

SECOND EDITION

ELECTROCHEMICAL METHODS

Fundamentals and
Applications

Allen J. Bard

Larry R. Faulkner


*Department of Chemistry and Biochemistry
University of Texas at Austin*



JOHN WILEY & SONS, INC.
*New York • Chichester • Weinheim
Brisbane • Singapore • Toronto*

Acquisitions Editor David Harris
Senior Production Editor Elizabeth Swain
Senior Marketing Manager Charity Robey
Illustration Editor Eugene Aiello

This book was set in 10/12 Times Roman by University Graphics and printed and bound by Hamilton. The cover was printed by Phoenix.

This book is printed on acid-free paper. 

Copyright 2001 © John Wiley & Sons, Inc. All rights reserved.

No part of this publication may be reproduced, stored in a retrieval system or transmitted in any form or by any means, electronic, mechanical, photocopying, recording, scanning or otherwise, except as permitted under Sections 107 or 108 of the 1976 United States Copyright Act, without either the prior written permission of the Publisher, or authorization through payment of the appropriate per-copy fee to the Copyright Clearance Center, 222 Rosewood Drive, Danvers, MA 01923, (978) 750-8400, fax (978) 750-4470. Requests to the Publisher for permission should be addressed to the Permissions Department, John Wiley & Sons, Inc., 605 Third Avenue, New York, NY 10158-0012, (212) 850-6011, fax (212) 850-6008, E-Mail: PERMREQ@WILEY.COM.

To order books or for customer service, call 1(800)-CALL-WILEY (225-5945).

Library of Congress Cataloging in Publication Data:

Bard, Allen J.

Electrochemical methods : fundamentals and applications / Allen J. Bard, Larry R.

Faulkner.—2nd ed.

p. cm.

Includes index.

ISBN 0-471-04372-9 (cloth : alk. paper)

1. Electrochemistry. I. Faulkner, Larry R., 1944— II. Title.

QD553.B37 2000

541.3'7—dc21

00-038210

Printed in the United States of America

10 9 8 7 6 5 4 3 2 1



PREFACE

In the twenty years since the appearance of our first edition, the fields of electrochemistry and electroanalytical chemistry have evolved substantially. An improved understanding of phenomena, the further development of experimental tools already known in 1980, and the introduction of new methods have all been important to that evolution. In the preface to the 1980 edition, we indicated that the focus of electrochemical research seemed likely to shift from the development of methods toward their application in studies of chemical behavior. By and large, history has justified that view. There have also been important changes in practice, and our 1980 survey of methodology has become dated. In this new edition, we have sought to update the book in a way that will extend its value as a general introduction to electrochemical methods.

We have maintained the philosophy and approach of the original edition, which is to provide comprehensive coverage of fundamentals for electrochemical methods now in widespread use. This volume is intended as a textbook and includes numerous problems and chemical examples. Illustrations have been employed to clarify presentations, and the style is pedagogical throughout. The book can be used in formal courses at the senior undergraduate and beginning graduate levels, but we have also tried to write in a way that enables self-study by interested individuals. A knowledge of basic physical chemistry is assumed, but the discussions generally begin at an elementary level and develop upward. We have sought to make the volume self-contained by developing almost all ideas of any importance to our subject from very basic principles of chemistry and physics. Because we stress foundations and limits of application, the book continues to emphasize the mathematical theory underlying methodology; however the key ideas are discussed consistently apart from the mathematical basis. Specialized mathematical background is covered as needed. The problems following each chapter have been devised as teaching tools. They often extend concepts introduced in the text or show how experimental data are reduced to fundamental results. The cited literature is extensive, but mainly includes only seminal papers and reviews. It is impossible to cover the huge body of primary literature in this field, so we have made no attempt in that direction.

Our approach is first to give an overview of electrode processes (Chapter 1), showing the way in which the fundamental components of the subject come together in an electrochemical experiment. Then there are individual discussions of thermodynamics and potential, electron-transfer kinetics, and mass transfer (Chapters 2–4). Concepts from these basic areas are integrated together in treatments of the various methods (Chapters 5–11). The effects of homogeneous kinetics are treated separately in a way that provides a comparative view of the responses of different methods (Chapter 12). Next are discussions of interfacial structure, adsorption, and modified electrodes (Chapters 13 and 14); then there is a taste of electrochemical instrumentation (Chapter 15), which is followed by an extensive introduction to experiments in which electrochemistry is coupled with other tools (Chapters 16–18). Appendix A teaches the mathematical background; Appendix B provides an introduction to digital simulation; and Appendix C contains tables of useful data.

This structure is generally that of the 1980 edition, but important additions have been made to cover new topics or subjects that have evolved extensively. Among them are applications of ultramicroelectrodes, phenomena at well-defined surfaces, modified electrodes, modern electron-transfer theory, scanning probe methods, LCEC, impedance spectrometry, modern forms of pulse voltammetry, and various aspects of spectroelectrochemistry. Chapter 5 in the first edition (“Controlled Potential Microelectrode Techniques—Potential Step Methods”) has been divided into the new Chapter 5 (“Basic Potential Step Methods”) and the new Chapter 7 (“Polarography and Pulse Voltammetry”). Chapter 12 in the original edition (“Double Layer Structure and Adsorbed Intermediates in Electrode Processes”) has become two chapters in the new edition: Chapter 12 (“Double-Layer Structure and Adsorption”) and Chapter 13 (“Electroactive Layers and Modified Electrodes”). Whereas the original edition covered in a single chapter experiments in which other characterization methods are coupled to electrochemical systems (Chapter 14, “Spectrometric and Photochemical Experiments”), this edition features a wholly new chapter on “Scanning Probe Techniques” (Chapter 16), plus separate chapters on “Spectroelectrochemistry and Other Coupled Characterization Methods” (Chapter 17) and “Photoelectrochemistry and Electrogenerated Chemiluminescence” (Chapter 18). The remaining chapters and appendices of the new edition directly correspond with counterparts in the old, although in most there are quite significant revisions.

The mathematical notation is uniform throughout the book and there is minimal duplication of symbols. The List of Major Symbols and the List of Abbreviations offer definitions, units, and section references. Usually we have adhered to the recommendations of the IUPAC Commission on Electrochemistry [R. Parsons et al., *Pure Appl. Chem.*, **37**, 503 (1974)]. Exceptions have been made where customary usage or clarity of notation seemed compelling.

Of necessity, compromises have been made between depth, breadth of coverage, and reasonable size. “Classical” topics in electrochemistry, including many aspects of thermodynamics of cells, conductance, and potentiometry are not covered here. Similarly, we have not been able to accommodate discussions of many techniques that are useful but not widely practiced. The details of laboratory procedures, such as the design of cells, the construction of electrodes, and the purification of materials, are beyond our scope. In this edition, we have deleted some topics and have shortened the treatment of others. Often, we have achieved these changes by making reference to the corresponding passages in the first edition, so that interested readers can still gain access to a deleted or attenuated topic.

As with the first edition, we owe thanks to many others who have helped with this project. We are especially grateful to Rose McCord and Susan Faulkner for their conscientious assistance with myriad details of preparation and production. Valuable comments have been provided by S. Amemiya, F. C. Anson, D. A. Buttry, R. M. Crooks, P. He, W. R. Heineman, R. A. Marcus, A. C. Michael, R. W. Murray, A. J. Nozik, R. A. Osteryoung, J.-M. Savéant, W. Schmickler, M. P. Soriaga, M. J. Weaver, H. S. White, R. M. Wightman, and C. G. Zoski. We thank them and our many other colleagues throughout the electrochemical community, who have taught us patiently over the years. Yet again, we also thank our families for affording us the time and freedom required to undertake such a large project.

*Allen J. Bard
Larry R. Faulkner*

CONTENTS

MAJOR SYMBOLS ix
STANDARD ABBREVIATIONS xix

- 1 ► INTRODUCTION AND OVERVIEW OF ELECTRODE PROCESSES 1
 - 2 ► POTENTIALS AND THERMODYNAMICS OF CELLS 44
 - 3 ► KINETICS OF ELECTRODE REACTIONS 87
 - 4 ► MASS TRANSFER BY MIGRATION AND DIFFUSION 137
 - 5 ► BASIC POTENTIAL STEP METHODS 156
 - 6 ► POTENTIAL SWEEP METHODS 226
 - 7 ► POLAROGRAPHY AND PULSE VOLTAMMETRY 261
 - 8 ► CONTROLLED-CURRENT TECHNIQUES 305
 - 9 ► METHODS INVOLVING FORCED CONVECTION—HYDRODYNAMIC METHODS 331
 - 10 ► TECHNIQUES BASED ON CONCEPTS OF IMPEDANCE 368
 - 11 ► BULK ELECTROLYSIS METHODS 417
 - 12 ► ELECTRODE REACTIONS WITH COUPLED HOMOGENEOUS CHEMICAL REACTIONS 471
 - 13 ► DOUBLE-LAYER STRUCTURE AND ADSORPTION 534
 - 14 ► ELECTROACTIVE LAYERS AND MODIFIED ELECTRODES 580
 - 15 ► ELECTROCHEMICAL INSTRUMENTATION 632
 - 16 ► SCANNING PROBE TECHNIQUES 659
 - 17 ► SPECTROELECTROCHEMISTRY AND OTHER COUPLED CHARACTERIZATION METHODS 680
 - 18 ► PHOTOELECTROCHEMISTRY AND ELECTROGENERATED CHEMILUMINESCENCE 736
- APPENDICES
- A ► MATHEMATICAL METHODS 769
 - B ► DIGITAL SIMULATIONS OF ELECTROCHEMICAL PROBLEMS 785
 - C ► REFERENCE TABLES 808
- INDEX 814

MAJOR SYMBOLS

Listed below are symbols used in several chapters or in large portions of a chapter. Symbols similar to some of these may have different local meanings. In most cases, the usage follows the recommendations of the IUPAC Commission on Electrochemistry [R. Parsons et al., *Pure Appl. Chem.*, **37**, 503 (1974).]; however there are exceptions.

A bar over a concentration or a current [e.g., $\bar{C}_O(x, s)$] indicates the Laplace transform of the variable. The exception is when i indicates an average current in polarography.

► STANDARD SUBSCRIPTS

a	anodic	dl	double layer	O	pertaining to species O in $O + ne \rightleftharpoons R$
c	(a) cathodic (b) charging	eq	equilibrium	p	peak
D	disk	f	(a) forward (b) faradaic	R	(a) pertaining to species R in $O + ne \rightleftharpoons R$ (b) ring
d	diffusion	l	limiting	r	reverse

► ROMAN SYMBOLS

Symbol	Meaning	Usual Units	Section References
A	(a) area (b) cross-sectional area of a porous electrode (c) frequency factor in a rate expression (d) open-loop gain of an amplifier	cm ² cm ² depends on order none	1.3.2 11.6.2 3.1.2 15.1.1
\mathcal{A}	absorbance	none	17.1.1
a	(a) internal area of a porous electrode (b) tip radius in SECM	cm ² μm	11.6.2 16.4.1
a_j^α	activity of substance j in a phase α	none	2.1.5
b	$\alpha Fv/RT$	s ⁻¹	6.3.1
b_j	$\beta_j \Gamma_{j,s}^\circ$	mol/cm ²	13.5.3
C	capacitance	F	1.2.2, 10.1.2
C_B	series equivalent capacitance of a cell	F	10.4
C_d	differential capacitance of the double layer	F, F/cm ²	1.2.2, 13.2.2
C_i	integral capacitance of the double layer	F, F/cm ²	13.2.2
C_j	concentration of species j	M , mol/cm ³	
C_j^*	bulk concentration of species j	M , mol/cm ³	1.4.2, 4.4.3
$C_j(x)$	concentration of species j at distance x	M , mol/cm ³	1.4

Symbol	Meaning	Usual Units	Section References
$C_j(x=0)$	concentration of species j at the electrode surface	$M, \text{mol/cm}^3$	1.4.2
$C_j(x, t)$	concentration of species j at distance x at time t	$M, \text{mol/cm}^3$	4.4
$C_j(0, t)$	concentration of species j at the electrode surface at time t	$M, \text{mol/cm}^3$	4.4.3
$C_j(y)$	concentration of species j at distance y away from rotating electrode	$M, \text{mol/cm}^3$	9.3.3
$C_j(y=0)$	surface concentration of species j at a rotating electrode	$M, \text{mol/cm}^3$	9.3.4
C_{SC}	space charge capacitance	F/cm^2	18.2.2
C_s	pseudocapacity	F	10.1.3
c	speed of light <i>in vacuo</i>	cm/s	17.1.2
D_E	diffusion coefficient for electrons within the film at a modified electrode	cm^2/s	14.4.2
D_j	diffusion coefficient of species j	cm^2/s	1.4.1, 4.4
$D_j(\lambda, E)$	concentration density of states for species j	$\text{cm}^3 \text{eV}^{-1}$	3.6.3
\mathbf{D}_M	model diffusion coefficient in simulation	none	B.1.3, B.1.8
D_S	diffusion coefficient for the primary reactant within the film at a modified electrode	cm^2/s	14.4.2
d	distance of the tip from the substrate in SECM	$\mu\text{m}, \text{nm}$	16.4.1
d_j	density of phase j	g/cm^3	
E	(a) potential of an electrode versus a reference	V	1.1, 2.1
	(b) emf of a reaction	V	2.1
	(c) amplitude of an ac voltage	V	10.1.2
ΔE	(a) pulse height in DPV	mV	7.3.4
	(b) step height in fast or staircase voltammetry	mV	7.3.1
	(c) amplitude (1/2 p-p) of ac excitation in ac voltammetry	mV	10.5.1
E	electron energy	eV	2.2.5, 3.6.3
\mathcal{E}	electric field strength vector	V/cm	2.2.1
\mathcal{E}	electric field strength	V/cm	2.2.1
\dot{E}	voltage or potential phasor	V	10.1.2
E^0	(a) standard potential of an electrode or a couple	V	2.1.4
	(b) standard emf of a half-reaction	V	2.1.4
ΔE^0	difference in standard potentials for two couples	V	6.6
E^0	electron energy corresponding to the standard potential of a couple	eV	3.6.3
$E^{0'}$	formal potential of an electrode	V	2.1.6
E_A	activation energy of a reaction	kJ/mol	3.1.2
E_{ac}	ac component of potential	mV	10.1.1
E_b	base potential in NPV and RPV	V	7.3.2, 7.3.3
E_{dc}	dc component of potential	V	10.1.1

Symbol	Meaning	Usual Units	Section References
E_{eq}	equilibrium potential of an electrode	V	1.3.2, 3.4.1
\mathbf{E}_F	Fermi level	eV	2.2.5, 3.6.3
E_{fb}	flat-band potential	V	18.2.2
\mathbf{E}_g	bandgap of a semiconductor	eV	18.2.2
E_i	initial potential	V	6.2.1
E_j	junction potential	mV	2.3.4
E_m	membrane potential	mV	2.4
E_p	peak potential	V	6.2.2
ΔE_p	(a) $ E_{\text{pa}} - E_{\text{pc}} $ in CV	V	6.5
	(b) pulse height in SWV	mV	7.3.5
$E_{p/2}$	potential where $i = i_p/2$ in LSV	V	6.2.2
E_{pa}	anodic peak potential	V	6.5
E_{pc}	cathodic peak potential	V	6.5
ΔE_s	staircase step height in SWV	mV	7.3.5
E_z	potential of zero charge	V	13.2.2
E_λ	switching potential for cyclic voltammetry	V	6.5
$E_{\tau/4}$	quarter-wave potential in chronopotentiometry	V	8.3.1
$E_{1/2}$	(a) measured or expected half-wave potential in voltammetry	V	1.4.2, 5.4, 5.5
	(b) in derivations, the “reversible” half-wave potential, $E^{0'} + (RT/nF) \ln(D_R/D_O)^{1/2}$	V	5.4
$E_{1/4}$	potential where $i/i_d = 1/4$	V	5.4.1
$E_{3/4}$	potential where $i/i_d = 3/4$	V	5.4.1
e	(a) electronic charge	C	
	(b) voltage in an electric circuit	V	10.1.1, 15.1
e_i	input voltage	V	15.2
e_o	output voltage	V	15.1.1
e_s	voltage across the input terminals of an amplifier	μV	15.1.1
$\text{erf}(x)$	error function of x	none	A.3
$\text{erfc}(x)$	error function complement of x	none	A.3
F	the Faraday constant; charge on one mole of electrons	C	
f	(a) F/RT	V^{-1}	
	(b) frequency of rotation	r/s	9.3
	(c) frequency of a sinusoidal oscillation	s^{-1}	10.1.2
	(d) SWV frequency	s^{-1}	7.3.5
	(e) fraction titrated	none	11.5.2
$f(\mathbf{E})$	Fermi function	none	3.6.3
$f_i(j, k)$	fractional concentration of species i in box j after iteration k in a simulation	none	B.1.3
G	Gibbs free energy	kJ, kJ/mol	2.2.4
ΔG	Gibbs free energy change in a chemical process	kJ, kJ/mol	2.1.2, 2.1.3
\bar{G}	electrochemical free energy	kJ, kJ/mol	2.2.4
G^0	standard Gibbs free energy	kJ, kJ/mol	3.1.2

Symbol	Meaning	Usual Units	Section References
ΔG^0	standard Gibbs free energy change in a chemical process	kJ, kJ/mol	2.1.2, 2.1.3
ΔG^\ddagger	standard Gibbs free energy of activation	kJ/mol	3.1.2
$\Delta G_{\text{transfer}, j}^{0\alpha \rightarrow \beta}$	standard free energy of transfer for species j from phase α into phase β	kJ/mol	2.3.6
g	(a) gravitational acceleration (b) interaction parameter in adsorption isotherms	cm/s ² J-cm ² /mol ²	13.5.2
H	(a) enthalpy (b) $k_f/D_O^{1/2} + k_b/D_R^{1/2}$	kJ, kJ/mol s ^{-1/2}	2.1.2 5.5.1
ΔH	enthalpy change in a chemical process	kJ, kJ/mol	2.1.2
ΔH^0	standard enthalpy change in a chemical process	kJ, kJ/mol	2.1.2
ΔH^\ddagger	standard enthalpy of activation	kJ/mol	3.1.2
h	Planck constant	J-s	
h_{corr}	corrected mercury column height at a DME	cm	7.1.4
I	amplitude of an ac current	A	10.1.2
$I(t)$	convolutive transform of current; semi-integral of current	C/s ^{1/2}	6.7.1
\dot{I}	current phasor	A	10.1.2
\bar{I}	diffusion current constant for average current	$\mu\text{A}\cdot\text{s}^{1/2}/(\text{mg}^{2/3}\cdot\text{mM})$	7.1.3
$(I)_{\text{max}}$	diffusion current constant for maximum current	$\mu\text{A}\cdot\text{s}^{1/2}/(\text{mg}^{2/3}\cdot\text{mM})$	7.1.3
I_p	peak value of ac current amplitude	A	10.5.1
i	current	A	1.3.2
Δi	difference current in SWV = $i_f - i_r$	A	7.3.5
δi	difference current in DPV = $i(\tau) - i(\tau')$	A	7.3.4
$i(0)$	initial current in bulk electrolysis	A	11.3.1
i_A	characteristic current describing flux of the primary reactant to a modified RDE	A	14.4.2
i_a	anodic component current	A	3.2
i_c	(a) charging current (b) cathodic component current	A A	6.2.4 3.2
i_d	(a) current due to diffusive flux (b) diffusion-limited current	A A	4.1 5.2.1
\bar{i}_d	average diffusion-limited current flow over a drop lifetime at a DME	A	7.1.2
$(i_d)_{\text{max}}$	diffusion-limited current at t_{max} at a DME (maximum current)	A	7.1.2
i_E	characteristic current describing diffusion of electrons within the film at a modified electrode	A	14.4.2
i_f	(a) faradaic current (b) forward current	A A	5.7
i_K	kinetically limited current	A	9.3.4
i_k	characteristic current describing cross-reaction within the film at a modified electrode	A	14.4.2

Symbol	Meaning	Usual Units	Section References
i_l	limiting current	A	1.4.2
$i_{l,a}$	limiting anodic current	A	1.4.2
$i_{l,c}$	limiting cathodic current	A	1.4.2
i_m	migration current	A	4.1
i_p	characteristic current describing permeation of the primary reactant into the film at a modified electrode	A	14.4.2
i_p	peak current	A	6.2.2
i_{pa}	anodic peak current	A	6.5.1
i_{pc}	cathodic peak current	A	6.5.1
i_r	current during reversal step	A	5.7
i_S	(a) characteristic current describing diffusion of the primary reactant through the film at a modified electrode	A	14.4.2
	(b) substrate current in SECM	A	16.4.4
i_{ss}	steady-state current	A	5.3
i_T	tip current in SECM	A	16.4.2
$i_{T,\infty}$	tip current in SECM far from the substrate	A	16.4.1
i_0	exchange current	A	3.4.1, 3.5.4
$i_{0,t}$	true exchange current	A	13.7.1
$\text{Im}(w)$	imaginary part of complex function w		A.5
$J_j(x, t)$	flux of species j at location x at time t	$\text{mol cm}^{-2} \text{s}^{-1}$	1.4.1, 4.1
j	(a) current density	A/cm^2	1.3.2
	(b) box index in a simulation	none	B.1.2
	(c) $\sqrt{-1}$	none	A.5
j_0	exchange current density	A/cm^2	3.4.1, 3.5.4
K	equilibrium constant	none	
$K_{P,j}$	precursor equilibrium constant for reactant j	depends on case	3.6.1
k	(a) rate constant for a homogeneous reaction	depends on order	
	(b) iteration number in a simulation	none	B.1
	(c) extinction coefficient	none	17.1.2
k	Boltzmann constant	J/K	
k^0	standard heterogeneous rate constant	cm/s	3.3, 3.4
k_b	(a) heterogeneous rate constant for oxidation	cm/s	3.2
	(b) homogeneous rate constant for "backward" reaction	depends on order	3.1
k_f	(a) heterogeneous rate constant for reduction	cm/s	3.2
	(b) homogeneous rate constant for "forward" reaction	depends on order	3.1
$k_{i,j}^{\text{pot}}$	potentiometric selectivity coefficient of interferent j toward a measurement of species i	none	2.4
k_t^0	true standard heterogeneous rate constant	cm/s	13.7.1

Symbol	Meaning	Usual Units	Section References
L	length of a porous electrode	cm	11.6.2
$L\{f(t)\}$	Laplace transform of $f(t) = \bar{f}(s)$		A.1
$L^{-1}\{\bar{f}(s)\}$	inverse Laplace transform of $f(s)$		A.1
l	thickness of solution in a thin-layer cell	cm	11.7.2
ℓ	number of iterations corresponding to t_k in a simulation	none	B.1.4
m	mercury flow rate at a DME	mg/s	7.1.2
$m(t)$	convolutive transform of current; semi-integral of current	$C/s^{1/2}$	6.7.1
m_j	mass-transfer coefficient of species j	cm/s	1.4.2
N	collection efficiency at an RRDE	none	9.4.2
N_A	(a) acceptor density (b) Avogadro's number	cm^{-3} mol^{-1}	18.2.2
N_D	donor density	cm^{-3}	18.2.2
N_j	total number of moles of species j in a system	mol	11.3.1
n	(a) stoichiometric number of electrons involved in an electrode reaction (b) electron density in a semiconductor (c) refractive index	none cm^{-3} none	1.3.2 18.2.2 17.1.2
\hat{n}	complex refractive index	none	17.1.2
n^0	number concentration of each ion in a $z:z$ electrolyte	cm^{-3}	13.3.2
n_i	electron density in an intrinsic semiconductor	cm^{-3}	18.2.2
n_j	(a) number of moles of species j in a phase (b) number concentration of ion j in an electrolyte	mol cm^{-3}	2.2.4, 13.1.1 13.3.2
n_j^0	number concentration of ion j in the bulk electrolyte	cm^{-3}	13.3.2
O	oxidized form of the standard system $O + ne \rightleftharpoons R$; often used as a subscript denoting quantities pertaining to species O		
P	pressure	Pa, atm	
p	(a) hole density in a semiconductor (b) $m_j A/V$	cm^{-3} s^{-1}	18.2.2 11.3.1
p_i	hole density in an intrinsic semiconductor	cm^{-3}	18.3.2
Q	charge passed in electrolysis	C	1.3.2, 5.8.1, 11.3.1
Q^0	charge required for complete electrolysis of a component by Faraday's law	C	11.3.4
Q_d	chronocoulometric charge from a diffusing component	C	5.8.1
Q_{dl}	charge devoted to double-layer capacitance	C	5.8
q^j	excess charge on phase j	C, μC	1.2, 2.2
R	reduced form of the standard system, $O + ne \rightleftharpoons R$; often used as a subscript denoting quantities pertaining to species R		

Symbol	Meaning	Usual Units	Section References
R	(a) gas constant	$\text{J mol}^{-1} \text{K}^{-1}$	
	(b) resistance	Ω	10.1.2
	(c) fraction of substance electrolyzed in a porous electrode	none	11.6.2
	(d) reflectance	none	17.1.2
R_B	series equivalent resistance of a cell	Ω	10.4
R_{ct}	charge-transfer resistance	Ω	1.3.3, 3.4.3
R_f	feedback resistance	Ω	15.2
R_{mt}	mass-transfer resistance	Ω	1.4.2, 3.4.6
R_s	(a) solution resistance	Ω	1.3.4
	(b) series resistance in an equivalent circuit	Ω	1.2.4, 10.1.3
R_u	uncompensated resistance	Ω	1.3.4, 15.6
R_Ω	ohmic solution resistance	Ω	10.1.3
r	radial distance from the center of an electrode	cm	5.2.2, 5.3, 9.3.1
r_c	radius of a capillary	cm	7.1.3
r_0	radius of an electrode	cm	5.2.2, 5.3
r_1	radius of the disk in an RDE or RRDE	cm	9.3.5
r_2	inner radius of a ring electrode	cm	9.4.1
r_3	outer radius of a ring electrode	cm	9.4.1
Re	Reynolds number	none	9.2.1
Re(w)	real part of complex function w		A.5
ΔS	entropy change in a chemical process	$\text{kJ/K}, \text{kJ mol}^{-1} \text{K}^{-1}$	2.1.2
ΔS^0	standard entropy change in a chemical process	$\text{kJ/K}, \text{kJ mol}^{-1} \text{K}^{-1}$	2.1.2
ΔS^\ddagger	standard entropy of activation	$\text{kJ mol}^{-1} \text{K}^{-1}$	3.1.2
$S_\tau(t)$	unit step function rising at $t = \tau$	none	A.1.7
s	(a) Laplace plane variable, usually complementary to t		A.1
	(b) specific area of a porous electrode	cm^{-1}	11.6.2
T	absolute temperature	K	
t	time	s	
t_j	transference number of species j	none	2.3.3, 4.2
t_k	known characteristic time in a simulation	s	B.1.4
t_{\max}	drop time at a DME	s	7.1.2
t_p	pulse width in SWV	s	7.3.5
u_j	mobility of ion (or charge carrier) j	$\text{cm}^2 \text{V}^{-1} \text{s}^{-1}$	2.3.3, 4.2
V	volume	cm^3	
v	(a) linear potential scan rate	V/s	6.1
	(b) homogeneous reaction rate	$\text{mol cm}^{-3} \text{s}^{-1}$	1.3.2, 3.1
	(c) heterogeneous reaction rate	$\text{mol cm}^{-2} \text{s}^{-1}$	1.3.2, 3.2
	(d) linear velocity of solution flow, usually a function of position	cm/s	1.4.1, 9.2
v_b	(a) "backward" homogeneous reaction rate	$\text{mol cm}^{-3} \text{s}^{-1}$	3.1
	(b) anodic heterogeneous reaction rate	$\text{mol cm}^{-2} \text{s}^{-1}$	3.2
v_f	(a) "forward" homogeneous reaction rate	$\text{mol cm}^{-3} \text{s}^{-1}$	3.1
	(b) cathodic heterogeneous reaction rate	$\text{mol cm}^{-2} \text{s}^{-1}$	3.2
v_j	component of velocity in the j direction	cm/s	9.2.1

Symbol	Meaning	Usual Units	Section References
v_{mt}	rate of mass transfer to a surface	$\text{mol cm}^{-2} \text{s}^{-1}$	1.4.1
$W_j(\lambda, \mathbf{E})$	probability density function for species j	eV^{-1}	3.6.3
w	width of a band electrode	cm	5.3
w_j	work term for reactant j in electron transfer	eV	3.6.2
X_C	capacitive reactance	Ω	10.1.2
X_j	mole fraction of species j	none	13.1.2
x	distance, often from a planar electrode	cm	
x_1	distance of the IHP from the electrode surface	cm	1.2.3, 13.3.3
x_2	distance of the OHP from the electrode surface	cm	1.2.3, 13.3.3
Y	admittance	Ω^{-1}	10.1.2
\mathbf{Y}	admittance vector	Ω^{-1}	10.1.2
y	distance from an RDE or RRDE	cm	9.3.1
Z	(a) impedance	Ω	10.1.2
	(b) dimensionless current parameter in simulation	none	B.1.6
\mathbf{Z}	impedance vector	Ω	10.1.2
Z_f	faradaic impedance	Ω	10.1.3
Z_{Im}	imaginary part of impedance	Ω	10.1.2
Z_{Re}	real part of impedance	Ω	10.1.2
Z_w	Warburg impedance	Ω	10.1.3
z	(a) distance normal to the surface of a disk electrode or along a cylindrical electrode	cm	5.3
	(b) charge magnitude of each ion in a $z:z$ electrolyte	none	13.3.2
z_j	charge on species j in signed units of electronic charge	none	2.3

► GREEK SYMBOLS

Symbol	Meaning	Usual Units	Section References
α	(a) transfer coefficient	none	3.3
	(b) absorption coefficient	cm^{-1}	17.1.2
β	(a) distance factor for extended charge transfer	\AA^{-1}	3.6.4
	(b) geometric parameter for an RRDE	none	9.4.1
	(c) $1 - \alpha$	none	10.5.2
β_j	(a) $\partial E / \partial C_j(0, t)$	$\text{V}\cdot\text{cm}^3/\text{mol}$	10.2.2
	(b) equilibrium parameter in an adsorption isotherm for species j	none	13.5.2
Γ_j	surface excess of species j at equilibrium	mol/cm^2	13.1.2
$\Gamma_{j(r)}$	relative surface excess of species j with respect to component r	mol/cm^2	13.1.2

Symbol	Meaning	Usual Units	Section References
$\Gamma_{j,s}$	surface excess of species j at saturation	mol/cm ²	13.5.2
γ	(a) surface tension (b) dimensionless parameter used to define frequency (time) regimes in step experiments at spherical electrodes	dyne/cm none	5.4.2, 5.5.2
γ_j	activity coefficient for species j	none	2.1.5
Δ	ellipsometric parameter	none	17.1.2
δ	$r_0(s/D_O)^{1/2}$, used to define diffusional regimes at a spherical electrode	none	5.5.2
δ_j	“diffusion” layer thickness for species j at an electrode fed by convective transfer	cm	1.4.2, 9.3.2
ε	(a) dielectric constant (b) optical-frequency dielectric constant (c) porosity	none none none	13.3.1 17.1.2 11.6.2
$\hat{\varepsilon}$	complex optical-frequency dielectric constant	none	17.1.2
ε_j	molar absorptivity of species j	M ⁻¹ cm ⁻¹	17.1.1
ε_0	permittivity of free space	C ² N ⁻¹ m ⁻²	13.3.1
ζ	zeta potential	mV	9.8.1
η	overpotential, $E - E_{eq}$	V	1.3.2, 3.4.2
η_{ct}	charge-transfer overpotential	V	1.3.3, 3.4.6
η_j	viscosity of fluid j	g cm ⁻¹ s ⁻¹ = poise	9.2.2
η_{mt}	mass-transfer overpotential	V	1.3.3, 3.4.6
θ	(a) $\exp[(nF/RT)(E - E^0)]$ (b) $\tau^{1/2} + (t - \tau)^{1/2} - t^{1/2}$	none s ^{1/2}	5.4.1 5.8.2
θ_j	fractional coverage of an interface by species j	none	13.5.2
κ	(a) conductivity of a solution (b) transmission coefficient of a reaction (c) $r_0 k_f / D_O$, used to define kinetic regimes at a spherical electrode (d) double-layer thickness parameter (e) partition coefficient for the primary reactant in a modified electrode system	S/cm = Ω^{-1} cm ⁻¹ none none cm ⁻¹ none	2.3.3, 4.2 3.1.3 5.5.2 13.3.2 14.4.2
κ_{el}	electronic transmission coefficient	none	3.6
Λ	equivalent conductivity of a solution	cm ² Ω^{-1} equiv ⁻¹	2.3.3
λ	(a) reorganization energy for electron transfer (b) $k_f \tau^{1/2} (1 + \xi \theta) / D_O^{1/2}$ (c) dimensionless homogeneous kinetic parameter, specific to a method and mechanism (d) switching time in CV (e) wavelength of light <i>in vacuo</i>	eV none none s nm	3.6 5.5.1 12.3 6.5 17.1.2
λ_i	inner component of the reorganization energy	eV	3.6.2
λ_j	equivalent ionic conductivity for ion j	cm ² Ω^{-1} equiv ⁻¹	2.3.3
λ_{0j}	equivalent ionic conductivity of ion j extrapolated to infinite dilution	cm ² Ω^{-1} equiv ⁻¹	2.3.3

Symbol	Meaning	Usual Units	Section References
λ_o	outer component of the reorganization energy	eV	3.6.2
μ	(a) reaction layer thickness (b) magnetic permeability	cm none	1.5.2, 12.4.2 17.1.2
$\bar{\mu}_e^\alpha$	electrochemical potential of electrons in phase α	kJ/mol	2.2.4, 2.2.5
$\bar{\mu}_j^\alpha$	electrochemical potential of species j in phase α	kJ/mol	2.2.4
μ_j^α	chemical potential of species j in phase α	kJ/mol	2.2.4
μ_j^0	standard chemical potential of species j in phase α	kJ/mol	2.2.4
ν	(a) kinematic viscosity (b) frequency of light	cm ² /s s ⁻¹	9.2.2
ν_j	stoichiometric coefficient for species j in a chemical process	none	2.1.5
ν_n	nuclear frequency factor	s ⁻¹	3.6
ξ	$(D_O/D_R)^{1/2}$	none	5.4.1
ρ	(a) resistivity (b) roughness factor	Ω -cm none	4.2 5.2.3
$\rho(\mathbf{E})$	electronic density of states	cm ² eV ⁻¹	3.6.3
σ	(a) nFv/RT (b) $(1/nFA\sqrt{2})[\beta_O/D_O^{1/2} - \beta_R/D_R^{1/2}]$	s ⁻¹ Ω -s ^{1/2}	6.2.1 10.2.3
σ^j	excess charge density on phase j	C/cm ²	1.2, 2.2
σ_j	parameter describing potential dependence of adsorption energy	none	13.3.4
τ	(a) transition time in chronopotentiometry (b) sampling time in sampled-current voltammetry (c) forward step duration in a double-step experiment (d) generally, a characteristic time defined by the properties of an experiment (e) in treatments of UMEs, $4D_O t/r_0^2$	s s s s none	8.2.2 5.1, 7.3 5.7.1 5.3
τ'	start of potential pulse in pulse voltammetry	s	7.3
τ_L	longitudinal relaxation time of a solvent	s	3.6.2
Φ	work function of a phase	eV	3.6.4
ϕ	(a) electrostatic potential (b) phase angle between two sinusoidal signals (c) phase angle between \dot{I}_{ac} and \dot{E}_{ac} (d) film thickness in a modified electrode	V degrees, radians degrees, radians cm	2.2.1 10.1.2 10.1.2 14.4.2
$\Delta\phi$	(a) electrostatic potential difference between two points or phases (b) potential drop in the space charge region of a semiconductor	V V	2.2 18.2.2
ϕ^j	absolute electrostatic potential of phase j	V	2.2.1
$\Delta_\beta^\alpha\phi$	junction potential at a liquid-liquid interface	V	6.8

Symbol	Meaning	Usual Units	Section References
$\Delta_{\beta}^{\alpha}\phi_j^0$	standard Galvani potential of ion transfer for species j from phase α to phase β	V	6.8
ϕ_0	total potential drop across the solution side of the double layer	mV	13.3.2
ϕ_2	potential at the OHP with respect to bulk solution	V	1.2.3, 13.3.3
χ	$(12/7)^{1/2}k_r\tau^{1/2}/D_O^{1/2}$	none	7.2.2
$\chi(j)$	dimensionless distance of box j in a simulation	none	B.1.5
$\chi(bt)$	normalized current for a totally irreversible system in LSV and CV	none	6.3.1
$\chi(\sigma t)$	normalized current for a reversible system in LSV and CV	none	6.2.1
χ_f	rate constant for permeation of the primary reactant into the film at a modified electrode	cm/s	14.4.2
ψ	(a) ellipsometric parameter	none	17.1.2
	(b) dimensionless rate parameter in CV	none	6.5.2
ω	(a) angular frequency of rotation; $2\pi \times$ rotation rate	s^{-1}	9.3
	(b) angular frequency of a sinusoidal oscillation; $2\pi f$	s^{-1}	10.1.2

▶ STANDARD ABBREVIATIONS

Abbreviation	Meaning	Section Reference
ADC	analog-to-digital converter	15.8
AES	Auger electron spectrometry	17.3.3
AFM	atomic force microscopy	16.3
ASV	anodic stripping voltammetry	11.8
BV	Butler-Volmer	3.3
CB	conduction band	18.2.2
CE	homogeneous chemical process preceding heterogeneous electron transfer ¹	12.1.1
CV	cyclic voltammetry	6.1, 6.5
CZE	capillary zone electrophoresis	11.6.4
DAC	digital-to-analog converter	15.8
DME	(a) dropping mercury electrode (b) 1,2-dimethoxyethane	7.1.1
DMF	<i>N,N</i> -dimethylformamide	
DMSO	Dimethylsulfoxide	
DPP	differential pulse polarography	7.3.4
DPV	differential pulse voltammetry	7.3.4

¹Letters may be subscripted *i*, *q*, or *r* to indicate irreversible, quasi-reversible, or reversible reactions.

Abbreviation	Meaning	Section Reference
EC	heterogeneous electron transfer followed by homogeneous chemical reaction ¹	12.1.1
EC'	catalytic regeneration of the electroactive species in a following homogeneous reaction ¹	12.1.1
ECE	heterogeneous electron transfer, homogeneous chemical reaction, and heterogeneous electron transfer, in sequence ¹	12.1.1
ECL	electrogenerated chemiluminescence	18.1
ECM	electrocapillary maximum	13.2.2
EE	stepwise heterogeneous electron transfers to accomplish a 2-electron reduction or oxidation of a species ¹	12.1.1
EIS	electrochemical impedance spectroscopy	10.1.1
emf	electromotive force	2.1.3
EMIRS	electrochemically modulated infrared reflectance spectroscopy	17.2.1
ESR	electron spin resonance	17.4.1
ESTM	electrochemical scanning tunneling microscopy	16.2
EXAFS	extended X-ray absorption fine structure	17.6.1
FFT	fast Fourier transform	A.6
GCS	Gouy-Chapman-Stern	13.3.3
GDP	galvanostatic double pulse	8.6
HCP	hexagonal close-packed	13.4.2
HMDE	hanging mercury drop electrode	5.2.2
HOPG	highly oriented pyrolytic graphite	13.4.2
IHP	inner Helmholtz plane	1.2.3, 13.3.3
IPE	ideal polarized electrode	1.2.1
IRRAS	infrared reflection absorption spectroscopy	17.2.1
IR-SEC	infrared spectroelectrochemistry	17.2.1
ISE	ion-selective electrode	2.4
ITIES	interface between two immiscible electrolyte solutions	6.8
ITO	indium-tin oxide thin film	18.2.5
LB	Langmuir-Blodgett	14.2.1
LCEC	liquid chromatography with electrochemical detection	11.6.4
LEED	low-energy electron diffraction	17.3.3
LSV	linear sweep voltammetry	6.1
MFE	mercury film electrode	11.8
NHE	normal hydrogen electrode = SHE	1.1.1
NCE	normal calomel electrode, Hg/Hg ₂ Cl ₂ /KCl (1.0 M)	
NPP	normal pulse polarography	7.3.2
NPV	normal pulse voltammetry	7.3.2
OHP	outer Helmholtz plane	1.2.3, 13.3.3
OTE	optically transparent electrode	17.1.1
OTTLE	optically transparent thin-layer electrode	17.1.1
PAD	pulsed amperometric detection	11.6.4
PC	propylene carbonate	
PDIRS	potential difference infrared spectroscopy	17.2.1
PZC	potential of zero charge	13.2.2
QCM	quartz crystal microbalance	17.5

¹Letters may be subscripted *i*, *q*, or *r* to indicate irreversible, quasi-reversible, or reversible reactions.

Abbreviation	Meaning	Section Reference
QRE	quasi-reference electrode	2.1.7
RDE	rotating disk electrode	9.3
RDS	rate-determining step	3.5
RPP	reverse pulse polarography	7.3.4
RPV	reverse pulse voltammetry	7.3.4
RRDE	rotating ring-disk electrode	9.4.2
SAM	self-assembled monolayer	14.2.2
SCE	saturated calomel electrode	1.1.1
SECM	scanning electrochemical microscopy	16.4
SERS	surface enhanced Raman spectroscopy	17.2.2
SHE	standard hydrogen electrode = NHE	1.1.1
SHG	second harmonic generation	17.1.5
SMDE	static mercury drop electrode	7.1.1
SNIFTIRS	subtractively normalized interfacial Fourier transform infrared spectroscopy	17.2.1
SPE	solid polymer electrolyte	14.2.6
SPR	surface plasmon resonance	17.1.3
SSCE	sodium saturated calomel electrode, Hg/Hg ₂ Cl ₂ /NaCl (sat'd)	
STM	scanning tunneling microscopy	16.2
SWV	square wave voltammetry	7.3.5
TBABF ₄	tetra- <i>n</i> -butylammonium fluoborate	
TBAI	tetra- <i>n</i> -butylammonium iodide	
TBAP	tetra- <i>n</i> -butylammonium perchlorate	
TEAP	tetraethylammonium perchlorate	
THF	tetrahydrofuran	
UHV	ultrahigh vacuum	17.3
UME	ultramicroelectrode	5.3
UPD	underpotential deposition	11.2.1
XPS	X-ray photoelectron spectrometry	17.3.2
VB	valence band	18.2.2

INTRODUCTION AND OVERVIEW OF ELECTRODE PROCESSES

▶ 1.1 INTRODUCTION

Electrochemistry is the branch of chemistry concerned with the interrelation of electrical and chemical effects. A large part of this field deals with the study of chemical changes caused by the passage of an electric current and the production of electrical energy by chemical reactions. In fact, the field of electrochemistry encompasses a huge array of different phenomena (e.g., electrophoresis and corrosion), devices (electrochromic displays, electroanalytical sensors, batteries, and fuel cells), and technologies (the electroplating of metals and the large-scale production of aluminum and chlorine). While the basic principles of electrochemistry discussed in this text apply to all of these, the main emphasis here is on the application of electrochemical methods to the study of chemical systems.

Scientists make electrochemical measurements on chemical systems for a variety of reasons. They may be interested in obtaining thermodynamic data about a reaction. They may want to generate an unstable intermediate such as a radical ion and study its rate of decay or its spectroscopic properties. They may seek to analyze a solution for trace amounts of metal ions or organic species. In these examples, electrochemical methods are employed as tools in the study of chemical systems in just the way that spectroscopic methods are frequently applied. There are also investigations in which the electrochemical properties of the systems themselves are of primary interest, for example, in the design of a new power source or for the electrosynthesis of some product. Many electrochemical methods have been devised. Their application requires an understanding of the fundamental principles of electrode reactions and the electrical properties of electrode–solution interfaces.

In this chapter, the terms and concepts employed in describing electrode reactions are introduced. In addition, before embarking on a detailed consideration of methods for studying electrode processes and the rigorous solutions of the mathematical equations that govern them, we will consider approximate treatments of several different types of electrode reactions to illustrate their main features. The concepts and treatments described here will be considered in a more complete and rigorous way in later chapters.

1.1.1 Electrochemical Cells and Reactions

In electrochemical systems, we are concerned with the processes and factors that affect the transport of charge across the interface between chemical phases, for example, between an electronic conductor (an *electrode*) and an ionic conductor (an *electrolyte*). Throughout this book, we will be concerned with the electrode/electrolyte interface and the events that occur there when an electric potential is applied and current passes. Charge is transported through the electrode by the movement of electrons (and holes). Typical electrode materials include solid metals (e.g., Pt, Au), liquid metals (Hg, amalgams), carbon (graphite), and semiconductors (indium–tin oxide, Si). In the electrolyte phase, charge is carried by the movement of ions. The most frequently used electrolytes are liquid solutions containing ionic species, such as, H^+ , Na^+ , Cl^- , in either water or a non-aqueous solvent. To be useful in an electrochemical cell, the solvent/electrolyte system must be of sufficiently low resistance (i.e., sufficiently conductive) for the electrochemical experiment envisioned. Less conventional electrolytes include fused salts (e.g., molten NaCl–KCl eutectic) and ionically conductive polymers (e.g., Nafion, polyethylene oxide– LiClO_4). Solid electrolytes also exist (e.g., sodium β -alumina, where charge is carried by mobile sodium ions that move between the aluminum oxide sheets).

It is natural to think about events at a single interface, but we will find that one cannot deal experimentally with such an isolated boundary. Instead, one must study the properties of collections of interfaces called *electrochemical cells*. These systems are defined most generally as two electrodes separated by at least one electrolyte phase.

In general, a difference in electric potential can be measured between the electrodes in an electrochemical cell. Typically this is done with a high impedance voltmeter. This *cell potential*, measured in volts (V), where $1 \text{ V} = 1 \text{ joule/coulomb (J/C)}$, is a measure of the energy available to drive charge externally between the electrodes. It is a manifestation of the collected differences in electric potential between all of the various phases in the cell. We will find in Chapter 2 that the transition in electric potential in crossing from one conducting phase to another usually occurs almost entirely at the interface. The sharpness of the transition implies that a very high electric field exists at the interface, and one can expect it to exert effects on the behavior of charge carriers (electrons or ions) in the interfacial region. Also, the magnitude of the potential difference at an interface affects the relative energies of the carriers in the two phases; hence it controls the direction and the rate of charge transfer. Thus, the measurement and control of cell potential is one of the most important aspects of experimental electrochemistry.

Before we consider how these operations are carried out, it is useful to set up a shorthand notation for expressing the structures of cells. For example, the cell pictured in Figure 1.1.1a is written compactly as



In this notation, a slash represents a phase boundary, and a comma separates two components in the same phase. A double slash, not yet used here, represents a phase boundary whose potential is regarded as a negligible component of the overall cell potential. When a gaseous phase is involved, it is written adjacent to its corresponding conducting element. For example, the cell in Figure 1.1.1b is written schematically as



The overall chemical reaction taking place in a cell is made up of two independent *half-reactions*, which describe the real chemical changes at the two electrodes. Each half-reaction (and, consequently, the chemical composition of the system near the electrodes)

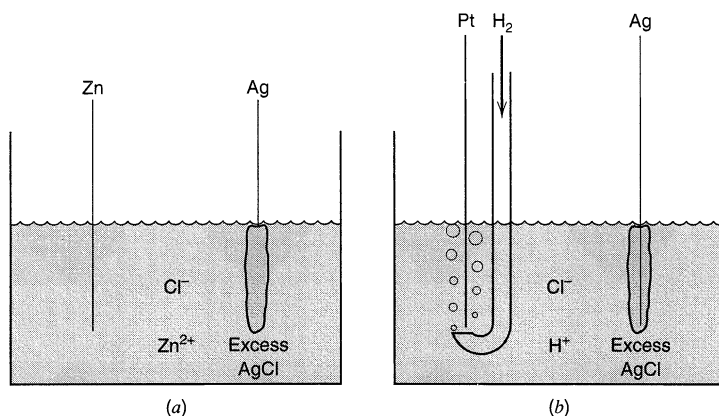
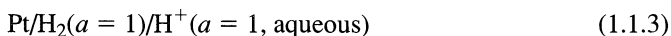


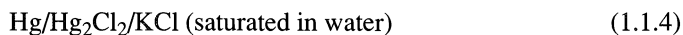
Figure 1.1.1 Typical electrochemical cells. (a) Zn metal and Ag wire covered with AgCl immersed in a ZnCl₂ solution. (b) Pt wire in a stream of H₂ and Ag wire covered with AgCl in HCl solution.

responds to the interfacial potential difference at the corresponding electrode. Most of the time, one is interested in only one of these reactions, and the electrode at which it occurs is called the *working* (or *indicator*) *electrode*. To focus on it, one standardizes the other half of the cell by using an electrode (called a *reference electrode*) made up of phases having essentially constant composition.

The internationally accepted primary reference is the *standard hydrogen electrode* (SHE), or *normal hydrogen electrode* (NHE), which has all components at unit activity:



Potentials are often measured and quoted with respect to reference electrodes other than the NHE, which is not very convenient from an experimental standpoint. A common reference is the *saturated calomel electrode* (SCE), which is



Its potential is 0.242 V vs. NHE. Another is the *silver–silver chloride electrode*,



with a potential of 0.197 V vs. NHE. It is common to see potentials identified in the literature as “vs. Ag/AgCl” when this electrode is used.

Since the reference electrode has a constant makeup, its potential is fixed. Therefore, any changes in the cell are ascribable to the working electrode. We say that we observe or control the *potential* of the working electrode *with respect to* the reference, and that is equivalent to observing or controlling the energy of the electrons within the working electrode (1, 2). By driving the electrode to more negative potentials (e.g., by connecting a battery or power supply to the cell with its negative side attached to the working electrode), the energy of the electrons is raised. They can reach a level high enough to transfer into vacant electronic states on species in the electrolyte. In that case, a flow of electrons from electrode to solution (a *reduction current*) occurs (Figure 1.1.2a). Similarly, the energy of the electrons can be lowered by imposing a more positive potential, and at some point electrons on solutes in the electrolyte will find a more favorable energy on the electrode and will transfer there. Their flow, from solution to electrode, is an *oxidation current* (Figure 1.1.2b). The critical potentials at which these processes occur are related to the *standard potentials*, E^0 , for the specific chemical substances in the system.

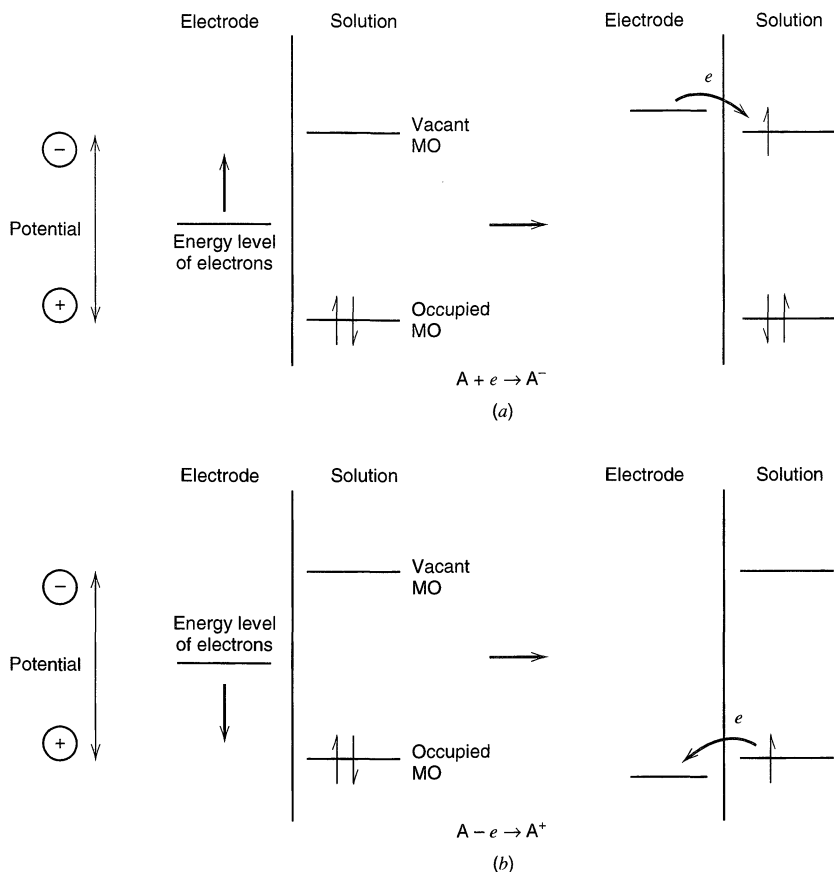


Figure 1.1.2 Representation of (a) reduction and (b) oxidation process of a species, A, in solution. The molecular orbitals (MO) of species A shown are the highest occupied MO and the lowest vacant MO. These correspond in an approximate way to the E^0 's of the A/A^- and A^+/A couples, respectively. The illustrated system could represent an aromatic hydrocarbon (e.g., 9,10-diphenylanthracene) in an aprotic solvent (e.g., acetonitrile) at a platinum electrode.

Consider a typical electrochemical experiment where a working electrode and a reference electrode are immersed in a solution, and the potential difference between the electrodes is varied by means of an external power supply (Figure 1.1.3). This variation in potential, E , can produce a current flow in the external circuit, because electrons cross the electrode/solution interfaces as reactions occur. Recall that the number of electrons that cross an interface is related stoichiometrically to the extent of the chemical reaction (i.e., to the amounts of reactant consumed and product generated). The number of electrons is measured in terms of the total charge, Q , passed in the circuit. Charge is expressed in units of coulombs (C), where 1 C is equivalent to 6.24×10^{18} electrons. The relationship between charge and amount of product formed is given by *Faraday's law*; that is, the passage of 96,485.4 C causes 1 equivalent of reaction (e.g., consumption of 1 mole of reactant or production of 1 mole of product in a one-electron reaction). The current, i , is the rate of flow of coulombs (or electrons), where a current of 1 ampere (A) is equivalent to 1 C/s. When one plots the current as a function of the potential, one obtains a *current-potential* (i vs. E) curve. Such curves can be quite informative about the nature of the solution and the electrodes and about the reactions that occur at the interfaces. Much of the remainder of this book deals with how one obtains and interprets such curves.

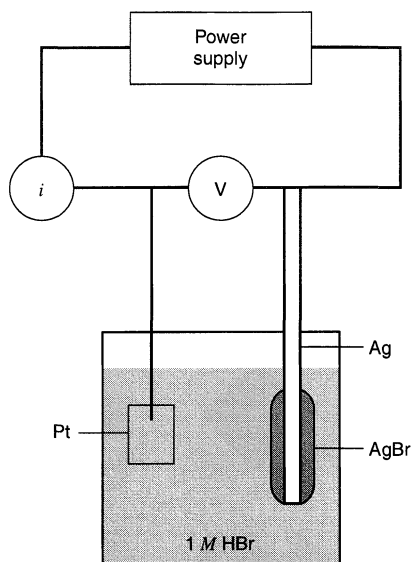
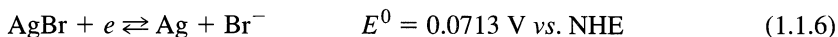


Figure 1.1.3 Schematic diagram of the electrochemical cell Pt/HBr(1 M)/AgBr/Ag attached to power supply and meters for obtaining a current-potential (i - E) curve.

Let us now consider the particular cell in Figure 1.1.3 and discuss in a qualitative way the current-potential curve that might be obtained with it. In Section 1.4 and in later chapters, we will be more quantitative. We first might consider simply the potential we would measure when a high impedance voltmeter (i.e., a voltmeter whose internal resistance is so high that no appreciable current flows through it during a measurement) is placed across the cell. This is called the *open-circuit potential* of the cell.¹

For some electrochemical cells, like those in Figure 1.1.1, it is possible to calculate the open-circuit potential from thermodynamic data, that is, from the standard potentials of the half-reactions involved at both electrodes via the Nernst equation (see Chapter 2). The key point is that a true equilibrium is established, because a pair of redox forms linked by a given half-reaction (i.e., a *redox couple*) is present at each electrode. In Figure 1.1.1*b*, for example, we have H^+ and H_2 at one electrode and Ag and AgCl at the other.²

The cell in Figure 1.1.3 is different, because an overall equilibrium cannot be established. At the Ag/AgBr electrode, a couple is present and the half-reaction is



Since AgBr and Ag are both solids, their activities are unity. The activity of Br^- can be found from the concentration in solution; hence the potential of this electrode (with respect to NHE) could be calculated from the Nernst equation. This electrode is at equilibrium. However, we cannot calculate a thermodynamic potential for the Pt/ H^+ , Br^- electrode, because we cannot identify a pair of chemical species coupled by a given half-reaction. The controlling pair clearly is not the H_2 , H^+ couple, since no H_2 has been introduced into the cell. Similarly, it is not the O_2 , H_2O couple, because by leaving O_2 out of the cell formulation we imply that the solutions in the cell have been deaerated. Thus, the Pt electrode and the cell as a whole are not at equilibrium, and an equilibrium potential

¹In the electrochemical literature, the open-circuit potential is also called the *zero-current potential* or the *rest potential*.

²When a redox couple is present at each electrode and there are no contributions from liquid junctions (yet to be discussed), the open-circuit potential is also the *equilibrium potential*. This is the situation for each cell in Figure 1.1.1.

does not exist. Even though the open-circuit potential of the cell is not available from thermodynamic data, we can place it within a potential range, as shown below.

Let us now consider what occurs when a power supply (e.g., a battery) and a microammeter are connected across the cell, and the potential of the Pt electrode is made more negative with respect to the Ag/AgBr reference electrode. The first electrode reaction that occurs at the Pt is the reduction of protons,



The direction of electron flow is from the electrode to protons in solution, as in Figure 1.1.2a, so a reduction (*cathodic*) current flows. In the convention used in this book, cathodic currents are taken as positive, and negative potentials are plotted to the right.³ As shown in Figure 1.1.4, the onset of current flow occurs when the potential of the Pt electrode is near E^0 for the H^+/H_2 reaction (0 V vs. NHE or -0.07 V vs. the Ag/AgBr electrode). While this is occurring, the reaction at the Ag/AgBr (which we consider the reference electrode) is the oxidation of Ag in the presence of Br^- in solution to form AgBr. The concentration of Br^- in the solution near the electrode surface is not changed appreciably with respect to the original concentration (1 M), therefore the potential of the Ag/AgBr electrode will be almost the same as at open circuit. The conservation of charge requires that the rate of oxidation at the Ag electrode be equal to the rate of reduction at the Pt electrode.

When the potential of the Pt electrode is made sufficiently positive with respect to the reference electrode, electrons cross from the solution phase into the electrode, and the ox-

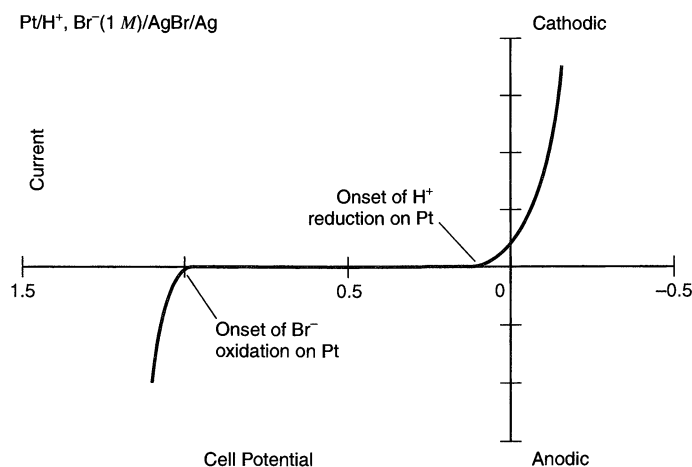


Figure 1.1.4 Schematic current-potential curve for the cell $\text{Pt}/\text{H}^+, \text{Br}^-(1 \text{ M})/\text{AgBr}/\text{Ag}$, showing the limiting proton reduction and bromide oxidation processes. The cell potential is given for the Pt electrode with respect to the Ag electrode, so it is equivalent to E_{Pt} (V vs. AgBr). Since $E_{\text{Ag}/\text{AgBr}} = 0.07$ V vs. NHE, the potential axis could be converted to E_{Pt} (V vs. NHE) by adding 0.07 V to each value of potential.

³The convention of taking i positive for a cathodic current stems from the early polarographic studies, where reduction reactions were usually studied. This convention has continued among many analytical chemists and electrochemists, even though oxidation reactions are now studied with equal frequency. Other electrochemists prefer to take an anodic current as positive. When looking over a derivation in the literature or examining a published i - E curve, it is important to decide, first, which convention is being used (i.e., “Which way is up?”).

idation of Br^- to Br_2 (and Br_3^-) occurs. An oxidation current, or *anodic* current, flows at potentials near the E^0 of the half-reaction,



which is +1.09 V vs. NHE or +1.02 V vs. Ag/AgBr. While this reaction occurs (right-to-left) at the Pt electrode, AgBr in the reference electrode is reduced to Ag and Br^- is liberated into solution. Again, because the composition of the Ag/AgBr/ Br^- interface (i.e., the activities of AgBr, Ag, and Br^-) is almost unchanged with the passage of modest currents, the potential of the reference electrode is essentially constant. Indeed, the essential characteristic of a reference electrode is that its potential remains practically constant with the passage of small currents. When a potential is applied between Pt and Ag/AgBr, nearly all of the potential change occurs at the Pt/solution interface.

The *background limits* are the potentials where the cathodic and anodic currents start to flow at a working electrode when it is immersed in a solution containing only an electrolyte added to decrease the solution resistance (a *supporting electrolyte*). Moving the potential to more extreme values than the background limits (i.e., more negative than the limit for H_2 evolution or more positive than that for Br_2 generation in the example above) simply causes the current to increase sharply with no additional electrode reactions, because the reactants are present at high concentrations. This discussion implies that one can often estimate the background limits of a given electrode–solution interface by considering the thermodynamics of the system (i.e., the standard potentials of the appropriate half-reactions). This is frequently, but not always, true, as we shall see in the next example.

From Figure 1.1.4, one can see that the open-circuit potential is not well defined in the system under discussion. One can say only that the open-circuit potential lies somewhere between the background limits. The value found experimentally will depend upon trace impurities in the solution (e.g., oxygen) and the previous history of the Pt electrode.

Let us now consider the same cell, but with the Pt replaced with a mercury electrode:



We still cannot calculate an open-circuit potential for the cell, because we cannot define a redox couple for the Hg electrode. In examining the behavior of this cell with an applied external potential, we find that the electrode reactions and the observed current-potential behavior are very different from the earlier case. When the potential of the Hg is made negative, there is essentially no current flow in the region where thermodynamics predict that H_2 evolution should occur. Indeed, the potential must be brought to considerably more negative values, as shown in Figure 1.1.5, before this reaction takes place. The thermodynamics have not changed, since the equilibrium potential of half-reaction 1.1.7 is independent of the metal electrode (see Section 2.2.4). However, when mercury serves as the locale for the hydrogen evolution reaction, the rate (characterized by a *heterogeneous rate constant*) is much lower than at Pt. Under these circumstances, the reaction does not occur at values one would predict from thermodynamics. Instead considerably higher electron energies (more negative potentials) must be applied to make the reaction occur at a measurable rate. The rate constant for a heterogeneous electron-transfer reaction is a function of applied potential, unlike one for a homogeneous reaction, which is a constant at a given temperature. The additional potential (beyond the thermodynamic requirement) needed to drive a reaction at a certain rate is called the *overpotential*. Thus, it is said that mercury shows “a high overpotential for the hydrogen evolution reaction.”

When the mercury is brought to more positive values, the anodic reaction and the potential for current flow also differ from those observed when Pt is used as the electrode.

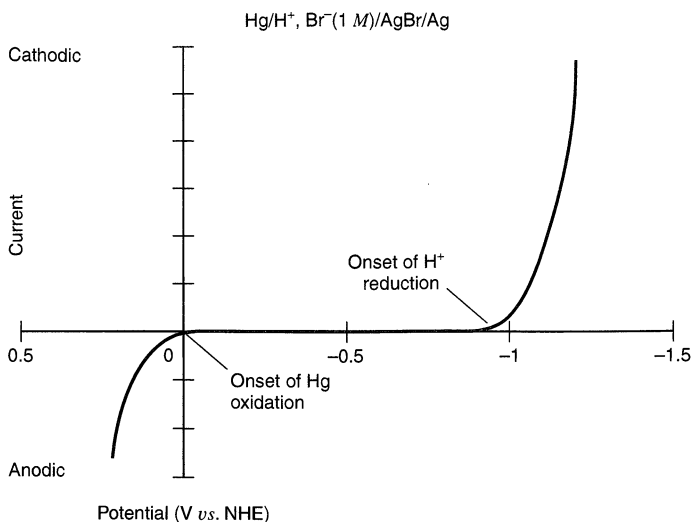
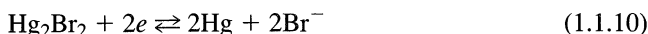


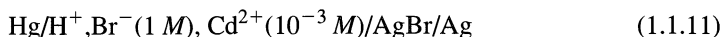
Figure 1.1.5 Schematic current-potential curve for the Hg electrode in the cell $\text{Hg}/\text{H}^+, \text{Br}^-(1 \text{ M})/\text{AgBr}/\text{Ag}$, showing the limiting processes: proton reduction with a large negative overpotential and mercury oxidation. The potential axis is defined through the process outlined in the caption to Figure 1.1.4.

With Hg, the anodic background limit occurs when Hg is oxidized to Hg_2Br_2 at a potential near 0.14 V vs. NHE (0.07 V vs. Ag/AgBr), characteristic of the half-reaction

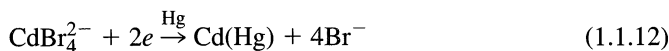


In general, the background limits depend upon both the electrode material and the solution employed in the electrochemical cell.

Finally let us consider the same cell with the addition of a small amount of Cd^{2+} to the solution,



The qualitative current-potential curve for this cell is shown in Figure 1.1.6. Note the appearance of the *reduction wave* at about -0.4 V vs. NHE arising from the reduction reaction



where $\text{Cd}(\text{Hg})$ denotes cadmium amalgam. The shape and size of such waves will be covered in Section 1.4.2. If Cd^{2+} were added to the cell in Figure 1.1.3 and a current-potential curve taken, it would resemble that in Figure 1.1.4, found in the absence of Cd^{2+} . At a Pt electrode, proton reduction occurs at less positive potentials than are required for the reduction of Cd(II), so the cathodic background limit occurs in 1 M HBr before the cadmium reduction wave can be seen.

In general, when the potential of an electrode is moved from its open-circuit value toward more negative potentials, the substance that will be reduced first (assuming all possible electrode reactions are rapid) is the oxidant in the couple with the least negative (or most positive) E^0 . For example, for a platinum electrode immersed in an aqueous solution containing 0.01 M each of Fe^{3+} , Sn^{4+} , and Ni^{2+} in 1 M HCl, the first substance reduced will be Fe^{3+} , since the E^0 of this couple is most positive (Figure 1.1.7a). When the poten-

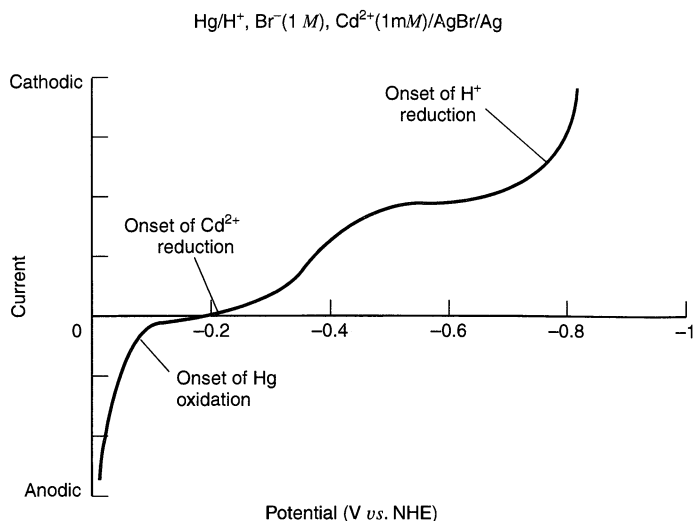


Figure 1.1.6 Schematic current-potential curve for the Hg electrode in the cell Hg/H⁺, Br⁻(1 M), Cd²⁺(10⁻³ M)/AgBr/Ag, showing reduction wave for Cd²⁺.

tial of the electrode is moved from its zero-current value toward more positive potentials, the substance that will be oxidized first is the reductant in the couple of least positive (or most negative) E^0 . Thus, for a gold electrode in an aqueous solution containing 0.01 M each of Sn²⁺ and Fe²⁺ in 1 M HI, the Sn²⁺ will be first oxidized, since the E^0 of this couple is least positive (Figure 1.1.7b). On the other hand, one must remember that these predictions are based on thermodynamic considerations (i.e., reaction energetics), and slow kinetics might prevent a reaction from occurring at a significant rate in a potential region where the E^0 would suggest the reaction was possible. Thus, for a mercury electrode immersed in a solution of 0.01 M each of Cr³⁺ and Zn²⁺, in 1 M HCl, the first reduction process predicted is the evolution of H₂ from H⁺ (Figure 1.1.7c). As discussed earlier, this reaction is very slow on mercury, so the first process actually observed is the reduction of Cr³⁺.

1.1.2 Faradaic and Nonfaradaic Processes

Two types of processes occur at electrodes. One kind comprises reactions like those just discussed, in which charges (e.g., electrons) are transferred across the metal–solution interface. Electron transfer causes oxidation or reduction to occur. Since such reactions are governed by Faraday’s law (i.e., the amount of chemical reaction caused by the flow of current is proportional to the amount of electricity passed), they are called *faradaic processes*. Electrodes at which faradaic processes occur are sometimes called *charge-transfer electrodes*. Under some conditions, a given electrode–solution interface will show a range of potentials where no charge-transfer reactions occur because such reactions are thermodynamically or kinetically unfavorable (e.g., the region in Figure 1.1.5 between 0 and -0.8 V vs. NHE). However, processes such as adsorption and desorption can occur, and the structure of the electrode–solution interface can change with changing potential or solution composition. These processes are called *nonfaradaic processes*. Although charge does not cross the interface, external currents can flow (at least transiently) when the potential, electrode area, or solution composition changes. Both faradaic and

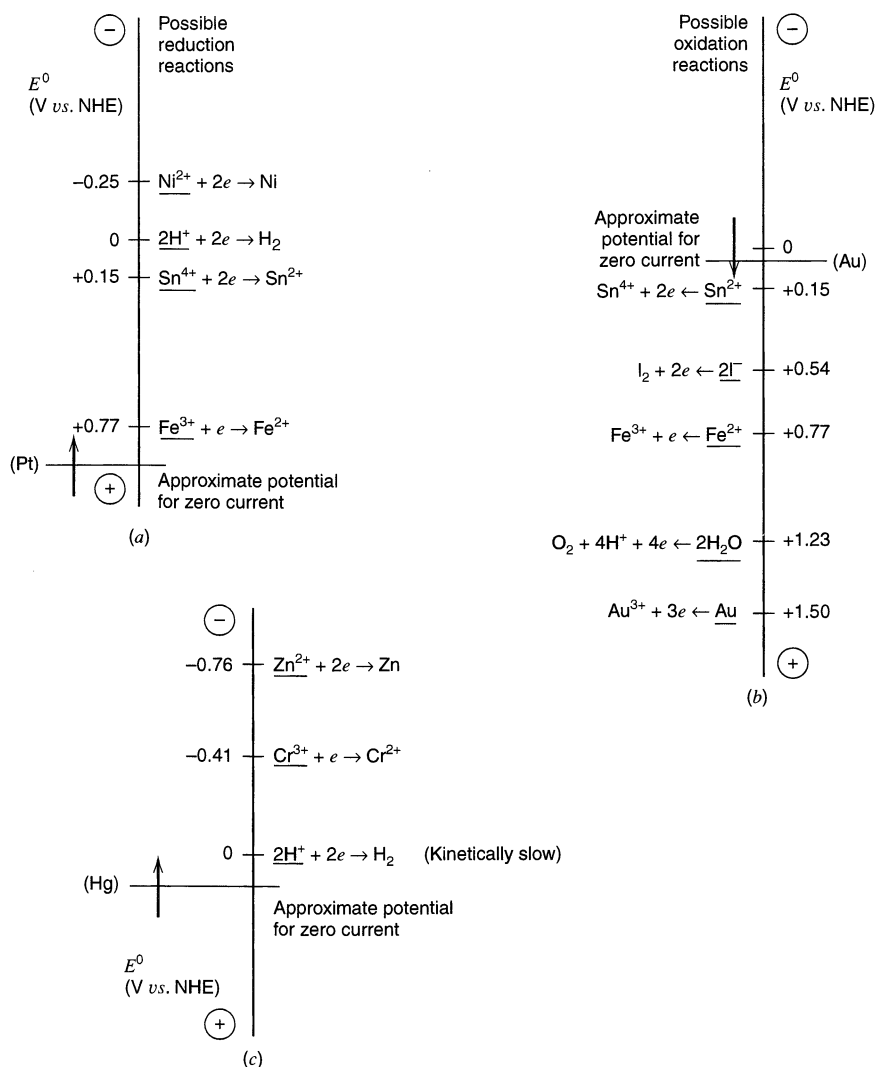


Figure 1.1.7 (a) Potentials for possible reductions at a platinum electrode, initially at ~ 1 V vs. NHE in a solution of 0.01 M each of Fe^{3+} , Sn^{4+} , and Ni^{2+} in 1 M HCl. (b) Potentials for possible oxidation reactions at a gold electrode, initially at ~ 0.1 V vs. NHE in a solution of 0.01 M each of Sn^{2+} and Fe^{2+} in 1 M HCl. (c) Potentials for possible reductions at a mercury electrode in 0.01 M Cr^{3+} and Zn^{2+} in 1 M HCl. The arrows indicate the directions of potential change discussed in the text.

nonfaradaic processes occur when electrode reactions take place. Although the faradaic processes are usually of primary interest in the investigation of an electrode reaction (except in studies of the nature of the electrode–solution interface itself), the effects of the nonfaradaic processes must be taken into account in using electrochemical data to obtain information about the charge transfer and associated reactions. Consequently, we next proceed by discussing the simpler case of a system where only nonfaradaic processes occur.

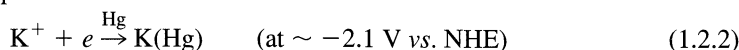
▶ 1.2 NONFARADAIC PROCESSES AND THE NATURE OF THE ELECTRODE–SOLUTION INTERFACE

1.2.1 The Ideal Polarized Electrode

An electrode at which no charge transfer can occur across the metal–solution interface, regardless of the potential imposed by an outside source of voltage, is called an *ideal polarized* (or *ideal polarizable*) *electrode* (IPE). While no real electrode can behave as an IPE over the whole potential range available in a solution, some electrode–solution systems can approach ideal polarizability over limited potential ranges. For example, a mercury electrode in contact with a deaerated potassium chloride solution approaches the behavior of an IPE over a potential range about 2 V wide. At sufficiently positive potentials, the mercury can oxidize in a charge-transfer reaction:



and at very negative potentials K^+ can be reduced:



In the potential range between these processes, charge-transfer reactions are not significant. The reduction of water:



is thermodynamically possible, but occurs at a very low rate at a mercury surface unless quite negative potentials are reached. Thus, the only faradaic current that flows in this region is due to charge-transfer reactions of trace impurities (e.g., metal ions, oxygen, and organic species), and this current is quite small in clean systems. Another electrode that behaves as an IPE is a gold surface hosting an adsorbed self-assembled monolayer of alkane thiol (see Section 14.5.2).

1.2.2 Capacitance and Charge of an Electrode

Since charge cannot cross the IPE interface when the potential across it is changed, the behavior of the electrode–solution interface is analogous to that of a capacitor. A capacitor is an electrical circuit element composed of two metal sheets separated by a dielectric material (Figure 1.2.1a). Its behavior is governed by the equation

$$\frac{q}{E} = C \quad (1.2.4)$$

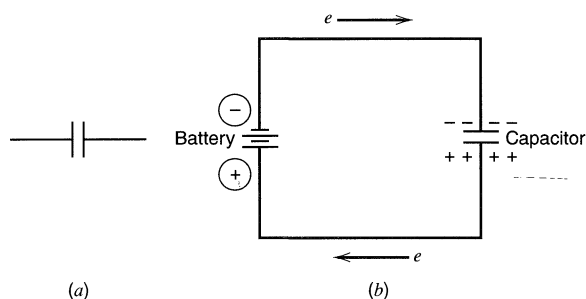


Figure 1.2.1 (a) A capacitor. (b) Charging a capacitor with a battery.

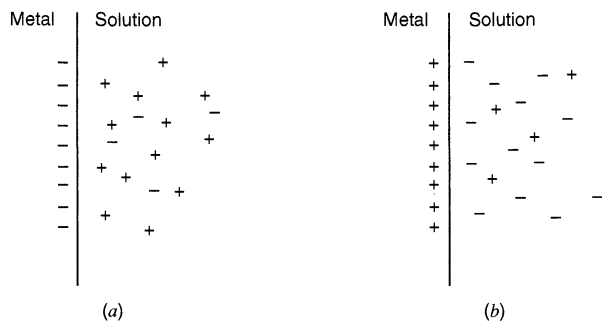


Figure 1.2.2 The metal–solution interface as a capacitor with a charge on the metal, q^M , (a) negative and (b) positive.

where q is the charge stored on the capacitor (in coulombs, C), E is the potential across the capacitor (in volts, V), and C is the capacitance (in farads, F). When a potential is applied across a capacitor, charge will accumulate on its metal plates until q satisfies equation 1.2.4. During this charging process, a current (called the *charging current*) will flow. The charge on the capacitor consists of an excess of electrons on one plate and a deficiency of electrons on the other (Figure 1.2.1b). For example, if a 2-V battery is placed across a 10- μF capacitor, current will flow until 20 μC has accumulated on the capacitor plates. The magnitude of the current depends on the resistance in the circuit (see also Section 1.2.4).

The electrode–solution interface has been shown experimentally to behave like a capacitor, and a model of the interfacial region somewhat resembling a capacitor can be given. At a given potential, there will exist a charge on the metal electrode, q^M , and a charge in the solution, q^S (Figure 1.2.2). Whether the charge on the metal is negative or positive with respect to the solution depends on the potential across the interface and the composition of the solution. At all times, however, $q^M = -q^S$. (In an actual experimental arrangement, two metal electrodes, and thus two interfaces, would have to be considered; we concentrate our attention here on one of these and ignore what happens at the other.) The charge on the metal, q^M , represents an excess or deficiency of electrons and resides in a very thin layer ($<0.1 \text{ \AA}$) on the metal surface. The charge in solution, q^S , is made up of an excess of either cations or anions in the vicinity of the electrode surface. The charges q^M and q^S are often divided by the electrode area and expressed as *charge densities*, such as, $\sigma^M = q^M/A$, usually given in $\mu\text{C}/\text{cm}^2$. The whole array of charged species and oriented dipoles existing at the metal–solution interface is called the *electrical double layer* (although its structure only very loosely resembles two charged layers, as we will see in Section 1.2.3). At a given potential, the electrode–solution interface is characterized by a double-layer capacitance, C_d , typically in the range of 10 to 40 $\mu\text{F}/\text{cm}^2$. However, unlike real capacitors, whose capacitances are independent of the voltage across them, C_d is often a function of potential.⁴

1.2.3 Brief Description of the Electrical Double Layer

The solution side of the double layer is thought to be made up of several “layers.” That closest to the electrode, the *inner layer*, contains solvent molecules and sometimes other species (ions or molecules) that are said to be *specifically adsorbed* (Figure 1.2.3). This inner layer is also called the *compact*, *Helmholtz*, or *Stern layer*. The locus of the electri-

⁴In various equations in the literature and in this book, C_d may express the capacitance per unit area and be given in $\mu\text{F}/\text{cm}^2$, or it may express the capacitance of a whole interface and be given in μF . The usage for a given situation is always apparent from the context or from a dimensional analysis.

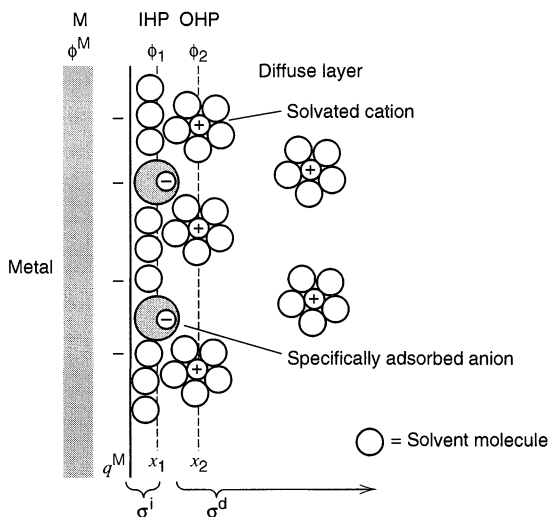


Figure 1.2.3 Proposed model of the double-layer region under conditions where anions are specifically adsorbed.

cal centers of the specifically adsorbed ions is called the *inner Helmholtz plane* (IHP), which is at a distance x_1 . The total charge density from specifically adsorbed ions in this inner layer is σ^i ($\mu\text{C}/\text{cm}^2$). Solvated ions can approach the metal only to a distance x_2 ; the locus of centers of these nearest solvated ions is called the *outer Helmholtz plane* (OHP). The interaction of the solvated ions with the charged metal involves only long-range electrostatic forces, so that their interaction is essentially independent of the chemical properties of the ions. These ions are said to be *nonspecifically adsorbed*. Because of thermal agitation in the solution, the nonspecifically adsorbed ions are distributed in a three-dimensional region called the *diffuse layer*, which extends from the OHP into the bulk of the solution. The excess charge density in the diffuse layer is σ^d , hence the total excess charge density on the solution side of the double layer, σ^S , is given by

$$\sigma^S = \sigma^i + \sigma^d = -\sigma^M \quad (1.2.5)$$

The thickness of the diffuse layer depends on the total ionic concentration in the solution; for concentrations greater than $10^{-2} M$, the thickness is less than $\sim 100 \text{ \AA}$. The potential profile across the double-layer region is shown in Figure 1.2.4.

The structure of the double layer can affect the rates of electrode processes. Consider an electroactive species that is not specifically adsorbed. This species can approach the electrode only to the OHP, and the total potential it experiences is less than the potential between the electrode and the solution by an amount $\phi_2 - \phi^S$, which is the potential drop across the diffuse layer. For example, in $0.1 M \text{ NaF}$, $\phi_2 - \phi^S$ is -0.021 V at $E = -0.55 \text{ V vs. SCE}$, but it has somewhat larger magnitudes at more negative and more positive potentials. Sometimes one can neglect double-layer effects in considering electrode reaction kinetics. At other times they must be taken into account. The importance of adsorption and double-layer structure is considered in greater detail in Chapter 13.

One usually cannot neglect the existence of the double-layer capacitance or the presence of a charging current in electrochemical experiments. Indeed, during electrode reactions involving very low concentrations of electroactive species, the charging current can be much larger than the faradaic current for the reduction or oxidation reaction. For this reason, we will briefly examine the nature of the charging current at an IPE for several types of electrochemical experiments.

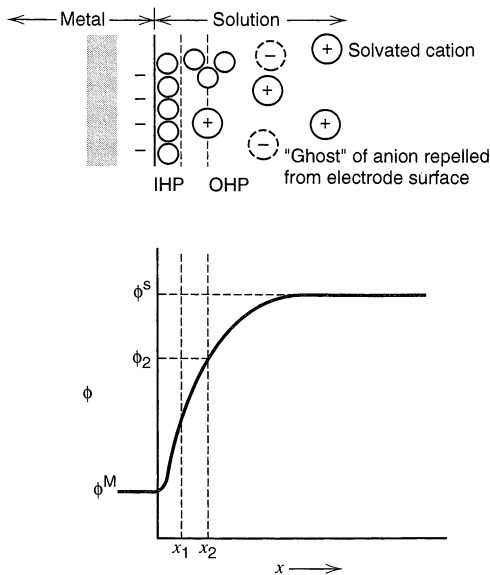


Figure 1.2.4 Potential profile across the double-layer region in the absence of specific adsorption of ions. The variable ϕ , called the *inner potential*, is discussed in detail in Section 2.2. A more quantitative representation of this profile is shown in Figure 12.3.6.

1.2.4 Double-Layer Capacitance and Charging Current in Electrochemical Measurements

Consider a cell consisting of an IPE and an ideal reversible electrode. We can approximate such a system with a mercury electrode in a potassium chloride solution that is also in contact with an SCE. This cell, represented by $\text{Hg}/\text{K}^+, \text{Cl}^-/\text{SCE}$, can be approximated by an electrical circuit with a resistor, R_s , representing the solution resistance and a capacitor, C_d , representing the double layer at the $\text{Hg}/\text{K}^+, \text{Cl}^-$ interface (Figure 1.2.5).⁵ Since

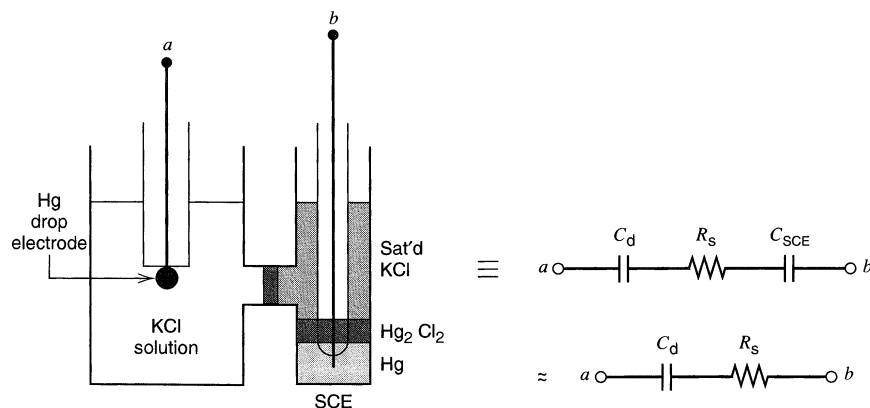


Figure 1.2.5 *Left:* Two-electrode cell with an ideal polarized mercury drop electrode and an SCE. *Right:* Representation of the cell in terms of linear circuit elements.

⁵Actually, the capacitance of the SCE, C_{SCE} , should also be included. However, the series capacitance of C_d and C_{SCE} is $C_T = C_d C_{\text{SCE}} / [C_d + C_{\text{SCE}}]$, and normally $C_{\text{SCE}} \gg C_d$, so that $C_T \approx C_d$. Thus, C_{SCE} can be neglected in the circuit.

C_d is generally a function of potential, the proposed model in terms of circuit elements is strictly accurate only for experiments where the overall cell potential does not change very much. Where it does, approximate results can be obtained using an “average” C_d over the potential range.

Information about an electrochemical system is often gained by applying an electrical perturbation to the system and observing the resulting changes in the characteristics of the system. In later sections of this chapter and later chapters of this book, we will encounter such experiments over and over. It is worthwhile now to consider the response of the IPE system, represented by the circuit elements R_s and C_d in series, to several common electrical perturbations.

(a) Voltage (or Potential) Step

The result of a potential step to the IPE is the familiar RC circuit problem (Figure 1.2.6). The behavior of the current, i , with time, t , when applying a potential step of magnitude E , is

$$i = \frac{E}{R_s} e^{-t/R_s C_d} \quad (1.2.6)$$

This equation is derived from the general equation for the charge, q , on a capacitor as a function of the voltage across it, E_C :

$$q = C_d E_C \quad (1.2.7)$$

At any time the sum of the voltages, E_R and E_C , across the resistor and the capacitor, respectively, must equal the applied voltage; hence

$$E = E_R + E_C = iR_s + \frac{q}{C_d} \quad (1.2.8)$$

Noting that $i = dq/dt$ and rearranging yields

$$\frac{dq}{dt} = \frac{-q}{R_s C_d} + \frac{E}{R_s} \quad (1.2.9)$$

If we assume that the capacitor is initially uncharged ($q = 0$ at $t = 0$), then the solution of (1.2.9) is

$$q = EC_d [1 - e^{-t/R_s C_d}] \quad (1.2.10)$$

By differentiating (1.2.10), one obtains (1.2.6). Hence, for a potential step input, there is an exponentially decaying current having a time constant, $\tau = R_s C_d$ (Figure 1.2.7). The current for charging the double-layer capacitance drops to 37% of its initial value at $t = \tau$, and to 5% of its initial value at $t = 3\tau$. For example, if $R_s = 1 \Omega$ and $C_d = 20 \mu\text{F}$, then $\tau = 20 \mu\text{s}$ and double-layer charging is 95% complete in $60 \mu\text{s}$.

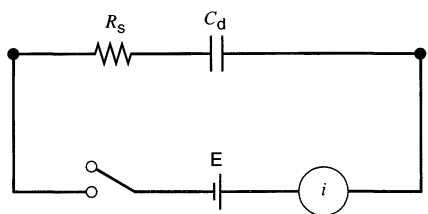


Figure 1.2.6 Potential step experiment for an RC circuit.

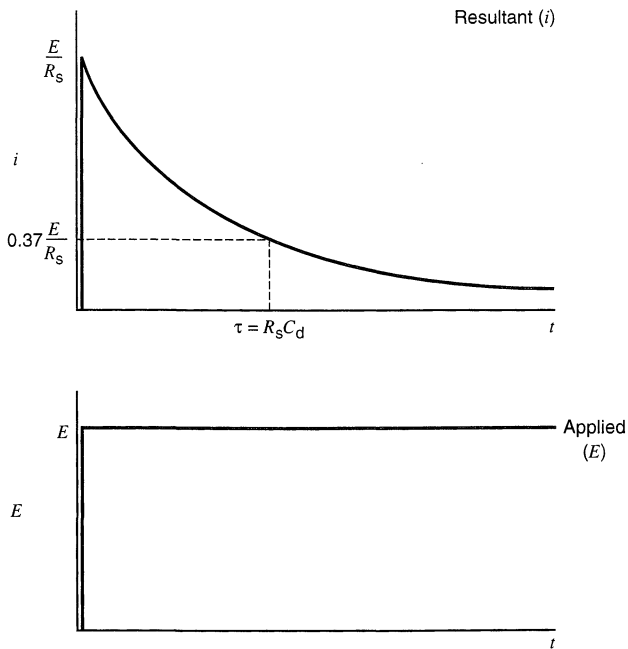


Figure 1.2.7 Current transient (i vs. t) resulting from a potential step experiment.

(b) Current Step

When the $R_s C_d$ circuit is charged by a constant current (Figure 1.2.8), then equation 1.2.8 again applies. Since $q = \int i dt$, and i is a constant,

$$E = iR_s + \frac{i}{C_d} \int_0^t dt \tag{1.2.11}$$

or

$$E = i(R_s + t/C_d) \tag{1.2.12}$$

Hence, the potential increases linearly with time for a current step (Figure 1.2.9).

(c) Voltage Ramp (or Potential Sweep)

A *voltage ramp* or *linear potential sweep* is a potential that increases linearly with time starting at some initial value (here assumed to be zero) at a sweep rate v (in $V s^{-1}$) (see Figure 1.2.10a).

$$E = vt \tag{1.2.13}$$

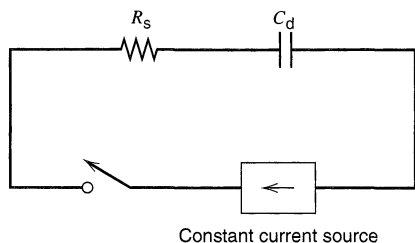


Figure 1.2.8 Current step experiment for an RC circuit.

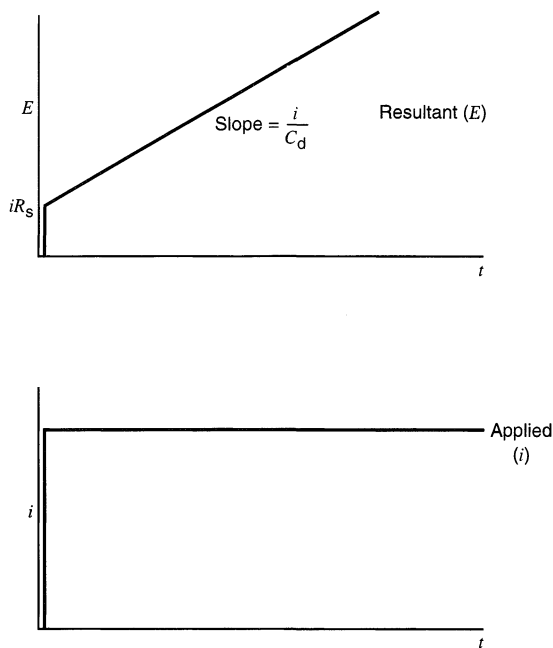


Figure 1.2.9 E - t behavior resulting from a current step experiment.

If such a ramp is applied to the $R_s C_d$ circuit, equation 1.2.8 still applies; hence

$$vt = R_s(dq/dt) + q/C_d \quad (1.2.14)$$

If $q = 0$ at $t = 0$,

$$i = vC_d [1 - \exp(-t/R_s C_d)] \quad (1.2.15)$$

The current rises from zero as the scan starts and attains a steady-state value, vC_d (Figure 1.2.10*b*). This steady-state current can then be used to estimate C_d . If the time constant,

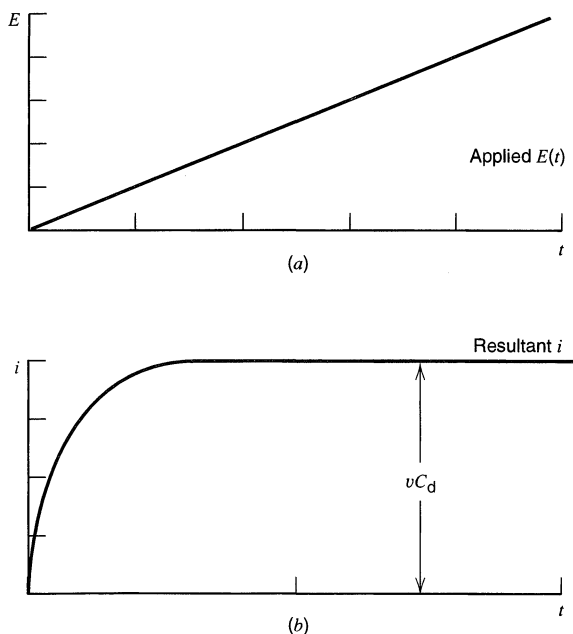


Figure 1.2.10 Current-time behavior resulting from a linear potential sweep applied to an RC circuit.

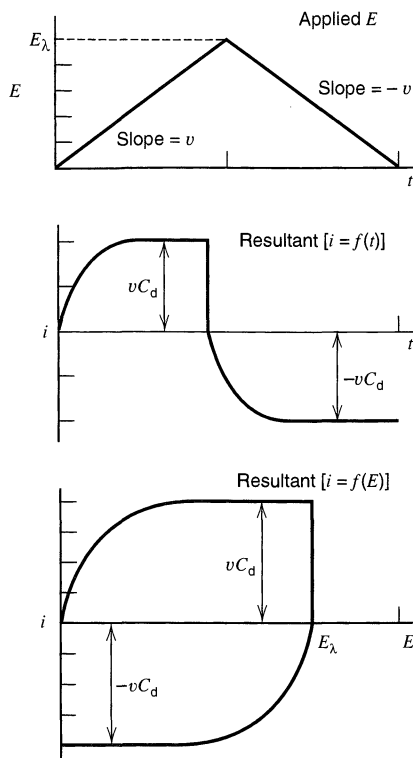


Figure 1.2.11 Current-time and current-potential plots resulting from a cyclic linear potential sweep (or triangular wave) applied to an RC circuit.

$R_s C_d$ is small compared to v , the instantaneous current can be used to measure C_d as a function of E .

If one instead applies a *triangular wave* (i.e., a ramp whose sweep rate switches from v to $-v$ at some potential, E_λ), then the steady-state current changes from vC_d during the forward (increasing E) scan to $-vC_d$ during the reverse (decreasing E) scan. The result for a system with constant C_d is shown in Figure 1.2.11.

▶ 1.3 FARADAIC PROCESSES AND FACTORS AFFECTING RATES OF ELECTRODE REACTIONS

1.3.1 Electrochemical Cells—Types and Definitions

Electrochemical cells in which faradaic currents are flowing are classified as either *galvanic* or *electrolytic* cells. A *galvanic cell* is one in which reactions occur spontaneously at the electrodes when they are connected externally by a conductor (Figure 1.3.1a). These cells are often employed in converting chemical energy into electrical energy. Galvanic cells of commercial importance include *primary (nonrechargeable) cells* (e.g., the Leclanché Zn–MnO₂ cell), *secondary (rechargeable) cells* (e.g., a charged Pb–PbO₂ storage battery), and *fuel cells* (e.g., an H₂–O₂ cell). An *electrolytic cell* is one in which reactions are effected by the imposition of an external voltage greater than the open-circuit potential of the cell (Figure 1.3.1b). These cells are frequently employed to carry out desired chemical reactions by expending electrical energy. Commercial processes involving electrolytic cells include electrolytic syntheses (e.g., the production of chlorine and aluminum), electrorefining (e.g., copper), and electroplating (e.g., silver and gold). The lead–acid storage cell, when it is being “recharged,” is an electrolytic cell.

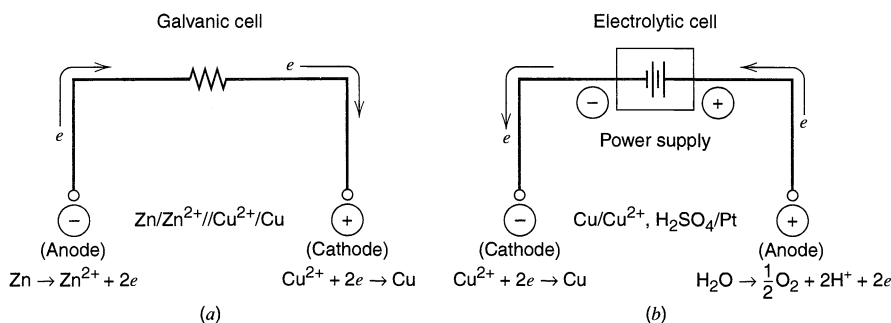


Figure 1.3.1 (a) Galvanic and (b) electrolytic cells.

Although it is often convenient to make a distinction between galvanic and electrolytic cells, we will most often be concerned with reactions occurring at only one of the electrodes. Treatment is simplified by concentrating our attention on only one-half of the cell at a time. If necessary, the behavior of a whole cell can be ascertained later by combining the characteristics of the individual half-cells. The behavior of a single electrode and the fundamental nature of its reactions are independent of whether the electrode is part of a galvanic or electrolytic cell. For example, consider the cells in Figure 1.3.1. The nature of the reaction $\text{Cu}^{2+} + 2e \rightarrow \text{Cu}$ is the same in both cells. If one desires to plate copper, one could accomplish this either in a galvanic cell (using a counter half-cell with a more negative potential than that of Cu/Cu^{2+}) or in an electrolytic cell (using any counter half-cell and supplying electrons to the copper electrode with an external power supply). Thus, *electrolysis* is a term that we define broadly to include chemical changes accompanying faradaic reactions at electrodes in contact with electrolytes. In discussing cells, one calls the electrode at which reductions occur the *cathode*, and the electrode at which oxidations occur the *anode*. A current in which electrons cross the interface from the electrode to a species in solution is a *cathodic current*, while electron flow from a solution species into the electrode is an *anodic current*. In an electrolytic cell, the cathode is negative with respect to the anode; but in a galvanic cell, the cathode is positive with respect to the anode.⁶

1.3.2 The Electrochemical Experiment and Variables in Electrochemical Cells

An investigation of electrochemical behavior consists of holding certain variables of an electrochemical cell constant and observing how other variables (usually current, potential, or concentration) vary with changes in the controlled variables. The parameters of importance in electrochemical cells are shown in Figure 1.3.2. For example, in *potentiometric* experiments, $i = 0$ and E is determined as a function of C . Since no current flows in this experiment, no net faradaic reaction occurs, and the potential is frequently (but not always) governed by the thermodynamic properties of the system. Many of the variables (electrode area, mass transfer, electrode geometry) do not affect the potential directly.

⁶Because a cathodic current and a cathodic reaction can occur at an electrode that is either positive or negative with respect to another electrode (e.g., an auxiliary or reference electrode, see Section 1.3.4), it is poor usage to associate the term “cathodic” or “anodic” with potentials of a particular sign. For example, one should not say, “The potential shifted in a cathodic direction,” when what is meant is, “The potential shifted in a *negative* direction.” The terms anodic and cathodic refer to electron flow or current direction, not to potential.

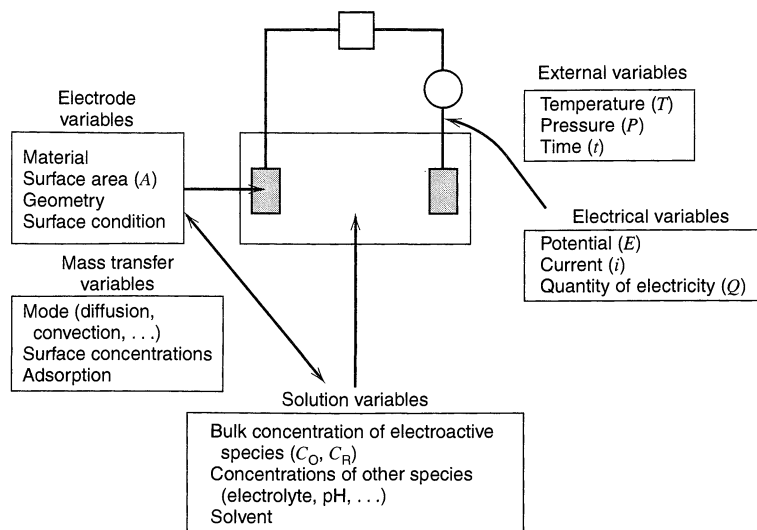
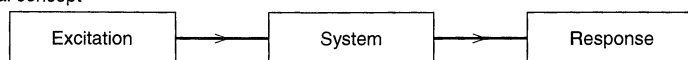


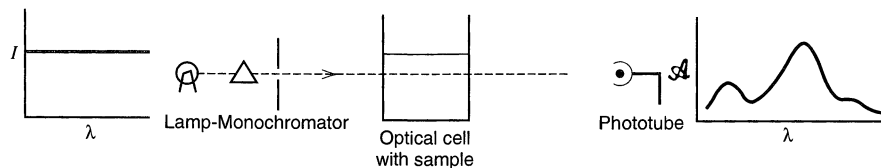
Figure 1.3.2 Variables affecting the rate of an electrode reaction.

Another way of visualizing an electrochemical experiment is in terms of the way in which the system responds to a perturbation. The electrochemical cell is considered as a “black box” to which a certain excitation function (e.g., a potential step) is applied, and a certain response function (e.g., the resulting variation of current with time) is measured, with all other system variables held constant (Figure 1.3.3). The aim of the experiment is to obtain information (thermodynamic, kinetic, analytical, etc.) from observation of the

(a) General concept



(b) Spectrophotometric experiment



(c) Electrochemical experiment

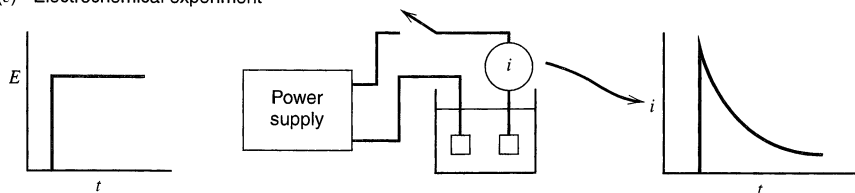


Figure 1.3.3 (a) General principle of studying a system by application of an excitation (or perturbation) and observation of response. (b) In a spectrophotometric experiment, the excitation is light of different wavelengths (λ), and the response is the absorbance (\mathcal{A}) curve. (c) In an electrochemical (potential step) experiment, the excitation is the application of a potential step, and the response is the observed $i-t$ curve.

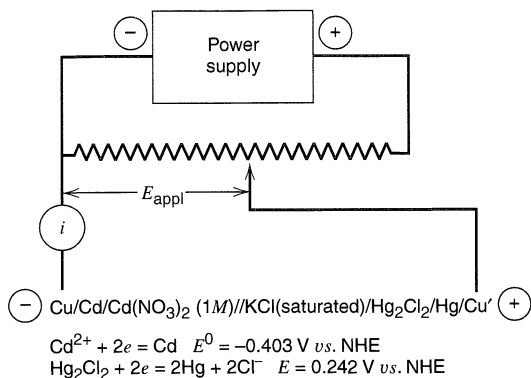


Figure 1.3.4 Schematic cell connected to an external power supply. The double slash indicates that the KCl solution contacts the Cd(NO₃)₂ solution in such a way that there is no appreciable potential difference across the junction between the two liquids. A “salt bridge” (Section 2.3.5) is often used to achieve that condition.

excitation and response functions and a knowledge of appropriate models for the system. This same basic idea is used in many other types of investigation, such as circuit testing or spectrophotometric analysis. In spectrophotometry, the excitation function is light of different wavelengths; the response function is the fraction of light transmitted by the system at these wavelengths; the system model is Beer’s law or a molecular model; and the information content includes the concentrations of absorbing species, their absorptivities, or their transition energies.

Before developing some simple models for electrochemical systems, let us consider more closely the nature of the current and potential in an electrochemical cell. Consider the cell in which a cadmium electrode immersed in 1 M Cd(NO₃)₂ is coupled to an SCE (Figure 1.3.4). The open-circuit potential of the cell is 0.64 V, with the copper wire attached to the cadmium electrode being negative with respect to that attached to the mercury electrode.⁷ When the voltage applied by the external power supply, E_{appl} , is 0.64 V, $i = 0$. When E_{appl} is made larger (i.e., $E_{\text{appl}} > 0.64 \text{ V}$, such that the cadmium electrode is made even more negative with respect to the SCE), the cell behaves as an electrolytic cell and a current flows. At the cadmium electrode, the reaction $\text{Cd}^{2+} + 2e \rightarrow \text{Cd}$ occurs, while at the SCE, mercury is oxidized to Hg₂Cl₂. A question of interest might be: “If $E_{\text{appl}} = 0.74 \text{ V}$ (i.e., if the potential of the cadmium electrode is made -0.74 V vs. the SCE), what current will flow?” Since i represents the number of electrons reacting with Cd²⁺ per second, or the number of coulombs of electric charge flowing per second, the question “What is i ?” is essentially the same as “What is the rate of the reaction, $\text{Cd}^{2+} + 2e \rightarrow \text{Cd}$?” The following relations demonstrate the direct proportionality between faradaic current and electrolysis rate:

$$i \text{ (amperes)} = \frac{dQ}{dt} \text{ (coulombs/s)} \quad (1.3.1)$$

$$\frac{Q}{nF} \text{ (coulombs)} = N \text{ (mol electrolyzed)} \quad (1.3.2)$$

where n is the stoichiometric number of electrons consumed in the electrode reaction (e.g., 2 for reduction of Cd²⁺).

$$\text{Rate (mol/s)} = \frac{dN}{dt} = \frac{i}{nF} \quad (1.3.3)$$

⁷This value is calculated from the information in Figure 1.3.4. The experimental value would also include the effects of activity coefficients and the liquid junction potential, which are neglected here. See Chapter 2.

Interpreting the rate of an electrode reaction is often more complex than doing the same for a reaction occurring in solution or in the gas phase. The latter is called a *homogeneous reaction*, because it occurs everywhere within the medium at a uniform rate. In contrast, an electrode process is a *heterogeneous reaction* occurring only at the electrode–electrolyte interface. Its rate depends on mass transfer to the electrode and various surface effects, in addition to the usual kinetic variables. Since electrode reactions are heterogeneous, their reaction rates are usually described in units of mol/s per unit area; that is,

$$\text{Rate} \left(\text{mol s}^{-1} \text{cm}^{-2} \right) = \frac{i}{nFA} = \frac{j}{nF} \quad (1.3.4)$$

where j is the *current density* (A/cm^2).

Information about an electrode reaction is often gained by determining current as a function of potential (by obtaining i - E curves). Certain terms are sometimes associated with features of the curves.⁸ If a cell has a defined equilibrium potential (Section 1.1.1), that potential is an important reference point of the system. The departure of the electrode potential (or cell potential) from the equilibrium value upon passage of faradaic current is termed *polarization*. The extent of polarization is measured by the *overpotential*, η ,

$$\eta = E - E_{\text{eq}} \quad (1.3.5)$$

Current-potential curves, particularly those obtained under steady-state conditions, are sometimes called *polarization curves*. We have seen that an ideal polarized electrode (Section 1.2.1) shows a very large change in potential upon the passage of an infinitesimal current; thus ideal polarizability is characterized by a horizontal region of an i - E curve (Figure 1.3.5a). A substance that tends to cause the potential of an electrode to be nearer to its equilibrium value by virtue of being oxidized or reduced is called a *depolarizer*.⁹ An

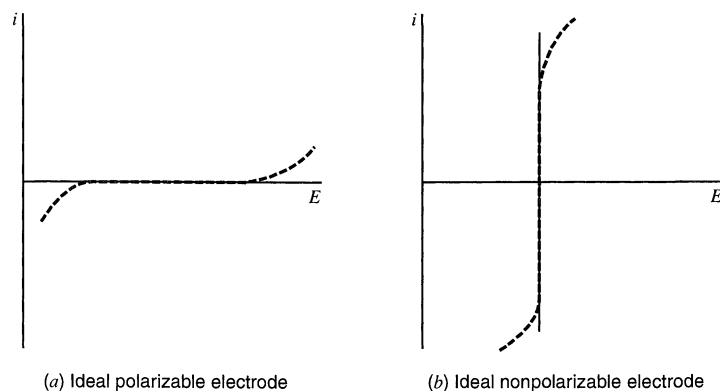


Figure 1.3.5 Current-potential curves for ideal (a) polarizable and (b) nonpolarizable electrodes. Dashed lines show behavior of actual electrodes that approach the ideal behavior over limited ranges of current or potential.

⁸These terms are carryovers from older electrochemical studies and models and, indeed, do not always represent the best possible terminology. However, their use is so ingrained in electrochemical jargon that it seems wisest to keep them and to define them as precisely as possible.

⁹The term *depolarizer* is also frequently used to denote a substance that is preferentially oxidized or reduced, to prevent an undesirable electrode reaction. Sometimes it is simply another name for an electroactive substance.

ideal nonpolarizable electrode (or *ideal depolarized electrode*) is thus an electrode whose potential does not change upon passage of current, that is, an electrode of fixed potential. Nonpolarizability is characterized by a vertical region on an i - E curve (Figure 1.3.5b). An SCE constructed with a large-area mercury pool would approach ideal nonpolarizability at small currents.

1.3.3 Factors Affecting Electrode Reaction Rate and Current

Consider an overall electrode reaction, $O + ne \rightleftharpoons R$, composed of a series of steps that cause the conversion of the dissolved oxidized species, O, to a reduced form, R, also in solution (Figure 1.3.6). In general, the current (or electrode reaction rate) is governed by the rates of processes such as (1, 2):

1. Mass transfer (e.g., of O from the bulk solution to the electrode surface).
2. Electron transfer at the electrode surface.
3. Chemical reactions preceding or following the electron transfer. These might be homogeneous processes (e.g., protonation or dimerization) or heterogeneous ones (e.g., catalytic decomposition) on the electrode surface.
4. Other surface reactions, such as adsorption, desorption, or crystallization (electrodeposition).

The rate constants for some of these processes (e.g., electron transfer at the electrode surface or adsorption) depend upon the potential.

The simplest reactions involve only mass transfer of a reactant to the electrode, heterogeneous electron transfer involving nonadsorbed species, and mass transfer of the product to the bulk solution. A representative reaction of this sort is the reduction of the aromatic hydrocarbon 9,10-diphenylanthracene (DPA) to the radical anion (DPA \cdot^-) in an aprotic solvent (e.g., *N,N*-dimethylformamide). More complex reaction sequences involving a series of electron transfers and protonations, branching mechanisms, parallel paths, or modifications of the electrode surface are quite common. When a steady-state current is obtained, the rates of all reaction steps in a series are the same. The magnitude of this current is often limited by the inherent sluggishness of one or more reactions called *rate-determining steps*. The more facile reactions are held back from their maximum rates by

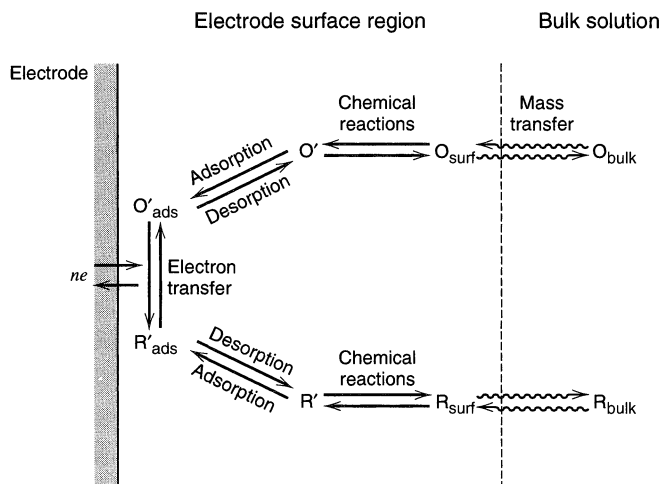


Figure 1.3.6 Pathway of a general electrode reaction.

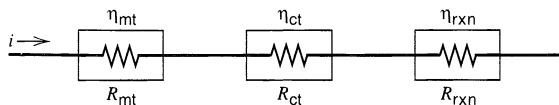


Figure 1.3.7 Processes in an electrode reaction represented as resistances.

the slowness with which a rate-determining step disposes of their products or creates their reactants.

Each value of current density, j , is driven by a certain overpotential, η . This overpotential can be considered as a sum of terms associated with the different reaction steps: η_{mt} (the *mass-transfer overpotential*), η_{ct} (the *charge-transfer overpotential*), η_{rxn} (the overpotential associated with a preceding reaction), etc. The electrode reaction can then be represented by a resistance, R , composed of a series of resistances (or more exactly, impedances) representing the various steps: R_{mt} , R_{ct} , etc. (Figure 1.3.7). A fast reaction step is characterized by a small resistance (or impedance), while a slow step is represented by a high resistance. However, except for very small current or potential perturbations, these impedances are functions of E (or i), unlike the analogous actual electrical elements.

1.3.4 Electrochemical Cells and Cell Resistance

Consider a cell composed of two ideal nonpolarizable electrodes, for example, two SCEs immersed in a potassium chloride solution: SCE/KCl/SCE. The i - E characteristic of this cell would look like that of a pure resistance (Figure 1.3.8), because the only limitation on current flow is imposed by the resistance of the solution. In fact, these conditions (i.e., paired, nonpolarizable electrodes) are exactly those sought in measurements of solution conductivity. For any real electrodes (e.g., actual SCEs), mass-transfer and charge-transfer overpotentials would also become important at high enough current densities.

When the potential of an electrode is measured against a nonpolarizable reference electrode during the passage of current, a voltage drop equal to iR_s is always included in the measured value. Here, R_s is the solution resistance between the electrodes, which, unlike the impedances describing the mass transfer and activation steps in the electrode reaction, actually behaves as a true resistance over a wide range of conditions. For example, consider once again the cell in Figure 1.3.4. At open circuit ($i = 0$), the potential of the cadmium electrode is the equilibrium value, $E_{eq,Cd}$ (about -0.64 V vs. SCE). We saw ear-

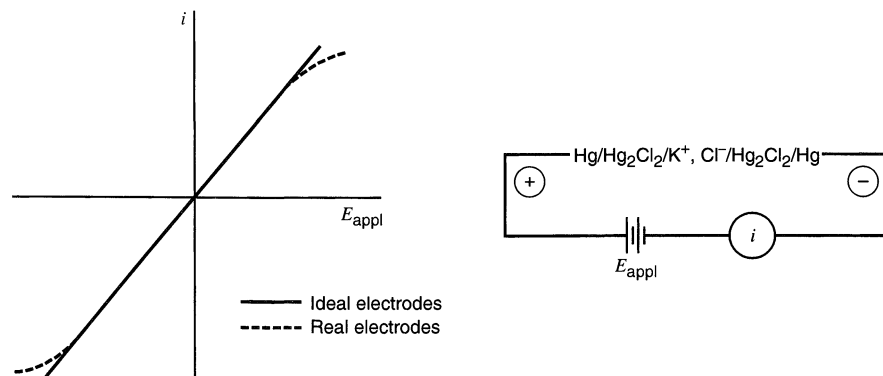


Figure 1.3.8 Current-potential curve for a cell composed of two electrodes approaching ideal nonpolarizability.

lier that with $E_{\text{appl}} = -0.64 \text{ V}$ (Cd vs. SCE), no current would flow through the ammeter. If E_{appl} is increased in magnitude to -0.80 V (Cd vs. SCE), current flows. The extra applied voltage is distributed in two parts. First, to deliver the current, the potential of the Cd electrode, E_{Cd} , must shift to a new value, perhaps -0.70 V vs. SCE. The remainder of the applied voltage (-0.10 V in this example) represents the ohmic drop caused by current flow in solution. We assume that the SCE is essentially nonpolarizable at the extant current level and does not change its potential. In general,

$$E_{\text{appl}} (\text{vs. SCE}) = E_{\text{Cd}} (\text{vs. SCE}) - iR_s = E_{\text{eq,Cd}} (\text{vs. SCE}) + \eta - iR_s \quad (1.3.6)$$

The last two terms of this equation are related to current flow. When there is a cathodic current at the cadmium electrode, both are negative. Conversely, both are positive for an anodic current. In the cathodic case, E_{appl} must manifest the (negative) overpotential ($E_{\text{Cd}} - E_{\text{eq,Cd}}$) needed to support the electrochemical reaction rate corresponding to the current. (In the example above, $\eta = -0.06 \text{ V}$.) In addition E_{appl} must encompass the ohmic drop, iR_s , required to drive the ionic current in solution (which corresponds to the passage of negative charge from the cadmium electrode to the SCE).¹⁰ The ohmic potential drop in the solution should not be regarded as a form of overpotential, because it is characteristic of the bulk solution and not of the electrode reaction. Its contribution to the measured electrode potential can be minimized by proper cell design and instrumentation.

Most of the time, one is interested in reactions that occur at only one electrode. An experimental cell could be composed of the electrode system of interest, called the *working (or indicator) electrode*, coupled with an electrode of known potential that approaches ideal nonpolarizability (such as an SCE with a large-area mercury pool), called the *reference electrode*. If the passage of current does not affect the potential of the reference electrode, the E of the working electrode is given by equation 1.3.6. Under conditions when iR_s is small (say less than 1–2 mV), this *two-electrode cell* (Figure 1.3.9) can be used to determine the i - E curve, with E either taken as equal to E_{appl} or corrected for the small iR_s drop. For example, in classic polarographic experiments in aqueous solutions, two-electrode cells were often used. In these systems, it is often true that $i < 10 \mu\text{A}$ and $R_s < 100 \Omega$, so that $iR_s < (10^{-5} \text{ A})(100 \Omega)$ or $iR_s < 1 \text{ mV}$, which is negligible for most purposes. With more highly resistive solutions, such as those based on many nonaqueous solvents, a very small electrode (an *ultramicroelectrode*, Section 5.3) must be used if a two-electrode cell is to be employed without serious complica-

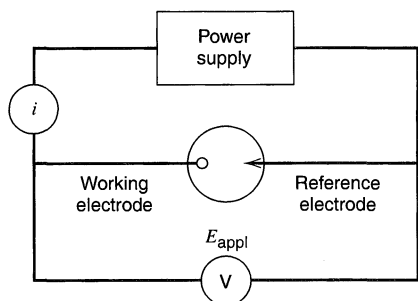


Figure 1.3.9 Two-electrode cell.

¹⁰The sign preceding the ohmic drop in (1.3.6) is negative as a consequence of the sign convention adopted here for currents (cathodic currents taken as positive).

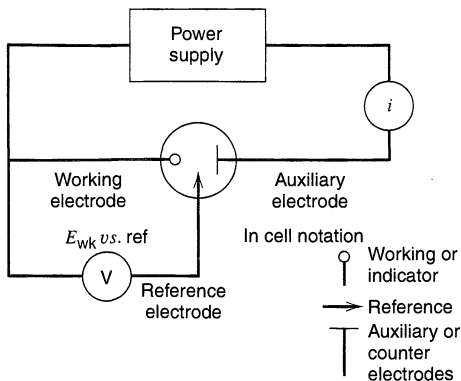


Figure 1.3.10 Three-electrode cell and notation for the different electrodes.

tions from the ohmic drop in solution. With such electrodes, currents of the order of 1 nA are typical; hence R_s values even in the $M\Omega$ range can be acceptable.

In experiments where iR_s may be high (e.g., in large-scale electrolytic or galvanic cells or in experiments involving nonaqueous solutions with low conductivities), a *three-electrode cell* (Figure 1.3.10) is preferable. In this arrangement, the current is passed between the working electrode and a *counter* (or *auxiliary*) *electrode*. The auxiliary electrode can be any convenient one, because its electrochemical properties do not

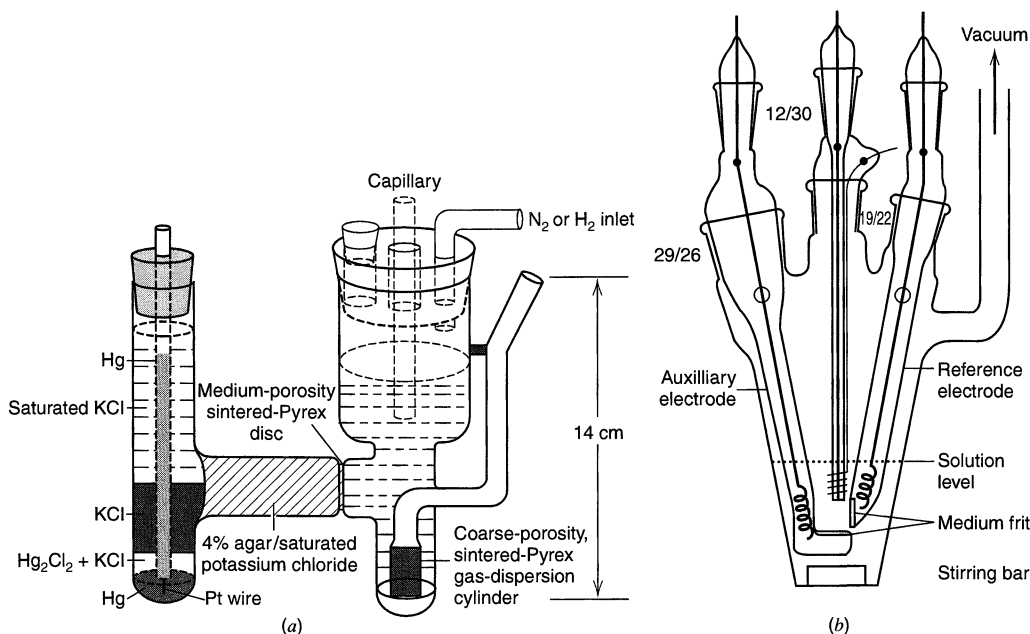


Figure 1.3.11 Typical two- and three-electrode cells used in electrochemical experiments. (a) Two-electrode cell for polarography. The working electrode is a dropping mercury electrode (capillary) and the N_2 inlet tube is for deaeration of the solution. [From L. Meites, *Polarographic Techniques*, 2nd ed., Wiley-Interscience, New York, 1965, with permission.] (b) Three-electrode cell designed for studies with nonaqueous solutions at a platinum-disk working electrode, with provision for attachment to a vacuum line. [Reprinted with permission from A. Demortier and A. J. Bard, *J. Am. Chem. Soc.*, **95**, 3495 (1973). Copyright 1973, American Chemical Society.] Three-electrode cells for bulk electrolysis are shown in Figure 11.2.2.

affect the behavior of the electrode of interest. It is usually chosen to be an electrode that does not produce substances by electrolysis that will reach the working electrode surface and cause interfering reactions there. Frequently, it is placed in a compartment separated from the working electrode by a sintered-glass disk or other separator. The potential of the working electrode is monitored relative to a separate reference electrode, positioned with its tip nearby. The device used to measure the potential difference between the working electrode and the reference electrode has a high input impedance, so that a negligible current is drawn through the reference electrode. Consequently, its potential will remain constant and equal to its open-circuit value. This three-electrode arrangement is used in most electrochemical experiments; several practical cells are shown in Figure 1.3.11.

Even in this arrangement, not all of the iR_s term is removed from the reading made by the potential-measuring device. Consider the potential profile in solution between the working and auxiliary electrodes, shown schematically in Figure 1.3.12. (The potential profile in an actual cell depends on the electrode shapes, geometry, solution conductance, etc.) The solution between the electrodes can be regarded as a potentiometer (but not necessarily a linear one). If the reference electrode is placed anywhere but exactly at the electrode surface, some fraction of iR_s , (called iR_u , where R_u is the *uncompensated resistance*) will be included in the measured potential. Even when the tip of the reference electrode is designed for very close placement to the working electrode by use of a fine tip called a *Luggin–Haber capillary*, some uncompensated resistance usually remains. This uncompensated potential drop can sometimes be removed later, for example, from steady-state measurements by measurement of R_u and point-by-point correction of each measured potential. Modern electrochemical instrumentation frequently includes circuitry for electronic compensation of the iR_u term (see Chapter 15).

If the reference capillary has a tip diameter d , it can be placed as close as $2d$ from the working electrode surface without causing appreciable shielding error. *Shielding* denotes a blockage of part of the solution current path at the working electrode surface, which causes nonuniform current densities to arise at the electrode surface. For a planar electrode with uniform current density across its surface,

$$R_u = x/\kappa A \quad (1.3.7)$$

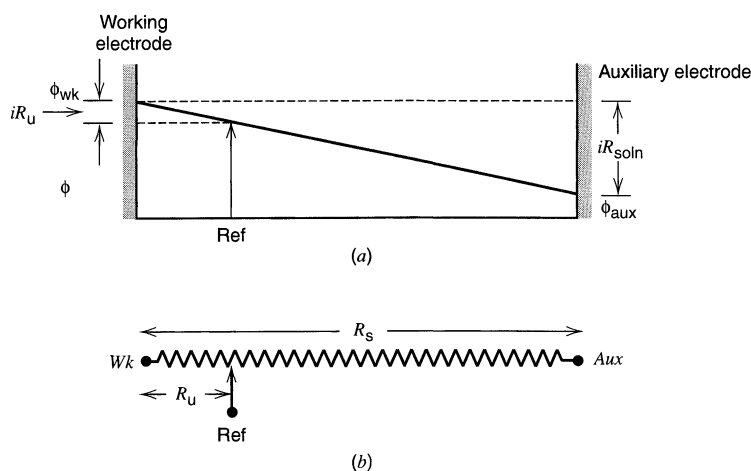


Figure 1.3.12 (a) Potential drop between working and auxiliary electrodes in solution and iR_u measured at the reference electrode. (b) Representation of the cell as a potentiometer.

where x is the distance of the capillary tip from the electrode, A is the electrode area, and κ is the solution conductivity. The effect of iR_u can be particularly serious for spherical microelectrodes, such as the hanging mercury drop electrode or the dropping mercury electrode (DME). For a spherical electrode of radius r_0 ,

$$R_u = \frac{1}{4\pi\kappa r_0} \left(\frac{x}{x + r_0} \right) \quad (1.3.8)$$

In this case, most of the resistive drop occurs close to the electrode. For a reference electrode tip placed just one electrode radius away ($x = r_0$), R_u is already half of the value for the tip placed infinitely far away. Any resistances in the working electrode itself (e.g., in thin wires used to make ultramicroelectrodes, in semiconductor electrodes, or in resistive films on the electrode surface) will also appear in R_u .

▶ 1.4 INTRODUCTION TO MASS-TRANSFER-CONTROLLED REACTIONS

1.4.1 Modes of Mass Transfer

Let us now be more quantitative about the size and shape of current-potential curves. As shown in equation 1.3.4, if we are to understand i , we must be able to describe the rate of the reaction, v , at the electrode surface. The simplest electrode reactions are those in which the rates of all associated chemical reactions are very rapid compared to those of the mass-transfer processes. Under these conditions, the chemical reactions can usually be treated in a particularly simple way. If, for example, an electrode process involves only fast heterogeneous charge-transfer kinetics and mobile, reversible homogeneous reactions, we will find below that (a) the homogeneous reactions can be regarded as being at equilibrium and (b) the *surface concentrations* of species involved in the faradaic process are related to the electrode potential by an equation of the Nernst form. The net rate of the electrode reaction, v_{rxn} , is then governed totally by the rate at which the electroactive species is brought to the surface by mass transfer, v_{mt} . Hence, from equation 1.3.4,

$$v_{\text{rxn}} = v_{\text{mt}} = i/nFA \quad (1.4.1)$$

Such electrode reactions are often called *reversible* or *nernstian*, because the principal species obey thermodynamic relationships at the electrode surface. Since mass transfer plays a big role in electrochemical dynamics, we review here its three modes and begin a consideration of mathematical methods for treating them.

Mass transfer, that is, the movement of material from one location in solution to another, arises either from differences in electrical or chemical potential at the two locations or from movement of a volume element of solution. The modes of mass transfer are:

1. *Migration*. Movement of a charged body under the influence of an electric field (a gradient of electrical potential).
2. *Diffusion*. Movement of a species under the influence of a gradient of chemical potential (i.e., a concentration gradient).
3. *Convection*. Stirring or hydrodynamic transport. Generally fluid flow occurs because of *natural convection* (convection caused by density gradients) and *forced convection*, and may be characterized by stagnant regions, laminar flow, and turbulent flow.

Mass transfer to an electrode is governed by the *Nernst–Planck equation*, written for one-dimensional mass transfer along the x -axis as

$$J_i(x) = -D_i \frac{\partial C_i(x)}{\partial x} - \frac{z_i F}{RT} D_i C_i \frac{\partial \phi(x)}{\partial x} + C_i v(x) \quad (1.4.2)$$

where $J_i(x)$ is the flux of species i ($\text{mol s}^{-1} \text{cm}^{-2}$) at distance x from the surface, D_i is the diffusion coefficient (cm^2/s), $\partial C_i(x)/\partial x$ is the concentration gradient at distance x , $\partial \phi(x)/\partial x$ is the potential gradient, z_i and C_i are the charge (dimensionless) and concentration (mol cm^{-3}) of species i , respectively, and $v(x)$ is the velocity (cm/s) with which a volume element in solution moves along the axis. This equation is derived and discussed in more detail in Chapter 4. The three terms on the right-hand side represent the contributions of diffusion, migration, and convection, respectively, to the flux.

While we will be concerned with particular solutions of this equation in later chapters, a rigorous solution is generally not very easy when all three forms of mass transfer are in effect; hence electrochemical systems are frequently designed so that one or more of the contributions to mass transfer are negligible. For example, the migrational component can be reduced to negligible levels by addition of an inert electrolyte (a *supporting electrolyte*) at a concentration much larger than that of the electroactive species (see Section 4.3.2). Convection can be avoided by preventing stirring and vibrations in the electrochemical cell. In this chapter, we present an approximate treatment of steady-state mass transfer, which will provide a useful guide for these processes in later chapters and will give insight into electrochemical reactions without encumbrance by mathematical details.

1.4.2 Semiempirical Treatment of Steady-State Mass Transfer

Consider the reduction of a species O at a cathode: $\text{O} + ne \rightleftharpoons \text{R}$. In an actual case, the oxidized form, O, might be $\text{Fe}(\text{CN})_6^{3-}$ and R might be $\text{Fe}(\text{CN})_6^{4-}$, with only $\text{Fe}(\text{CN})_6^{3-}$ initially present at the millimolar level in a solution of 0.1 M K_2SO_4 . We envision a three-electrode cell having a platinum cathode, platinum anode, and SCE reference electrode. In addition, we furnish provision for agitation of the solution, such as by a stirrer. A particularly reproducible way to realize these conditions is to make the cathode in the form of a disk embedded in an insulator and to rotate the assembly at a known rate; this is called the *rotating disk electrode* (RDE) and is discussed in Section 9.3.

Once electrolysis of species O begins, its concentration at the electrode surface, $C_O(x=0)$ becomes smaller than the value, C_O^* , in the *bulk solution* (far from the electrode). We assume here that stirring is ineffective at the electrode surface, so the solution velocity term need not be considered at $x=0$. This simplified treatment is based on the idea that a stagnant layer of thickness δ_O exists at the electrode surface (*Nernst diffusion layer*), with stirring maintaining the concentration of O at C_O^* beyond $x=\delta_O$ (Figure 1.4.1). Since we also assume that there is an excess of supporting electrolyte, migration is not important, and the rate of mass transfer is proportional to the concentration gradient at the electrode surface, as given by the first (diffusive) term in equation 1.4.2:

$$v_{\text{mt}} \propto (dC_O/dx)_{x=0} = D_O(dC_O/dx)_{x=0} \quad (1.4.3)$$

If one further assumes a linear concentration gradient within the diffusion layer, then, from equation 1.4.3

$$v_{\text{mt}} = D_O[C_O^* - C_O(x=0)]/\delta_O \quad (1.4.4)$$

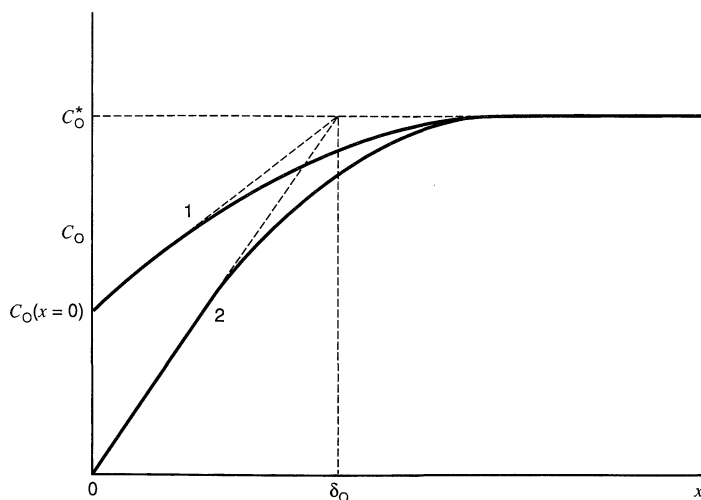


Figure 1.4.1 Concentration profiles (solid lines) and diffusion layer approximation (dashed lines). $x = 0$ corresponds to the electrode surface and δ_O is the diffusion layer thickness. Concentration profiles are shown at two different electrode potentials: (1) where $C_O(x = 0)$ is about $C_O^*/2$, (2) where $C_O(x = 0) \approx 0$ and $i = i_l$.

Since δ_O is often unknown, it is convenient to combine it with the diffusion coefficient to produce a single constant, $m_O = D_O/\delta_O$, and to write equation 1.4.4 as

$$v_{\text{mt}} = m_O[C_O^* - C_O(x = 0)] \quad (1.4.5)$$

The proportionality constant, m_O , called the *mass-transfer coefficient*, has units of cm/s (which are those of a rate constant of a first-order heterogeneous reaction; see Chapter 3). These units follow from those of v and C_O , but can also be thought of as volume flow/s per unit area ($\text{cm}^3 \text{s}^{-1} \text{cm}^{-2}$).¹¹ Thus, from equations 1.4.1 and 1.4.5 and taking a reduction current as positive [i.e., i is positive when $C_O^* > C_O(x = 0)$], we obtain

$$\frac{i}{nFA} = m_O[C_O^* - C_O(x = 0)] \quad (1.4.6)$$

Under the conditions of a net cathodic reaction, R is produced at the electrode surface, so that $C_R(x = 0) > C_R^*$ (where C_R^* is the bulk concentration of R). Therefore,

$$\frac{i}{nFA} = m_R[C_R(x = 0) - C_R^*] \quad (1.4.7)$$

¹¹While m_O is treated here as a phenomenological parameter, in more exact treatments the value of m_O can sometimes be specified in terms of measurable quantities. For example, for the rotating disk electrode, $m_O = 0.62D_O^{2/3}\omega^{1/2}\nu^{-1/6}$, where ω is the angular velocity of the disk (i.e., $2\pi f$, with f as the frequency in revolutions per second) and ν is the kinematic viscosity (i.e., viscosity/density, with units of cm^2/s) (see Section 9.3.2). Steady-state currents can also be obtained with a very small electrode (such as a Pt disk with a radius, r_0 , in the μm range), called an ultramicroelectrode (UME, Section 5.3). At a disk UME, $m_O = 4D_O/\pi r_0$.

or for the particular case when $C_R^* = 0$ (no R in the bulk solution),

$$\boxed{\frac{i}{nFA} = m_R C_R(x=0)} \quad (1.4.8)$$

The values of $C_O(x=0)$ and $C_R(x=0)$ are functions of electrode potential, E . The largest rate of mass transfer of O occurs when $C_O(x=0) = 0$ (or more precisely, when $C_O(x=0) \ll C_O^*$, so that $C_O^* - C_O(x=0) \approx C_O^*$). The value of the current under these conditions is called the *limiting current*, i_l , where

$$\boxed{i_l = nFAm_O C_O^*} \quad (1.4.9)$$

When the limiting current flows, the electrode process is occurring at the maximum rate possible for a given set of mass-transfer conditions, because O is being reduced as fast as it can be brought to the electrode surface. Equations 1.4.6 and 1.4.9 can be used to obtain expressions for $C_O(x=0)$:

$$\boxed{\frac{C_O(x=0)}{C_O^*} = 1 - \frac{i}{i_l}} \quad (1.4.10)$$

$$C_O(x=0) = \frac{i_l - i}{nFAm_O} \quad (1.4.11)$$

Thus, the concentration of species O at the electrode surface is linearly related to the current and varies from C_O^* , when $i = 0$, to a negligible value, when $i = i_l$.

If the kinetics of electron transfer are rapid, the concentrations of O and R at the electrode surface can be assumed to be at equilibrium with the electrode potential, as governed by the Nernst equation for the half-reaction¹²

$$E = E^{0'} + \frac{RT}{nF} \ln \frac{C_O(x=0)}{C_R(x=0)} \quad (1.4.12)$$

Such a process is called a *nernstian reaction*. We can derive the steady-state i - E curves for nernstian reactions under several different conditions.

(a) R Initially Absent

When $C_R^* = 0$, $C_R(x=0)$ can be obtained from (1.4.8):

$$C_R(x=0) = i/nFAm_R \quad (1.4.13)$$

Then, combining equations 1.4.11 to 1.4.13, we obtain

$$E = E^{0'} - \frac{RT}{nF} \ln \frac{m_O}{m_R} + \frac{RT}{nF} \ln \left(\frac{i_l - i}{i} \right) \quad (1.4.14)$$

An i - E plot is shown in Figure 1.4.2a. Note that when $i = i_l/2$,

$$\boxed{E = E_{1/2} = E^{0'} - \frac{RT}{nF} \ln \frac{m_O}{m_R}} \quad (1.4.15)$$

¹²Equation 1.4.12 is written in terms of $E^{0'}$, called the *formal potential*, rather than the standard potential E^0 . The formal potential is an adjusted form of the standard potential, manifesting activity coefficients and some chemical effects of the medium. In Section 2.1.6, it will be introduced in more detail. For the present it is not necessary to distinguish between $E^{0'}$ and E^0 .

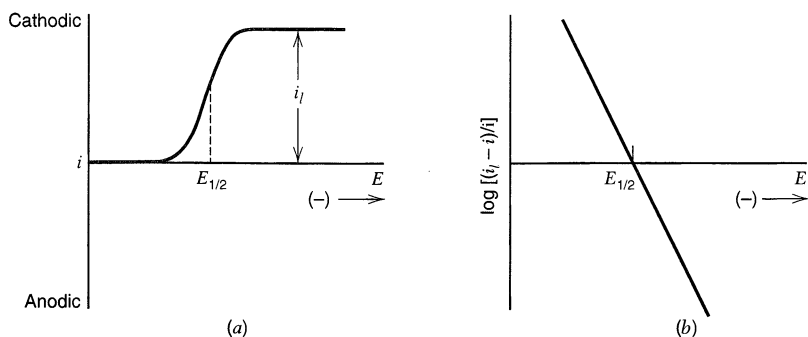


Figure 1.4.2 (a) Current-potential curve for a Nernstian reaction involving two soluble species with only oxidant present initially. (b) $\log[(i_l - i)/i]$ vs. E for this system.

where $E_{1/2}$ is independent of the substrate concentration and is therefore characteristic of the O/R system. Thus,

$$E = E_{1/2} + \frac{RT}{nF} \ln \left(\frac{i_l - i}{i} \right) \quad (1.4.16)$$

When a system conforms to this equation, a plot of E vs. $\log[(i_l - i)/i]$ is a straight line with a slope of $2.3RT/nF$ (or $59.1/n$ mV at 25°C). Alternatively (Figure 1.4.2b), $\log[(i_l - i)/i]$ vs. E is linear with a slope of $nF/2.3RT$ (or $n/59.1$ mV^{-1} at 25°C) and has an E -intercept of $E_{1/2}$. When m_O and m_R have similar values, $E_{1/2} \approx E^{0'}$.

(b) Both O and R Initially Present

When both members of the redox couple exist in the bulk, we must distinguish between a *cathodic* limiting current, $i_{l,c}$, when $C_O(x=0) \approx 0$, and an *anodic* limiting current, $i_{l,a}$, when $C_R(x=0) \approx 0$. We still have $C_O(x=0)$ given by (1.4.11), but with i_l now specified as $i_{l,c}$. The limiting anodic current naturally reflects the maximum rate at which R can be brought to the electrode surface for conversion to O. It is obtained from (1.4.7):

$$i_{l,a} = -nFAm_R C_R^* \quad (1.4.17)$$

(The negative sign arises because of our convention that cathodic currents are taken as positive and anodic ones as negative.) Thus $C_R(x=0)$ is given by

$$C_R(x=0) = \frac{i - i_{l,a}}{nFAm_R} \quad (1.4.18)$$

$$\frac{C_R(x=0)}{C_R^*} = 1 - \frac{i}{i_{l,a}} \quad (1.4.19)$$

The i - E curve is then

$$E = E^{0'} - \frac{RT}{nF} \ln \frac{m_O}{m_R} + \frac{RT}{nF} \ln \left(\frac{i_{l,c} - i}{i - i_{l,a}} \right) \quad (1.4.20)$$

A plot of this equation is shown in Figure 1.4.3. When $i = 0$, $E = E_{\text{eq}}$ and the system is at equilibrium. Surface concentrations are then equal to the bulk values. When current flows,

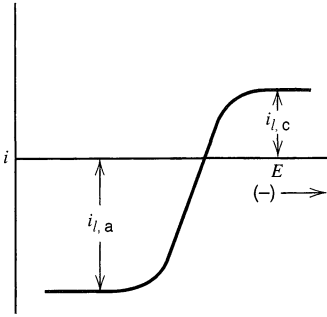


Figure 1.4.3 Current-potential curve for a Nernstian system involving two soluble species with both forms initially present.

the potential deviates from E_{eq} , and the extent of this deviation is the concentration overpotential. (An equilibrium potential cannot be defined when $C_{\text{R}}^* = 0$, of course.)

(c) R Insoluble

Suppose species R is a metal and can be considered to be at essentially unit activity as the electrode reaction takes place on bulk R.¹³ When $a_{\text{R}} = 1$, the Nernst equation is

$$E = E^{0'} + \frac{RT}{nF} \ln C_{\text{O}}(x = 0) \quad (1.4.21)$$

or, using the value of $C_{\text{O}}(x = 0)$ from equation 1.4.11,

$$E = E^{0'} + \frac{RT}{nF} \ln C_{\text{O}}^* + \frac{RT}{nF} \ln \left(\frac{i_l - i}{i_l} \right) \quad (1.4.22)$$

When $i = 0$, $E = E_{\text{eq}} = E^{0'} + (RT/nF) \ln C_{\text{O}}^*$ (Figure 1.4.4). If we define the *concentration overpotential*, η_{conc} (or the *mass-transfer overpotential*, η_{mt}), as

$$\eta_{\text{conc}} = E - E_{\text{eq}} \quad (1.4.23)$$

then

$$\eta_{\text{conc}} = \frac{RT}{nF} \ln \left(\frac{i_l - i}{i_l} \right) \quad (1.4.24)$$

When $i = i_l$, $\eta_{\text{conc}} \rightarrow \infty$. Since η is a measure of polarization, this condition is sometimes called *complete concentration polarization*.

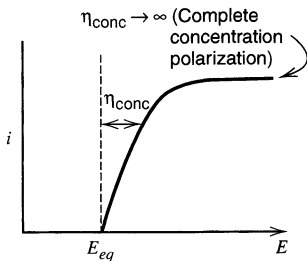


Figure 1.4.4 Current-potential curve for a Nernstian system where the reduced form is insoluble.

¹³This will not be the case for R plated onto an inert substrate in amounts less than a monolayer (e.g., the substrate electrode being Pt and R being Cu). Under those conditions, a_{R} may be considerably less than unity (see Section 11.2.1).

Equation 1.4.24 can be written in exponential form:

$$1 - \frac{i}{i_l} = \exp\left(\frac{nF\eta_{\text{conc}}}{RT}\right) \quad (1.4.25)$$

The exponential can be expanded as a power series, and the higher-order terms can be dropped if the argument is kept small; that is,

$$e^x = 1 + x + \frac{x^2}{2} + \dots \approx 1 + x \text{ (when } x \text{ is small)} \quad (1.4.26)$$

Thus, under conditions of small deviations of potential from E_{eq} , the i - η_{conc} characteristic is linear:

$$\eta_{\text{conc}} = \frac{-RTi}{nFi_l} \quad (1.4.27)$$

Since $-\eta/i$ has dimensions of resistance (ohms), we can define a “small signal” mass-transfer resistance, R_{mt} , as

$$R_{\text{mt}} = \frac{RT}{nF|i_l|} \quad (1.4.28)$$

Here we see that the mass-transfer-limited electrode reaction resembles an actual resistance element only at small overpotentials.

1.4.3 Semiempirical Treatment of the Transient Response

The treatment in Section 1.4.2 can also be employed in an approximate way to time-dependent (transient) phenomena, for example, the buildup of the diffusion layer, either in a stirred solution (before steady state is attained) or in an unstirred solution where the diffusion layer continues to grow with time. Equation 1.4.4 still applies, but in this case we consider the diffusion layer thickness to be a time-dependent quantity, so that

$$i/nFA = v_{\text{mt}} = D_{\text{O}}[C_{\text{O}}^* - C_{\text{O}}(x=0)]/\delta_{\text{O}}(t) \quad (1.4.29)$$

Consider what happens when a potential step of magnitude E is applied to an electrode immersed in a solution containing a species O. If the reaction is nernstian, the concentrations of O and R at $x = 0$ instantaneously adjust to the values governed by the Nernst equation, (1.4.12). The thickness of the approximately linear diffusion layer, $\delta_{\text{O}}(t)$, grows with time (Figure 1.4.5). At any time, the volume of the diffusion layer is

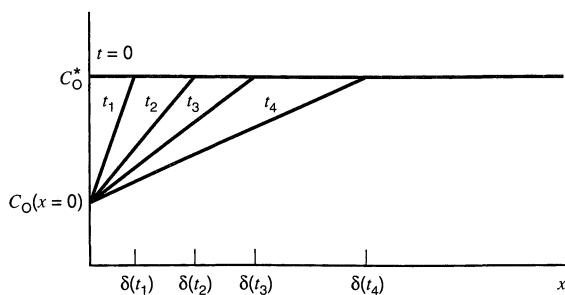


Figure 1.4.5 Growth of the diffusion-layer thickness with time.

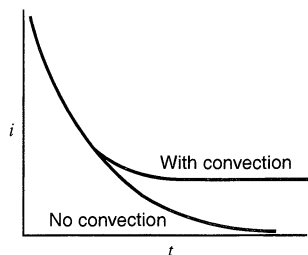


Figure 1.4.6 Current-time transient for a potential step to a stationary electrode (no convection) and to an electrode in stirred solution (with convection) where a steady-state current is attained.

$A\delta_{\text{O}}(t)$. The current flow causes a depletion of O, where the amount of O electrolyzed is given by

$$\text{Moles of O electrolyzed in diffusion layer} \cong [C_{\text{O}}^* - C_{\text{O}}(x=0)] \frac{A\delta(t)}{2} = \int_0^t \frac{i}{nF} dt \quad (1.4.30)$$

By differentiation of (1.4.30) and use of (1.4.29),

$$\frac{[C_{\text{O}}^* - C_{\text{O}}(x=0)] A}{2} \frac{d\delta(t)}{dt} = \frac{i}{nF} = \frac{D_{\text{O}}A}{\delta(t)} [C_{\text{O}}^* - C_{\text{O}}(x=0)] \quad (1.4.31)$$

or

$$\frac{d\delta(t)}{dt} = \frac{2D_{\text{O}}}{\delta(t)} \quad (1.4.32)$$

Since $\delta(t) = 0$ at $t = 0$, the solution of (1.4.32) is

$$\delta(t) = 2\sqrt{D_{\text{O}}t} \quad (1.4.33)$$

and

$$\frac{i}{nFA} = \frac{D_{\text{O}}^{1/2}}{2t^{1/2}} [C_{\text{O}}^* - C_{\text{O}}(x=0)] \quad (1.4.34)$$

This approximate treatment predicts a diffusion layer that grows with $t^{1/2}$ and a current that decays with $t^{-1/2}$. In the absence of convection, the current continues to decay, but in a convective system, it ultimately approaches the steady-state value characterized by $\delta(t) = \delta_{\text{O}}$ (Figure 1.4.6). Even this simplified approach approximates reality quite closely; equation 1.4.34 differs only by a factor of $2/\pi^{1/2}$ from the rigorous description of current arising from a nernstian system during a potential step (see Section 5.2.1).

▶ 1.5 SEMIEMPIRICAL TREATMENT OF NERNSTIAN REACTIONS WITH COUPLED CHEMICAL REACTIONS

The current-potential curves discussed so far can be used to measure concentrations, mass-transfer coefficients, and standard potentials. Under conditions where the electron-transfer rate at the interface is rate-determining, they can be employed to measure heterogeneous kinetic parameters as well (see Chapters 3 and 9). Often, however, one is interested in using electrochemical methods to find equilibrium constants and rate constants of homogeneous reactions that are coupled to the electron-transfer step. This section provides a brief introduction to these applications.

1.5.1 Coupled Reversible Reactions

If a homogeneous process, fast enough to be considered always in thermodynamic equilibrium (a reversible process), is coupled to a Nernstian electron-transfer reaction, then one can use a simple extension of the steady-state treatment to derive the i - E curve. Consider, for example, a species O involved in an equilibrium that precedes the electron-transfer reaction¹⁴



For example, A could be a metal complex, MY_q^{n+} ; O could be the free metal ion, M^{n+} ; and Y could be the free, neutral ligand (see Section 5.4.4). For reaction 1.5.2, the Nernst equation still applies at the electrode surface,

$$E = E^{0'} + \frac{RT}{nF} \ln \frac{C_O(x=0)}{C_R(x=0)} \quad (1.5.3)$$

and (1.5.1) is assumed to be at equilibrium everywhere:

$$\frac{C_O C_Y^q}{C_A} = K \quad (\text{all } x) \quad (1.5.4)$$

Hence

$$E = E^{0'} + \frac{RT}{nF} \ln \left[\frac{K C_A(x=0)}{C_Y^q(x=0) C_R(x=0)} \right] \quad (1.5.5)$$

Assuming (1) that at $t = 0$, $C_A = C_A^*$, $C_Y = C_Y^*$, and $C_R = 0$ (for all x); (2) that C_Y^* is so large compared to C_A^* that $C_Y(x=0) = C_Y^*$ at all times; and (3) that $K \ll 1$; then at steady state

$$\frac{i}{nFA} = m_A [C_A^* - C_A(x=0)] \quad (1.5.6)$$

$$\frac{i_l}{nFA} = m_A C_A^* \quad (1.5.7)$$

$$\frac{i}{nFA} = m_R C_R(x=0) \quad (1.5.8)$$

Then, as previously,

$$C_A(x=0) = \frac{(i_l - i)}{nFA m_A} \quad C_R(x=0) = \frac{i}{nFA m_R} \quad (1.5.9)$$

$$E = E^{0'} + \frac{RT}{nF} \ln K + \frac{RT}{nF} \ln \frac{m_R}{m_A} - \frac{RT}{nF} q \ln C_Y^* + \frac{RT}{nF} \ln \left(\frac{i_l - i}{i} \right) \quad (1.5.10)$$

$$E = E_{1/2} + (0.059/n) \log \frac{i_l - i}{i} \quad (T = 25^\circ) \quad (1.5.11)$$

where

$$E_{1/2} = E^{0'} + \frac{0.059}{n} \log \frac{m_R}{m_A} + \frac{0.059}{n} \log K - \frac{0.059}{n} q \log C_Y^* \quad (1.5.12)$$

¹⁴To simplify notation, charges on all species are omitted.

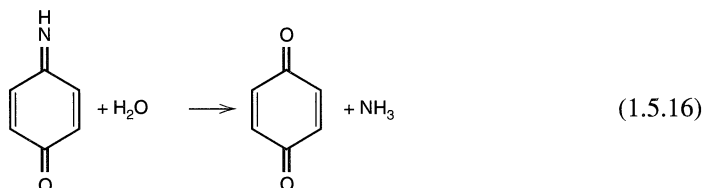
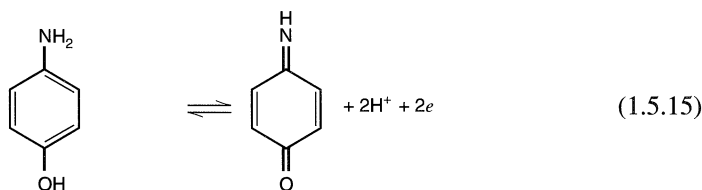
Thus, the i - E curve, (1.5.11), has the usual nernstian shape, but $E_{1/2}$ is shifted in a negative direction (since $K \ll 1$) from the position that would be found for process 1.5.2 unperturbed by the homogeneous equilibrium. From the shift of $E_{1/2}$ with $\log C_Y$, both $q [= -(n/0.059)(dE_{1/2}/d \log C_Y^*)]$ and K can be determined. Although these thermodynamic and stoichiometric quantities are available, no kinetic or mechanistic information can be obtained when both reactions are reversible.

1.5.2 Coupled Irreversible Chemical Reactions

When an irreversible chemical reaction is coupled to a nernstian electron transfer, the i - E curves can be used to provide kinetic information about the reaction in solution. Consider a nernstian charge-transfer reaction with a following first-order reaction:



where k is the rate constant (in s^{-1}) for the decomposition of R . (Note that k could be a pseudo-first-order constant, such as when R reacts with protons in a buffered solution and $k = k' C_{H^+}$.) As an example of this sequence, consider the oxidation of p -aminophenol in acid solution.



Reaction 1.5.16 does not affect the mass transfer and reduction of O , so (1.4.6) and (1.4.9) still apply (assuming $C_O = C_O^*$ and $C_R = 0$ at all x at $t = 0$). However, the reaction causes R to disappear from the electrode surface at a higher rate, and this difference affects the i - E curve.

In the absence of the following reaction, we think of the concentration profile for R as decreasing linearly from a value $C_R(x = 0)$ at the surface to the point where $C_R = 0$ at δ , the outer boundary of the Nernst diffusion layer. The coupled reaction adds a channel for disappearance of R , so the R profile in the presence of the reaction does not extend as far into the solution as δ . Thus, the added reaction steepens the profile and augments mass transfer away from the electrode surface. For steady-state behavior, such as at a rotating disk, we assume the rate at which R disappears from the surface to be the rate of diffusion in the absence of the reaction [$(m_R C_R(x = 0))$; see (1.4.8)] plus an increment proportional to the rate of reaction [$\mu k C_R(x = 0)$]. Since the rate of formation of R , given by (1.4.6), equals its total rate of disappearance, we have

$$\frac{i}{nFA} = m_O [C_O^* - C_O(x = 0)] = m_R C_R(x = 0) + \mu k C_R(x = 0) \quad (1.5.17)$$

where μ is a proportionality constant having units of cm, so that the product μk has dimensions of cm/s as required. In the literature (3), μ is called the *reaction layer thickness*. For our purpose, it is best just to think of μ as an adjustable parameter. From (1.5.17),

$$C_O(x=0) = \frac{i_l - i}{nFAm_O} \quad (1.5.18)$$

$$C_R(x=0) = \frac{i}{nFA(m_R + \mu k)} \quad (1.5.19)$$

Substituting these values into the Nernst equation for (1.5.13) yields

$$E = E^{0'} + \frac{RT}{nF} \ln \frac{m_R + \mu k}{m_O} + \frac{RT}{nF} \ln \left(\frac{i_l - i}{i} \right) \quad (1.5.20)$$

or

$$E = E'_{1/2} + \frac{0.059}{n} \log \left(\frac{i_l - i}{i} \right) \quad (\text{at } 25^\circ \text{C}) \quad (1.5.21)$$

where

$$E'_{1/2} = E^{0'} + \frac{0.059}{n} \log \left(\frac{m_R + \mu k}{m_O} \right) \quad (1.5.22)$$

or

$$E'_{1/2} = E_{1/2} + \frac{0.059}{n} \log \left(1 + \frac{\mu k}{m_R} \right) \quad (1.5.23)$$

where $E_{1/2}$ is the half-wave potential for the kinetically unperturbed reaction.

Two limiting cases can be defined: (a) When $\mu k/m_R \ll 1$, that is $\mu k \ll m_R$, the effect of the following reaction, (1.5.14), is negligible, and the unperturbed i - E curve results. (b) When $\mu k/m_R \gg 1$, the following reaction dominates the behavior and

$$E'_{1/2} = E_{1/2} + \frac{0.059}{n} \log \frac{\mu k}{m_R} \quad (1.5.24)$$

The effect is to shift the reduction wave in a *positive* direction without a change in shape. For the rotating disk electrode, where $m_R = 0.62D_R^{2/3}\omega^{1/2}\nu^{-1/6}$, (1.5.24) becomes [assuming $\mu \neq f(\omega)$]

$$E'_{1/2} = E_{1/2} + \frac{0.059}{n} \log \frac{\mu k}{0.62D_R^{2/3}\nu^{-1/6}} - \frac{0.059}{2n} \log \omega \quad (1.5.25)$$

An increase of rotation rate, ω , will cause the wave to shift in a *negative* direction (toward the unperturbed wave; see Figure 1.5.1). A tenfold change in ω causes a shift of $0.03/n$ V.

A similar treatment can be given for other chemical reactions coupled to the charge-transfer reaction (4). This approach is often useful in formulating a qualitative or semi-quantitative interpretation of i - E curves. Notice, however, that unless explicit expressions for m_R and μ can be given in a particular case, the exact values of k cannot be determined. The rigorous treatment of electrode reactions with coupled homogeneous chemical reactions is discussed in Chapter 12.

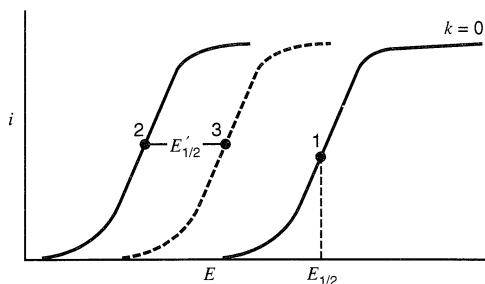


Figure 1.5.1 Effect of an irreversible following homogeneous chemical reaction on Nernstian i - E curves at a rotating disk electrode. (1) Unperturbed curve. (2) and (3) Curves with following reaction at two rotation rates, where the rotation rate for (3) is greater than for (2).

▶ 1.6 THE LITERATURE OF ELECTROCHEMISTRY

We now embark on more detailed and rigorous considerations of the fundamental principles of electrode reactions and the methods used to study them. At the outset, we list the general monographs and review series in which many of these topics are treated in much greater depth. This listing is not at all comprehensive, but does represent the recent English-language sources on general electrochemical subjects. References to the older literature can be found in these and in the first edition. Monographs and reviews on particular subjects are listed in the appropriate chapter. We also list the journals in which papers relating to electrochemical methods are published regularly.

1.6.1 Books and Monographs

(a) *General Electrochemistry*

Albery, W. J., "Electrode Kinetics," Clarendon, Oxford, 1975.

Bockris, J. O'M., and A. K. N. Reddy, "Modern Electrochemistry," Plenum, New York, 1970 (2 volumes); 2nd ed., (Vol. 1) 1998.

Christensen, P. A., and A. Hamnett, "Techniques and Mechanisms in Electrochemistry," Blackie Academic and Professional, New York, 1994.

Conway, B. E., "Theory and Principles of Electrode Processes," Ronald, New York, 1965.

Gileadi, E., "Electrode Kinetics for Chemists, Chemical Engineers, and Materials Scientists," VCH, New York, 1993.

Goodisman, J., "Electrochemistry: Theoretical Foundations, Quantum and Statistical Mechanics, Thermodynamics, the Solid State," Wiley, New York, 1987.

Hamann, C. H., A. Hamnett, and W. Vielstich, "Electrochemistry," Wiley-VCH, Weinheim, Germany, 1997.

Koryta, J., J., Dvořák, and L. Kavan, "Principles of Electrochemistry," 2nd ed, Wiley, New York, 1993.

MacInnes, D. A., "The Principles of Electrochemistry," Dover, New York, 1961 (Corrected version of 1947 edition).

Newman, J. S., "Electrochemical Systems," 2nd ed., Prentice-Hall, Englewood Cliffs, NJ, 1991.

Oldham, K. B., and J. C. Myland, "Fundamentals of Electrochemical Science," Academic, New York, 1994.

Rieger, P. H., "Electrochemistry," 2nd ed., Chapman and Hall, New York, 1994.

Rubinstein, I., Ed., "Physical Electrochemistry: Principles, Methods, and Applications," Marcel Dekker, New York, 1995.

Schmickler, W., "Interfacial Electrochemistry," Oxford University Press, New York, 1996.

(b) *Electrochemical Methodology*

Adams, R. N., "Electrochemistry at Solid Electrodes," Marcel Dekker, New York, 1969.

Delahay, P., "New Instrumental Methods in Electrochemistry," Interscience, New York, 1954.

Galus, Z., "Fundamentals of Electrochemical Analysis," 2nd ed, Wiley, New York, 1994.

Gileadi, E., E. Kirowa-Eisner, and J. Penciner, "Interfacial Electrochemistry—An Experimental Approach," Addison-Wesley, Reading, MA, 1975.

Kissinger, P. T., and W. R. Heineman, Eds., "Laboratory Techniques in Electroanalytical Chemistry," 2nd ed., Marcel Dekker, New York, 1996.

Lingane, J. J., "Electroanalytical Chemistry," 2nd ed., Interscience, New York, 1958.

Macdonald, D. D., "Transient Techniques in Electrochemistry," Plenum, New York, 1977.

Sawyer, D. T., A. Sobkowiak, and J. L. Roberts, Jr., "Electrochemistry for Chemists," 2nd ed., Wiley, New York, 1995.

Southampton Electrochemistry Group, "Instrumental Methods in Electrochemistry," Ellis Horwood, Chichester, UK, 1985.

Vanýsek, P., Ed., "Modern Techniques in Electroanalysis," Wiley, New York, 1996.

(c) *Descriptive Electrochemistry*

Bard, A. J., and H. Lund, Eds., "Encyclopedia of the Electrochemistry of the Elements," Marcel Dekker, New York, 1973–1986, (16 volumes).

Lund, H., and M. M. Baizer, "Organic Electrochemistry: an Introduction and Guide," 3rd ed., Marcel Dekker, New York, 1991.

Mann, C. K., and K. K. Barnes, "Electrochemical Reactions in Nonaqueous Systems," Marcel Dekker, New York, 1970.

(d) *Compilations of Electrochemical Data*

Bard, A. J., R. Parsons, and J. Jordan, Eds., "Standard Potentials in Aqueous Solutions," Marcel Dekker, New York, 1985.

Conway, B. E., "Electrochemical Data," Elsevier, Amsterdam, 1952.

Horvath, A. L., "Handbook of Aqueous Electrolyte Solutions: Physical Properties, Estimation, and Correlation Methods," Ellis Horwood, Chichester, UK, 1985.

Janz, G. J., and R. P. T. Tomkins, "Nonaqueous Electrolytes Handbook," Academic, New York, 1972 (2 volumes).

Meites, L., and P. Zuman, "Electrochemical Data," Wiley, New York, 1974.

Meites, L., and P. Zuman et al., "CRC Handbook Series in Organic Electrochemistry," (6 volumes) CRC, Boca Raton, FL, 1977–1983.

Meites, L., and P. Zuman et al., "CRC Handbook Series in Inorganic Electrochemistry," (8 volumes), CRC, Boca Raton, FL, 1980–1988.

Parsons, R., "Handbook of Electrochemical Data," Butterworths, London, 1959.

Zemaitis, J. F., D. M. Clark, M. Rafal, and N. C. Scrivner, "Handbook of Aqueous Electrolyte Thermodynamics: Theory and Applications," Design Institute for Physical Property Data (for the American Institute of Chemical Engineers), New York, 1986.

1.6.2 Review Series

A number of review series dealing with electrochemistry and related areas exist. Volumes are published every year or few years and contain chapters written by authorities in particular subject areas.¹⁵

Bard, A. J., Ed., (from Vol. 19 with I. Rubinstein), "Electroanalytical Chemistry," Marcel Dekker, New York, 1966–1998, (20 volumes).

Bockris, J. O'M., and B. E. Conway, et al., Eds., "Modern Aspects of Electrochemistry," Plenum, New York, 1954–1997, (31 volumes).

Delahay, P., and C. W. Tobias (from Vol. 10, H. Gerischer and C. W. Tobias), Eds., "Advances in Electrochemistry and Electrochemical Engineering," Wiley, New York, 1961–1984, (13 volumes).

Gerischer, H., C.W. Tobias, et al., Eds., "Advances in Electrochemical Science and Engineering," Wiley-VCH, Weinheim, Germany, 1990–1997, (5 volumes).

Specialist Periodical Reports, "Electrochemistry," G. J. Hills (Vols. 1–3), H. R. Thirsk (Vols. 4–7), and D. Pletcher (Vols. 8–10) Senior Reporters, The Chemical Society, London, 1971–1985, (10 volumes).

Steckhan, E., Ed., "Electrochemistry (Topics in Current Chemistry)," Springer, New York, 1987–1997, (6 volumes).

Yeager, E., J. O'M. Bockris, B. E. Conway, et al., Eds., "Comprehensive Treatise of Electrochemistry," Plenum, New York, 1984, (10 volumes).

Yeager, E., and A. J. Salkind, Eds., "Techniques of Electrochemistry," Wiley-Interscience, New York, 1972–1978, (3 volumes).

Reviews on electrochemical topics also appear from time to time in the following:

Accounts of Chemical Research, The American Chemical Society, Washington.

Analytical Chemistry (Annual Reviews), The American Chemical Society, Washington.

Annual Reviews of Physical Chemistry, Annual Reviews, Inc., Palo Alto, CA, from 1950.

Chemical Reviews, The American Chemical Society, Washington.

1.6.3 Journals

The following journals are primarily devoted to electrochemistry:

Electroanalysis (1989–).

Electrochimica Acta (1959–).

Electrochemical and Solid State Letters (1998–)

Electrochemistry Communications (1999–)

Journal of Applied Electrochemistry (1971–).

Journal of Electroanalytical Chemistry (1959–).

Journal of the Electrochemical Society (1902–).

Journal of Solid State Electrochemistry (1997–).

¹⁵Articles in the first three series listed below are cited in this book, and often elsewhere in the literature, in journal reference format with the abbreviations *Electroanal. Chem.*, *Mod. Asp. Electrochem.*, and *Adv. Electrochem. Electrochem. Engr.*, respectively. Note that the first should not be confused with *J. Electroanal Chem.*

1.6.4 World Wide Web

A number of web pages contain bibliographies of books and chapters on electrochemical topics, simulation programs, information about societies, and meetings in the area of electrochemistry. Links to these pages, and other information of interest to readers of this book will be maintained at <http://www.wiley.com/college/bard>.

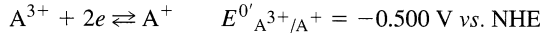
▶ 1.7 REFERENCES

1. L. R. Faulkner, *J. Chem. Educ.*, **60**, 262 (1983).
2. L. R. Faulkner in "Physical Methods in Modern Chemical Analysis," Vol. 3, T. Kuwana, Ed., Academic, New York, 1983, pp. 137–248.
3. P. Delahay, "New Instrumental Methods in Electrochemistry," Wiley-Interscience, New York, 1954, p. 92 ff.
4. See, for example, G. J. Hoytink, J. Van Schooten, E. de Boer, and W. Aalbersberg, *Rec. Trav. Chim.*, **73**, 355 (1954), for an application of this type of method to the study of reactions coupled to the reduction of aromatic hydrocarbons.

▶ 1.8 PROBLEMS

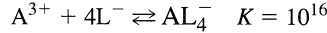
- 1.1 Consider each of the following electrode–solution interfaces, and write the equation for the electrode reaction that occurs first when the potential is moved in (1) a negative direction and (2) a positive direction from the open-circuit potential. Next to each reaction write the approximate potential for the reaction in V vs. SCE (assuming the reaction is reversible).
 - (a) Pt/Cu²⁺(0.01 M), Cd²⁺(0.01 M), H₂SO₄(1 M)
 - (b) Pt/Sn²⁺(0.01 M), Sn⁴⁺(0.01 M), HCl(1 M)
 - (c) Hg/Cd²⁺(0.01 M), Zn²⁺(0.01 M), HCl(1 M)
- 1.2 For a rotating disk electrode, the treatment of steady-state, mass-transfer-controlled electrode reactions applies, where the mass-transfer coefficient is $m_O = 0.62D_O^{2/3} \omega^{1/2} \nu^{-1/6}$. Here, D_O is the diffusion coefficient (cm²/s), ω is the angular velocity of the disk (s⁻¹) ($\omega = 2\pi f$, where f is the frequency of rotation in revolutions per second), and ν is the kinematic viscosity ($\nu = \eta/d$, η = viscosity, and d = density; for aqueous solutions $\nu \sim 0.010$ cm²/s). A rotating disk electrode of area 0.30 cm² is used for the reduction of 0.010 M Fe³⁺ to Fe²⁺ in 1 M H₂SO₄. Given D_O for Fe³⁺ at 5.2×10^{-6} cm²/s, calculate the limiting current for the reduction for a disk rotation rate of 10 r/s. Include units on variables during calculation and give units of current in the answer.
- 1.3 A solution of volume 50 cm³ contains 2.0×10^{-3} M Fe³⁺ and 1.0×10^{-3} M Sn⁴⁺ in 1 M HCl. This solution is examined by voltammetry at a rotating platinum disk electrode of area 0.30 cm². At the rotation rate employed, both Fe³⁺ and Sn⁴⁺ have mass-transfer coefficients, m , of 10⁻² cm/s.
 - (a) Calculate the limiting current for the reduction of Fe³⁺ under these conditions.
 - (b) A current-potential scan is taken from +1.3 to -0.40 V vs. NHE. Make a labeled, quantitatively correct, sketch of the i - E curve that would be obtained. Assume that no changes in the bulk concentrations of Fe³⁺ and Sn⁴⁺ occur during this scan and that all electrode reactions are nernstian.
- 1.4 The conductivity of a 0.1 M KCl solution is 0.013 Ω⁻¹cm⁻¹ at 25°C.
 - (a) Calculate the solution resistance between two parallel planar platinum electrodes of 0.1 cm² area placed 3 cm apart in this solution.
 - (b) A reference electrode with a Luggin capillary is placed the following distances from a planar platinum working electrode ($A = 0.1$ cm²) in 0.1 M KCl: 0.05, 0.1, 0.5, 1.0 cm. What is R_u in each case?
 - (c) Repeat the calculations in part (b) for a spherical working electrode of the same area. [In parts (b) and (c) it is assumed that a large counter electrode is employed.]
- 1.5 A 0.1 cm² electrode with $C_d = 20$ μF/cm² is subjected to a potential step under conditions where R_s is 1, 10, or 100 Ω. In each case, what is the time constant, and what is the time required for the double-layer charging to be 95% complete?

- 1.6 For the electrode in Problem 1.5, what nonfaradaic current will flow (neglecting any transients) when the electrode is subjected to linear sweeps at 0.02, 1, 20 V/s?
- 1.7 Consider the nernstian half-reaction:



The i - E curve for a solution at 25°C containing 2.00 mM A^{3+} and 1.00 mM A^+ in excess electrolyte shows $i_{l,c} = 4.00 \mu\text{A}$ and $i_{l,a} = -2.40 \mu\text{A}$. (a) What is $E_{1/2}$ (V vs. NHE)? (b) Sketch the expected i - E curve for this system. (c) Sketch the “log plot” (see Figure 1.4.2b) for the system.

- 1.8 Consider the system in Problem 1.7 under the conditions that a complexing agent, L^- , which reacts with A^{3+} according to the reaction



is added to the system. For a solution at 25°C containing only 2.0 mM A^{3+} and 0.1 M L^- in excess inert electrolyte, answer parts (a), (b), and (c) in Problem 1.7. (Assume m_O is the same for A^{3+} and AL_4^- .)

- 1.9 Derive the current-potential relationship under the conditions of Section 1.4.2 for a system where R is initially present at a concentration C_R^* and $C_O^* = 0$. Consider both O and R soluble. Sketch the expected i - E curve.
- 1.10 Suppose a mercury pool of 1 cm² area is immersed in a 0.1 M sodium perchlorate solution. How much charge (order of magnitude) would be required to change its potential by 1 mV? How would this be affected by a change in the electrolyte concentration to 10⁻² M? Why?
- 1.11 Rearrangement of equation 1.4.16 yields the following expression for i as a function of E , which is convenient for calculating i - E curves for nernstian reactions:

$$i/i_l = \{1 + \exp[(nF/RT)(E - E_{1/2})]\}^{-1}$$

(a) Derive this expression. (b) Consider the half-reaction $\text{Ru}(\text{NH}_3)_6^{3+} + e \rightleftharpoons \text{Ru}(\text{NH}_3)_6^{2+}$. The E^0 for this reaction is given in Appendix C. A steady-state i - E curve is obtained with a solution containing 10 mM $\text{Ru}(\text{NH}_3)_6^{3+}$ and 1 M KCl (as supporting electrolyte). The working electrode is a Pt disk of area 0.10 cm² operating under conditions where $m = 10^{-3}$ cm/s for both Ru species. Use a spreadsheet program to calculate and plot the expected i - E curve.

- 1.12 (a) Derive an expression for i as a function of E , analogous to that in Problem 1.11, from equation 1.4.20, using (1.4.15) as the definition of $E_{1/2}$, for use in solutions that contain both components of a redox couple. (b) Consider the same system as in Problem 1.11, but for a solution containing 10 mM $\text{Ru}(\text{NH}_3)_6^{3+}$ and 5.0 mM $\text{Ru}(\text{NH}_3)_6^{2+}$ in 1M KCl. Use a spreadsheet program to calculate the i - E curve and plot the results. (c) What is η_{conc} at a cathodic current density of 0.48 mA/cm²? (d) Estimate R_{mt} .

POTENTIALS AND THERMODYNAMICS OF CELLS

In Chapter 1, we sought to obtain a working feeling for potential as an electrochemical variable. Here we will explore the physical meaning of that variable in more detail. Our goal is to understand how potential differences are established and what kinds of chemical information can be obtained from them. At first, these questions will be approached through thermodynamics. We will find that potential differences are related to free energy changes in an electrochemical system, and this discovery will open the way to the experimental determination of all sorts of chemical information through electrochemical measurements. Later in this chapter, we will explore the mechanisms by which potential differences are established. Those considerations will provide insights that will prove especially useful when we start to examine experiments involving the active control of potential in an electrochemical system.

► 2.1 BASIC ELECTROCHEMICAL THERMODYNAMICS

2.1.1 Reversibility

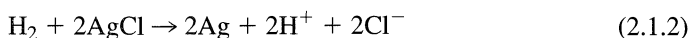
Since thermodynamics can strictly encompass only systems at equilibrium, the concept of *reversibility* is important in treating real processes thermodynamically. After all, the concept of equilibrium involves the idea that a process can move in either of two opposite directions from the equilibrium position. Thus, the adjective *reversible* is an essential one. Unfortunately, it takes on several different, but related, meanings in the electrochemical literature, and we need to distinguish three of them now.

(a) *Chemical Reversibility*

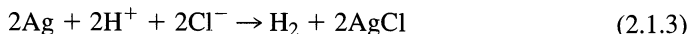
Consider the electrochemical cell shown in Figure 1.1.1b:



Experimentally, one finds that the difference in potential between the silver wire and the platinum wire is 0.222 V when all substances are in their standard states. Furthermore, the platinum wire is the negative electrode, and when the two electrodes are shorted together, the following reaction takes place:



If one overcomes the cell voltage by opposing it with the output of a battery or other direct current (dc) source, the current flow through the cell will reverse, and the new cell reaction is



Reversing the cell current merely reverses the cell reaction. No new reactions appear, thus the cell is termed *chemically reversible*.

On the other hand, the system



is not chemically reversible. The zinc electrode is negative with respect to platinum, and discharging the cell causes the reaction



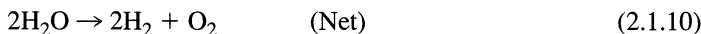
to occur there. At the platinum electrode, hydrogen evolves:



Thus the net cell reaction is¹



By applying an opposing voltage larger than the cell voltage, the current flow reverses, but the reactions observed are

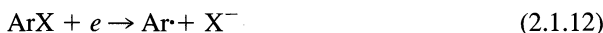


One has different electrode reactions as well as a different net process upon current reversal; hence this cell is said to be *chemically irreversible*.

One can similarly characterize half-reactions by their chemical reversibility. The reduction of nitrobenzene in oxygen-free, dry acetonitrile produces a stable radical anion in a chemically reversible, one-electron process:



The reduction of an aromatic halide, ArX, under similar conditions will often be chemically irreversible, since the radical anion product of the electron-transfer reaction rapidly decomposes:



Whether or not a half-reaction exhibits chemical reversibility depends upon solution conditions and the time scale of the experiment. For example, if the nitrobenzene reaction is carried out in an acidic acetonitrile solution, the reaction will become chemically irreversible, because $\text{PhNO}_2^- \cdot$ reacts with protons under these conditions. Alternatively, if the reduction of ArX is studied by a technique that takes only a very short time, then the reaction can be chemically reversible in that time regime:



¹The net reaction will also occur without a flow of electrons in the external circuit, because H^+ in solution will attack the zinc. This "side reaction," which happens to be identical with the electrochemical process, is slow if dilute acid is involved.

(b) Thermodynamic Reversibility

A process is thermodynamically reversible when an infinitesimal reversal in a driving force causes it to reverse direction. Obviously this cannot happen unless the system feels only an infinitesimal driving force at any time; hence it must essentially be always at equilibrium. A reversible path between two states of the system is therefore one that connects a continuous series of equilibrium states. Traversing it would require an infinite length of time.

A cell that is chemically irreversible cannot behave reversibly in a thermodynamic sense. A chemically reversible cell may or may not operate in a manner approaching thermodynamic reversibility.

(c) Practical Reversibility

Since all actual processes occur at finite rates, they cannot proceed with strict thermodynamic reversibility. However, a process may in practice be carried out in such a manner that thermodynamic equations apply to a desired accuracy. Under these circumstances, one might term the process reversible. *Practical reversibility* is not an absolute term; it includes certain attitudes and expectations an observer has toward the process.

A useful analogy involves the removal of a large weight from a spring balance. Carrying out this process strictly reversibly requires continuous equilibrium; the “thermodynamic” equation that always applies is

$$kx = mg \quad (2.1.14)$$

where k is the force constant, x is the distance the spring is stretched when mass m is added, and g is the earth’s gravitational acceleration. In the reversible process, the spring is never prone to contract more than an infinitesimal distance, because the large weight is removed progressively in infinitesimal portions.

Now if the same final state is reached by simply removing the weight all at once, equation 2.1.14 applies at no time during the process, which is characterized by severe disequilibrium and is grossly irreversible.

On the other hand, one could remove the weight as pieces, and if there were enough pieces, the thermodynamic relation, (2.1.14), would begin to apply a very large fraction of the time. In fact, one might not be able to distinguish the real (but slightly irreversible) process from the strictly reversible path. One could then legitimately label the real transformation as “practically reversible.”

In electrochemistry, one frequently relies on the Nernst equation:

$$E = E^{\circ} + \frac{RT}{nF} \ln \frac{C_{\text{O}}}{C_{\text{R}}} \quad (2.1.15)$$

to provide a linkage between electrode potential E and the concentrations of participants in the electrode process:



If a system follows the Nernst equation or an equation derived from it, the electrode reaction is often said to be thermodynamically or electrochemically reversible (or *nernstian*).

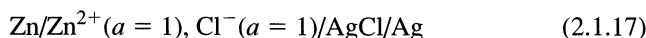
Whether a process appears reversible or not depends on one’s ability to detect the signs of disequilibrium. In turn, that ability depends on the time domain of the possible measurements, the rate of change of the force driving the observed process, and the speed with which the system can reestablish equilibrium. If the perturbation applied to the system is small enough, or if the system can attain equilibrium rapidly enough compared to

the measuring time, thermodynamic relations will apply. A given system may behave reversibly in one experiment and irreversibly in another, even of the same genre, if the experimental conditions have a wide latitude. This theme will be met again and again throughout this book.

2.1.2 Reversibility and Gibbs Free Energy

Consider three different methods (1) of carrying out the reaction $\text{Zn} + 2\text{AgCl} \rightarrow \text{Zn}^{2+} + 2\text{Ag} + 2\text{Cl}^-$:

- (a) Suppose zinc and silver chloride are mixed directly in a calorimeter at constant, atmospheric pressure and at 25°C . Assume also that the extent of reaction is so small that the activities of all species remain unchanged during the experiment. It is found that the amount of heat liberated when all substances are in their standard states is 233 kJ/mol of Zn reacted. Thus, $\Delta H^0 = -233 \text{ kJ}$.²
- (b) Suppose we now construct the cell of Figure 1.1.1a, that is,



and discharge it through a resistance R . Again assume that the extent of reaction is small enough to keep the activities essentially unchanged. During the discharge, heat will evolve from the resistor and from the cell, and we could measure the total heat change by placing the entire apparatus inside a calorimeter. We would find that the heat evolved is 233 kJ/mol of Zn, independent of R . That is, $\Delta H^0 = -233 \text{ kJ}$, regardless of the rate of cell discharge.

- (c) Let us now repeat the experiment with the cell and the resistor in separate calorimeters. Assume that the wires connecting them have no resistance and do not conduct any heat between the calorimeters. If we take Q_C as the heat change in the cell and Q_R as that in the resistor, we find that $Q_C + Q_R = -233 \text{ kJ/mol}$ of Zn reacted, independent of R . However, the balance between these quantities does depend on the rate of discharge. As R increases, $|Q_C|$ decreases and $|Q_R|$ increases. In the limit of infinite R , Q_C approaches -43 kJ (per mole of zinc) and Q_R tends toward -190 kJ .

In this example, the energy Q_R was dissipated as heat, but it was obtained as electrical energy, and it might have been converted to light or mechanical work. In contrast, Q_C is an energy change that is inevitably thermal. Since discharge through $R \rightarrow \infty$ corresponds to a thermodynamically reversible process, the energy that must appear as heat in traversing a reversible path, Q_{rev} , is identified as $\lim_{R \rightarrow \infty} Q_C$. The entropy change, ΔS , is defined as Q_{rev}/T (2), therefore for our example, where all species are in their standard states,

$$T\Delta S^0 = \lim_{R \rightarrow \infty} Q_C = -43 \text{ kJ} \quad (2.1.18)$$

Because $\Delta G^0 = \Delta H^0 - T\Delta S^0$,

$$\Delta G^0 = -190 \text{ kJ} = \lim_{R \rightarrow \infty} Q_R \quad (2.1.19)$$

Note that we have now identified $-\Delta G$ with the maximum *net work* obtainable from the cell, where net work is defined as work other than PV work (2). For any finite R , $|Q_R|$

²We adopt the thermodynamic convention in which absorbed quantities are positive.

(and the net work) is *less* than the limiting value. Note also that the cell may absorb or evolve heat as it discharges. In the former case, $|\Delta G^0| > |\Delta H^0|$.

2.1.3 Free Energy and Cell emf

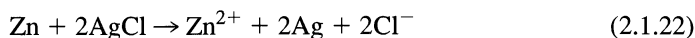
We found just above that if we discharged the electrochemical cell (2.1.17) through an infinite load resistance, the discharge would be reversible. The potential difference is therefore always the equilibrium (open-circuit) value. Since the extent of reaction is supposed to be small enough that all activities remain constant, the potential also remains constant. Then, the energy dissipated in R is given by

$$|\Delta G| = \text{charge passed} \times \text{reversible potential difference} \quad (2.1.20)$$

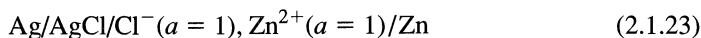
$$|\Delta G| = nF|E| \quad (2.1.21)$$

where n is the number of electrons passed per atom of zinc reacted (or the number of moles of electrons per mole of Zn reacted), and F is the charge on a mole of electrons, which is about 96,500 C. However, we also recognize that the free energy change has a *sign* associated with the *direction* of the net cell reaction. We can reverse the sign by reversing the direction. On the other hand, only an infinitesimal change in the overall cell potential is required to reverse the direction of the reaction; hence E is essentially constant and independent of the direction of a (reversible) transformation. We have a quandary. We want to relate a direction-sensitive quantity (ΔG) to a direction-insensitive observable (E). This desire is the origin of almost all of the confusion that exists over electrochemical sign conventions. Moreover the actual meaning of the signs $-$ and $+$ is different for free energy and potential. For free energy, $-$ and $+$ signify energy lost or gained from the system, a convention that traces back to the early days of thermodynamics. For potential, $-$ and $+$ signify the excess or deficiency of electronic charge, an electrostatic convention proposed by Benjamin Franklin even before the discovery of the electron. In most scientific discussions, this difference in meaning is not important, since the context, thermodynamic *vs.* electrostatic, is clear. But when one considers electrochemical cells, where both thermodynamic and electrostatic concepts are needed, it is necessary to distinguish clearly between these two conventions.

When we are interested in thermodynamic aspects of electrochemical systems, we rationalize this difficulty by inventing a thermodynamic construct called the *emf of the cell reaction*. This quantity is assigned to the reaction (not to the physical cell); hence it has a directional aspect. In a formal way, we also associate a given chemical reaction with each cell schematic. For the one in (2.1.17), the reaction is



The right electrode corresponds to reduction in the implied cell reaction, and the left electrode is identified with oxidation. Thus, the reverse of (2.1.22) would be associated with the opposite schematic:



The cell reaction emf, E_{rxn} , is then defined as the electrostatic potential of the electrode written on the right in the cell schematic with respect to that on the left.

For example, in the cell of (2.1.17), the measured potential difference is 0.985 V and the zinc electrode is negative; thus the emf of reaction 2.1.22, the spontaneous direction, is +0.985 V. Likewise, the emf corresponding to (2.1.23) and the reverse of (2.1.22) is -0.985 V. By adopting this convention, we have managed to rationalize an (observable) *electrostatic* quantity (the cell potential difference), which is not sensitive to the direction

of the cell's operation, with a (defined) *thermodynamic* quantity (the Gibbs free energy), which is sensitive to that direction. One can avoid completely the common confusion about sign conventions of cell potentials if one understands this formal relationship between electrostatic measurements and thermodynamic concepts (3,4).

Because our convention implies a positive emf when a reaction is spontaneous,

$$\Delta G = -nFE_{\text{rxn}} \quad (2.1.24)$$

or as above, when all substances are at unit activity,

$$\Delta G^0 = -nFE_{\text{rxn}}^0 \quad (2.1.25)$$

where E_{rxn}^0 is called the *standard emf of the cell reaction*.

Other thermodynamic quantities can be derived from electrochemical measurements now that we have linked the potential difference across the cell to the free energy. For example, the entropy change in the cell reaction is given by the temperature dependence of ΔG :

$$\Delta S = -\left(\frac{\partial \Delta G}{\partial T}\right)_P \quad (2.1.26)$$

hence

$$\Delta S = nF\left(\frac{\partial E_{\text{rxn}}}{\partial T}\right)_P \quad (2.1.27)$$

and

$$\Delta H = \Delta G + T\Delta S = nF\left[T\left(\frac{\partial E_{\text{rxn}}}{\partial T}\right)_P - E_{\text{rxn}}\right] \quad (2.1.28)$$

The equilibrium constant of the reaction is given by

$$RT \ln K_{\text{rxn}} = -\Delta G^0 = nFE_{\text{rxn}}^0 \quad (2.1.29)$$

Note that these relations are also useful for predicting electrochemical properties from thermochemical data. Several problems following this chapter illustrate the usefulness of that approach. Large tabulations of thermodynamic quantities exist (5–8).

2.1.4 Half-Reactions and Reduction Potentials

Just as the overall cell reaction comprises two independent half-reactions, one might think it reasonable that the cell potential could be broken into two individual electrode potentials. This view has experimental support, in that a self-consistent set of half-reaction emfs and half-cell potentials has been devised.

To establish the absolute potential of any conducting phase according to definition, one must evaluate the work required to bring a unit positive charge, without associated matter, from the point at infinity to the interior of the phase. Although this quantity is not measurable by thermodynamically rigorous means, it can sometimes be estimated from a series of nonelectrochemical measurements and theoretical calculations, if the demand for thermodynamic rigor is relaxed. Even if we could determine these absolute phase potentials, they would have limited utility because they would

depend on magnitudes of the adventitious fields in which the phase is immersed (see Section 2.2). Much more meaningful is the *difference* in absolute phase potentials between an electrode and its electrolyte, for this difference is the chief factor determining the state of an electrochemical equilibrium. Unfortunately, we will find that it also is not rigorously measurable. Experimentally, we can find only the absolute potential difference between two electronic conductors. Still, a useful scale results when one refers electrode potentials and half-reaction emfs to a standard reference electrode featuring a standard half-reaction.

The primary reference, chosen by convention, is the *normal hydrogen electrode* (NHE), also called the *standard hydrogen electrode* (SHE):

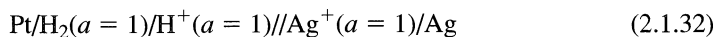


Its potential (the electrostatic standard) is taken as zero at all temperatures. Similarly, the standard emfs of the half-reactions:

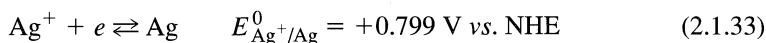


have also been assigned values of zero at all temperatures (the thermodynamic standard).

We can record half-cell potentials by measuring them in whole cells against the NHE.³ For example, in the system



the cell potential is 0.799 V and silver is positive. Thus, we say that the *standard potential of the Ag⁺/Ag couple* is +0.799 V vs. NHE. Moreover, the *standard emf of the Ag⁺ reduction* is also +0.799 V vs. NHE, but that of the Ag oxidation is -0.799 V vs. NHE. Another valid expression is that the *standard electrode potential of Ag⁺/Ag* is +0.799 V vs. NHE. To sum all of this up, we write:⁴



For the general system, (2.1.16), the electrostatic potential of the R/O electrode (with respect to NHE) and the emf for the *reduction* of O always coincide. Therefore, one can condense the electrostatic and thermodynamic information into one list by tabulating electrode potentials and writing the half-reactions as reductions. Appendix C provides some frequently encountered potentials. Reference (5) is an authoritative general source for aqueous systems.

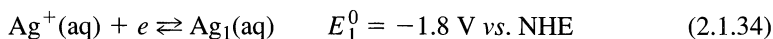
Tables of this sort are extremely useful, because they feature much chemical and electrical information condensed into quite a small space. A few electrode potentials can characterize quite a number of cells and reactions. Since the potentials are really indices of free energies, they are also ready means for evaluating equilibrium constants, complexation constants, and solubility products. Also, they can be taken in linear combinations to supply electrochemical information about additional half-reactions. One can tell from a glance at an ordered list of potentials whether or not a given redox process will proceed spontaneously.

³Note that an NHE is an ideal device and cannot be constructed. However, real hydrogen electrodes can approximate it, and its properties can be defined by extrapolation.

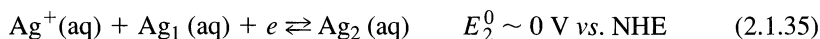
⁴In some of the older literature, the standard emfs of reduction and oxidation are, respectively, called the "reduction potential" and the "oxidation potential." These terms are intrinsically confusing and should be avoided altogether, because they conflate the chemical concept of reaction direction with the physical concept of electrical potential.

It is important to recognize that it is the electrostatic potential (not the emf) that is experimentally controlled and measured. When a half-reaction is chemically reversible, the potential of its electrode will usually have the same sign, whether the reaction proceeds as an oxidation or a reduction. [See also reference (9), and Sections 1.3.4, and 1.4.2(b).]

The standard potential of a cell or half-reaction is obtained under conditions where all species are in their standard states (10). For solids, like Ag in cell 2.1.32 or reaction 2.1.33, the standard state is the pure crystalline (bulk) metal. It is interesting to consider how many atoms or what particle size is needed to produce “bulk metal” and whether the standard potential is a function of particle size when one deals with metal clusters. These questions have been addressed (11–13); and for clusters containing n atoms (where $n < 20$), E_n^0 indeed turns out to be very different from the value for the bulk metal ($n \gg 20$). Consider, for example, silver clusters, Ag_n . For a silver atom ($n = 1$), the value of E_1^0 can be related to E^0 for the bulk metal through a thermodynamic cycle involving the ionization potential of Ag and the hydration energy of Ag and Ag^+ . This process yields



which is 2.6 V more negative than for bulk Ag. This result implies that it is much easier energetically to remove an electron from a single isolated Ag atom than to remove an electron from Ag atoms within a lattice of other Ag atoms. Experimental work carried out with larger silver clusters shows that as the cluster size increases, E_n^0 moves toward the value for the bulk metal. For example, for $n = 2$



These differences in standard potential can be explained by the greater *surface energy* of small clusters compared to bulk metal and is consistent with the tendency of small particles to grow into larger ones (e.g., the dimerization of 2Ag_1 into Ag_2 or the Ostwald ripening of colloidal particles to form precipitates). Surface atoms are bonded to fewer neighbors than atoms within a crystal; thus an extra surface free energy is required to create additional surface area by subdivision of a metal. Conversely, the total energy of a system can be minimized by decreasing the surface area, such as by taking on a spherical shape or by fusing small particles into larger ones. If one adopts a microscopic viewpoint, one can see that the tendency for surfaces to reconstruct (see Section 13.4.2) and for different sites on surfaces to etch at different rates implies that even the standard potential for reduction to the “bulk metal” is actually an average of E^0 values for reduction at the different sites (14).

2.1.5 emf and Concentration

Consider a general cell in which the half-reaction at the right-hand electrode is



where the ν 's are stoichiometric coefficients. The cell reaction is then



and its free energy is given from basic thermodynamics (2) by

$$\Delta G = \Delta G^0 + RT \ln \frac{a_{\text{R}}^{\nu_{\text{R}}} a_{\text{H}^+}^{\nu_{\text{H}^+}}}{a_{\text{O}}^{\nu_{\text{O}}} a_{\text{H}_2}^{\nu_{\text{H}_2}}} \quad (2.1.38)$$

where a_i is the activity of species i .⁵ Since $\Delta G = -nFE$ and $\Delta G^0 = -nFE^0$,

$$E = E^0 - \frac{RT}{nF} \ln \frac{a_{\text{R}}^{\nu_{\text{R}}} a_{\text{H}^+}^{\nu_{\text{H}^+}}}{a_{\text{O}}^{\nu_{\text{O}}} a_{\text{H}_2}^{\nu_{\text{H}_2}}} \quad (2.1.39)$$

but since $a_{\text{H}^+} = a_{\text{H}_2} = 1$,

$$E = E^0 + \frac{RT}{nF} \ln \frac{a_{\text{O}}^{\nu_{\text{O}}}}{a_{\text{R}}^{\nu_{\text{R}}}} \quad (2.1.40)$$

This relation, the *Nernst equation*, furnishes the potential of the O/R electrode vs. NHE as a function of the activities of O and R. In addition, it defines the activity dependence of the emf for reaction 2.1.36.

It is now clear that the emf of any cell reaction, in terms of the electrode potentials of the two half-reactions, is

$$E_{\text{rxn}} = E_{\text{right}} - E_{\text{left}} \quad (2.1.41)$$

where E_{right} and E_{left} refer to the cell schematic and are given by the appropriate Nernst equation. The cell potential is the magnitude of this value.

2.1.6 Formal Potentials

It is usually inconvenient to deal with activities in evaluations of half-cell potentials, because activity coefficients are almost always unknown. A device for avoiding them is the *formal potential*, $E^{0'}$. This quantity is the *measured* potential of the half-cell (vs. NHE) when (a) the species O and R are present at concentrations such that the ratio $C_{\text{O}}^{\nu_{\text{O}}}/C_{\text{R}}^{\nu_{\text{R}}}$ is unity and (b) other specified substances, for example, miscellaneous components of the medium, are present at designated concentrations. At the least, the formal potential incorporates the standard potential and some activity coefficients, γ_i . For example, consider



Its Nernst relation is simply

$$E = E^0 + \frac{RT}{nF} \ln \frac{a_{\text{Fe}^{3+}}}{a_{\text{Fe}^{2+}}} = E^0 + \frac{RT}{nF} \ln \frac{\gamma_{\text{Fe}^{3+}} [\text{Fe}^{3+}]}{\gamma_{\text{Fe}^{2+}} [\text{Fe}^{2+}]} \quad (2.1.43)$$

which is

$$E = E^{0'} + \frac{RT}{nF} \ln \frac{[\text{Fe}^{3+}]}{[\text{Fe}^{2+}]} \quad (2.1.44)$$

where

$$E^{0'} = E^0 + \frac{RT}{nF} \ln \frac{\gamma_{\text{Fe}^{3+}}}{\gamma_{\text{Fe}^{2+}}} \quad (2.1.45)$$

⁵For a solute i , the activity is $a_i = \gamma_i (C_i/C^0)$, where C_i is the concentration of the solute, C^0 is the standard concentration (usually 1 M), and γ_i is the activity coefficient, which is unitless. For a gas, $a_i = \gamma_i (P_i/P^0)$, where P_i is the partial pressure of i , P^0 is the standard pressure, and γ_i is the activity coefficient, which is again unitless. For most of the published literature, including all before the late 1980s, the standard pressure was 1 atm (101,325 Pa). The new standard pressure adopted by the International Union of Pure and Applied Chemistry is 10^5 Pa. A consequence of this change is that the potential of the NHE now differs from that used historically. The “new NHE” is +0.169 mV vs. the “old NHE” (based on a standard state of 1 atm). This difference is rarely significant, and is never so in this book. Most tabulated standard potentials, including those in Table C.1 are referred to the old NHE See reference 15.

Because the ionic strength affects the activity coefficients, $E^{0'}$ will vary from medium to medium. Table C.2 contains values for this couple in 1 M HCl, 10 M HCl, 1 M HClO₄, 1 M H₂SO₄, and 2 M H₃PO₄. The values of standard potentials for half-reactions and cells are actually determined by measuring formal potentials values at different ionic strengths and extrapolating to zero ionic strength, where the activity coefficients approach unity.

Often $E^{0'}$ also contains factors related to complexation and ion pairing; as it does in fact for the Fe(III)/Fe(II) couple in HCl, H₂SO₄, and H₃PO₄ solutions. Both iron species are complexed in these media; hence (2.1.42) does not accurately describe the half-cell reaction. However, one can sidestep a full description of the complex competitive equilibria by using the empirical formal potentials. In such cases, $E^{0'}$ contains terms involving equilibrium constants and concentrations of some species involved in the equilibria.

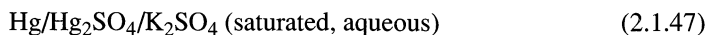
2.1.7 Reference Electrodes

Many reference electrodes other than the NHE and the SCE have been devised for electrochemical studies in aqueous and nonaqueous solvents. Several authors have provided discussions on the subject (16–18).

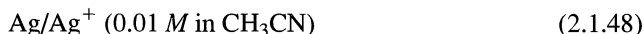
Usually there are experimental reasons for the choice of a reference electrode. For example, the system



has a smaller temperature coefficient of potential than an SCE and can be built more compactly. When chloride is not acceptable, the mercurous sulfate electrode may be used:



With a nonaqueous solvent, one may be concerned with the leakage of water from an aqueous reference electrode; hence a system like



might be preferred.

Because of the difficulty in finding a reference electrode for a nonaqueous solvent that does not contaminate the test solution with undesirable species, a *quasireference electrode* (QRE)⁶ is often employed. This is usually just a metal wire, Ag or Pt, used with the expectation that in experiments where there is essentially no change in the bulk solution, the potential of this wire, although unknown, will not change during a series of measurements. The actual potential of the quasireference electrode *vs.* a true reference electrode must be calibrated before reporting potentials with reference to the QRE. Typically the calibration is achieved simply by measuring (e.g., by voltammetry) the standard or formal potential *vs.* the QRE of a couple whose standard or formal potential is already known *vs.* a true reference under the same conditions. The ferrocene/ferrocenium (Fc/Fc⁺) couple is recommended as a calibrating redox couple, since both forms are soluble and stable in many solvents, and since the couple usually shows nernstian behavior (19). Voltammograms for ferrocene oxidation might be recorded to establish the value of $E_{\text{Fc/Fc}^+}^{0'}$ *vs.* the QRE, so that the potentials of other reactions can be reported against $E_{\text{Fc/Fc}^+}^{0'}$. It is unacceptable to report potentials *vs.* an uncalibrated quasireference electrode. Moreover a QRE is not suitable in experiments, such as bulk electrolysis, where changes in the composition of the bulk solu-

⁶*Quasi* implies that it is “almost” or “essentially” a reference electrode. Sometimes such electrodes are also called *pseudoreference electrodes* (*pseudo*, meaning false); this terminology seems less appropriate.

$E^0(\text{Zn}^{2+}/\text{Zn})$	-0.763	-1.00	3.7	-3.7
NHE	0	-0.242	4.5	-4.5
SCE	0.242	0	4.7	-4.7
$E^0(\text{Fe}^{3+}/\text{Fe}^{2+})$	0.77	0.53	5.3	-5.3
	E vs. NHE (volts)	E vs. SCE (volts)	E vs. vacuum (volts)	E_F (Fermi energy) (eV)

Figure 2.1.1 Relationship between potentials on the NHE, SCE, and “absolute” scales. The potential on the absolute scale is the electrical work required to bring a unit positive test charge into the conducting phase of the electrode from a point *in vacuo* just outside the system (see Section 2.2.5). At right is the Fermi energy corresponding to each of the indicated potentials. The Fermi energy is the electrochemical potential of electrons on the electrode (see Section 2.2.4).

tion can cause concomitant variations in the potential of the QRE. A proposed alternative approach (20) is to employ a reference electrode in which Fc and Fc^+ are immobilized at a known concentration ratio in a polymer layer on the electrode surface (see Chapter 14).

Since the potential of a reference electrode vs. NHE or SCE is typically specified in experimental papers, interconversion of scales can be accomplished easily. Figure 2.1.1 is a schematic representation of the relationship between the SCE and NHE scales. The inside back cover contains a tabulation of the potentials of the most common reference electrodes.

▶ 2.2 A MORE DETAILED VIEW OF INTERFACIAL POTENTIAL DIFFERENCES

2.2.1 The Physics of Phase Potentials

In the thermodynamic considerations of the previous section, we were not required to advance a mechanistic basis for the observable differences in potentials across certain phase boundaries. However, it is difficult to think chemically without a mechanistic model, and we now find it helpful to consider the kinds of interactions between phases that could create these interfacial differences. First, let us consider two prior questions: (1) Can we expect the potential within a phase to be uniform? (2) If so, what governs its value?

One certainly can speak of the potential at any particular point within a phase. That quantity, $\phi(x, y, z)$, is defined as the work required to bring a unit positive charge, without material interactions, from an infinite distance to point (x, y, z) . From electrostatics, we have assurance that $\phi(x, y, z)$ is independent of the path of the test charge (21). The work is done against a coulombic field; hence we can express the potential generally as

$$\phi(x, y, z) = \int_{\infty}^{x,y,z} -\mathcal{E} \cdot d\mathbf{l} \quad (2.2.1)$$

where \mathcal{E} is the electric field strength vector (i.e., the force exerted on a unit charge at any point), and $d\mathbf{l}$ is an infinitesimal tangent to the path in the direction of movement. The integral is carried out over any path to (x, y, z) . The difference in potential between points (x', y', z') and (x, y, z) is then

$$\phi(x', y', z') - \phi(x, y, z) = \int_{x,y,z}^{x',y',z'} -\mathcal{E} \cdot d\mathbf{l} \quad (2.2.2)$$

In general, the electric field strength is not zero everywhere between two points and the integral does not vanish; hence some potential difference usually exists.

Conducting phases have some special properties of great importance. Such a phase is one with mobile charge carriers, such as a metal, a semiconductor, or an electrolyte solution. When no current passes through a conducting phase, there is no net movement of charge carriers, so the electric field at all interior points must be zero. If it were not, the carriers would move in response to it to eliminate the field. From equation 2.2.2, one can see that the difference in potential between any two points in the interior of the phase must also be zero under these conditions; thus the entire phase is an *equipotential volume*. We designate its potential as ϕ , which is known as the *inner potential* (or *Galvani potential*) of the phase.

Why does the inner potential have the value that it does? A very important factor is any excess charge that might exist on the phase itself, because a test charge would have to work against the coulombic field arising from that charge. Other components of the potential can arise from miscellaneous fields resulting from charged bodies outside the sample. As long as the charge distribution throughout the system is constant, the phase potential will remain constant, but alterations in charge distributions inside or outside the phase will change the phase potential. Thus, we have our first indication that differences in potential arising from chemical interactions between phases have some sort of *charge separation* as their basis.

An interesting question concerns the location of any excess charge on a conducting phase. The Gauss law from elementary electrostatics is extremely helpful here (22). It states that if we enclose a volume with an imaginary surface (a *Gaussian surface*), we will find that the net charge q inside the surface is given by an integral of the electric field over the surface:

$$q = \epsilon_0 \oint \mathcal{E} \cdot d\mathbf{S} \quad (2.2.3)$$

where ϵ_0 is a proportionality constant,⁷ and $d\mathbf{S}$ is an infinitesimal vector normal outward from the surface. Now consider a Gaussian surface located within a conductor that is uniform in its interior (i.e., without voids or interior phases). If no current flows, \mathcal{E} is zero at all points on the Gaussian surface, hence the net charge within the boundary is zero. The situation is depicted in Figure 2.2.1. This conclusion applies to any Gaussian surface, even one situated just inside the phase boundary; thus we must infer that the excess charge actually resides on the surface of the conducting phase.⁸

⁷The parameter ϵ_0 is called the *permittivity of free space* or the *electric constant* and has the value $8.85419 \times 10^{-12} \text{ C}^2 \text{ N}^{-1} \text{ m}^{-1}$. See the footnote in Section 13.3.1 for a fuller explanation of electrostatic conventions followed in this book.

⁸There can be a finite thickness to this surface layer. The critical aspect is the size of the excess charge with respect to the bulk carrier concentration in the phase. If the charge is established by drawing carriers from a significant volume, thermal processes will impede the compact accumulation of the excess strictly on the surface. Then, the charged zone is called a *space charge region*, because it has three-dimensional character. Its thickness can range from a few angstroms to several thousand angstroms in electrolytes and semiconductors. In metals, it is negligibly thick. See Chapters 13 and 18 for more detailed discussion along this line.

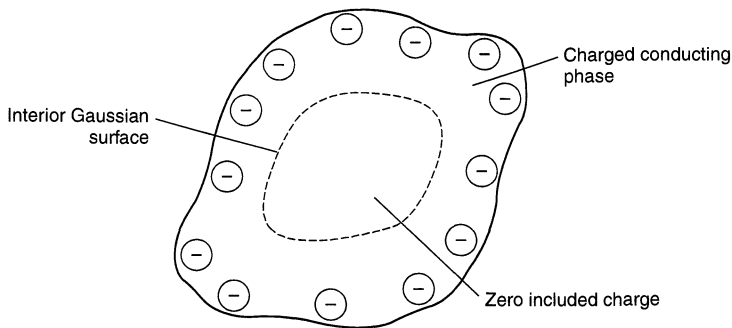


Figure 2.2.1 Cross-section of a three-dimensional conducting phase containing a Gaussian enclosure. Illustration that the excess charge resides on the surface of the phase.

A view of the way in which phase potentials are established is now beginning to emerge:

1. Changes in the potential of a conducting phase can be effected by altering the charge distributions on or around the phase.
2. If the phase undergoes a change in its excess charge, its charge carriers will adjust such that the excess becomes wholly distributed over an entire boundary of the phase.
3. The surface distribution is such that the electric field strength within the phase is zero under null-current conditions.
4. The interior of the phase features a constant potential, ϕ .

The excess charge needed to change the potential of a conductor by electrochemically significant amounts is often not very large. Consider, for example, a spherical mercury drop of 0.5 mm radius. Changing its potential requires only about 5×10^{-14} C/V (about 300,000 electrons/V), if it is suspended in air or in a vacuum (21).

2.2.2 Interactions Between Conducting Phases

When two conductors, for example, a metal and an electrolyte, are placed in contact, the situation becomes more complicated because of the coulombic interaction between the phases. Charging one phase to change its potential tends to alter the potential of the neighboring phase as well. This point is illustrated in the idealization of Figure 2.2.2, which portrays a situation where there is a charged metal sphere of macroscopic size, perhaps a mercury droplet 1 mm in diameter, surrounded by a layer of uncharged electrolyte a few millimeters in thickness. This assembly is suspended in a vacuum. We know that the

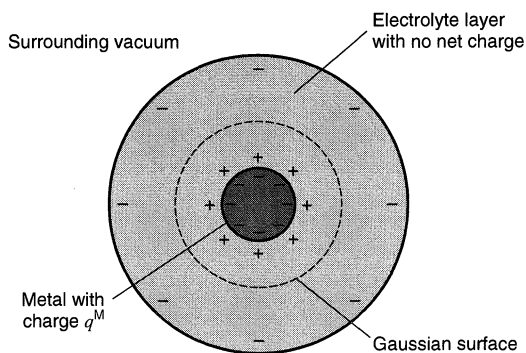


Figure 2.2.2 Cross-sectional view of the interaction between a metal sphere and a surrounding electrolyte layer. The Gaussian enclosure is a sphere containing the metal phase and part of the electrolyte.

charge on the metal, q^M , resides on its surface. This unbalanced charge (negative in the diagram) creates an excess cation concentration near the electrode in the solution. What can we say about the magnitudes and distributions of the obvious charge imbalances in solution?

Consider the integral of equation 2.2.3 over the Gaussian surface shown in Figure 2.2.2. Since this surface is in a conducting phase where current is not flowing, \mathcal{E} at every point is zero and the net enclosed charge is also zero. We could place the Gaussian surface just outside the surface region bounding the metal and solution, and we would reach the same conclusion. Thus, we know now that the excess positive charge in the solution, q^S , resides at the metal–solution interface and exactly compensates the excess metal charge. That is,

$$q^S = -q^M \quad (2.2.4)$$

This fact is very useful in the treatment of interfacial charge arrays, which we have already seen as *electrical double layers* (see Chapters 1 and 13).⁹

Alternatively, we might move the Gaussian surface to a location just inside the outer boundary of the electrolyte. The enclosed charge must still be zero, yet we know that the net charge on the whole system is q^M . A negative charge equal to q^M must therefore reside at the outer surface of the electrolyte.

Figure 2.2.3 is a display of potential vs. distance from the center of this assembly, that is, the work done to bring a unit positive test charge from infinitely far away to a given distance from the center. As the test charge is brought from the right side of the diagram, it is attracted by the charge on the outer surface of the electrolyte; thus negative work is required to traverse any distance toward the electrolyte surface in the surrounding vacuum, and the potential steadily drops in that direction. Within the electrolyte, \mathcal{E} is zero everywhere, so there is no work in moving the test charge, and the potential is constant at ϕ^S . At the metal–solution interface, there is a strong field because of the double layer there, and it is oriented such that negative work is done in taking the positive test charge through the interface. Thus there is a sharp change in potential from ϕ^S to ϕ^M over the distance scale of the double layer.¹⁰ Since the metal is a field-free volume, the

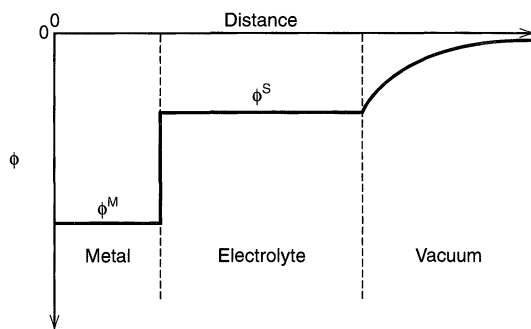


Figure 2.2.3 Potential profile through the system shown in Figure 2.2.2. Distance is measured radially from the center of the metallic sphere.

⁹Here we are considering the problem on a macroscopic distance scale, and it is accurate to think of q^S as residing strictly at the metal–solution interface. On a scale of $1 \mu\text{m}$ or finer, the picture is more detailed. One finds that q^S is still near the metal–solution interface, but is distributed in one or more zones that can be as thick as 1000 \AA (Section 13.3).

¹⁰The diagram is drawn on a macroscopic scale, so the transition from ϕ^S to ϕ^M appears vertical. The theory of the double layer (Section 13.3) indicates that most of the change occurs over a distance equivalent to one to several solvent monolayers, with a smaller portion being manifested over the diffuse layer in solution.

potential is constant in its interior. If we were to increase the negative charge on the metal, we would naturally lower ϕ^M , but we would also lower ϕ^S , because the excess negative charge on the outer boundary of the solution would increase, and the test charge would be attracted more strongly to the electrolyte layer at every point on the path through the vacuum.

The difference $\phi^M - \phi^S$, called the *interfacial potential difference*, depends on the charge imbalance at the interface and the physical size of the interface. That is, it depends on the charge density (C/cm^2) at the interface. Making a change in this interfacial potential difference requires sizable alterations in charge density. For the spherical mercury drop considered above ($A = 0.03 \text{ cm}^2$), now surrounded by 0.1 M strong electrolyte, one would need about 10^{-6} C (or 6×10^{12} electrons) for a 1-V change. These numbers are more than 10^7 larger than for the case where the electrolyte is absent. The difference appears because the coulombic field of any surface charge is counterbalanced to a very large degree by polarization in the adjacent electrolyte.

In practical electrochemistry, metallic electrodes are partially exposed to an electrolyte and partially insulated. For example, one might use a 0.1 cm^2 platinum disk electrode attached to a platinum lead that is almost fully sealed in glass. It is interesting to consider the location of excess charge used in altering the potential of such a phase. Of course, the charge must be distributed over the entire surface, including both the insulated and the electrochemically active area. However, we have seen that the coulombic interaction with the electrolyte is so strong that essentially all of the charge at any potential will lie adjacent to the solution, unless the percentage of the phase area in contact with electrolyte is really minuscule.¹¹

What real mechanisms are there for charging a phase at all? An important one is simply to pump electrons into or out of a metal or semiconductor with a power supply of some sort. In fact, we will make great use of this approach as the basis for control over the kinetics of electrode processes. In addition, there are chemical mechanisms. For example, we know from experience that a platinum wire dipped into a solution containing ferricyanide and ferrocyanide will have its potential shift toward a predictable equilibrium value given by the Nernst equation. This process occurs because the electron affinities of the two phases initially differ; hence there is a transfer of electrons from the metal to the solution or vice versa. Ferricyanide is reduced or ferrocyanide is oxidized. The transfer of charge continues until the resulting change in potential reaches the equilibrium point, where the electron affinities of the solution and the metal are equal. Compared to the total charge that could be transferred to or from ferri- and ferrocyanide in a typical system, only a tiny charge is needed to establish the equilibrium at Pt; consequently, the net chemical effects on the solution are unnoticeable. By this mechanism, the metal adapts to the solution and reflects its composition.

Electrochemistry is full of situations like this one, in which charged species (electrons or ions) cross interfacial boundaries. These processes generally create a net transfer of charge that sets up the equilibrium or steady-state potential differences that we observe. Considering them in more detail must, however, await the development of additional concepts (see Section 2.3 and Chapter 3).

Actually, interfacial potential differences can develop without an excess charge on either phase. Consider an aqueous electrolyte in contact with an electrode. Since the electrolyte interacts with the metal surface (e.g., wetting it), the water dipoles in contact with the metal generally have some preferential orientation. From a coulombic standpoint, this situation is equivalent to charge separation across the interface, because the dipoles are

¹¹As it can be with an ultramicroelectrode. See Section 5.3.

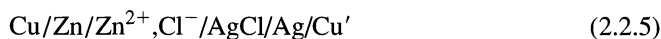
not randomized with time. Since moving a test charge through the interface requires work, the interfacial potential difference is not zero (23–26).¹²

2.2.3 Measurement of Potential Differences

We have already noted that the difference in the inner potentials, $\Delta\phi$, of two phases in contact is a factor of primary importance to electrochemical processes occurring at the interface between them. Part of its influence comes from the local electric fields reflecting the large changes in potential in the boundary region. These fields can reach values as high as 10^7 V/cm. They are large enough to distort electroreactants so as to alter reactivity, and they can affect the kinetics of charge transport across the interface. Another aspect of $\Delta\phi$ is its direct influence over the relative energies of charged species on either side of the interface. In this way, $\Delta\phi$ controls the relative electron affinities of the two phases; hence it controls the direction of reaction.

Unfortunately, $\Delta\phi$ cannot be measured for a single interface, because one cannot sample the electrical properties of the solution without introducing at least one more interface. It is characteristic of devices for measuring potential differences (e.g., potentiometers, voltmeters, or electrometers) that they can be calibrated only to register potential differences between two phases of the same composition, such as the two metal contacts available at most instruments. Consider $\Delta\phi$ at the interface Zn/Zn^{2+} , Cl^- . Shown in Figure 2.2.4a is the simplest approach one could make to $\Delta\phi$ using a potentiometric instrument with copper contacts. The measurable potential difference between the copper phases clearly includes interfacial potential differences at the Zn/Cu interface and the $\text{Cu}/\text{electrolyte}$ interface in addition to $\Delta\phi$. We might simplify matters by constructing a voltmeter wholly from zinc but, as shown in Figure 2.2.4b, the measurable voltage would still contain contributions from two separate interfacial potential differences.

By now we realize that a measured cell potential is a sum of several interfacial differences, none of which we can evaluate independently. For example, one could sketch the potential profile through the cell



according to Vetter's representation (24) in the manner of Figure 2.2.5.¹³

Even with these complications, it is still possible to focus on a single interfacial potential difference, such as that between zinc and the electrolyte in (2.2.5). If we can maintain constant interfacial potentials at all of the other junctions in the cell, then any *change* in E must be wholly attributed to a *change* in $\Delta\phi$ at the zinc/electrolyte boundary. Keeping the other junctions at a constant potential difference is not so difficult, for the metal-

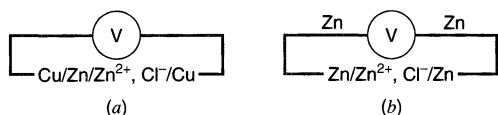


Figure 2.2.4 Two devices for measuring the potential of a cell containing the Zn/Zn^{2+} interface.

¹²Sometimes it is useful to break the inner potential into two components called the *outer* (or *Volta*) potential, ψ , and the *surface potential*, χ . Thus, $\phi = \psi + \chi$. There is a large, detailed literature on the establishment, the meaning, and the measurement of interfacial potential differences and their components. See references 23–26.

¹³Although silver chloride is a separate phase, it does not contribute to the cell potential, because it does not physically separate silver from the electrolyte. In fact, it need not even be present; one merely requires a solution saturated in silver chloride to measure the same cell potential.

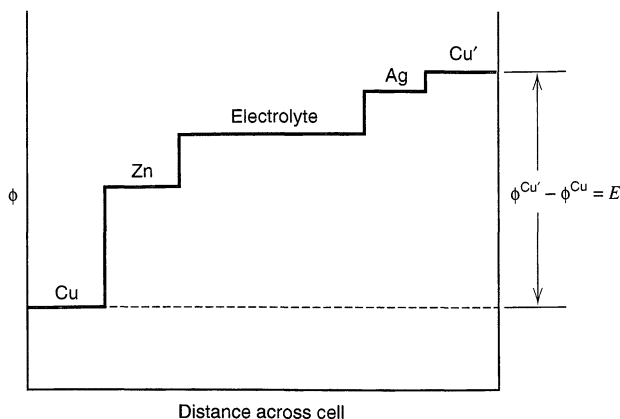


Figure 2.2.5 Potential profile across a whole cell at equilibrium.

metal junctions always remain constant (at constant temperature) without attention, and the silver/electrolyte junction can be fixed if the activities of the participants in its half-reaction remain fixed. When this idea is realized, the whole rationale behind half-cell potentials and the choice of reference electrodes becomes much clearer.

2.2.4 Electrochemical Potentials

Let us consider again the interface Zn/Zn^{2+} , Cl^- (aqueous) and focus on zinc ions in metallic zinc and in solution. In the metal, Zn^{2+} is fixed in a lattice of positive zinc ions, with free electrons permeating the structure. In solution, zinc ion is hydrated and may interact with Cl^- . The energy state of Zn^{2+} in any location clearly depends on the chemical environment, which manifests itself through short-range forces that are mostly electrical in nature. In addition, there is the energy required simply to bring the +2 charge, disregarding the chemical effects, to the location in question. This second energy is clearly proportional to the potential ϕ at the location; hence it depends on the electrical properties of an environment very much larger than the ion itself. Although one cannot experimentally separate these two components for a single species, the differences in the scales of the two environments responsible for them makes it plausible to separate them mathematically (23–26). Butler (27) and Guggenheim (28) developed the conceptual separation and introduced the *electrochemical potential*, $\bar{\mu}_i^\alpha$, for species i with charge z_i in phase α :

$$\boxed{\bar{\mu}_i^\alpha = \mu_i^\alpha + z_i F \phi^\alpha} \quad (2.2.6)$$

The term μ_i^α is the familiar *chemical potential*

$$\mu_i^\alpha = \left(\frac{\partial G}{\partial n_i} \right)_{T,P,n_j \neq i} \quad (2.2.7)$$

where n_i is the number of moles of i in phase α . Thus, the electrochemical potential would be

$$\bar{\mu}_i^\alpha = \left(\frac{\partial \bar{G}}{\partial n_i} \right)_{T,P,n_j \neq i} \quad (2.2.8)$$

where the *electrochemical free energy*, \bar{G} , differs from the *chemical free energy*, G , by the inclusion of effects from the large-scale electrical environment.

(a) Properties of the Electrochemical Potential

1. For an uncharged species: $\bar{\mu}_i^\alpha = \mu_i^\alpha$.
2. For any substance: $\mu_i^\alpha = \mu_i^{0\alpha} + RT \ln a_i^\alpha$, where $\mu_i^{0\alpha}$ is the standard chemical potential, and a_i^α is the activity of species i in phase α .
3. For a pure phase at unit activity (e.g., solid Zn, AgCl, Ag, or H₂ at unit fugacity): $\bar{\mu}_i^\alpha = \mu_i^{0\alpha}$.
4. For electrons in a metal ($z = -1$): $\bar{\mu}_e^\alpha = \mu_e^{0\alpha} - F\phi^\alpha$. Activity effects can be disregarded because the electron concentration never changes appreciably.
5. For equilibrium of species i between phases α and β : $\bar{\mu}_i^\alpha = \bar{\mu}_i^\beta$.

(b) Reactions in a Single Phase

Within a single conducting phase, ϕ is constant everywhere and exerts no effect on a chemical equilibrium. The ϕ terms drop out of relations involving electrochemical potentials, and only chemical potentials will remain. Consider, for example, the acid–base equilibrium:



This requires that

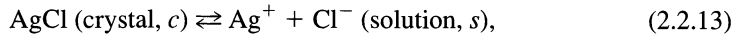
$$\bar{\mu}_{\text{HOAc}} = \bar{\mu}_{\text{H}^+} + \bar{\mu}_{\text{OAc}^-} \quad (2.2.10)$$

$$\mu_{\text{HOAc}} = \mu_{\text{H}^+} + F\phi + \mu_{\text{OAc}^-} - F\phi \quad (2.2.11)$$

$$\mu_{\text{HOAc}} = \mu_{\text{H}^+} + \mu_{\text{OAc}^-} \quad (2.2.12)$$

(c) Reactions Involving Two Phases Without Charge Transfer

Let us now examine the solubility equilibrium



which can be treated in two ways. First, one can consider separate equilibria involving Ag^+ and Cl^- in solution and in the solid. Thus

$$\bar{\mu}_{\text{Ag}^+}^{\text{AgCl}} = \bar{\mu}_{\text{Ag}^+}^s \quad (2.2.14)$$

$$\bar{\mu}_{\text{Cl}^-}^{\text{AgCl}} = \bar{\mu}_{\text{Cl}^-}^s \quad (2.2.15)$$

Recognizing that

$$\bar{\mu}_{\text{AgCl}}^{\text{AgCl}} = \bar{\mu}_{\text{Ag}^+}^{\text{AgCl}} + \bar{\mu}_{\text{Cl}^-}^{\text{AgCl}} \quad (2.2.16)$$

one has from the sum of (2.2.14) and (2.2.15),

$$\mu_{\text{AgCl}}^{0\text{AgCl}} = \bar{\mu}_{\text{Ag}^+}^s + \bar{\mu}_{\text{Cl}^-}^s \quad (2.2.17)$$

Expanding, we obtain

$$\mu_{\text{AgCl}}^{0\text{AgCl}} = \mu_{\text{Ag}^+}^{0s} + RT \ln a_{\text{Ag}^+}^s + F\phi^s + \mu_{\text{Cl}^-}^{0s} + RT \ln a_{\text{Cl}^-}^s - F\phi^s \quad (2.2.18)$$

and rearrangement gives

$$\mu_{\text{AgCl}}^{0\text{AgCl}} - \mu_{\text{Ag}^+}^{0s} - \mu_{\text{Cl}^-}^{0s} = RT \ln (a_{\text{Ag}^+}^s a_{\text{Cl}^-}^s) = RT \ln K_{\text{sp}} \quad (2.2.19)$$

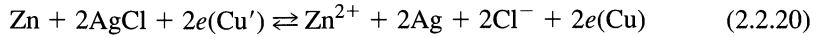
where K_{sp} is the solubility product. A quicker route to this well-known result is to write down (2.2.17) directly from the chemical equation, (2.2.13).

Note that the ϕ^s terms canceled in (2.2.18), and that an implicit cancellation of ϕ^{AgCl} terms occurred in (2.2.16). Since the final result depends only on chemical potentials, the

equilibrium is unaffected by the potential difference across the interface. This is a general feature of interphase reactions without transfer of charge (either ionic or electronic). When charge transfer does occur, the ϕ terms will not cancel and the interfacial potential difference strongly affects the chemical process. We can use that potential difference either to probe or to alter the equilibrium position.

(d) Formulation of a Cell Potential

Consider now the cell (2.2.5), for which the cell reaction can be written



At equilibrium,

$$\bar{\mu}_{\text{Zn}}^{\text{Zn}} + 2\bar{\mu}_{\text{AgCl}}^{\text{AgCl}} + 2\bar{\mu}_{\text{e}}^{\text{Cu}'} = \bar{\mu}_{\text{Zn}^{2+}}^{\text{Zn}^{2+}} + 2\bar{\mu}_{\text{Ag}}^{\text{Ag}} + 2\bar{\mu}_{\text{Cl}^-}^{\text{Cl}^-} + 2\bar{\mu}_{\text{e}}^{\text{Cu}} \quad (2.2.21)$$

$$2(\bar{\mu}_{\text{e}}^{\text{Cu}'} - \bar{\mu}_{\text{e}}^{\text{Cu}}) = \bar{\mu}_{\text{Zn}^{2+}}^{\text{Zn}^{2+}} + 2\bar{\mu}_{\text{Ag}}^{\text{Ag}} + 2\bar{\mu}_{\text{Cl}^-}^{\text{Cl}^-} - \bar{\mu}_{\text{Zn}}^{\text{Zn}} - 2\bar{\mu}_{\text{AgCl}}^{\text{AgCl}} \quad (2.2.22)$$

But,

$$2(\bar{\mu}_{\text{e}}^{\text{Cu}'} - \bar{\mu}_{\text{e}}^{\text{Cu}}) = -2F(\phi^{\text{Cu}'} - \phi^{\text{Cu}}) = -2FE \quad (2.2.23)$$

Expanding (2.2.22), we have

$$-2FE = \mu_{\text{Zn}^{2+}}^{0\text{s}} + RT \ln a_{\text{Zn}^{2+}}^{\text{s}} + 2F\phi^{\text{s}} + 2\mu_{\text{Ag}}^{0\text{Ag}} + 2\mu_{\text{Cl}^-}^{0\text{s}} \quad (2.2.24)$$

$$+ 2RT \ln a_{\text{Cl}^-}^{\text{s}} - 2F\phi^{\text{s}} - \mu_{\text{Zn}}^{0\text{Zn}} - 2\mu_{\text{AgCl}}^{0\text{AgCl}} \quad (2.2.25)$$

$$-2FE = \Delta G^0 + RT \ln a_{\text{Zn}^{2+}}^{\text{s}} (a_{\text{Cl}^-}^{\text{s}})^2$$

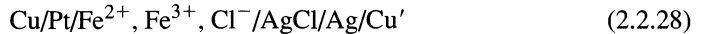
where

$$\Delta G^0 = \mu_{\text{Zn}^{2+}}^{0\text{s}} + 2\mu_{\text{Cl}^-}^{0\text{s}} + 2\mu_{\text{Ag}}^{0\text{Ag}} - \mu_{\text{Zn}}^{0\text{Zn}} - 2\mu_{\text{AgCl}}^{0\text{AgCl}} = -2FE^0 \quad (2.2.26)$$

Thus, we arrive at

$$E = E^0 - \frac{RT}{2F} \ln(a_{\text{Zn}^{2+}}^{\text{s}})(a_{\text{Cl}^-}^{\text{s}})^2, \quad (2.2.27)$$

which is the Nernst equation for the cell. This corroboration of an earlier result displays the general utility of electrochemical potentials for treating interfacial reactions with charge transfer. They are powerful tools. For example, they are easily used to consider whether the two cells



would have the same cell potential. This point is left to the reader as Problem 2.8.

2.2.5 Fermi Level and Absolute Potential

The electrochemical potential of electrons in a phase α , $\bar{\mu}_{\text{e}}^{\alpha}$, is called the *Fermi level* or *Fermi energy* and corresponds to an electron energy (not an electrical potential) $\mathbf{E}_{\text{F}}^{\alpha}$. The Fermi level represents the average energy of available electrons in phase α and is related to the chemical potential of electrons in that phase, μ_{e}^{α} , and the inner potential of α .¹⁴ The Fermi level of a metal or semiconductor depends on the work function of the material (see Section 18.2.2). For a solution phase, it is a function of the electrochemical potentials of

¹⁴More exactly, it is the energy where the occupation probability is 0.5 in the distribution of electrons among the various energy levels (the Fermi–Dirac distribution). See Sections 3.6.3 and 18.2.2 for more discussion of \mathbf{E}_{F} .

the dissolved oxidized and reduced species. For example, for a solution containing Fe^{3+} and Fe^{2+}

$$\bar{\mu}_e^s = \bar{\mu}_{\text{Fe}^{2+}}^s - \bar{\mu}_{\text{Fe}^{3+}}^s \quad (2.2.30)$$

For an inert metal in contact with a solution, the condition for electrical (or electronic) equilibrium is that the Fermi levels of the two phases be equal, that is,

$$\mathbf{E}_F^s = \mathbf{E}_F^M \quad (2.2.31)$$

This condition is equivalent to saying that the electrochemical potentials of electrons in both phases are equal, or that the average energies of available (i.e., transferable) electrons are the same in both phases. When an initially uncharged metal is brought into contact with an initially uncharged solution, the Fermi levels will not usually be equal. As discussed in Section 2.2.2, equality is attained by the transfer of electrons between the phases, with electrons flowing from the phase with the higher Fermi level (higher $\bar{\mu}_e$ or more energetic electrons) to the phase with the lower Fermi level. This electron flow causes the potential difference between the phases (the electrode potential) to shift.

For most purposes in electrochemistry, it is sufficient to reference the potentials of electrodes (and half-cell emfs) arbitrarily to the NHE, but it is sometimes of interest to have an estimate of the *absolute* or *single electrode potential* (i.e., vs. the potential of a free electron in vacuum). This interest arises, for example, if one would like to estimate relative potentials of metals or semiconductors based on their work functions. The absolute potential of the NHE can be estimated as 4.5 ± 0.1 V, based on certain extrathermodynamic assumptions, such as about the energy involved in moving a proton from the gas phase into an aqueous solution (10, 29). Thus, the amount of energy needed to remove an electron from $\text{Pt}/\text{H}_2/\text{H}^+$ ($a = 1$) to vacuum is about 4.5 eV or 434 kJ.¹⁵ With this value, the standard potentials of other couples and reference electrodes can be expressed on the absolute scale (Figure 2.1.1).

2.3 LIQUID JUNCTION POTENTIALS

2.3.1 Potential Differences at an Electrolyte–Electrolyte Boundary

To this point, we have examined only systems at equilibrium, and we have learned that the potential differences in equilibrium electrochemical systems can be treated exactly by thermodynamics. However, many real cells are never at equilibrium, because they feature different electrolytes around the two electrodes. There is somewhere an interface between the two solutions, and at that point, mass transport processes work to mix the solutes. Unless the solutions are the same initially, the *liquid junction* will not be at equilibrium, because net flows of mass occur continuously across it.

Such a cell is



for which we can depict the equilibrium processes as in Figure 2.3.1. The overall cell potential at null current is then

$$E = (\phi^{\text{Cu}'} - \phi^\beta) - (\phi^{\text{Cu}} - \phi^\alpha) + (\phi^\beta - \phi^\alpha) \quad (2.3.2)$$

¹⁵The potential and the Fermi energy of an electrode have different signs, because the potential is based on energy changes involving a positive test charge, while the Fermi energy refers to a negative electron.

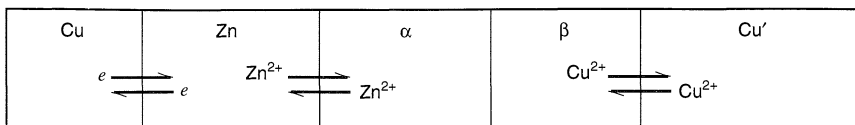


Figure 2.3.1 Schematic view of the phases in cell (2.3.1). Equilibrium is established for certain charge carriers as shown, but at the liquid junction between the two electrolyte phases α and β , equilibrium is not reached.

Obviously, the first two components of E are the expected interfacial potential differences at the copper and zinc electrodes. The third term shows that the measured cell potential depends also on the potential difference between the electrolytes, that is, on the *liquid junction potential*. This discovery is a real threat to our system of electrode potentials, because it is based on the idea that all contributions to E can be assigned unambiguously to one electrode or to the other. How could the junction potential possibly be assigned properly? We must evaluate the importance of these phenomena.

2.3.2 Types of Liquid Junctions

The reality of junction potentials is easily understood by considering the boundary shown in Figure 2.3.2a. At the junction, there is a steep concentration gradient in H^+ and Cl^- ; hence both ions tend to diffuse from right to left. Since the hydrogen ion has a much larger mobility than Cl^- , it initially penetrates the dilute phase at a higher rate. This process gives a positive charge to the dilute phase and a negative charge to the concentrated one, with the result that a boundary potential difference develops. The corresponding electric field then retards the movement of H^+ and speeds up the passage of Cl^- until the two cross the boundary at equal rates. Thus, there is a detectable steady-state potential, which is not due to an equilibrium process (3, 24, 30, 31). From its origin, this interfacial potential is sometimes called a *diffusion potential*.

Lingane (3) classified liquid junctions into three types:

1. Two solutions of the same electrolyte at different concentrations, as in Figure 2.3.2a.
2. Two solutions at the same concentration with different electrolytes having an ion in common, as in Figure 2.3.2b.
3. Two solutions not satisfying conditions 1 or 2, as in Figure 2.3.2c.

We will find this classification useful in the treatments of junction potentials that follow.

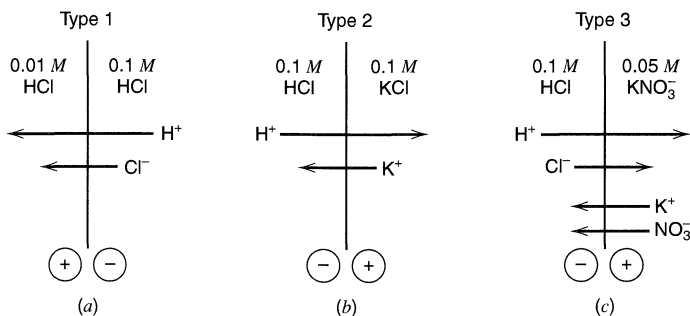
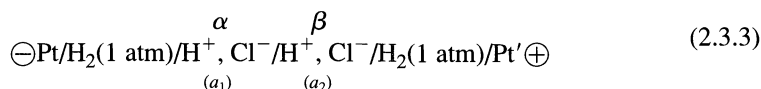


Figure 2.3.2 Types of liquid junctions. Arrows show the direction of net transfer for each ion, and their lengths indicate relative mobilities. The polarity of the junction potential is indicated in each case by the circled signs. [Adapted from J. J. Lingane, "Electroanalytical Chemistry," 2nd ed., Wiley-Interscience, New York, 1958, p. 60, with permission.]

Even though the boundary region cannot be at equilibrium, it has a composition that is effectively constant over long time periods, and the reversible transfer of electricity through the region can be considered.

Conductance, Transference Numbers, and Mobility

When an electric current flows in an electrochemical cell, the current is carried in solution by the movement of ions. For example, take the cell:



where $a_2 > a_1$.¹⁶ When the cell operates galvanically, an oxidation occurs at the left electrode,



and a reduction happens on the right,



Therefore, there is a tendency to build up a positive charge in the α phase and a negative charge in β . This tendency is overcome by the movement of ions: H^+ to the right and Cl^- to the left. For each mole of electrons passed, 1 mole of H^+ is produced in α , and 1 mole of H^+ is consumed in β . The total amount of H^+ and Cl^- migrating across the boundary between α and β must equal 1 mole.

The fractions of the current carried by H^+ and Cl^- are called their *transference numbers* (or *transport numbers*). If we let t_+ be the transference number for H^+ and t_- be that for Cl^- , then clearly,

$$t_+ + t_- = 1 \quad (2.3.6)$$

In general, for an electrolyte containing many ions, i ,

$$\sum_i t_i = 1 \quad (2.3.7)$$

Schematically, the process can be represented as shown in Figure 2.3.3. The cell initially features a higher activity of hydrochloric acid (+ as H^+ , - as Cl^-) on the right (Figure

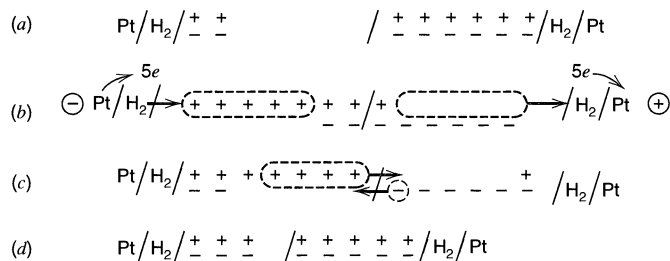


Figure 2.3.3 Schematic diagram showing the redistribution of charge during electrolysis of a system featuring a high concentration of HCl on the right and a low concentration on the left.

¹⁶A cell like (2.3.3), having electrodes of the same type on both sides, but with differing activities of one or both of the redox forms, is called a *concentration cell*.

2.3.3a); hence discharging it spontaneously produces H^+ on the left and consumes it on the right. Assume that five units of H^+ are reacted as shown in Figure 2.3.3b. For hydrochloric acid, $t_+ \approx 0.8$ and $t_- \approx 0.2$; therefore, four units of H^+ must migrate to the right and one unit of Cl^- to the left to maintain electroneutrality. This process is depicted in Figure 2.3.3c, and the final state of the solution is represented in Figure 2.3.3d.

A charge imbalance like that suggested in Figure 2.3.3b could not actually occur, because a very large electric field would be established, and it would work to erase the imbalance. On a macroscopic scale, electroneutrality is always maintained throughout the solution. The migration represented in Figure 2.3.3c occurs simultaneously with the electron-transfer reactions.

Transference numbers are determined by the details of ionic conduction, which are understood mainly through measurements of either the resistance to current flow in solution or its reciprocal, the conductance, L (31, 32). The value of L for a segment of solution immersed in an electric field is directly proportional to the cross-sectional area perpendicular to the field vector and is inversely proportional to the length of the segment along the field. The proportionality constant is the *conductivity*, κ , which is an intrinsic property of the solution:

$$L = \kappa A/l \quad (2.3.8)$$

The conductance, L , is given in units of siemens ($\text{S} = \Omega^{-1}$), and κ is expressed in S cm^{-1} or $\Omega^{-1} \text{cm}^{-1}$.

Since the passage of current through the solution is accomplished by the independent movement of different species, κ is the sum of contributions from all ionic species, i . It is intuitive that each component of κ is proportional to the concentration of the ion, the magnitude of its charge $|z_i|$, and some index of its migration velocity.

That index is the *mobility*, u_i , which is the limiting velocity of the ion in an electric field of unit strength. Mobility usually carries dimensions of $\text{cm}^2 \text{V}^{-1} \text{s}^{-1}$ (i.e., cm/s per V/cm). When a field of strength \mathcal{E} is applied to an ion, it will accelerate under the force imposed by the field until the frictional drag exactly counterbalances the electric force. Then, the ion continues its motion at that terminal velocity. This balance is represented in Figure 2.3.4.

The magnitude of the force exerted by the field is $|z_i| e \mathcal{E}$, where e is the electronic charge. The frictional drag can be approximated from the Stokes law as $6\pi\eta r v$, where η is the viscosity of the medium, r is the radius of the ion, and v is the velocity. When the terminal velocity is reached, we have by equation and rearrangement,

$$u_i = \frac{v}{\mathcal{E}} = \frac{|z_i| e}{6\pi\eta r} \quad (2.3.9)$$

The proportionality factor relating an individual ionic conductivity to charge, mobility, and concentration turns out to be the Faraday constant; thus

$$\kappa = F \sum_i |z_i| u_i C_i \quad (2.3.10)$$

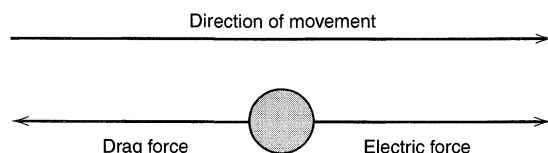


Figure 2.3.4 Forces on a charged particle moving in solution under the influence of an electric field. The forces balance at the terminal velocity.

The transference number for species i is merely the contribution to conductivity made by that species divided by the total conductivity:

$$t_i = \frac{|z_i|u_i C_i}{\sum_j |z_j|u_j C_j} \quad (2.3.11)$$

For solutions of simple, pure electrolytes (i.e., one positive and one negative ionic species), such as KCl, CaCl₂, and HNO₃, conductance is often quantified in terms of the *equivalent conductivity*, Λ , which is defined by

$$\Lambda = \frac{\kappa}{C_{\text{eq}}} \quad (2.3.12)$$

where C_{eq} is the concentration of positive (or negative) charges. Thus, Λ expresses the conductivity per unit concentration of charge. Since $C|z| = C_{\text{eq}}$ for either ionic species in these systems, one finds from (2.3.10) and (2.3.12) that

$$\Lambda = F(u_+ + u_-) \quad (2.3.13)$$

where u_+ refers to the cation and u_- to the anion. This relation suggests that Λ could be regarded as the sum of individual *equivalent ionic conductivities*,

$$\Lambda = \lambda_+ + \lambda_- \quad (2.3.14)$$

hence we find

$$\lambda_i = F u_i \quad (2.3.15)$$

In these simple solutions, then, the transference number t_i is given by

$$t_i = \frac{\lambda_i}{\Lambda} \quad (2.3.16)$$

or, alternatively,

$$t_i = \frac{u_i}{u_+ + u_-} \quad (2.3.17)$$

Transference numbers can be measured by several approaches (31, 32), and numerous data for pure solutions appear in the literature. Frequently, transference numbers are measured by noting concentration changes caused by electrolysis, as in the experiment shown in Figure 2.3.3 (see Problem 2.11). Table 2.3.1 displays a few values for aqueous solutions at 25°C. From results of this sort, one can evaluate the individual ionic conductivities, λ_i . Both λ_i and t_i depend on the concentration of the pure electrolyte, because interactions between ions tend to alter the mobilities (31–33). Lists of λ values, like Table 2.3.2, usually give figures for λ_{0i} , which are obtained by extrapolation to infinite dilution. In the absence of measured transference numbers, it is convenient to use these to estimate t_i for pure solutions by (2.3.16), or for mixed electrolytes by the following equivalent to (2.3.11),

$$t_i = \frac{|z_i|C_i\lambda_i}{\sum_j |z_j|C_j\lambda_j} \quad (2.3.18)$$

In addition to the liquid electrolytes that we have been considering, *solid electrolytes*, such as sodium β -alumina, the silver halides, and polymers like polyethylene

TABLE 2.3.1 Cation Transference Numbers for Aqueous Solutions at 25°C^a

Electrolyte	Concentration, C_{eq}^b			
	0.01	0.05	0.1	0.2
HCl	0.8251	0.8292	0.8314	0.8337
NaCl	0.3918	0.3876	0.3854	0.3821
KCl	0.4902	0.4899	0.4898	0.4894
NH ₄ Cl	0.4907	0.4905	0.4907	0.4911
KNO ₃	0.5084	0.5093	0.5103	0.5120
Na ₂ SO ₄	0.3848	0.3829	0.3828	0.3828
K ₂ SO ₄	0.4829	0.4870	0.4890	0.4910

^aFrom D. A. MacInnes, "The Principles of Electrochemistry," Dover, New York, 1961, p. 85 and references cited therein.

^bMoles of positive (or negative) charge per liter.

oxide/LiClO₄ (34, 35), are sometimes used in electrochemical cells. In these materials, ions move under the influence of an electric field, even in the absence of solvent. For example, the conductivity of a single crystal of sodium β -alumina at room temperature is 0.035 S/cm, a value similar to that of aqueous solutions. Solid electrolytes are technologically important in the fabrication of batteries and electrochemical devices. In some of these materials (e.g., α -Ag₂S and AgBr), and unlike essentially all liquid electrolytes,

TABLE 2.3.2 Ionic Properties at Infinite Dilution in Aqueous Solutions at 25°C

Ion	$\lambda_0, \text{cm}^2 \Omega^{-1} \text{equiv}^{-1a}$	$u, \text{cm}^2 \text{sec}^{-1} \text{V}^{-1b}$
H ⁺	349.82	3.625×10^{-3}
K ⁺	73.52	7.619×10^{-4}
Na ⁺	50.11	5.193×10^{-4}
Li ⁺	38.69	4.010×10^{-4}
NH ₄ ⁺	73.4	7.61×10^{-4}
$\frac{1}{3}\text{Ca}^{2+}$	59.50	6.166×10^{-4}
OH ⁻	198	2.05×10^{-3}
Cl ⁻	76.34	7.912×10^{-4}
Br ⁻	78.4	8.13×10^{-4}
I ⁻	76.85	7.96×10^{-4}
NO ₃ ⁻	71.44	7.404×10^{-4}
OAc ⁻	40.9	4.24×10^{-4}
ClO ₄ ⁻	68.0	7.05×10^{-4}
$\frac{1}{2}\text{SO}_4^{2-}$	79.8	8.27×10^{-4}
HCO ₃ ⁻	44.48	4.610×10^{-4}
$\frac{1}{3}\text{Fe}(\text{CN})_6^{3-}$	101.0	1.047×10^{-3}
$\frac{1}{4}\text{Fe}(\text{CN})_6^{4-}$	110.5	1.145×10^{-3}

^aFrom D. A. MacInnes, "The Principles of Electrochemistry," Dover, New York, 1961, p. 342

^bCalculated from λ_0 .

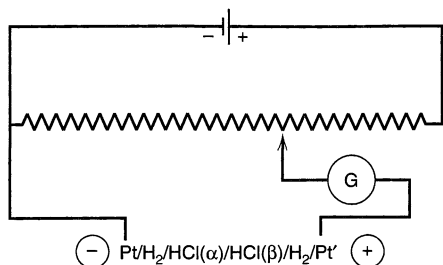


Figure 2.3.5 Experimental system for demonstrating reversible flow of charge through a cell with a liquid junction.

there is electronic conductivity as well as ionic conductivity. The relative contribution of electronic conduction through the solid electrolyte can be found by applying a potential to a cell that is too small to drive electrochemical reactions and noting the magnitude of the (nonfaradaic) current. Alternatively, an electrolysis can be carried out and the faradaic contribution determined separately (see Problem 2.12).

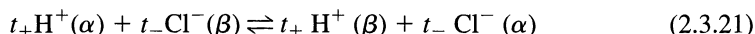
2.3.4 Calculation of Liquid Junction Potentials

Imagine the concentration cell (2.3.3) connected to a power supply as shown in Figure 2.3.5. The voltage from the supply opposes that from the cell, and one finds experimentally that it is possible to oppose the cell voltage exactly, so that no current flows through the galvanometer, G . If the magnitude of the opposing voltage is reduced very slightly, the cell operates spontaneously as described above, and electrons flow from Pt to Pt' in the external circuit. The process occurring at the liquid junction is the passage of an equivalent negative charge from right to left. If the opposing voltage is increased from the null point, the entire process reverses, including charge transfer through the interface between the electrolytes. The fact that an infinitesimal change in the driving force can reverse the direction of charge passage implies that the *electrochemical* free energy change for the whole process is zero.

These events can be divided into those involving the chemical transformations at the metal–solution interfaces:



and that effecting charge transport at the liquid junction depicted in Figure 2.3.6:



Note that (2.3.19) and (2.3.20) are at strict equilibrium under the null-current condition; hence the electrochemical free energy change for each of them individually is zero. Of course, this is also true for their sum:

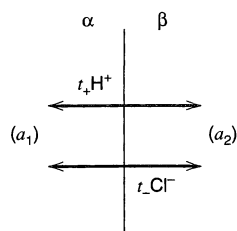
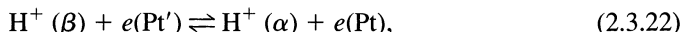


Figure 2.3.6 Reversible charge transfer through the liquid junction in Figure 2.3.5.

which describes the chemical change in the system. The sum of this equation and the charge transport relation, (2.3.21), describes the overall cell operation. However, since we have just learned that the electrochemical free energy changes for both the overall process and (2.3.22) are zero, we must conclude that the electrochemical free energy change for (2.3.21) is also zero. In other words, charge transport across the junction occurs in such a way that the electrochemical free energy change vanishes, even though it cannot be considered as a process at equilibrium. This important conclusion permits an approach to the calculation of junction potentials.

Let us focus first on the net chemical reaction, (2.3.22). Since the electrochemical free energy change is zero,

$$\bar{\mu}_{H^+}^\beta + \bar{\mu}_e^{Pt'} = \bar{\mu}_{H^+}^\alpha + \bar{\mu}_e^{Pt} \quad (2.3.23)$$

$$FE = F(\phi^{Pt'} - \phi^{Pt}) = \bar{\mu}_{H^+}^\beta - \bar{\mu}_{H^+}^\alpha \quad (2.3.24)$$

$$E = \frac{RT}{F} \ln \frac{a_2}{a_1} + (\phi^\beta - \phi^\alpha) \quad (2.3.25)$$

The first component of E in (2.3.25) is merely the Nernst relation for the reversible chemical change, and $\phi^\beta - \phi^\alpha$ is the liquid junction potential. In general, for a chemically reversible system under null current conditions,

$$E_{\text{cell}} = E_{\text{Nernst}} + E_j \quad (2.3.26)$$

hence the junction potential is always an additive perturbation onto the nernstian response.

To evaluate E_j , we consider (2.3.21), for which

$$t_+ \bar{\mu}_{H^+}^\alpha + t_- \bar{\mu}_{Cl^-}^\beta = t_+ \bar{\mu}_{H^+}^\beta + t_- \bar{\mu}_{Cl^-}^\alpha \quad (2.3.27)$$

Thus,

$$t_+(\bar{\mu}_{H^+}^\alpha - \bar{\mu}_{H^+}^\beta) + t_-(\bar{\mu}_{Cl^-}^\beta - \bar{\mu}_{Cl^-}^\alpha) = 0 \quad (2.3.28)$$

$$t_+ \left[RT \ln \frac{a_{H^+}^\alpha}{a_{H^+}^\beta} + F(\phi^\alpha - \phi^\beta) \right] + t_- \left[RT \ln \frac{a_{Cl^-}^\beta}{a_{Cl^-}^\alpha} - F(\phi^\beta - \phi^\alpha) \right] = 0 \quad (2.3.29)$$

Activity coefficients for single ions cannot be measured with thermodynamic rigor (30, 36, 37–38); hence they are usually equated to a measurable *mean ionic activity coefficient*. Under this procedure, $a_{H^+}^\alpha = a_{Cl^-}^\alpha = a_1$ and $a_{H^+}^\beta = a_{Cl^-}^\beta = a_2$. Since $t_+ + t_- = 1$, we have

$$E_j = (\phi^\beta - \phi^\alpha) = (t_+ - t_-) \frac{RT}{F} \ln \frac{a_1}{a_2} \quad (2.3.30)$$

for a type 1 junction involving 1:1 electrolytes.

Consider, for example, HCl solutions with $a_1 = 0.01$ and $a_2 = 0.1$. We can see from Table 2.3.1 that $t_+ = 0.83$ and $t_- = 0.17$; hence at 25°C

$$E_j = (0.83 - 0.17)(59.1) \log \left(\frac{0.01}{0.1} \right) = -39.1 \text{ mV} \quad (2.3.31)$$

For the total cell,

$$E = 59.1 \log \frac{a_2}{a_1} + E_j = 59.1 - 39.1 = 20.0 \text{ mV} \quad (2.3.32)$$

thus, the junction potential is a substantial component of the measured cell potential.

In the derivation above, we made the implicit assumption that the transference numbers were constant throughout the system. This is a very good approximation for junctions

of type 1; hence (2.3.30) is not seriously compromised. For type 2 and type 3 systems, it clearly cannot be true. To consider these cases, one must imagine the junction region to be sectioned into an infinite number of volume elements having compositions that range smoothly from the pure α -phase composition to that of pure β . Transporting charge across one of these elements involves every ionic species in the element, and $t_i/|z_i|$ moles of species i must move for each mole of charge passed. Thus, the passage of positive charge from α toward β might be depicted as in Figure 2.3.7. One can see that the change in electrochemical free energy upon moving any species is $(t_i/z_i)d\bar{\mu}_i$ (recall that z_i is a signed quantity); therefore, the differential in free energy is

$$d\bar{G} = \sum_i \frac{t_i}{z_i} d\bar{\mu}_i \quad (2.3.33)$$

Integrating from the α phase to the β phase, we have

$$\int_{\alpha}^{\beta} d\bar{G} = 0 = \sum_i \int_{\alpha}^{\beta} \frac{t_i}{z_i} d\bar{\mu}_i \quad (2.3.34)$$

If μ_i^0 for the α phase is the same as that for the β phase (e.g., if both are aqueous solutions),

$$\sum_i \int_{\alpha}^{\beta} \frac{t_i}{z_i} RT d \ln a_i + \left(\sum_i t_i \right) F \int_{\alpha}^{\beta} d\phi = 0 \quad (2.3.35)$$

Since $\sum_i t_i = 1$,

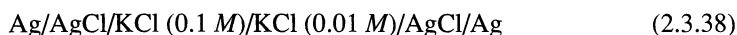
$$E_j = \phi^{\beta} - \phi^{\alpha} = \frac{-RT}{F} \sum_i \int_{\alpha}^{\beta} \frac{t_i}{z_i} d \ln a_i \quad (2.3.36)$$

which is the general expression for the junction potential.

It is easy to see now that (2.3.30) is a special case for type 1 junctions between 1:1 electrolytes having constant t_i . Note that E_j is a strong function of t_+ and t_- , and that it actually vanishes if $t_+ = t_-$. The value of E_j as a function of t_+ for a 1:1 electrolyte with $a_1/a_2 = 10$ is

$$E_j = 59.1 (2t_+ - 1) \text{ mV} \quad (2.3.37)$$

at 25°C. For example, the cell



has $t_+ = 0.49$; hence $E_j = -1.2 \text{ mV}$.

While type 1 junctions can be treated with some rigor and are independent of the method of forming the junction, type 2 and type 3 junctions have potentials that depend on the technique of junction formation (e.g., static or flowing) and can be treated only in an approximate manner. Different approaches to junction formation apparently lead to

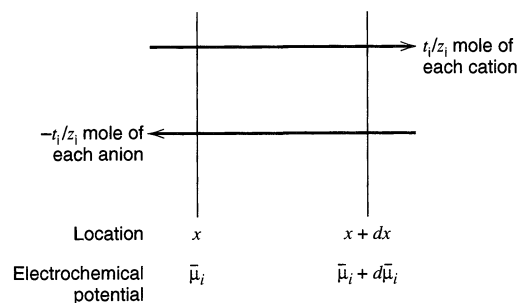


Figure 2.3.7 Transfer of net positive charge from left to right through an infinitesimal segment of a junction region. Each species must contribute t_i moles of charge per mole of overall charge transported; hence $t_i/|z_i|$ moles of that species must migrate.

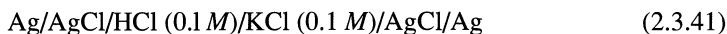
different profiles of t_i through the junction, which in turn lead to different integrals for (2.3.36). Approximate values for E_j can be obtained by assuming (a) that concentrations of ions everywhere in the junction are equivalent to activities and (b) that the concentration of each ion follows a linear transition between the two phases. Then, (2.3.36) can be integrated to give the *Henderson equation* (24, 30):

$$E_j = \frac{\sum_i \frac{|z_i| u_i}{z_i} [C_i(\beta) - C_i(\alpha)]}{\sum_i |z_i| u_i [C_i(\beta) - C_i(\alpha)]} \frac{RT}{F} \ln \frac{\sum_i |z_i| u_i C_i(\alpha)}{\sum_i |z_i| u_i C_i(\beta)} \quad (2.3.39)$$

where u_i is the mobility of species i , and C_i is its molar concentration. For type 2 junctions between 1:1 electrolytes, this equation collapses to the *Lewis–Sargent relation*:

$$E_j = \pm \frac{RT}{F} \ln \frac{\Lambda_\beta}{\Lambda_\alpha} \quad (2.3.40)$$

where the positive sign corresponds to a junction with a common cation in the two phases, and the negative sign applies to the case with a common anion. As an example, consider the cell



for which E_{cell} is essentially E_j . The measured value at 25°C is 28 ± 1 mV, depending on the technique of junction formation (30), while the estimated value from (2.3.40) and the data of Table 2.3.2 is 26.8 mV.

2.3.5 Minimizing Liquid Junction Potentials

In most electrochemical experiments, the junction potential is an additional troublesome factor, so attempts are often made to minimize it. Alternatively, one hopes that it is small or that it at least remains constant. A familiar method for minimizing E_j is to replace the junction, for example,



with a system featuring a concentrated solution in an intermediate *salt bridge*, where the solution in the bridge has ions of nearly equal mobility. Such a system is

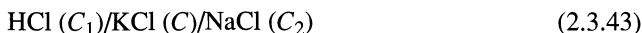


Table 2.3.3 lists some measured junction potentials for the cell,



As C increases, E_j falls markedly, because ionic transport at the two junctions is dominated more and more extensively by the massive amounts of KCl. The series junctions become more similar in magnitude and have opposite polarities; hence they tend to cancel. Solutions used in aqueous salt bridges usually contain KCl ($t_+ = 0.49$, $t_- = 0.51$) or, where Cl^- is deleterious, KNO_3 ($t_+ = 0.51$, $t_- = 0.49$). Other concentrated solutions with equitransferent ions that have been suggested (39) for salt bridges include CsCl ($t_+ = 0.5025$), RbBr ($t_+ = 0.4958$), and NH_4I ($t_+ = 0.4906$). In many measurements, such as the determination of pH, it is sufficient if the junction potential remains constant between calibra-

TABLE 2.3.3 Effect of a Salt Bridge on Measured Junction Potentials^a

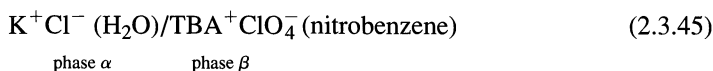
Concentration of KCl, $C(M)$	E_j, mV
0.1	27
0.2	20
0.5	13
1.0	8.4
2.5	3.4
3.5	1.1
4.2 (saturated)	<1

^aSee J. J. Lingane, "Electroanalytical Chemistry," Wiley-Interscience, New York, 1958, p. 65. Original data from H. A. Fales and W. C. Vosburgh, *J. Am. Chem. Soc.*, **40**, 1291 (1918); E. A. Guggenheim, *ibid.*, **52**, 1315 (1930); and A. L. Ferguson, K. Van Lente, and R. Hitchens, *ibid.*, **54**, 1285 (1932).

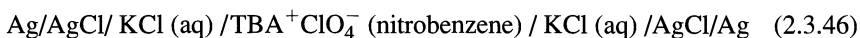
tion (e.g., with a standard buffer or solution) and measurement. However, variations in E_j of 1–2 mV can be expected, and should be considered in any interpretations made from potentiometric data.

2.3.6 Junctions of Two Immiscible Liquids

Another junction of interest is that between two immiscible electrolyte solutions (40–44). A typical junction of this type would be



where $TBA^+ ClO_4^-$ is tetra-*n*-butylammonium perchlorate. Of interest in connection with ion-selective electrodes (Section 2.4.3) and as models for biological membranes are related cells with immiscible liquids between two aqueous phases, such as



where the intermediate liquid layer behaves as a membrane. The treatment of the potentials across junctions like (2.3.45) is similar to that given earlier in this section, except that the standard free energies of a species i in the two phases, $\mu_i^{0\alpha}$ and $\mu_i^{0\beta}$, are now different. The junction potential then becomes (40, 41)

$$\phi^\beta - \phi^\alpha = -\frac{1}{z_i F} \left[\Delta G_{\text{transfer},i}^{0\alpha \rightarrow \beta} + RT \ln \left(\frac{a_i^\beta}{a_i^\alpha} \right) \right] \quad (2.3.47)$$

where $\Delta G_{\text{transfer},i}^{0\alpha \rightarrow \beta}$ is the standard free energy required to transfer species i with charge z_i between the two phases and is defined as

$$\Delta G_{\text{transfer},i}^{0\alpha \rightarrow \beta} = \mu_i^{0\beta} - \mu_i^{0\alpha} \quad (2.3.48)$$

This quantity can be estimated, for example, from solubility data, but only with an extrathermodynamic assumption of some kind. For example, for the salt tetraphenylarsonium tetraphenylborate ($TPAs^+ TPB^-$), it is widely assumed that the free energy of solvation ($\Delta G_{\text{solvn}}^0$) of $TPAs^+$ is equal to that of TPB^- , since both are large ions with most of the charge buried deep inside the surrounding phenyl rings (45). Consequently, the in-

dividual ion solvation energies are taken as one-half of the solvation energy of the salt, which is measurable from the solubility product in a given solvent. That is,

$$\Delta G_{\text{solvn}}^0(\text{TPAs}^+) = \Delta G_{\text{solvn}}^0(\text{TPB}^-) = \frac{1}{2}\Delta G_{\text{solvn}}^0(\text{TPAs}^+\text{TPB}^-) \quad (2.3.49)$$

$$\Delta G_{\text{transfer, TPAs}^+}^{0\alpha\rightarrow\beta} = \Delta G_{\text{solvn}}^0(\text{TPAs}^+, \beta) - \Delta G_{\text{solvn}}^0(\text{TPAs}^+, \alpha) \quad (2.3.50)$$

The free energy of transfer can also be obtained from the partitioning of the salt between the phases α and β . For each ion, the value determined in this way should be the same as that calculated in (2.3.50), if the intersolubility of α and β is very small.

The *rate* of transfer of ions across interfaces between immiscible liquids is also of interest and can be obtained from electrochemical measurements (Section 6.8).

► 2.4 SELECTIVE ELECTRODES (46–55)

2.4.1 Selective Interfaces

Suppose one could create an interface between two electrolyte phases across which only a single ion could penetrate. A selectively permeable membrane might be used as a separator to accomplish this end. Equation 2.3.34 would still apply; but it could be simplified by recognizing that the transference number for the permeating ion is unity, while that for every other ion is zero. If both electrolytes are in a common solvent, one obtains by integration

$$\frac{RT}{z_i} \ln \frac{a_i^\beta}{a_i^\alpha} + F(\phi^\beta - \phi^\alpha) = 0 \quad (2.4.1)$$

where ion i is the permeating species. Rearrangement gives

$$E_m = -\frac{RT}{z_i F} \ln \frac{a_i^\beta}{a_i^\alpha} \quad (2.4.2)$$

If the activity of species i is held constant in one phase, the potential difference between the two phases (often called the *membrane potential*, E_m) responds in a Nernst-like fashion to the ion's activity in the other phase.

This idea is the essence of ion-selective electrodes. Measurements with these devices are essentially determinations of membrane potentials, which themselves comprise junction potentials between electrolyte phases. The performance of any single system is determined largely by the degree to which the species of interest can be made to dominate charge transport in part of the membrane. We will see below that real devices are fairly complicated, and that selectivity in charge transport throughout the membrane is both rarely achieved and actually unnecessary.

Many ion-selective interfaces have been studied, and several different types of electrodes have been marketed commercially. We will examine the basic strategies for introducing selectivity by considering a few of them here. The glass membrane is our starting point because it offers a fairly complete view of the fundamentals as well as the usual complications found in practical devices.

2.4.2 Glass Electrodes

The ion-selective properties of glass/electrolyte interfaces were recognized early in the 20th century, and glass electrodes have been used since then for measurements of pH and the activities of alkali ions (24, 37, 46–55). Figure 2.4.1 depicts the construction of a typi-

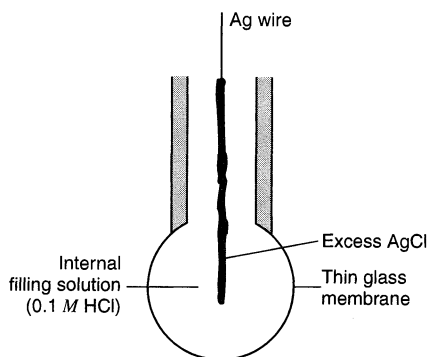
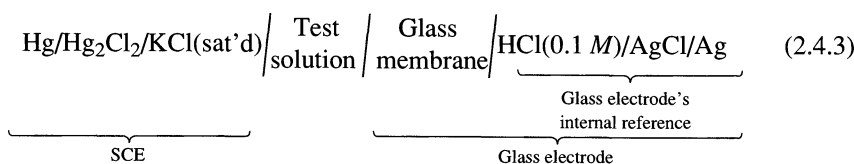


Figure 2.4.1 A typical glass electrode.

cal device. To make measurements, the thin membrane is fully immersed in the test solution, and the potential of the electrode is registered with respect to a reference electrode such as an SCE. Thus, the cell becomes,



The properties of the test solution influence the overall potential difference of the cell at two points. One of them is the liquid junction between the SCE and the test solution. From the considerations of Section 2.3.5, we can hope that the potential difference there is small and constant. The remaining contribution from the test solution comes from its effect on the potential difference across the glass membrane. Since all of the other interfaces in the cell feature phases of constant composition, changes in the cell potential can be wholly ascribed to the junction between the glass membrane and the test solution. If that interface is selective toward a single species i , the cell potential is

$$E = \text{constant} + \frac{RT}{z_i F} \ln a_i^{\text{soln}} \quad (2.4.4)$$

where the constant term is the sum of potential differences at all of the other interfaces.¹⁷ The constant term is evaluated by “standardizing” the electrode, that is, by measuring E for a cell in which the test solution is replaced by a standard solution having a known activity for species i .¹⁸

Actually, the operation of the glass phase is rather complicated (24, 37, 46–48, 51). The bulk of the membrane, which might be about 50 μm thick, is dry glass through which charge transport occurs exclusively by the mobile cations present in the glass. Usually, these are alkali ions, such as Na^+ or Li^+ . Hydrogen ion from solution does not contribute to conduction in this region. The faces of the membrane in contact with solution differ from the bulk, in that the silicate structure of the glass is hydrated. As shown in Figure 2.4.2, the hydrated layers are thin. Interactions between the glass and the adjacent solution, which occur exclusively in the hydrated zone, are facilitated kinetically by the swelling that accompanies the hydration.

¹⁷Equation 2.4.4 is derived from (2.4.2) by recognizing the test solution as phase α and the internal filling solution of the electrode as phase β . See also Figures 2.3.5 and 2.3.6.

¹⁸By the phrase “activity for species i ” we mean the concentration of i multiplied by the mean ionic activity coefficient. See Section 2.3.4 for a commentary and references related to the concept of single-ion activities.

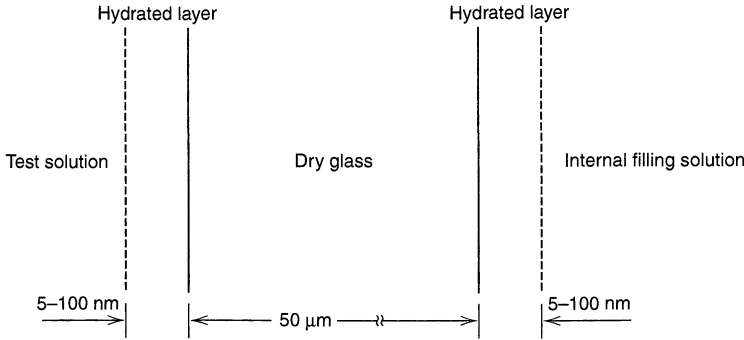


Figure 2.4.2 Schematic profile through a glass membrane.

The membrane potentials appear because the silicate network has an affinity for certain cations, which are adsorbed (probably at fixed anionic sites) within the structure. This action creates a charge separation that alters the interfacial potential difference. That potential difference, in turn, alters the rates of adsorption and desorption. Thus, the rates are gradually brought into balance by a mechanism resembling the one responsible for the establishment of junction potentials, as discussed above.

Obviously, the glass membrane does not adhere to the simplified idea of a selectively permeable membrane. In fact, it may not be at all permeable to some of the ions of greatest interest, such as H^+ . Thus, the transference number of such an ion cannot be unity throughout the membrane, and it may actually be zero in certain zones. Can we still understand the observed selective response? The answer is yes, provided that the ion of interest dominates charge transport in the interfacial regions of the membrane.

Let us consider a model for the glass membrane like that shown in Figure 2.4.3. The glass will be considered as comprising three regions. In the interfacial zones, m' and m'' , there is rapid attainment of equilibrium with constituents in solution, so that each adsorbing cation has an activity reflecting its corresponding activity in the adjacent solution. The bulk of the glass is denoted by m , and we presume that conduction there takes place by a single species, which is taken as Na^+ for the sake of this argument. The whole system therefore comprises five phases, and the overall difference in potential across the membrane is the sum of four contributions from the junctions between the various zones:

$$E_m = (\phi^\beta - \phi^{m''}) + (\phi^{m''} - \phi^m) + (\phi^m - \phi^{m'}) + (\phi^{m'} - \phi^\alpha) \quad (2.4.5)$$

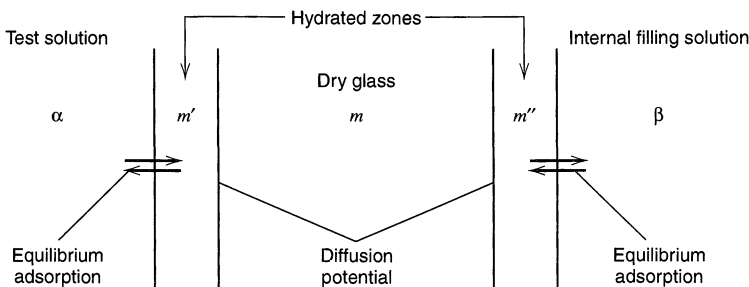


Figure 2.4.3 Model for treating the membrane potential across a glass barrier.

The first and last terms are interfacial potential differences arising from an *equilibrium balance* of selective charge exchange across an interface. This condition is known as *Donnan equilibrium* (24, 51). The magnitude of the resulting potential difference can be evaluated from electrochemical potentials. Suppose we have Na^+ and H^+ as interfacially active ions. Then at the α/m' interface,

$$\bar{\mu}_{\text{H}^+}^{\alpha} = \bar{\mu}_{\text{H}^+}^{m'} \quad (2.4.6)$$

$$\bar{\mu}_{\text{Na}^+}^{\alpha} = \bar{\mu}_{\text{Na}^+}^{m'} \quad (2.4.7)$$

Expanding (2.4.6), we have

$$\mu_{\text{H}^+}^{0\alpha} + RT \ln a_{\text{H}^+}^{\alpha} + F\phi^{\alpha} = \mu_{\text{H}^+}^{0m'} + RT \ln a_{\text{H}^+}^{m'} + F\phi^{m'} \quad (2.4.8)$$

and rearrangement gives

$$(\phi^{m'} - \phi^{\alpha}) = \frac{\mu_{\text{H}^+}^{0\alpha} - \mu_{\text{H}^+}^{0m'}}{F} + \frac{RT}{F} \ln \frac{a_{\text{H}^+}^{\alpha}}{a_{\text{H}^+}^{m'}} \quad (2.4.9)$$

An equivalent treatment of the interface between β and m'' gives

$$(\phi^{\beta} - \phi^{m''}) = \frac{\mu_{\text{H}^+}^{0m''} - \mu_{\text{H}^+}^{0\beta}}{F} + \frac{RT}{F} \ln \frac{a_{\text{H}^+}^{m''}}{a_{\text{H}^+}^{\beta}} \quad (2.4.10)$$

Note that $\mu_{\text{H}^+}^{0\alpha} = \mu_{\text{H}^+}^{0\beta}$, because both α and β are aqueous solutions. Similarly, $\mu_{\text{H}^+}^{0m'} = \mu_{\text{H}^+}^{0m''}$. When we add (2.4.9) and (2.4.10) later in this development, these equivalencies will cause the terms involving μ^0 to disappear.

The second and third components in (2.4.5) are junction potentials within the glass membrane. In the specialized literature, they are called *diffusion potentials*, because they arise from differential ionic diffusion in the manner discussed in Section 2.3.2. The systems correspond to type 3 junctions as defined there.

We can treat them through a variant of the Henderson equation, (2.3.39), which was introduced earlier in Section 2.3.4. The usual form of this equation is derived from (2.3.36) by neglecting activity effects and assuming linear concentration profiles through the junction. Here, we are interested only in univalent positive charge carriers; hence we can specialize (2.3.39) for the interface between m and m' as

$$(\phi^m - \phi^{m'}) = \frac{RT}{F} \ln \frac{u_{\text{H}^+} a_{\text{H}^+}^{m'} + u_{\text{Na}^+} a_{\text{Na}^+}^{m'}}{u_{\text{Na}^+} a_{\text{Na}^+}^m} \quad (2.4.11)$$

where the concentrations have been replaced by activities. Also, for the interface between m and m'' ,

$$(\phi^{m''} - \phi^m) = \frac{RT}{F} \ln \frac{u_{\text{Na}^+} a_{\text{Na}^+}^m}{u_{\text{H}^+} a_{\text{H}^+}^{m''} + u_{\text{Na}^+} a_{\text{Na}^+}^{m''}} \quad (2.4.12)$$

Now let us add the component potential differences, (2.4.9)–(2.4.12), as dictated by (2.4.5), to obtain the whole potential difference across the membrane.¹⁹

$$\begin{aligned} E_m &= \frac{RT}{F} \ln \frac{a_{\text{H}^+}^{\alpha} a_{\text{H}^+}^{m''}}{a_{\text{H}^+}^{\beta} a_{\text{H}^+}^{m'}} && \text{(Donnan Term)} \\ &+ \frac{RT}{F} \ln \frac{(u_{\text{Na}^+}/u_{\text{H}^+})a_{\text{Na}^+}^{m'} + a_{\text{H}^+}^{m'}}{(u_{\text{Na}^+}/u_{\text{H}^+})a_{\text{Na}^+}^{m''} + a_{\text{H}^+}^{m''}} && \text{(Diffusion term)} \end{aligned} \quad (2.4.13)$$

¹⁹Note that the diffusion term here is the same as that which would be predicted by the Henderson equation from the compositions of m' and m'' without considering m as a separate phase. Many treatments of this problem follow such an approach. We have added the phase m because the three-phase model for the membrane is more realistic with regard to the assumptions underlying the Henderson equation.

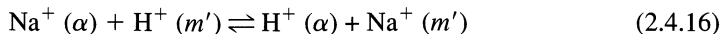
Some important simplifications can be made in this result. First, we combine the two terms in (2.4.13) and rearrange the parameters to give

$$E_m = \frac{RT}{F} \ln \frac{(u_{\text{Na}^+}/u_{\text{H}^+})(a_{\text{H}^+}^\alpha a_{\text{Na}^+}^{m'}/a_{\text{H}^+}^{m'}) + a_{\text{H}^+}^\alpha}{(u_{\text{Na}^+}/u_{\text{H}^+})(a_{\text{H}^+}^\beta a_{\text{Na}^+}^{m'}/a_{\text{H}^+}^{m'}) + a_{\text{H}^+}^\beta} \quad (2.4.14)$$

Now consider (2.4.6) and (2.4.7), which apply simultaneously. Their sum must also be true:

$$\bar{\mu}_{\text{Na}^+}^\alpha + \bar{\mu}_{\text{H}^+}^{m'} = \bar{\mu}_{\text{H}^+}^\alpha + \bar{\mu}_{\text{Na}^+}^{m'} \quad (2.4.15)$$

This equation is a free energy balance for the ion-exchange reaction:



Since it does not involve net charge transfer, it is not sensitive to the interfacial potential difference [see Section 2.2.4(c)], and it has an equilibrium constant given by

$$K_{\text{H}^+, \text{Na}^+} = \frac{a_{\text{H}^+}^\alpha a_{\text{Na}^+}^{m'}}{a_{\text{H}^+}^{m'} a_{\text{Na}^+}^\alpha} \quad (2.4.17)$$

An equivalent expression, involving the same numeric value of $K_{\text{H}^+, \text{Na}^+}$, would apply to the interface between phases β and m' . These relations can be substituted into (2.4.14) to give

$$E_m = \frac{RT}{F} \ln \frac{(u_{\text{Na}^+}/u_{\text{H}^+})K_{\text{H}^+, \text{Na}^+} a_{\text{Na}^+}^\alpha + a_{\text{H}^+}^\alpha}{(u_{\text{Na}^+}/u_{\text{H}^+})K_{\text{H}^+, \text{Na}^+} a_{\text{Na}^+}^\beta + a_{\text{H}^+}^\beta} \quad (2.4.18)$$

Since $K_{\text{H}^+, \text{Na}^+}$ and $u_{\text{Na}^+}/u_{\text{H}^+}$ are constants of the experiment, it is convenient to define their product as the *potentiometric selectivity coefficient*, $k_{\text{H}^+, \text{Na}^+}^{\text{pot}}$:

$$E_m = \frac{RT}{F} \ln \frac{a_{\text{H}^+}^\alpha + k_{\text{H}^+, \text{Na}^+}^{\text{pot}} a_{\text{Na}^+}^\alpha}{a_{\text{H}^+}^\beta + k_{\text{H}^+, \text{Na}^+}^{\text{pot}} a_{\text{Na}^+}^\beta} \quad (2.3.19)$$

If the β phase is the internal filling solution (of constant composition) and the α phase is the test solution, then the overall potential of the cell is

$$E = \text{constant} + \frac{RT}{F} \ln (a_{\text{H}^+}^\alpha + k_{\text{H}^+, \text{Na}^+}^{\text{pot}} a_{\text{Na}^+}^\alpha) \quad (2.4.20)$$

This expression tells us that the cell potential is responsive to the activities of both Na^+ and H^+ in the test solution, and that the degree of selectivity between these species is defined $k_{\text{H}^+, \text{Na}^+}^{\text{pot}}$. If the product $k_{\text{H}^+, \text{Na}^+}^{\text{pot}} a_{\text{Na}^+}^\alpha$ is much less than $a_{\text{H}^+}^\alpha$, then the membrane responds essentially exclusively to H^+ . When that condition applies, charge exchange between the phases α and m' is dominated by H^+ .

We have formulated this problem in a manner that considers only Na^+ and H^+ as active species. Glass membranes also respond to other ions, such as Li^+ , K^+ , Ag^+ , and NH_4^+ . The relative responses can be expressed through the corresponding potentiometric selectivity coefficients (see Problem 2.16 for some typical numbers), which are influenced to a great extent by the composition of the glass. Different types of electrodes, based on different types of glass, are marketed. They are broadly classified as (a) *pH electrodes* with a selectivity order $\text{H}^+ \gg \gg \text{Na}^+ > \text{K}^+, \text{Rb}^+, \text{Cs}^+ \gg \text{Ca}^{2+}$, (b) *sodium-sensitive electrodes* with the order $\text{Ag}^+ > \text{H}^+ > \text{Na}^+ \gg \text{K}^+, \text{Li}^+ \gg \text{Ca}^{2+}$, and (c) a more general *cation-sensitive electrode* with a narrower range of selectivities in the order $\text{H}^+ > \text{K}^+ > \text{Na}^+ > \text{NH}_4^+, \text{Li}^+ \gg \text{Ca}^{2+}$.

There is a large literature on the design, performance, and theory of glass electrodes (37, 46–55). The interested reader is referred to it for more advanced discussions.

2.4.3 Other Ion-Selective Electrodes

The principles that we have just reviewed also apply to other types of selective membranes (48, 50–59). They fall generally into two categories.

(a) Solid-State Membranes

Like the glass membrane, which is a member of this group, the remaining common solid-state membranes are electrolytes having tendencies toward the preferential adsorption of certain ions on their surfaces.

Consider, for example, the single-crystal LaF_3 membrane, which is doped with EuF_2 to create fluoride vacancies that allow ionic conduction by fluoride. Its surface selectively accommodates F^- to the virtual exclusion of other species except OH^- .

Other devices are made from precipitates of insoluble salts, such as AgCl , AgBr , AgI , Ag_2S , CuS , CdS , and PbS . The precipitates are usually pressed into pellets or are suspended in polymer matrices. The silver salts conduct by mobile Ag^+ ions, but the heavy metal sulfides are usually mixed with Ag_2S , since they are not very conductive. The surfaces of these membranes are generally sensitive to the ions comprising the salts, as well as to other species that tend to form very insoluble precipitates with a constituent ion. For example, the Ag_2S membrane responds to Ag^+ , S^{2-} , and Hg^{2+} . Likewise, the AgCl membrane is sensitive to Ag^+ , Cl^- , Br^- , I^- , CN^- , and OH^- .

(b) Liquid and Polymer Membranes

An alternative structure utilizes a hydrophobic liquid membrane as the sensing element. The liquid is stabilized physically between an aqueous internal filling solution and an aqueous test solution by allowing it to permeate a porous, lipophilic diaphragm. A reservoir contacting the outer edges of the diaphragm contains this liquid. Chelating agents with selectivity toward ions of interest are dissolved in it, and they provide the mechanism for selective charge transport across the boundaries of the membrane.

A device based on these principles is a calcium-selective electrode. The hydrophobic solvent might be dioctylphenylphosphonate, and the chelating agent might be the sodium salt of an alkyl phosphate ester, $(\text{RO})_2\text{PO}_2\text{Na}^+$, where R is an aliphatic chain having 8–18 carbons. The membrane is sensitive to Ca^{2+} , Zn^{2+} , Fe^{2+} , Pb^{2+} , Cu^{2+} , tetra-alkylammonium ions, and still other species to lesser degrees. “Water hardness” electrodes are based on similar agents, but are designed to show virtually equal responses to Ca^{2+} and Mg^{2+} .

Other systems featuring liquid ion-exchangers are available for anions, such as NO_3^- , ClO_4^- , and Cl^- . Nitrate and perchlorate are sensed by membranes including alkylated 1,10-phenanthroline complexes of Ni^{2+} and Fe^{2+} , respectively. All three ions are active at other membranes based on quaternary ammonium salts.

In commercial electrodes, the liquid ion-exchanger is in a form in which the chelating agent is immobilized in a hydrophobic polymer membrane like poly(vinylchloride) (Figure 2.4.4). Electrodes based on this design (called *polymer* or *plastic membrane ISEs*) are more rugged and generally offer superior performance.

Liquid ion-exchangers all feature charged chelating agents, and various ion-exchange equilibria play a role in their operation. A related type of device, also featuring a stabilized liquid membrane, involves uncharged chelating agents that enable the transport of charge by selectively complexing certain ions. These agents are sometimes called *neutral carriers*. Systems based on them typically also involve the presence of some anionic sites in the membrane, either naturally occurring or added in the form of hydrophobic ions, and these anionic sites contribute to the ion-exchange process (56–58). It has also been proposed that electrodes based on neutral carriers operate by a phase-boundary (i.e., adsorption), rather than a carrier mechanism (59).

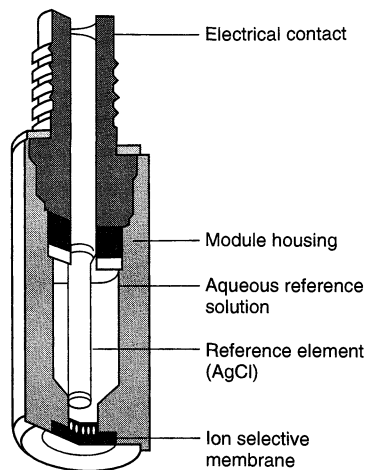


Figure 2.4.4 A typical plastic membrane ISE. [Courtesy of Orion Research, Inc.]

For example, potassium-selective electrodes can be constructed with the natural macrocycle valinomycin as a neutral carrier in diphenyl ether. This membrane has a much higher sensitivity to K^+ than to Na^+ , Li^+ , Mg^{2+} , Ca^{2+} , or H^+ ; but Rb^+ and Cs^+ are sensed to much the same degree as K^+ . The selectivity seems to rest mostly on the molecular recognition of the target ion by the complexing site of the carrier.

(c) Commercial Devices

Table 2.4.1 is a listing of typical commercial ion-selective electrodes, the pH and concentration ranges over which they operate, and typical interferences. Selectivity coefficients for many of these electrodes are available (55, 57).

TABLE 2.4.1 Typical Commercially Available Ion-Selective Electrodes

Species	Type ^a	Concentration Range(M)	pH Range	Interferences
Ammonium (NH_4^+)	L	10^{-1} to 10^{-6}	5–8	K^+ , Na^+ , Mg^{2+}
Barium (Ba^{2+})	L	10^{-1} to 10^{-5}	5–9	K^+ , Na^+ , Ca^{2+}
Bromide (Br^-)	S	1 to 10^{-5}	2–12	I^- , S^{2-} , CN^-
Cadmium (Cd^{2+})	S	10^{-1} to 10^{-7}	3–7	Ag^+ , Hg^{2+} , Cu^{2+} , Pb^{2+} , Fe^{3+}
Calcium (Ca^{2+})	L	1 to 10^{-7}	4–9	Ba^{2+} , Mg^{2+} , Na^+ , Pb^{2+}
Chloride (Cl^-)	S	1 to 5×10^{-5}	2–11	I^- , S^{2-} , CN^- , Br^-
Copper (Cu^{2+})	S	10^{-1} to 10^{-7}	0–7	Ag^+ , Hg^{2+} , S^{2-} , Cl^- , Br^-
Cyanide (CN^-)	S	10^{-2} to 10^{-6}	10–14	S^{2-}
Fluoride (F^-)	S	1 to 10^{-7}	5–8	OH^-
Iodide (I^-)	S	1 to 10^{-7}	3–12	S^{2-}
Lead (Pb^{2+})	S	10^{-1} to 10^{-6}	0–9	Ag^+ , Hg^{2+} , S^{2-} , Cd^{2+} , Cu^{2+} , Fe^{3+}
Nitrate (NO_3^-)	L	1 to 5×10^{-6}	3–10	Cl^- , Br^- , NO_2^- , F^- , SO_4^{2-}
Nitrite (NO_2^-)	L	1 to 10^{-6}	3–10	Cl^- , Br^- , NO_3^- , F^- , SO_4^{2-}
Potassium (K^+)	L	1 to 10^{-6}	4–9	Na^+ , Ca^{2+} , Mg^{2+}
Silver (Ag^+)	S	1 to 10^{-7}	2–9	S^{2-} , Hg^{2+}
Sodium (Na^+)	G	Sat'd to 10^{-6}	9–12	Li^+ , K^+ , NH_4^+
Sulfide (S^{2-})	S	1 to 10^{-7}	12–14	Ag^+ , Hg^{2+}

^aG = glass; L = liquid membrane; S = solid-state. Typical temperature ranges are 0–50°C for liquid-membrane and 0–80°C for solid-state electrodes.

(d) Detection Limits

As shown in Table 2.4.1, the lower limit for detection of an ion with an ISE is generally 10^{-6} to 10^{-7} M. This limit is largely governed by the leaching of ions from the internal electrolyte into the sample solution (60). The leakage can be prevented by using a lower concentration of the ion of interest in the internal electrolyte, so that the concentration gradient established in the membrane causes an ion flux from the sample to the inner electrolyte. This low concentration can be maintained with an *ion buffer*, that is, a mixture of the metal ion with an excess of a strong complexing agent. In addition, a high concentration of a second potential-determining ion is added to the internal solution. Under these conditions, the lower detection limit can be considerably improved. For example, for a conventional liquid-membrane Pb^{2+} electrode with an internal filling solution of 5×10^{-4} M Pb^{2+} and 5×10^{-2} M Mg^{2+} , the detection limit for Pb^{2+} was 4×10^{-6} M. When the internal solution was changed to 10^{-3} M Pb^{2+} and 5×10^{-2} M Na_2EDTA (yielding a free $[\text{Pb}^{2+}] = 10^{-12}$ M), the detection limit decreased to 5×10^{-12} M (61). In the internal solution, the dominant potential-determining ion is Na^+ at 0.1 M.

2.4.4 Gas-Sensing Electrodes

Figure 2.4.5 depicts the structure of a typical potentiometric gas-sensing electrode (62). In general, such a device involves a glass pH electrode that is protected from the test solution by a polymer diaphragm. Between the glass membrane and the diaphragm is a small volume of electrolyte. Small molecules, such as SO_2 , NH_3 , and CO_2 , can penetrate the membrane and interact with the trapped electrolyte by reactions that produce changes in pH. The glass electrode responds to the alterations in acidity.

Electrochemical cells that use a solid electrolyte composed of zirconium dioxide containing Y_2O_3 (yttria-stabilized zirconia) are available to measure the oxygen content of gases at high temperature. In fact, sensors of this type are widely used to monitor the exhaust gas from the internal combustion engines of motor vehicles, so that the air-to-fuel mixture can be controlled to minimize the emission of pollutants such as CO and NO_x . This solid electrolyte shows good conductivity only at high temperatures (500–1,000°C), where the conduction process is the migration of oxide ions. A typical sensor is composed of a tube of zirconia with Pt electrodes deposited on the inside and outside of the tube. The outside electrode contacts air with a known partial pressure of

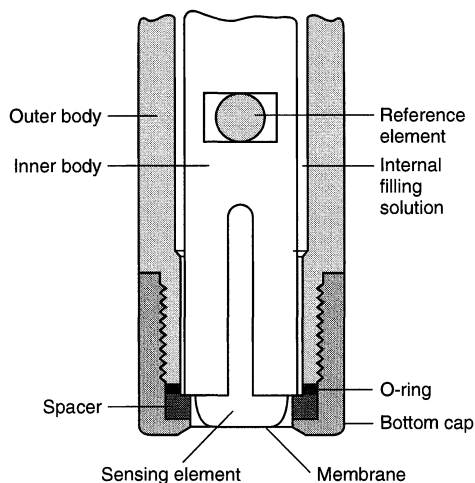
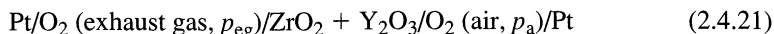


Figure 2.4.5 Structure of a gas-sensing electrode. [Courtesy of Orion Research, Inc.]

oxygen, p_a , and serves as the reference electrode. The inside of the tube is exposed to the hot exhaust gas with a lower oxygen partial pressure, p_{eg} . The cell configuration can thus be written



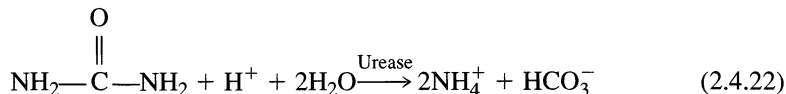
and the potential of this oxygen concentration cell can be used to measure p_{eg} (Problem 2.19).

We note here that the widely employed *Clark oxygen electrode* differs fundamentally from these devices (18, 63). The Clark device is similar in construction to the apparatus of Figure 2.4.5, in that a polymer membrane traps an electrolyte against a sensing surface. However, the sensor is a platinum electrode, and the analytical signal is the steady-state *current* flow due to the faradaic reduction of molecular oxygen.

2.4.5 Enzyme-Coupled Devices

The natural specificity of enzyme-catalyzed reactions can be used as the basis for selective detection of analytes (49, 64–68). One fruitful approach has featured potentiometric sensors with a structure similar to that of Figure 2.4.5, with the difference that the gap between the ion-selective electrode and the polymer diaphragm is filled with a matrix in which an enzyme is immobilized.

For example, urease, together with a buffered electrolyte, might be held in a cross-linked polyacrylamide gel. When the electrode is immersed in a test solution, there will be a selective response toward urea, which diffuses through the diaphragm into the gel. The response comes about because the urease catalyzes the process:



The resulting ammonium ions can be detected with a cation-sensitive glass membrane. Alternatively, one could use a gas-sensing electrode for ammonia in place of the glass electrode, so that interferences from H^+ , Na^+ , and K^+ are reduced.

The research literature features many examples of this basic strategy. Different enzymes allow selective determinations of single species, such as glucose (with glucose oxidase), or groups of substances such as the L-amino acids (with L-amino acid oxidase). Recent reviews should be consulted for a more complete view of the field (66–68).

Amperometric enzyme electrodes are discussed in Sections 14.2.5 and 14.4.2(c).

▶ 2.5 REFERENCES

1. The arguments presented here follow those given earlier by D. A. MacInnes (“The Principles of Electrochemistry,” Dover, New York, 1961, pp. 110–113) and by J. J. Lingane (“Electroanalytical Chemistry,” 2nd ed., Wiley-Interscience, New York, 1958, pp. 40–45). Experiments like those described here were actually carried out by H. Jahn (*Z. Physik. Chem.*, **18**, 399 (1895)).
2. I. M. Klotz and R. M. Rosenberg, “Chemical Thermodynamics,” 4th ed., Benjamin/Cummings, Menlo Park, CA, 1986.
3. J. J. Lingane, “Electroanalytical Chemistry,” 2nd ed., Wiley-Interscience, New York, 1958, Chap. 3.
4. F. C. Anson, *J. Chem. Educ.*, **36**, 394 (1959).
5. A. J. Bard, R. Parsons, and J. Jordan, Eds., “Standard Potentials in Aqueous Solutions,” Marcel Dekker, New York, 1985.
6. <http://webbook.nist.gov/>, National Institute of Standards and Technology.
7. A. J. Bard and H. Lund, Eds., “Encyclopedia of Electrochemistry of the Elements,” Marcel Dekker, New York, 1973–1980.

8. M. W. Chase, Jr., "NIST-JANAF Thermochemical Tables," 4th ed., American Chemical Society, Washington, and American Institute of Physics, New York, for the National Institute of Standards and Technology, 1998.
9. L. R. Faulkner, *J. Chem. Educ.*, **60**, 262 (1983).
10. R. Parsons in A. J. Bard, R. Parsons, and J. Jordan, Eds., *op.cit.*, Chap. 1.
11. A. Henglein, *Ber. Bunsenges. Phys. Chem.*, **94**, 600 (1990).
12. A. Henglein, *Top. Curr. Chem.*, **1988**, 113.
13. A. Henglein, *Accts. Chem. Res.*, **9**, 1861 (1989).
14. D. W. Suggs and A. J. Bard, *J. Am. Chem. Soc.*, **116**, 10725 (1994).
15. R. Parsons, *op. cit.*, p. 5.
16. D. J. G. Ives and G. J. Janz, Eds., "Reference Electrodes," Academic, New York, 1961.
17. J. N. Butler, *Adv. Electrochem. Electrochem. Engr.*, **7**, 77 (1970).
18. D. T. Sawyer, A. Sobkowiak, and J. L. Roberts, Jr., "Electrochemistry for Chemists," 2nd ed., Wiley, New York, 1995.
19. G. Gritzner and J. Kuta, *Pure Appl. Chem.*, **56**, 461 (1984).
20. (a) P. Pearce and A. J. Bard, *J. Electroanal. Chem.*, **108**, 121 (1980); (b) R. M. Kannuck, J. M. Bellama, E. A. Blubaugh, and R. A. Durst, *Anal. Chem.*, **59**, 1473 (1987).
21. D. Halliday and R. Resnick, "Physics," 3rd ed., Wiley, New York, 1978, Chap. 29.
22. *Ibid.*, Chap. 28.
23. J. O'M. Bockris and A. K. N. Reddy, "Modern Electrochemistry," Vol. 2, Plenum, New York, 1970, Chap. 7.
24. K. J. Vetter, "Electrochemical Kinetics," Academic, New York, 1967.
25. B. E. Conway, "Theory and Principles of Electrode Processes," Ronald, New York, 1965, Chap. 13.
26. R. Parsons, *Mod. Asp. Electrochem.*, **1**, 103 (1954).
27. J. A. V. Butler, *Proc. Roy. Soc., London*, **112A**, 129 (1926).
28. E. A. Guggenheim, *J. Phys. Chem.*, **33**, 842 (1929); **34**, 1540 (1930).
29. S. Trasatti, *Pure Appl. Chem.*, **58**, 955 (1986).
30. D. A. MacInnes, "Principles of Electrochemistry," Dover, New York, 1961, Chap. 13.
31. J. O'M. Bockris and A. K. N. Reddy, *op. cit.*, Vol. 1, Chap. 4.
32. D. A. MacInnes, *op. cit.*, Chap. 4.
33. *Ibid.*, Chap. 18.
34. D. O. Raleigh, *Electroanal. Chem.*, **6**, 87 (1973).
35. G. Holzäpfel, "Solid State Electrochemistry" in *Encycl. Phys. Sci. Technol.*, R. A. Meyers, Ed., Academic, New York, 1992, Vol. 15, p. 471.
36. J. O'M. Bockris and A. K. N. Reddy, *op. cit.*, Chap. 3.
37. R. G. Bates, "Determination of pH," 2nd ed., Wiley-Interscience, New York, 1973.
38. R. M. Garrels in "Glass Electrodes for Hydrogen and Other Cations," G. Eisenman, Ed., Marcel Dekker, New York, 1967, Chap. 13.
39. P. R. Mussini, S. Rondinini, A. Cipolli, R. Mamenti and M. Mauretti, *Ber. Bunsenges. Phys. Chem.*, **97**, 1034 (1993).
40. H. H. J. Girault and D. J. Schiffrin, *Electroanal. Chem.*, **15**, 1 (1989).
41. H. H. J. Girault, *Mod. Asp. Electrochem.*, **25**, 1 (1993).
42. P. Vanýšek, "Electrochemistry on Liquid/Liquid Interfaces," Springer, Berlin, 1985.
43. A. G. Volkov and D. W. Deamer, Eds., "Liquid-Liquid Interfaces," CRC, Boca Raton, FL, 1996.
44. A. G. Volkov, D. W. Deamer, D. L. Tanelian, and V. S. Markin, "Liquid Interfaces in Chemistry and Biology," Wiley-Interscience, New York, 1997.
45. E. Grunwald, G. Baughman, and G. Kohnstam, *J. Am. Chem. Soc.*, **82**, 5801 (1960).
46. M. Dole, "The Glass Electrode," Wiley, New York, 1941.
47. G. Eisenman, Ed., "Glass Electrodes for Hydrogen and Other Cations," Marcel Dekker, New York, 1967.
48. R. A. Durst, Ed., "Ion Selective Electrodes," Nat. Bur. Stand. Spec. Pub. 314, U.S. Government Printing Office, Washington, 1969.
49. N. Lakshminarayanaiah in "Electrochemistry," (A Specialist Periodical Report), Vols. 2, 4, 5, and 7; G. J. Hills (Vol. 2); and H. R. Thirsk (Vols. 4, 5, and 7); Senior Reporters, Chemical Society, London, 1972, 1974, 1975, and 1980.
50. H. Freiser, "Ion-Selective Electrodes in Analytical Chemistry," Plenum, New York, Vol. 1, 1979; Vol. 2, 1980.
51. J. Koryta and K. Štulík, "Ion-Selective Electrodes," 2nd ed., Cambridge University Press, Cambridge, 1983.
52. A. Evans, "Potentiometry and Ion Selective Electrodes," Wiley, New York, 1987.

53. D. Ammann, "Ion-Selective Microelectrodes: Principles, Design, and Application," Springer, Berlin, 1986.
54. E. Lindner, K. Toth, and E. Pungor, "Dynamic Characteristics of Ion-Sensitive Electrodes," CRC, Boca Raton, FL, 1988.
55. Y. Umezawa, Ed., "CRC Handbook of Ion-Selective Electrodes," CRC, Boca Raton, FL 1990.
56. E. Bakker, P. Bühlmann, and E. Pretsch, *Chem. Rev.*, **97**, 3083 (1997).
57. P. Bühlmann, E. Pretsch, and E. Bakker, *Chem. Rev.*, **98**, 1593 (1998).
58. R. P. Buck and E. Lindner, *Accts. Chem. Res.*, **31**, 257 (1998).
59. E. Pungor, *Pure Appl. Chem.*, **64**, 503 (1992).
60. S. Mathison and E. Bakker, *Anal. Chem.*, **70**, 303 (1998).
61. T. Sokalski, A. Ceresa, T. Zwicky, and E. Pretsch, *J. Am. Chem. Soc.*, **119**, 11347 (1997).
62. J. W. Ross, J. H. Riseman, and J. A. Krueger, *Pure Appl. Chem.*, **36**, 473 (1973).
63. L. C. Clark, Jr., *Trans. Am. Soc. Artif. Intern. Organs*, **2**, 41 (1956).
64. G. G. Guilbault, *Pure Appl. Chem.*, **25**, 727 (1971).
65. G. A. Rechnitz, *Chem. Engr. News*, **53** (4), 29 (1975).
66. E. A. H. Hall, "Biosensors," Prentice Hall, Englewood Cliffs, NJ, 1991, Chap. 9.
67. A. J. Cunningham, "Introduction to Bioanalytical Sensors," Wiley, New York, 1998, Chap. 4.
68. H. S. Yim, C. E. Kibbey, S. C. Ma, D. M. Kliza, D. Liu, S. B. Park, C. E. Torre, and M. E. Meyerhoff, *Biosens. Bioelectron.*, **8**, 1 (1993).

► 2.6 PROBLEMS

2.1 Devise electrochemical cells in which the following reactions could be made to occur. If liquid junctions are necessary, note them in the cell schematic appropriately, but neglect their effects.

- (a) $\text{H}_2\text{O} \rightleftharpoons \text{H}^+ + \text{OH}^-$
- (b) $2\text{H}_2 + \text{O}_2 \rightleftharpoons \text{H}_2\text{O}$
- (c) $2\text{PbSO}_4 + 2\text{H}_2\text{O} \rightleftharpoons \text{PbO}_2 + \text{Pb} + 4\text{H}^+ + 2\text{SO}_4^{2-}$
- (d) $\text{An}^- + \text{TMPD}^{\cdot+} \rightleftharpoons \text{An} + \text{TMPD}$ (in acetonitrile, where An and An^- are anthracene and its anion radical, and TMPD and $\text{TMPD}^{\cdot+}$ are *N,N,N',N'*-tetramethyl-*p*-phenylenediamine and its cation radical. Use anthracene potentials for DMF solutions given in Appendix C.3).
- (e) $2\text{Ce}^{3+} + 2\text{H}^+ + \text{BQ} \rightleftharpoons 2\text{Ce}^{4+} + \text{H}_2\text{Q}$ (aqueous, where BQ is *p*-benzoquinone and H_2Q is *p*-hydroquinone)
- (f) $\text{Ag}^+ + \text{I}^- \rightleftharpoons \text{AgI}$ (aqueous)
- (g) $\text{Fe}^{3+} + \text{Fe}(\text{CN})_6^{4-} \rightleftharpoons \text{Fe}^{2+} + \text{Fe}(\text{CN})_6^{3-}$ (aqueous)
- (h) $\text{Cu}^{2+} + \text{Pb} \rightleftharpoons \text{Pb}^{2+} + \text{Cu}$ (aqueous)
- (i) $\text{An}^- + \text{BQ} \rightleftharpoons \text{BO}^{\cdot-} + \text{An}$ (in *N,N*-dimethylformamide, where BQ, An, and An^- are defined above and $\text{BO}^{\cdot-}$ is the anion radical of *p*-benzoquinone. Use BQ potentials in acetonitrile given in Appendix C.3).

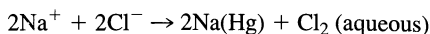
What half-reactions take place at the electrodes in each cell? What is the standard cell potential in each case? Which electrode is negative? Would the cell operate electrolytically or galvanically in carrying out a net reaction from left to right? Be sure your decisions accord with chemical intuition.

2.2 Several hydrocarbons and carbon monoxide have been studied as possible fuels for use in fuel cells. From thermodynamic data in references 5–8 and 16, derive E^0 s for the following reactions at 25°C:

- (a) $\text{CO}(g) + \text{H}_2\text{O}(l) \rightarrow \text{CO}_2(g) + 2\text{H}^+ + 2e$
- (b) $\text{CH}_4(g) + 2\text{H}_2\text{O}(l) \rightarrow \text{CO}_2(g) + 8\text{H}^+ + 8e$
- (c) $\text{C}_2\text{H}_6(g) + 4\text{H}_2\text{O}(l) \rightarrow 2\text{CO}_2(g) + 14\text{H}^+ + 14e$
- (d) $\text{C}_2\text{H}_2(g) + 4\text{H}_2\text{O}(l) \rightarrow 2\text{CO}_2(g) + 10\text{H}^+ + 10e$

Even though a reversible emf could not be established (Why not?), which half-cell would ideally yield the highest cell voltage when coupled with the standard oxygen half-cell in acid solution? Which of the fuels above could yield the highest net work per mole of fuel oxidized? Which would give the most net work per gram?

- 2.3 Devise a cell in which the following reaction is the overall cell process ($T = 298\text{ K}$):



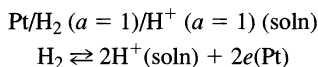
where Na(Hg) symbolizes the amalgam. Is the reaction spontaneous or not? What is the standard free energy change? Take the standard free energy of formation of Na(Hg) as -85 kJ/mol . From a thermodynamic standpoint, another reaction should occur more readily at the cathode of your cell. What is it? It is observed that the reaction written above takes place with good current efficiency. Why? Could your cell have a commercial value?

- 2.4 What are the cell reactions and their emfs in the following systems? Are the reactions spontaneous? Assume that all systems are aqueous.
- $\text{Ag/AgCl/K}^+, \text{Cl}^- (1\text{ M})/\text{Hg}_2\text{Cl}_2/\text{Hg}$
 - $\text{Pt/Fe}^{3+} (0.01\text{ M}), \text{Fe}^{2+} (0.1\text{ M}), \text{HCl} (1\text{ M})/\text{Cu}^{2+} (0.1\text{ M}), \text{HCl} (1\text{ M})/\text{Cu}$
 - $\text{Pt/H}_2 (1\text{ atm})/\text{H}^+, \text{Cl}^- (0.1\text{ M})/\text{H}^+, \text{Cl}^- (0.1\text{ M})/\text{O}_2 (0.2\text{ atm})/\text{Pt}$
 - $\text{Pt/H}_2 (1\text{ atm})/\text{Na}^+, \text{OH}^- (0.1\text{ M})/\text{Na}^+, \text{OH}^- (0.1\text{ M})/\text{O}_2 (0.2\text{ atm})/\text{Pt}$
 - $\text{Ag/AgCl/K}^+, \text{Cl}^- (1\text{ M})/\text{K}^+, \text{Cl}^- (0.1\text{ M})/\text{AgCl/Ag}$
 - $\text{Pt/Ce}^{3+} (0.01\text{ M}), \text{Ce}^{4+} (0.1\text{ M}), \text{H}_2\text{SO}_4 (1\text{ M})/\text{Fe}^{2+} (0.01\text{ M}), \text{Fe}^{3+} (0.1\text{ M}), \text{HCl} (1\text{ M})/\text{Pt}$
- 2.5 Consider the cell in part (f) of Problem 2.4. What would the composition of the system be at the end of a galvanic discharge to an equilibrium condition? What would the cell potential be? What would the potential of each electrode be vs. NHE? Vs. SCE? Take equal volumes on both sides.
- 2.6 Devise a cell for evaluating the solubility product of PbSO_4 . Calculate the solubility product from the appropriate E^0 values ($T = 298\text{ K}$).
- 2.7 Obtain the dissociation constant of water from the parameters of the cell constructed for reaction (a) in Problem 2.1 ($T = 298\text{ K}$).
- 2.8 Consider the cell:



Would the cell potential be independent of the identity of M (e.g., graphite, gold, platinum) as long as M is chemically inert? Use electrochemical potentials to prove your point.

- 2.9 Given the half-cell of the standard hydrogen electrode,

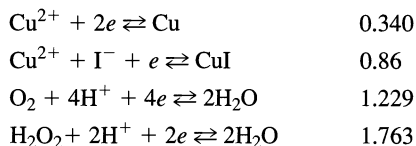


Show that although the emf of the cell half-reaction is taken as zero, the potential difference between the platinum and the solution, that is, $\phi^{\text{Pt}} - \phi^{\text{s}}$, is not zero.

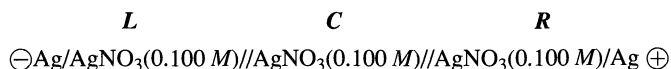
- 2.10 Devise a thermodynamically sound basis for obtaining the standard potentials for new half-reactions by taking linear combinations of other half-reactions ($T = 298\text{ K}$). As two examples, calculate E^0 values for

- $\text{CuI} + e \rightleftharpoons \text{Cu} + \text{I}^-$
- $\text{O}_2 + 2\text{H}^+ + 2e \rightleftharpoons \text{H}_2\text{O}_2$

given the following half-reactions and values for E^0 (V vs. NHE):

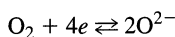


- 2.11 Transference numbers are often measured by the Hittorf method as illustrated in this problem. Consider the three-compartment cell:



where the double slashes (//) signify sintered glass disks that divide the compartments and prevent mixing, but not ionic movement. The volume of AgNO_3 solution in each compartment (L , C , R) is 25.00 mL. An external power supply is connected to the cell with the polarity shown, and current is applied until 96.5 C have passed, causing Ag to deposit on the left Ag electrode and Ag to dissolve from the right Ag electrode.

- (a) How many grams of Ag have deposited on the left electrode? How many mmol of Ag have deposited?
 - (b) If the transference number for Ag^+ were 1.00 (i.e., $t_{\text{Ag}^+} = 1.00$, $t_{\text{NO}_3^-} = 0.00$), what would the concentrations of Ag^+ be in the three compartments after electrolysis?
 - (c) Suppose the transference number for Ag^+ were 0.00 (i.e., $t_{\text{Ag}^+} = 0.00$, $t_{\text{NO}_3^-} = 1.00$), what would the concentrations of Ag^+ be in the three compartments after electrolysis?
 - (d) In an actual experiment like this, it is found experimentally that the concentration of Ag^+ in the anode compartment R has increased to 0.121 M . Calculate t_{Ag^+} and $t_{\text{NO}_3^-}$.
- 2.12 Suppose one wants to determine the contribution of electronic (as opposed to ionic) conduction through doped AgBr, a solid electrolyte. A cell is prepared with a film of AgBr between two Ag electrodes, each of mass 1.00 g, that is, $\ominus\text{Ag}/\text{AgBr}/\text{Ag}\oplus$. After passage of 200 mA through the cell for 10.0 min, the cell was disassembled and the cathode was found to have a mass of 1.12 g. If Ag deposition is the only faradaic process that occurs at the cathode, what fraction of the current through the cell represents electronic conduction in AgBr?
 - 2.13 Calculate the individual junction potentials at $T = 298$ K on either side of the salt bridge in (2.3.44) for the first two concentrations in Table 2.3.3. What is the sum of the two potentials in each case? How does it compare with the corresponding entry in the table?
 - 2.14 Estimate the junction potentials for the following situations ($T = 298$ K):
 - (a) HCl (0.1 M)/NaCl (0.1 M)
 - (b) HCl (0.1 M)/NaCl (0.01 M)
 - (c) KNO_3 (0.01 M)/NaOH (0.1 M)
 - (d) NaNO_3 (0.1 M)/NaOH (0.1 M)
 - 2.15 One often finds pH meters with direct readout to 0.001 pH unit. Comment on the accuracy of these readings in making comparisons of pH from test solution to test solution. Comment on their meaning in measurements of small changes in pH in a single solution (e.g., during a titration).
 - 2.16 The following values of $k_{\text{Na}^+,i}^{\text{pot}}$ are typical for interferents i at a sodium-selective glass electrode: K^+ , 0.001; NH_4^+ , 10^{-5} ; Ag^+ , 300; H^+ , 100. Calculate the activities of each interferent that would cause a 10% error when the activity of Na^+ is estimated to be 10^{-3} M from a potentiometric measurement.
 - 2.17 Would $\text{Na}_2\text{H}_2\text{EDTA}$ be a good ion-exchanger for a liquid membrane electrode? How about $\text{Na}_2\text{H}_2\text{EDTA-R}$, where R designates a C_{20} alkyl substituent? Why or why not?
 - 2.18 Comment on the feasibility of developing selective electrodes for the direct potentiometric determination of uncharged substances.
 - 2.19 Consider the exhaust gas analyzer based on the oxygen concentration cell, (2.4.21). The electrode reaction that occurs at high temperature at both of the Pt/ZrO₂ + Y₂O₃ interfaces is



Write the equation that governs the potential of this cell as a function of the pressures, p_{eg} and p_{a} . What would the cell voltage be when the partial pressure of oxygen in the exhaust gas is 0.01 atm (1,013 Pa)?

KINETICS OF ELECTRODE REACTIONS

In Chapter 1, we established a proportionality between the current and the net rate of an electrode reaction, v . Specifically, $v = i/nFA$. We also know that for a given electrode process, current does not flow in some potential regions, yet it flows to a variable degree in others. The reaction rate is a strong function of potential; thus, we require potential-dependent rate constants for an accurate description of interfacial charge-transfer dynamics.

In this chapter, our goal is to devise a theory that can quantitatively rationalize the observed behavior of electrode kinetics with respect to potential and concentration. Once constructed, the theory will serve often as an aid for understanding kinetic effects in new situations. We begin with a brief review of certain aspects of homogeneous kinetics, because they provide both a familiar starting ground and a basis for the construction, through analogy, of an electrochemical kinetic theory.

► 3.1 REVIEW OF HOMOGENEOUS KINETICS

3.1.1 Dynamic Equilibrium

Consider two substances, A and B, that are linked by simple unimolecular elementary reactions.¹



Both elementary reactions are active at all times, and the rate of the forward process, v_f (M/s), is

$$v_f = k_f C_A \quad (3.1.2)$$

whereas the rate of the reverse reaction is

$$v_b = k_b C_B \quad (3.1.3)$$

The rate constants, k_f and k_b , have dimensions of s^{-1} , and one can easily show that they are the reciprocals of the mean lifetimes of A and B, respectively (Problem 3.8). The net conversion rate of A to B is

$$v_{\text{net}} = k_f C_A - k_b C_B \quad (3.1.4)$$

¹An *elementary reaction* describes an actual, discrete chemical event. Many chemical reactions, as written, are not elementary, because the transformation of products to reactants involves several distinct steps. These steps are the elementary reactions that comprise the *mechanism* for the overall process.

At equilibrium, the net conversion rate is zero; hence

$$\frac{k_f}{k_b} = K = \frac{C_B}{C_A} \quad (3.1.5)$$

The kinetic theory therefore predicts a constant concentration ratio at equilibrium, just as thermodynamics does.

Such agreement is required of *any* kinetic theory. In the limit of equilibrium, the kinetic equations must collapse to relations of the thermodynamic form; otherwise the kinetic picture cannot be accurate. Kinetics describe the evolution of mass flow throughout the system, including both the *approach* to equilibrium and the *dynamic maintenance* of that state. Thermodynamics describe only equilibrium. Understanding of a system is not even at a crude level unless the kinetic view and the thermodynamic one agree on the properties of the equilibrium state.

On the other hand, thermodynamics provide no information about the mechanism required to maintain equilibrium, whereas kinetics can be used to describe the intricate balance quantitatively. In the example above, equilibrium features nonzero rates of conversion of A to B (and vice versa), but those rates are equal. Sometimes they are called the *exchange velocity* of the reaction, v_0 :

$$v_0 = k_f(C_A)_{\text{eq}} = k_b(C_B)_{\text{eq}} \quad (3.1.6)$$

We will see below that the idea of exchange velocity plays an important role in treatments of electrode kinetics.

3.1.2 The Arrhenius Equation and Potential Energy Surfaces (1, 2)

It is an experimental fact that most rate constants of solution-phase reactions vary with temperature in a common fashion: nearly always, $\ln k$ is linear with $1/T$. Arrhenius was first to recognize the generality of this behavior, and he proposed that rate constants be expressed in the form:

$$k = Ae^{-E_A/RT} \quad (3.1.7)$$

where E_A has units of energy. Since the exponential factor is reminiscent of the probability of using thermal energy to surmount an energy barrier of height E_A , that parameter has been known as the *activation energy*. If the exponential expresses the probability of surmounting the barrier, then A must be related to the frequency of attempts on it; thus A is known generally as the *frequency factor*. As usual, these ideas turn out to be oversimplifications, but they carry an essence of truth and are useful for casting a mental image of the ways in which reactions proceed.

The idea of activation energy has led to pictures of reaction paths in terms of potential energy along a *reaction coordinate*. An example is shown in Figure 3.1.1. In a simple unimolecular process, such as, the *cis-trans* isomerization of stilbene, the reaction coordinate might be an easily recognized molecular parameter, such as the twist angle about the central double bond in stilbene. In general, the reaction coordinate expresses progress along a favored path on the multidimensional surface describing potential energy as a function of all independent position coordinates in the system. One zone of this surface corresponds to the configuration we call “reactant,” and another corresponds to the structure of the “product.” Both must occupy minima on the energy surface, because they are the only arrangements possessing a significant lifetime. Even though other configurations are possible, they must lie at higher energies and lack the energy minimum required for

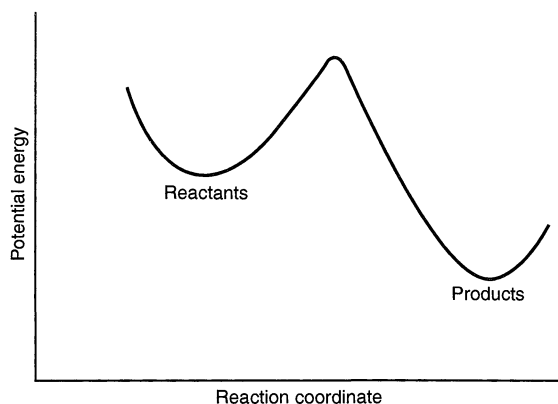


Figure 3.1.1 Simple representation of potential energy changes during a reaction.

stability. As the reaction takes place, the coordinates are changed from those of the reactant to those of the product. Since the path along the reaction coordinate connects two minima, it must rise, pass over a maximum, then fall into the product zone. Very often, the height of the maximum above a valley is identified with the activation energy, either $E_{A,f}$ or $E_{A,b}$, for the forward or backward reaction, respectively.

In another notation, we can understand E_A as the change in standard internal energy in going from one of the minima to the maximum, which is called the *transition state* or *activated complex*. We might designate it as the *standard internal energy of activation*, ΔE^\ddagger . The *standard enthalpy of activation*, ΔH^\ddagger , would then be $\Delta E^\ddagger + \Delta(PV)^\ddagger$, but $\Delta(PV)$ is usually negligible in a condensed-phase reaction, so that $\Delta H^\ddagger \approx \Delta E^\ddagger$. Thus, the Arrhenius equation could be recast as

$$k = A e^{-\Delta H^\ddagger/RT} \quad (3.1.8)$$

We are free also to factor the coefficient A into the product $A' \exp(\Delta S^\ddagger/R)$, because the exponential involving the *standard entropy of activation*, ΔS^\ddagger , is a dimensionless constant. Then

$$k = A' e^{-(\Delta H^\ddagger - T\Delta S^\ddagger)/RT} \quad (3.1.9)$$

or

$$k = A' e^{-\Delta G^\ddagger/RT} \quad (3.1.10)$$

where ΔG^\ddagger is the *standard free energy of activation*.² This relation, like (3.1.8), is really an equivalent statement of the Arrhenius equation, (3.1.7), which itself is an empirical generalization of reality. Equations 3.1.8 and 3.1.10 are derived from (3.1.7), but only by the *interpretation* we apply to the phenomenological constant E_A . Nothing we have written so far depends on a specific theory of kinetics.

²We are using *standard* thermodynamic quantities here, because the free energy and the entropy of a species are concentration-dependent. The rate constant is not concentration-dependent in dilute systems; thus the argument that leads to (3.1.10) needs to be developed in the context of a standard state of concentration. The choice of standard state is not critical to the discussion. It simply affects the way in which constants are apportioned in rate expressions. To simplify notation, we omit the superscript “0” from ΔE^\ddagger , ΔH^\ddagger , ΔS^\ddagger , and ΔG^\ddagger , but understand them throughout this book to be referred to the standard state of concentration.

3.1.3 Transition State Theory (1–4)

Many theories of kinetics have been constructed to illuminate the factors controlling reaction rates, and a prime goal of these theories is to predict the values of A and E_A for specific chemical systems in terms of quantitative molecular properties. An important general theory that has been adapted for electrode kinetics is the *transition state theory*, which is also known as the *absolute rate theory* or the *activated complex theory*.

Central to this approach is the idea that reactions proceed through a fairly well-defined transition state or activated complex, as shown in Figure 3.1.2. The standard free energy change in going from the reactants to the complex is ΔG_f^\ddagger , whereas the complex is elevated above the products by ΔG_b^\ddagger .

Let us consider the system of (3.1.1), in which two substances A and B are linked by unimolecular reactions. First we focus on the special condition in which the entire system—A, B, and all other configurations—is at thermal equilibrium. For this situation, the concentration of complexes can be calculated from the standard free energies of activation according to either of two equilibrium constants:

$$\frac{[\text{Complex}]}{[A]} = \frac{\gamma_A/C^0}{\gamma_\ddagger/C^0} K_f = \frac{\gamma_A}{\gamma_\ddagger} \exp(-\Delta G_f^\ddagger/RT) \quad (3.1.11)$$

$$\frac{[\text{Complex}]}{[B]} = \frac{\gamma_B}{\gamma_\ddagger} K_b = \frac{\gamma_B}{\gamma_\ddagger} \exp(-\Delta G_b^\ddagger/RT) \quad (3.1.12)$$

where C^0 is the concentration of the standard state (see Section 2.1.5), and γ_A , γ_B , and γ_\ddagger are dimensionless activity coefficients. Normally, we assume that the system is ideal, so that the activity coefficients approach unity and divide out of (3.1.11) and (3.1.12).

The activated complexes decay into either A or B according to a combined rate constant, k' , and they can be divided into four fractions: (a) those created from A and reverting back to A, f_{AA} , (b) those arising from A and decaying to B, f_{AB} , (c) those created from B and decaying to A, f_{BA} , and (d) those arising from B and reverting back to B, f_{BB} . Thus the rate of transforming A into B is

$$k_f [A] = f_{AB} k' [\text{Complex}] \quad (3.1.13)$$

and the rate of transforming B into A is

$$k_b [B] = f_{BA} k' [\text{Complex}] \quad (3.1.14)$$

Since we require $k_f [A] = k_b [B]$ at equilibrium, f_{AB} and f_{BA} must be the same. In the simplest version of the theory, both are taken as $1/2$. This assumption implies that

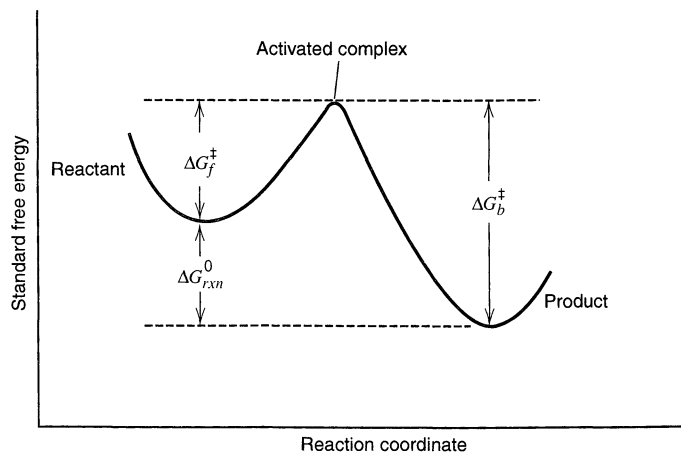


Figure 3.1.2 Free energy changes during a reaction. The activated complex (or transition state) is the configuration of maximum free energy.

$f_{AA} = f_{BB} \approx 0$; thus complexes are not considered as reverting to the source state. Instead, any system reaching the activated configuration is transmitted with unit efficiency into the product opposite the source. In a more flexible version, the fractions f_{AB} and f_{BA} are equated to $\kappa/2$, where κ , the *transmission coefficient*, can take a value from zero to unity.

Substitution for the concentration of the complex from (3.1.11) and (3.1.12) into (3.1.13) and (3.1.14), respectively, leads to the rate constants:

$$k_f = \frac{\kappa k'}{2} e^{-\Delta G_f^\ddagger/RT} \quad (3.1.15)$$

$$k_b = \frac{\kappa k'}{2} e^{-\Delta G_b^\ddagger/RT} \quad (3.1.16)$$

Statistical mechanics can be used to predict $\kappa k'/2$. In general, that quantity depends on the shape of the energy surface in the region of the complex, but for simple cases k' can be shown to be $2\mathcal{E}T/h$, where, \mathcal{E} and h are the Boltzmann and Planck constants. Thus the rate constants (equations 3.1.15 and 3.1.16) might both be expressed in the form:

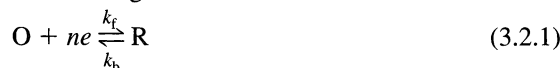
$$k = \kappa \frac{\mathcal{E}T}{h} e^{-\Delta G^\ddagger/RT} \quad (3.1.17)$$

which is the equation most frequently seen for calculating rate constants by the transition state theory.

To reach (3.1.17), we considered only a system at equilibrium. It is important to note now that the rate constant for an elementary process is fixed for a given temperature and pressure and does not depend on the reactant and product concentrations. Equation 3.1.17 is therefore a general expression. If it holds at equilibrium, it will hold away from equilibrium. The assumption of equilibrium, though useful in the derivation, does not constrain the equation's range of validity.³

▶ 3.2 ESSENTIALS OF ELECTRODE REACTIONS (6–14)

We noted above that an accurate kinetic picture of any dynamic process must yield an equation of the thermodynamic form in the limit of equilibrium. For an electrode reaction, equilibrium is characterized by the Nernst equation, which links the electrode potential to the bulk concentrations of the participants. In the general case:



this equation is

$$E = E^{0'} + \frac{RT}{nF} \ln \frac{C_O^*}{C_R^*} \quad (3.2.2)$$

where C_O^* and C_R^* are the bulk concentrations, and $E^{0'}$ is the formal potential. Any valid theory of electrode kinetics must predict this result for corresponding conditions.

³Note that $\mathcal{E}T/h$ has units of s^{-1} and that the exponential is dimensionless. Thus, the expression in (3.1.17) is dimensionally correct for a first-order rate constant. For a second-order reaction, the equilibrium corresponding to (3.1.11) would have the concentrations of two reactants in the denominator on the left side and the activity coefficient for each of those species divided by the standard-state concentration, C^0 , in the numerator on the right. Thus, C^0 no longer divides out altogether and is carried to the first power into the denominator of the final expression. Since it normally has a unit value (usually $1 M^{-1}$), its presence has no effect numerically, but it does dimensionally. The overall result is to create a prefactor having a numeric value equal to $\mathcal{E}T/h$ but having units of $M^{-1} s^{-1}$, as required. This point is often omitted in applications of transition state theory to processes more complicated than unimolecular decay. See Section 2.1.5 and reference 5.

We also require that the theory explain the observed dependence of current on potential under various circumstances. In Chapter 1, we saw that current is often limited wholly or partially by the rate at which the electroreactants are transported to the electrode surface. This kind of limitation does not concern a theory of interfacial kinetics. More to the point is the case of low current and efficient stirring, in which mass transport is not a factor determining the current. Instead, it is controlled by interfacial dynamics. Early studies of such systems showed that the current is often related exponentially to the overpotential η . That is,

$$i = a' e^{\eta/b'} \quad (3.2.3)$$

or, as given by Tafel in 1905,

$$\boxed{\eta = a + b \log i} \quad (3.2.4)$$

A successful model of electrode kinetics must explain the frequent validity of (3.2.4), which is known as the *Tafel equation*.

Let us begin by considering that reaction (3.2.1) has forward and backward paths as shown. The forward component proceeds at a rate, v_f , that must be proportional to the surface concentration of O. We express the concentration at distance x from the surface and at time t as $C_O(x, t)$; hence the surface concentration is $C_O(0, t)$. The constant of proportionality linking the forward reaction rate to $C_O(0, t)$ is the rate constant k_f .

$$v_f = k_f C_O(0, t) = \frac{i_c}{nFA} \quad (3.2.5)$$

Since the forward reaction is a reduction, there is a cathodic current, i_c , proportional to v_f . Likewise, we have for the backward reaction

$$v_b = k_b C_R(0, t) = \frac{i_a}{nFA} \quad (3.2.6)$$

where i_a is the anodic component to the total current. Thus the net reaction rate is

$$v_{\text{net}} = v_f - v_b = k_f C_O(0, t) - k_b C_R(0, t) = \frac{i}{nFA} \quad (3.2.7)$$

and we have overall

$$i = i_c - i_a = nFA[k_f C_O(0, t) - k_b C_R(0, t)] \quad (3.2.8)$$

Note that heterogeneous reactions are described differently than homogeneous ones. For example, reaction velocities in heterogeneous systems refer to unit interfacial area; hence they have units of $\text{mol s}^{-1} \text{cm}^{-2}$. Thus heterogeneous rate constants must carry units of cm/s , if the concentrations on which they operate are expressed in mol/cm^3 . Since the interface can respond only to its immediate surroundings, the concentrations entering rate expressions are always surface concentrations, which may differ from those of the bulk solution.

▶ 3.3 BUTLER-VOLMER MODEL OF ELECTRODE KINETICS (9, 11, 12, 15, 16)

Experience demonstrates that the potential of an electrode strongly affects the kinetics of reactions occurring on its surface. Hydrogen evolves rapidly at some potentials, but not at others. Copper dissolves from a metallic sample in a clearly defined potential range; yet the metal is stable outside that range. And so it is for all faradaic processes. Because the interfacial potential difference can be used to control reactivity, we want to be able to pre-

dict the precise way in which k_f and k_b depend on potential. In this section, we will develop a predictive model based purely on classical concepts. Even though it has significant limitations, it is very widely used in the electrochemical literature and must be understood by any student of the field. Section 3.6 will yield more modern models based on a microscopic view of electron transfer.

3.3.1 Effects of Potential on Energy Barriers

We saw in Section 3.1 that reactions can be visualized in terms of progress along a reaction coordinate connecting a reactant configuration to a product configuration on an energy surface. This idea applies to electrode reactions too, but the shape of the surface turns out to be a function of electrode potential.

One can see the effect easily by considering the reaction



where Na^+ is dissolved in acetonitrile or dimethylformamide. We can take the reaction coordinate as the distance of the sodium nucleus from the interface; then the free energy profile along the reaction coordinate would resemble Figure 3.3.1*a*. To

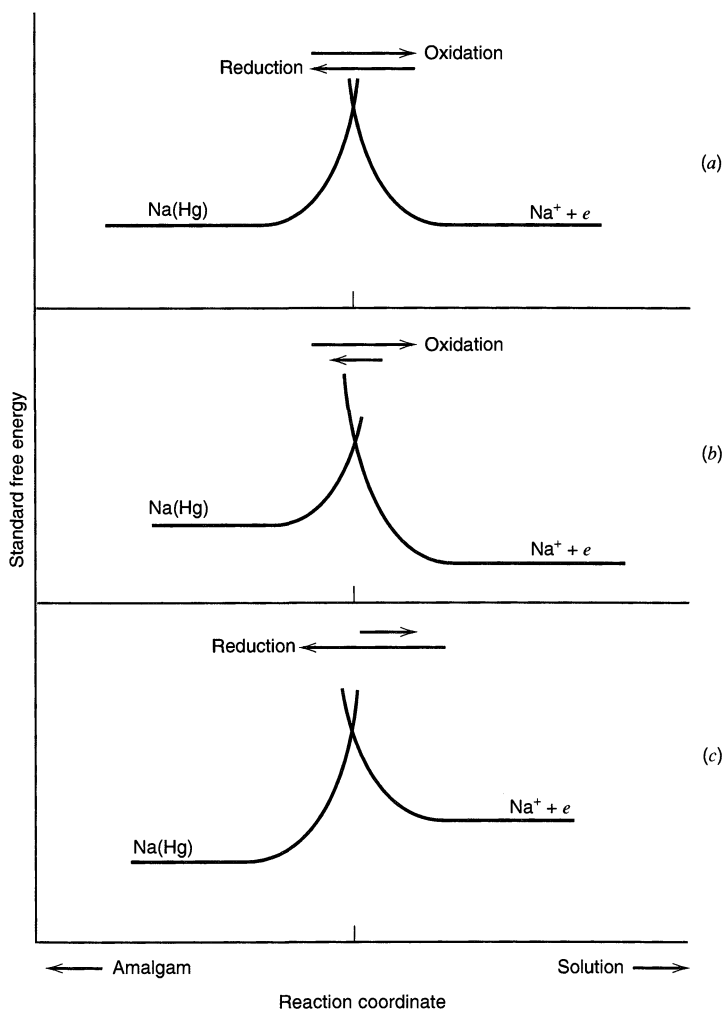


Figure 3.3.1 Simple representation of standard free energy changes during a faradaic process. (a) At a potential corresponding to equilibrium. (b) At a more positive potential than the equilibrium value. (c) At a more negative potential than the equilibrium value.

the right, we identify $\text{Na}^+ + e$. This configuration has an energy that depends little on the nuclear position in solution, unless the electrode is approached so closely that the ion must be partially or wholly desolvated. To the left, the configuration corresponds to a sodium atom dissolved in mercury. Within the mercury phase, the energy depends only slightly on position, but if the atom leaves the interior, its energy rises as the favorable mercury–sodium interaction is lost. The curves corresponding to these reactant and product configurations intersect at the transition state, and the heights of the barriers to oxidation and reduction determine their relative rates. When the rates are equal, as in Figure 3.3.1a, the system is at equilibrium, and the potential is E_{eq} .

Now suppose the potential is changed to a more positive value. The main effect is to lower the energy of the “reactant” electron; hence the curve corresponding to $\text{Na}^+ + e$ drops with respect to that corresponding to $\text{Na}(\text{Hg})$, and the situation resembles that of Figure 3.3.1b. Since the barrier for reduction is raised and that for oxidation is lowered, the net transformation is conversion of $\text{Na}(\text{Hg})$ to $\text{Na}^+ + e$. Setting the potential to a value more negative than E_{eq} , raises the energy of the electron and shifts the curve for $\text{Na}^+ + e$ to higher energies, as shown in Figure 3.3.1c. Since the reduction barrier drops and the oxidation barrier rises, relative to the condition at E_{eq} , a net cathodic current flows. These arguments show qualitatively the way in which the potential affects the net rates and directions of electrode reactions. By considering the model more closely, we can establish a quantitative relationship.

3.3.2 One-Step, One-Electron Process

Let us now consider the simplest possible electrode process, wherein species O and R engage in a one-electron transfer at the interface without being involved in any other chemical step,



Suppose also that the standard free energy profiles along the reaction coordinate have the parabolic shapes shown in Figure 3.3.2. The upper frame of that figure depicts the full path from reactants to products, while the lower frame is an enlargement of the region near the transition state. It is not important for this discussion that we know the shapes of these profiles in detail.

In developing a theory of electrode kinetics, it is convenient to express potential against a point of significance to the chemistry of the system, rather than against an arbitrary external reference, such as an SCE. There are two natural reference points, *viz.* the equilibrium potential of the system and the standard (or formal) potential of the couple under consideration. We actually used the equilibrium potential as a reference point in the discussion of the preceding section, and we will use it again in this section. However, it is possible to do so only when both members of the couple are present, so that an equilibrium is defined. The more general reference point is $E^{0'}$. Suppose the upper curve on the $\text{O} + e$ side of Figure 3.3.2 applies when the electrode potential is equal to $E^{0'}$. The cathodic and anodic activation energies are then ΔG_{0c}^\ddagger and ΔG_{0a}^\ddagger respectively.

If the potential is changed by ΔE to a new value, E , the relative energy of the electron resident on the electrode changes by $-F\Delta E = -F(E - E^{0'})$; hence the $\text{O} + e$ curve moves up or down by that amount. The lower curve on the left side of Figure 3.3.2 shows this effect for a positive ΔE . It is readily apparent that the barrier for oxidation, ΔG_a^\ddagger , has become less than ΔG_{0a}^\ddagger by a fraction of the total energy change. Let us call that fraction

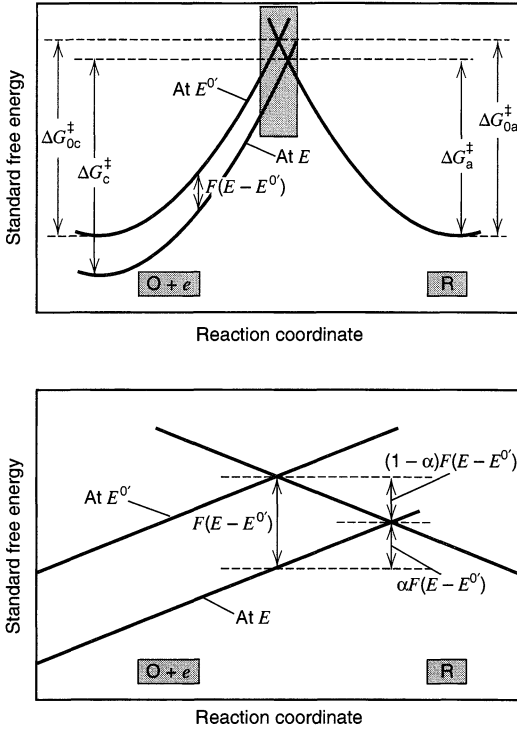


Figure 3.3.2 Effects of a potential change on the standard free energies of activation for oxidation and reduction. The lower frame is a magnified picture of the boxed area in the upper frame.

$1 - \alpha$, where α , the *transfer coefficient*, can range from zero to unity, depending on the shape of the intersection region. Thus,

$$\Delta G_a^\ddagger = \Delta G_{0a}^\ddagger - (1 - \alpha)F(E - E^0) \quad (3.3.3)$$

A brief study of the figure also reveals that at potential E the cathodic barrier, ΔG_c^\ddagger , is higher than ΔG_{0c}^\ddagger by $\alpha F(E - E^0)$; therefore,

$$\Delta G_c^\ddagger = \Delta G_{0c}^\ddagger + \alpha F(E - E^0) \quad (3.3.4)$$

Now let us assume that the rate constants k_f and k_b have an Arrhenius form that can be expressed as

$$k_f = A_f \exp(-\Delta G_c^\ddagger/RT) \quad (3.3.5)$$

$$k_b = A_b \exp(-\Delta G_a^\ddagger/RT) \quad (3.3.6)$$

Inserting the activation energies, (3.3.3) and (3.3.4), gives

$$k_f = A_f \exp(-\Delta G_{0c}^\ddagger/RT) \exp[-\alpha f(E - E^0)] \quad (3.3.7)$$

$$k_b = A_b \exp(-\Delta G_{0a}^\ddagger/RT) \exp[(1 - \alpha)f(E - E^0)] \quad (3.3.8)$$

where $f = F/RT$. The first two factors in each of these expressions form a product that is independent of potential and equal to the rate constant at $E = E^0$.⁴

Now consider the special case in which the interface is at equilibrium with a solution in which $C_O^* = C_R^*$. In this situation, $E = E^0$ and $k_f C_O^* = k_b C_R^*$, so that $k_f = k_b$. Thus, E^0 is the potential where the forward and reverse rate constants have the same value. That

⁴In other electrochemical literature, k_f and k_b are designated as k_c and k_a or as k_{ox} and k_{red} . Sometimes kinetic equations are written in terms of a complementary transfer coefficient, $\beta = 1 - \alpha$.

value is called the *standard rate constant*, k^0 .⁵ The rate constants at other potentials can then be expressed simply in terms of k^0 :

$$k_f = k^0 \exp[-\alpha f(E - E^{0'})] \quad (3.3.9)$$

$$k_b = k^0 \exp[(1 - \alpha)f(E - E^{0'})] \quad (3.3.10)$$

Insertion of these relations into (3.2.8) yields the complete *current-potential characteristic*:

$$i = F A k^0 \left[C_{\text{O}}(0, t) e^{-\alpha f(E - E^{0'})} - C_{\text{R}}(0, t) e^{(1-\alpha)f(E - E^{0'})} \right] \quad (3.3.11)$$

This relation is very important. It, or a variation derived from it, is used in the treatment of almost every problem requiring an account of heterogeneous kinetics. Section 3.4 will cover some of its ramifications. These results and the inferences derived from them are known broadly as the *Butler–Volmer* formulation of electrode kinetics, in honor of the pioneers in this area (17, 18).

One can derive the Butler–Volmer kinetic expressions by an alternative method based on electrochemical potentials (8, 10, 12, 19–21). Such an approach can be more convenient for more complicated cases, such as requiring the inclusion of double-layer effects or sequences of reactions in a mechanism. The first edition develops it in detail.⁶

3.3.3 The Standard Rate Constant

The physical interpretation of k^0 is straightforward. It simply is a measure of the kinetic facility of a redox couple. A system with a large k^0 will achieve equilibrium on a short time scale, but a system with small k^0 will be sluggish. The largest measured standard rate constants are in the range of 1 to 10 cm/s and are associated with particularly simple electron-transfer processes. For example, the standard rate constants for the reductions and oxidations of many aromatic hydrocarbons (such as substituted anthracenes, pyrene, and perylene) to the corresponding anion and cation radicals fall in this range (22–24). These processes involve only electron transfer and resolution. There are no significant alterations in the molecular forms. Similarly, some electrode processes involving the formation of amalgams [e.g., the couples $\text{Na}^+/\text{Na}(\text{Hg})$, $\text{Cd}^{2+}/\text{Cd}(\text{Hg})$, and $\text{Hg}_2^{2+}/\text{Hg}$] are rather facile (25, 26). More complicated reactions involving significant molecular rearrangement upon electron transfer, such as the reduction of molecular oxygen to hydrogen peroxide or water, or the reduction of protons to molecular hydrogen, can be very sluggish (25–27). Many of these systems involve multistep mechanisms and are discussed more fully in Section 3.5. Values of k^0 significantly lower than 10^{-9} cm/s have been reported (28–31); therefore, electrochemistry deals with a range of more than 10 orders of magnitude in kinetic reactivity.

Note that k_f and k_b can be made quite large, even if k^0 is small, by using a sufficiently extreme potential relative to $E^{0'}$. In effect, one drives the reaction by supplying the activation energy electrically. This idea is explored more fully in Section 3.4.

⁵The standard rate constant is also designated by $k_{s,h}$ or k_s in the electrochemical literature. Sometimes it is also called the *intrinsic rate constant*.

⁶First edition, Section 3.4.

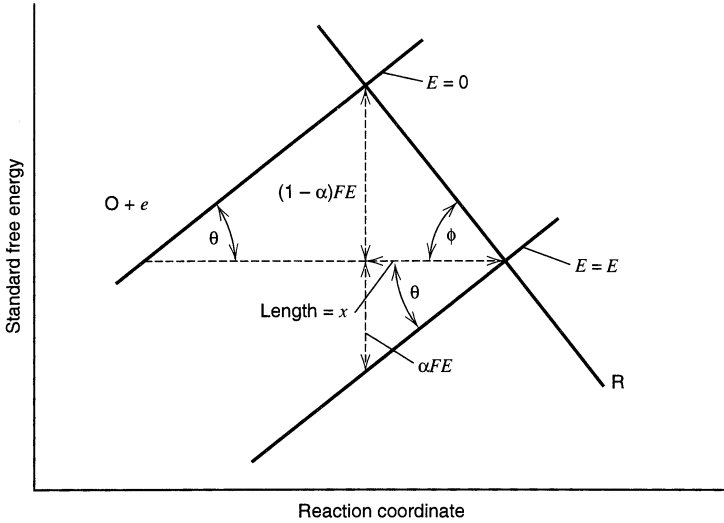


Figure 3.3.3 Relationship of the transfer coefficient to the angles of intersection of the free energy curves.

3.3.4 The Transfer Coefficient

The transfer coefficient, α , is a measure of the symmetry of the energy barrier. This idea can be amplified by considering α in terms of the geometry of the intersection region, as shown in Figure 3.3.3. If the curves are locally linear, then the angles θ and ϕ are defined by

$$\tan \theta = \alpha FE/x \quad (3.3.12)$$

$$\tan \phi = (1 - \alpha) FE/x \quad (3.3.13)$$

hence

$$\alpha = \frac{\tan \theta}{\tan \phi + \tan \theta} \quad (3.3.14)$$

If the intersection is symmetrical, $\phi = \theta$, and $\alpha = 1/2$. Otherwise $0 \leq \alpha < 1/2$ or $1/2 < \alpha \leq 1$, as shown in Figure 3.3.4. In most systems α turns out to lie between 0.3 and 0.7, and it can usually be approximated by 0.5 in the absence of actual measurements.

The free energy profiles are not likely to be linear over large ranges of the reaction coordinate; thus the angles θ and ϕ can be expected to change as the intersection between reactant and product curves shifts with potential. Consequently, α should generally be a

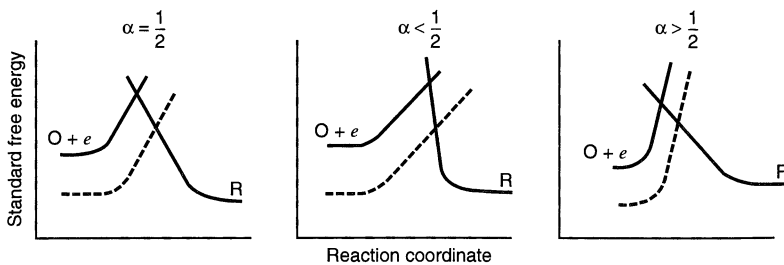


Figure 3.3.4 The transfer coefficient as an indicator of the symmetry of the barrier to reaction. The dashed lines show the shift in the curve for $O + e$ as the potential is made more positive.

potential-dependent factor (see Section 6.7.3). However, in the great majority of experiments, α appears to be constant, if only because the potential range over which kinetic data can be collected is fairly narrow. In a typical chemical system, the free energies of activation are in the range of a few electron volts, but the full range of measurable kinetics usually corresponds to a *change* in activation energy of only 50–200 meV, or a few percent of the total. Thus, the intersection point varies only over a small domain, such as, the boxed region in Figure 3.3.2, where the curvature in the profiles can hardly be seen. The kinetically operable potential range is narrow in most systems, because the rate constant for electron transfer rises exponentially with potential. Not far beyond the potential where a process first produces a detectable current, mass transfer becomes rate-limiting and the electron-transfer kinetics no longer control the experiment. These points are discussed in much detail throughout the remainder of this book. In a few systems, mass transfer is not an issue and kinetics can be measured over very wide ranges of potential. Figure 14.5.8 provides an example showing large variations of α with potential in a case involving a surface-bound electroactive species.

▶ 3.4 IMPLICATIONS OF THE BUTLER-VOLMER MODEL FOR THE ONE-STEP, ONE-ELECTRON PROCESS

In this section, we will develop a number of operational relationships that will prove valuable in the interpretation of electrochemical experiments. Each is derived under the assumption that the electrode reaction is the one-step, one-electron process for which the primary relations were derived above. The validity of the conclusions for a multistep process will be considered separately in Section 3.5.

3.4.1 Equilibrium Conditions. The Exchange Current (8–14)

At equilibrium, the net current is zero, and the electrode is known to adopt a potential based on the bulk concentrations of O and R as dictated by the Nernst equation. Let us see now if the kinetic model yields that thermodynamic relation as a special case. From equation 3.3.11 we have, at zero current,

$$FAk^0C_{\text{O}}(0, t)e^{-\alpha f(E_{\text{eq}}-E^{0'})} = FAk^0C_{\text{R}}(0, t)e^{(1-\alpha)f(E_{\text{eq}}-E^{0'})} \quad (3.4.1)$$

Since equilibrium applies, the bulk concentrations of O and R are found also at the surface; hence

$$e^{f(E_{\text{eq}}-E^{0'})} = \frac{C_{\text{O}}^*}{C_{\text{R}}^*} \quad (3.4.2)$$

which is simply an exponential form of the Nernst relation:

$$E_{\text{eq}} = E^{0'} + \frac{RT}{F} \ln \frac{C_{\text{O}}^*}{C_{\text{R}}^*} \quad (3.4.3)$$

Thus, the theory has passed its first test of compatibility with reality.

Even though the net current is zero at equilibrium, we still envision balanced faradaic activity that can be expressed in terms of the *exchange current*, i_0 , which is equal in magnitude to either component current, i_c or i_a . That is,

$$i_0 = FAk^0C_{\text{O}}^*e^{-\alpha f(E_{\text{eq}}-E^{0'})} \quad (3.4.4)$$

If both sides of (3.4.2) are raised to the $-\alpha$ power, we obtain

$$e^{-\alpha f(E_{\text{eq}} - E^{0'})} = \left(\frac{C_{\text{O}}^*}{C_{\text{R}}^*} \right)^{-\alpha} \quad (3.4.5)$$

Substitution of (3.4.5) into (3.4.4) gives⁷

$$i_0 = F A k^0 C_{\text{O}}^{*(1-\alpha)} C_{\text{R}}^{*\alpha} \quad (3.4.6)$$

The exchange current is therefore proportional to k^0 and can often be substituted for k^0 in kinetic equations. For the particular case where $C_{\text{O}}^* = C_{\text{R}}^* = C$,

$$i_0 = F A k^0 C \quad (3.4.7)$$

Often the exchange current is normalized to unit area to provide the *exchange current density*, $j_0 = i_0/A$.

3.4.2 The Current-Overpotential Equation

An advantage of working with i_0 rather than k^0 is that the current can be described in terms of the deviation from the equilibrium potential, that is, the overpotential, η , rather than the formal potential, $E^{0'}$. Dividing (3.3.11) by (3.4.6), we obtain

$$\frac{i}{i_0} = \frac{C_{\text{O}}(0, t) e^{-\alpha f(E - E^{0'})}}{C_{\text{O}}^{*(1-\alpha)} C_{\text{R}}^{*\alpha}} - \frac{C_{\text{R}}(0, t) e^{(1-\alpha) f(E - E^{0'})}}{C_{\text{O}}^{*(1-\alpha)} C_{\text{R}}^{*\alpha}} \quad (3.4.8)$$

or

$$\frac{i}{i_0} = \frac{C_{\text{O}}(0, t)}{C_{\text{O}}^*} e^{-\alpha f(E - E^{0'})} \left(\frac{C_{\text{O}}^*}{C_{\text{R}}^*} \right)^{\alpha} - \frac{C_{\text{R}}(0, t)}{C_{\text{R}}^*} e^{(1-\alpha) f(E - E^{0'})} \left(\frac{C_{\text{O}}^*}{C_{\text{R}}^*} \right)^{-(1-\alpha)} \quad (3.4.9)$$

The ratios $(C_{\text{O}}^*/C_{\text{R}}^*)^{\alpha}$ and $(C_{\text{O}}^*/C_{\text{R}}^*)^{-(1-\alpha)}$ are easily evaluated from equations 3.4.2 and 3.4.5, and by substitution we obtain

$$i = i_0 \left[\frac{C_{\text{O}}(0, t)}{C_{\text{O}}^*} e^{-\alpha f \eta} - \frac{C_{\text{R}}(0, t)}{C_{\text{R}}^*} e^{(1-\alpha) f \eta} \right] \quad (3.4.10)$$

where $\eta = E - E_{\text{eq}}$. This equation, known as the *current-overpotential equation*, will be used frequently in later discussions. Note that the first term describes the cathodic component current at any potential, and the second gives the anodic contribution.⁸

The behavior predicted by (3.4.10) is depicted in Figure 3.4.1. The solid curve shows the actual total current, which is the sum of the components i_c and i_a , shown as dashed traces. For large negative overpotentials, the anodic component is negligible; hence the total current curve merges with that for i_c . At large positive overpotentials, the cathodic component is negligible, and the total current is essentially the same as i_a . In going either direction from E_{eq} , the magnitude of the current rises rapidly, because the exponential factors dominate behavior, but at extreme η , the current levels off. In these

⁷The same equation for the exchange current can be derived from the anodic component current i_a at $E = E_{\text{eq}}$.

⁸Since double-layer effects have not been included in this treatment, k^0 and i_0 are, in Delahay's nomenclature (8), *apparent* constants of the system. Both depend on double-layer structure to some extent and are functions of the potential at the outer Helmholtz plane, ϕ_2 , relative to the solution bulk. This point will be discussed in more detail in Section 13.7.

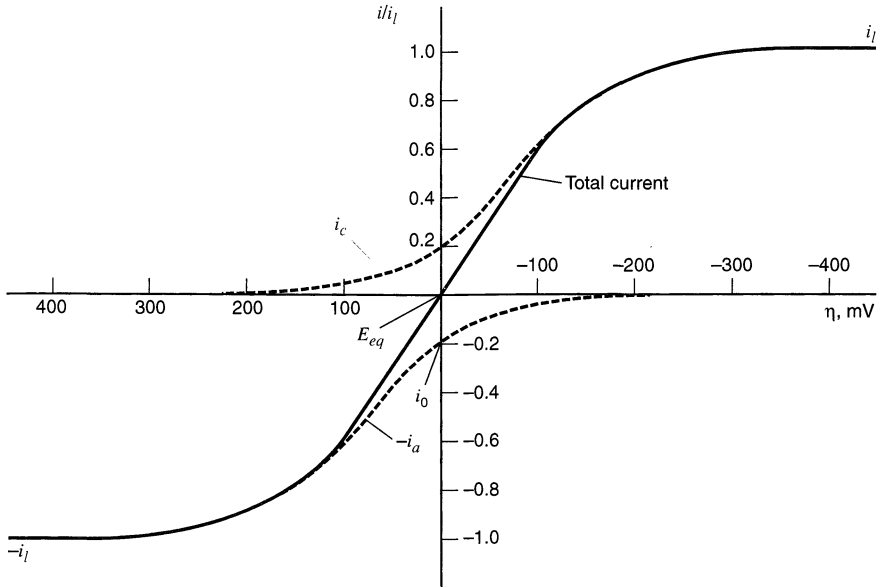


Figure 3.4.1 Current-overpotential curves for the system $O + e \rightleftharpoons R$ with $\alpha = 0.5$, $T = 298$ K, $i_{l,c} = -i_{l,a} = i_l$ and $i_0/i_l = 0.2$. The dashed lines show the component currents i_c and i_a .

level regions, the current is limited by mass transfer rather than heterogeneous kinetics. The exponential factors in (3.4.10) are then moderated by the factors $C_O(0, t)/C_O^*$ and $C_R(0, t)/C_R^*$, which manifest the reactant supply.

3.4.3 Approximate Forms of the i - η Equation

(a) No Mass-Transfer Effects

If the solution is well stirred, or currents are kept so low that the surface concentrations do not differ appreciably from the bulk values, then (3.4.10) becomes

$$i = i_0 \left[e^{-\alpha f \eta} - e^{(1-\alpha) f \eta} \right] \quad (3.4.11)$$

which is historically known as the *Butler–Volmer equation*. It is a good approximation of (3.4.10) when i is less than about 10% of the smaller limiting current, $i_{l,c}$ or $i_{l,a}$. Equations 1.4.10 and 1.4.19 show that $C_O(0, t)/C_O^*$ and $C_R(0, t)/C_R^*$ will then be between 0.9 and 1.1.

The curves in Figure 3.4.2 show the behavior of (3.4.11) for different exchange current densities. In each case $\alpha = 0.5$. Figure 3.4.3 shows the effect of α in a similar manner. There the exchange current density is 10^{-6} A/cm² for each curve. A notable feature of Figure 3.4.2 is the degree to which the inflection at E_{eq} depends on the exchange current density.

Since mass-transfer effects are not included here, the overpotential associated with any given current serves solely to provide the activation energy required to drive the heterogeneous process at the rate reflected by the current. The lower the exchange current, the more sluggish the kinetics; hence the larger this *activation overpotential* must be for any particular net current.

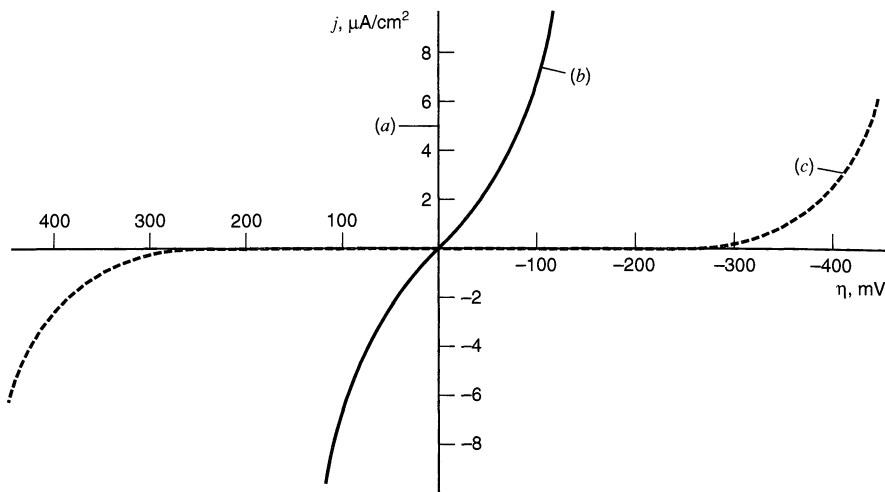


Figure 3.4.2 Effect of exchange current density on the activation overpotential required to deliver net current densities. (a) $j_0 = 10^{-3}$ A/cm² (curve is indistinguishable from the current axis), (b) $j_0 = 10^{-6}$ A/cm², (c) $j_0 = 10^{-9}$ A/cm². For all cases the reaction is $O + e \rightleftharpoons R$ with $\alpha = 0.5$ and $T = 298$ K.

If the exchange current is very large, as for case (a) in Figure 3.4.2, then the system can supply large currents, even the mass-transfer-limited current, with insignificant activation overpotential. In that case, any observed overpotential is associated with changing surface concentrations of species O and R. It is called a *concentration overpotential* and can be viewed as an activation energy required to drive mass transfer at the rate needed to support the current. If the concentrations of O and R are comparable, then E_{eq} will be near $E^{0'}$, and the limiting currents for both the anodic and cathodic segments will be reached within a few tens of millivolts of $E^{0'}$.

On the other hand, one might deal with a system with an exceedingly small exchange current because k^0 is very low, as for case (c) in Figure 3.4.2. In that circumstance, no sig-

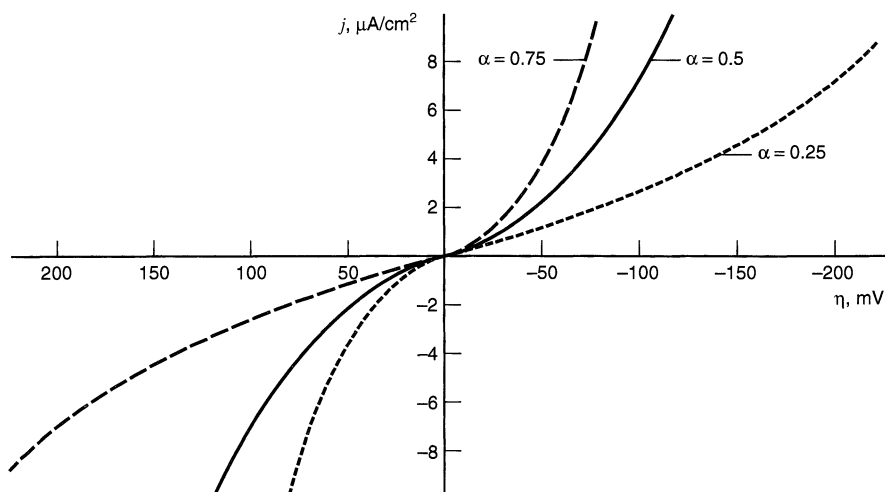


Figure 3.4.3 Effect of the transfer coefficient on the symmetry of the current-overpotential curves for $O + e \rightleftharpoons R$ with $T = 298$ K and $j_0 = 10^{-6}$ A/cm².

nificant current flows unless a large activation overpotential is applied. At a sufficiently extreme potential, the heterogeneous process can be driven fast enough that mass transfer controls the current, and a limiting plateau is reached. When mass-transfer effects start to manifest themselves, then a concentration overpotential will also contribute, but the bulk of the overpotential is for activation of charge transfer. In this kind of system, the reduction wave occurs at much more negative potentials than $E^{0'}$, and the oxidation wave lies at much more positive values.

The exchange current can be viewed as a kind of “idle current” for charge exchange across the interface. If we want to draw a net current that is only a small fraction of this bidirectional idle current, then only a tiny overpotential will be required to extract it. Even at equilibrium, the system is delivering charge across the interface at rates much greater than we require. The role of the slight overpotential is to unbalance the rates in the two directions to a small degree so that one of them predominates. On the other hand, if we ask for a net current that exceeds the exchange current, the job is much harder. We have to drive the system to deliver charge at the required rate, and we can only do that by applying a significant overpotential. From this perspective, we see that the exchange current is a measure of any system’s ability to deliver a net current without a significant energy loss due to activation.

Exchange current densities in real systems reflect the wide range in k^0 . They may exceed 10 A/cm^2 or be less than pA/cm^2 (8–14, 28–31).

(b) Linear Characteristic at Small η

For small values of x , the exponential e^x can be approximated as $1 + x$; hence for sufficiently small η , equation 3.4.11 can be reexpressed as

$$i = -i_0 f \eta \quad (3.4.12)$$

which shows that the net current is linearly related to overpotential in a narrow potential range near E_{eq} . The ratio $-\eta/i$ has units of resistance and is often called the *charge-transfer resistance*, R_{ct} :

$$R_{\text{ct}} = \frac{RT}{Fi_0} \quad (3.4.13)$$

This parameter is the negative reciprocal slope of the i - η curve where that curve passes through the origin ($\eta = 0, i = 0$). It can be evaluated directly in some experiments, and it serves as a convenient index of kinetic facility. For very large k^0 , it approaches zero (see Figure 3.4.2).

(c) Tafel Behavior at Large η

For large values of η (either negative or positive), one of the bracketed terms in (3.4.11) becomes negligible. For example, at large negative overpotentials, $\exp(-\alpha f \eta) \gg \exp[(1 - \alpha) f \eta]$ and (3.4.11) becomes

$$i = i_0 e^{-\alpha f \eta} \quad (3.4.14)$$

or

$$\eta = \frac{RT}{\alpha F} \ln i_0 - \frac{RT}{\alpha F} \ln i \quad (3.4.15)$$

Thus, we find that the kinetic treatment outlined above does yield a relation of the Tafel form, as required by observation, for the appropriate conditions. The empirical Tafel constants (see equation 3.2.4) can now be identified from theory as⁹

$$a = \frac{2.3RT}{\alpha F} \log i_0 \quad b = \frac{-2.3RT}{\alpha F} \quad (3.4.16)$$

The Tafel form can be expected to hold whenever the back reaction (i.e., the anodic process, when a net reduction is considered, and vice versa) contributes less than 1% of the current, or

$$\frac{e^{(1-\alpha)f\eta}}{e^{-\alpha f\eta}} = e^{f\eta} \leq 0.01, \quad (3.4.17)$$

which implies that $|\eta| > 118$ mV at 25°C. If the electrode kinetics are fairly facile, the system will approach the mass-transfer-limited current by the time such an extreme overpotential is established. Tafel relationships cannot be observed for such cases, because they require the absence of mass-transfer effects on the current. When electrode kinetics are sluggish and significant activation overpotentials are required, good Tafel relationships can be seen. This point underscores the fact that Tafel behavior is an indicator of *totally irreversible* kinetics. Systems in that category allow no significant current flow except at high overpotentials, where the faradaic process is effectively unidirectional and, therefore, chemically irreversible.

(d) Tafel Plots (8–11, 32)

A plot of $\log i$ vs. η , known as a *Tafel plot*, is a useful device for evaluating kinetic parameters. In general, there is an anodic branch with slope $(1 - \alpha)F/2.3RT$ and a cathodic branch with slope $-\alpha F/2.3RT$. As shown in Figure 3.4.4, both linear segments extrapolate to an intercept of $\log i_0$. The plots deviate sharply from linear behavior as η approaches zero, because the back reactions can no longer be regarded as negligible. The

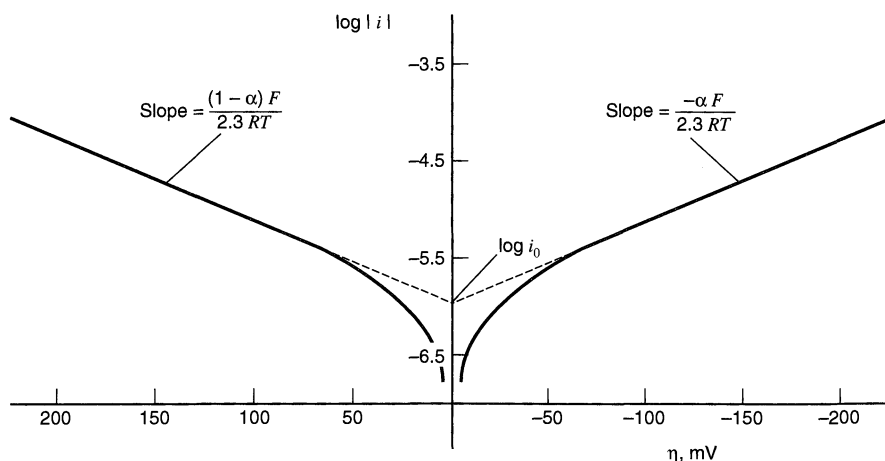


Figure 3.4.4 Tafel plots for anodic and cathodic branches of the current-overpotential curve for $O + e \rightleftharpoons R$ with $\alpha = 0.5$, $T = 298$ K, and $j_0 = 10^{-6}$ A/cm².

⁹Note that for $\alpha = 0.5$, $b = 0.118$ V, a value that is sometimes quoted as a “typical” Tafel slope.

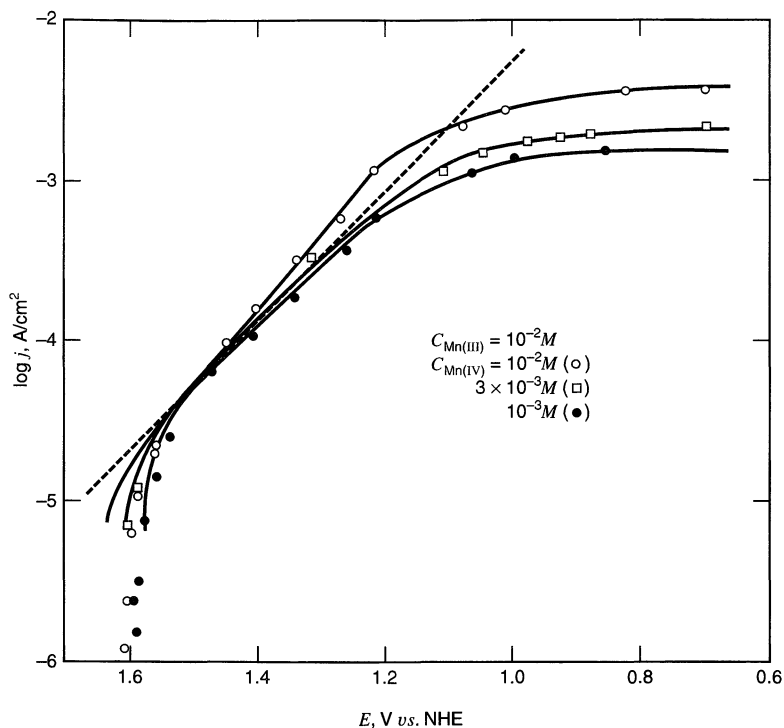


Figure 3.4.5 Tafel plots for the reduction of Mn(IV) to Mn(III) at Pt in 7.5 M H₂SO₄ at 298 K. The dashed line corresponds to $\alpha = 0.24$. [From K. J. Vetter and G. Manecke, *Z. Physik. Chem. (Leipzig)*, **195**, 337 (1950), with permission.]

transfer coefficient, α , and the exchange current, i_0 , are obviously readily accessible from this kind of presentation, when it can be applied.

Some real Tafel plots are shown in Figure 3.4.5 for the Mn(IV)/Mn(III) system in concentrated acid (33). The negative deviations from linearity at very large overpotentials come from limitations imposed by mass transfer. The region of very low overpotentials shows sharp falloffs for the reasons outlined just above.

Allen and Hickling (34) suggested an alternative method allowing the use of data obtained at low overpotentials. Equation 3.4.11 can be rewritten as

$$i = i_0 e^{-\alpha f \eta} (1 - e^{f \eta}) \quad (3.4.18)$$

or

$$\log \frac{i}{1 - e^{f \eta}} = \log i_0 - \frac{\alpha F \eta}{2.3 RT} \quad (3.4.19)$$

so that a plot of $\log [i/(1 - e^{f \eta})]$ vs. η yields an intercept of $\log i_0$ and a slope of $-\alpha F/2.3 RT$. This approach has the advantage of being applicable to electrode reactions that are not totally irreversible, that is, those in which both anodic and cathodic processes contribute significantly to the currents measured in the overpotential range where mass-transfer effects are not important. Such systems are often termed *quasireversible*, because the opposing charge-transfer reactions must both be considered, yet a noticeable activation overpotential is required to drive a given net current through the interface.

3.4.4 Exchange Current Plots (8–14)

From equation 3.4.4, we recognize that the exchange current can be restated as

$$\log i_0 = \log F A k^0 + \log C_O^* + \frac{\alpha F}{2.3RT} E^{0'} - \frac{\alpha F}{2.3RT} E_{\text{eq}} \quad (3.4.20)$$

Therefore, a plot of $\log i_0$ vs. E_{eq} at constant C_O^* should be linear with a slope of $-\alpha F/2.3RT$. The equilibrium potential E_{eq} can be varied experimentally by changing the bulk concentration of species R, while that of species O is held constant. This kind of plot is useful for obtaining α from experiments in which i_0 is measured essentially directly (e.g., see Chapters 8 and 10).

Another means for determining α is suggested by rewriting (3.4.6) as

$$\log i_0 = \log F A k^0 + (1 - \alpha) \log C_O^* + \alpha \log C_R^* \quad (3.4.21)$$

Thus

$$\left(\frac{\partial \log i_0}{\partial \log C_O^*} \right)_{C_R^*} = 1 - \alpha \quad \text{and} \quad \left(\frac{\partial \log i_0}{\partial \log C_R^*} \right)_{C_O^*} = \alpha \quad (3.4.22)$$

An alternative equation, which does not require holding either C_O^* or C_R^* constant, is

$$\frac{d \log (i_0/C_O^*)}{d \log (C_R^*/C_O^*)} = \alpha \quad (3.4.23)$$

The last relation is easily derived from (3.4.6).

3.4.5 Very Facile Kinetics and Reversible Behavior

To this point, we have discussed in detail only those systems for which appreciable activation overpotential is observed. Another very important limit is the case in which the electrode kinetics require a negligible driving force. As we noted above, that case corresponds to a very large exchange current, which in turn reflects a big standard rate constant k^0 . Let us rewrite the current-overpotential equation (3.4.10) as follows:

$$\frac{i}{i_0} = \frac{C_O(0, t)}{C_O^*} e^{-\alpha f \eta} - \frac{C_R(0, t)}{C_R^*} e^{(1-\alpha) f \eta} \quad (3.4.24)$$

and consider its behavior when i_0 becomes very large compared to any current of interest. The ratio i/i_0 then approaches zero, and we can rearrange the limiting form of equation 3.4.24 to

$$\frac{C_O(0, t)}{C_R(0, t)} = \frac{C_O^*}{C_R^*} e^{f(E-E_{\text{eq}})} \quad (3.4.25)$$

and, by substitution from the Nernst equation in form (3.4.2), we obtain

$$\frac{C_O(0, t)}{C_R(0, t)} = e^{f(E_{\text{eq}}-E^{0'})} e^{f(E-E_{\text{eq}})} \quad (3.4.26)$$

or

$$\frac{C_O(0, t)}{C_R(0, t)} = e^{f(E-E^{0'})} \quad (3.4.27)$$

This equation can be rearranged to the very important result:

$$E = E^{0'} + \frac{RT}{F} \ln \frac{C_{\text{O}}(0, t)}{C_{\text{R}}(0, t)} \quad (3.4.28)$$

Thus we see that the electrode potential and the *surface* concentrations of O and R are linked by an equation of the Nernst form, regardless of the current flow.

No kinetic parameters are present because the kinetics are so facile that no experimental manifestations can be seen. In effect, the potential and the surface concentrations are always kept in equilibrium with each other by the fast charge-transfer processes, and the *thermodynamic* equation, (3.4.28), characteristic of equilibrium, always holds. Net current flows because the surface concentrations are not at equilibrium with the bulk, and mass transfer continuously moves material to the surface, where it must be reconciled to the potential by electrochemical change.

We have already seen that a system that is always at equilibrium is termed a *reversible* system; thus it is logical that an electrochemical system in which the charge-transfer interface is always at equilibrium be called a *reversible* (or, alternatively, a *nernstian*) *system*. These terms simply refer to cases in which the interfacial redox kinetics are so fast that activation effects cannot be seen. Many such systems exist in electrochemistry, and we will consider this case frequently under different sets of experimental circumstances. We will also see that any given system may appear reversible, quasireversible, or totally irreversible, depending on the demands we make on the charge-transfer kinetics.

3.4.6 Effects of Mass Transfer

A more complete i - η relation can be obtained from (3.4.10) by substituting for $C_{\text{O}}(0, t)/C_{\text{O}}^*$ and $C_{\text{R}}(0, t)/C_{\text{R}}^*$ according to (1.4.10) and (1.4.19):

$$\frac{i}{i_0} = \left(1 - \frac{i}{i_{l,c}}\right) e^{-\alpha f \eta} - \left(1 - \frac{i}{i_{l,a}}\right) e^{(1-\alpha) f \eta} \quad (3.4.29)$$

This equation can be rearranged easily to give i as an explicit function of η over the whole range of η . In Figure 3.4.6, one can see i - η curves for several ratios of i_0/i_l , where $i_l = i_{l,c} = -i_{l,a}$.

For small overpotentials, a linearized relation can be used. The complete Taylor expansion (Section A.2) of (3.4.24) gives, for $\alpha f \eta \ll 1$,

$$\frac{i}{i_0} = \frac{C_{\text{O}}(0, t)}{C_{\text{O}}^*} - \frac{C_{\text{R}}(0, t)}{C_{\text{R}}^*} - \frac{F \eta}{RT} \quad (3.4.30)$$

which can be substituted as above and rearranged to give

$$\eta = i \frac{RT}{F} \left(\frac{1}{i_0} + \frac{1}{i_{l,c}} - \frac{1}{i_{l,a}} \right) \quad (3.4.31)$$

In terms of the charge- and mass-transfer pseudoresistances defined in equations 1.4.28 and 3.4.13, this equation is

$$\eta = -i(R_{\text{ct}} + R_{\text{mt,c}} + R_{\text{mt,a}}) \quad (3.4.32)$$

Here we see very clearly that when i_0 is much greater than the limiting currents, $R_{\text{ct}} \ll R_{\text{mt,c}} + R_{\text{mt,a}}$ and the overpotential, even near E_{eq} , is a concentration over-

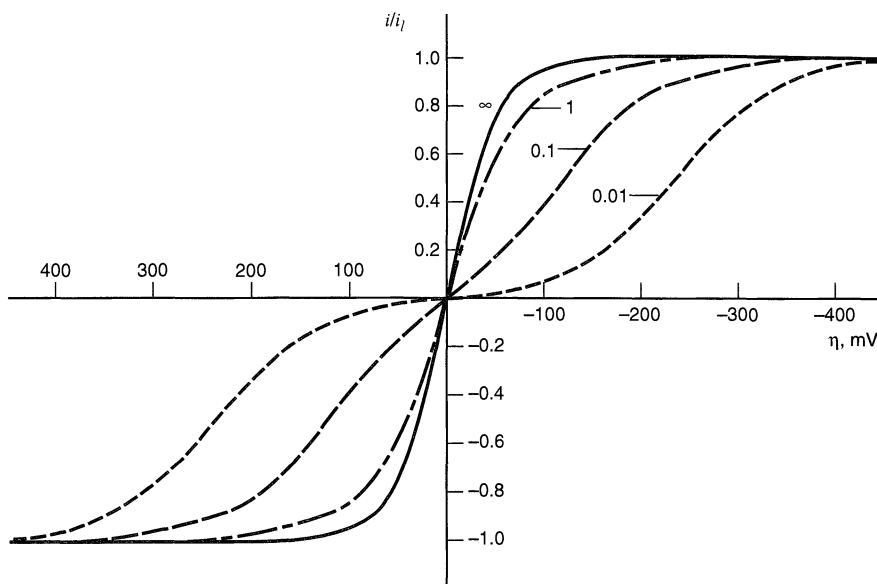


Figure 3.4.6 Relationship between the activation overpotential and net current demand relative to the exchange current. The reaction is $O + e \rightleftharpoons R$ with $\alpha = 0.5$, $T = 298$ K, and $i_{l,c} = -i_{l,a} = i_l$. Numbers by curves show i_0/i_l .

potential. On the other hand, if i_0 is much less than the limiting currents, then $R_{mt,c} + R_{mt,a} \ll R_{ct}$, and the overpotential near E_{eq} is due to activation of charge transfer. This argument is simply another way of looking at the points made earlier in Section 3.4.3(a).

In the Tafel regions, other useful forms of (3.4.29) can be obtained. For the cathodic branch at high η values, the anodic contribution is insignificant, and (3.4.29) becomes

$$\frac{i}{i_0} = \left(1 - \frac{i}{i_{l,c}}\right) e^{-\alpha f \eta} \quad (3.4.33)$$

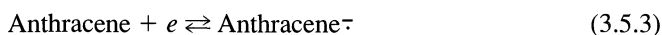
or

$$\eta = \frac{RT}{\alpha F} \ln \frac{i_0}{i_{l,c}} + \frac{RT}{\alpha F} \ln \frac{(i_{l,c} - i)}{i} \quad (3.4.34)$$

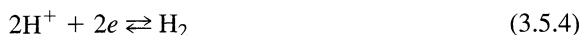
This equation can be useful for obtaining kinetic parameters for systems in which the normal Tafel plots are complicated by mass-transfer effects.

▶ 3.5 MULTISTEP MECHANISMS (11, 13, 14, 25, 26, 35)

The foregoing sections have concentrated on the potential dependences of the forward and reverse rate constants governing the simple one-step, one-electron electrode reaction. By restricting our view in this way, we have achieved a qualitative and quantitative understanding of the major features of electrode kinetics. Also, we have developed a set of relations that we can expect to fit a number of real chemical systems, for example,



But we must now recognize that most electrode processes are mechanisms of several steps. For example, the important reaction



clearly must involve several elementary reactions. The hydrogen nuclei are separated in the oxidized form, but are combined by reduction. Somehow, during reduction, there must be a pair of charge transfers and some chemical means for linking the two nuclei. Consider also the reduction



Is it realistic to regard two electrons as tunneling simultaneously through the interface? Or must we consider the reduction and oxidation sequences as two one-electron processes proceeding through the ephemeral intermediate Sn^{3+} ? Another case that looks simple at first glance is the deposition of silver from aqueous potassium nitrate:



However, there is evidence that this reduction involves at least a charge-transfer step, creating an adsorbed silver atom (*adatom*), and a crystallization step, in which the adatom migrates across the surface until it finds a vacant lattice site. Electrode processes may also involve adsorption and desorption kinetics of primary reactants, intermediates, and products.

Thus, electrode reactions generally can be expected to show complex behavior, and for each mechanistic sequence, one would obtain a distinct theoretical linkage between current and potential. That relation would have to take into account the potential dependences of all steps and the surface concentrations of all intermediates, in addition to the concentrations of the primary reactants and products.

A great deal of effort has been spent in studying the mechanisms of complex electrode reactions. One general approach is based on steady-state current-potential curves. Theoretical responses are derived on the basis of mechanistic alternatives, then one compares predicted behavior, such as the variation of exchange current with reactant concentration, with the behavior found experimentally. A number of excellent expositions of this approach are available in the literature (8–14, 25, 26, 35). We will not delve into specific cases in this chapter, except in Problems 3.7 and 3.10. More commonly, complex behavior is elucidated by studies of transient responses, such as cyclic voltammetry at different scan rates. The experimental study of multistep reactions by such techniques is covered in Chapter 12.

3.5.1 Rate-Determining Electron Transfer

In the study of chemical kinetics, one can often simplify the prediction and analysis of behavior by recognizing that a single step of a mechanism is much more sluggish than all the others, so that it controls the rate of the overall reaction. If the mechanism is an electrode process, this *rate-determining step* (RDS) can be a heterogeneous electron-transfer reaction.

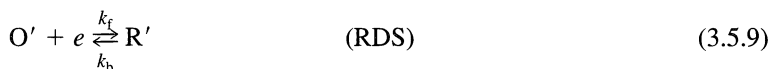
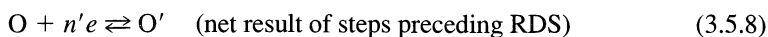
A widely held concept in electrochemistry is that truly elementary electron-transfer reactions always involve the exchange of one electron, so that an overall process involving a change of n electrons must involve n distinct electron-transfer steps. Of course, it may also involve other elementary reactions, such as adsorption, desorption, or various chemical reactions away from the interface. Within this view, a rate-determining electron-transfer is always a one-electron-process, and the results that we derived above for the

one-step, one-electron process can be used to describe the RDS, although the concentrations must often be understood as applying to intermediates, rather than to starting species or final products.

For example, consider an overall process in which O and R are coupled in an overall multielectron process



by a mechanism having the following general character:



Obviously $n' + n'' + 1 = n$.¹⁰

The current-potential characteristic can be written as

$$i = nFAk_{\text{rds}}^0 [C_{\text{O}'}(0, t)e^{-\alpha f(E-E_{\text{rds}}^{0'})} - C_{\text{R}'}(0, t)e^{(1-\alpha)f(E-E_{\text{rds}}^{0'})}] \quad (3.5.11)$$

where k_{rds}^0 , α , and $E_{\text{rds}}^{0'}$ apply to the RDS. This relation is (3.3.11) written for the RDS and multiplied by n , because each net conversion of O' to R' results in the flow of n electrons, not just one electron, across the interface. The concentrations $C_{\text{O}'}(0, t)$ and $C_{\text{R}'}(0, t)$ are controlled not only by the interplay between mass transfer and the kinetics of heterogeneous electron transfer, as we found in Section 3.4, but also by the properties of the preceding and following reactions. The situation can become quite complicated, so we will make no attempt to discuss the general problem. However, a few important simple cases exist, and we will develop them briefly now.¹¹

3.5.2 Multistep Processes at Equilibrium

If a true equilibrium exists for the overall process, all steps in the mechanism are individually at equilibrium. Thus, the surface concentrations of O' and R' are the values in equilibrium with the bulk concentrations of O and R, respectively. We designate them as $(C_{\text{O}'})_{\text{eq}}$ and $(C_{\text{R}'})_{\text{eq}}$. Recognizing that $i = 0$, we can proceed through the treatment leading to (3.4.2) to obtain the analogous relation

$$e^{f(E_{\text{eq}}-E_{\text{rds}}^{0'})} = \frac{(C_{\text{O}'})_{\text{eq}}}{(C_{\text{R}'})_{\text{eq}}} \quad (3.5.12)$$

For the mechanism in (3.5.8)–(3.5.10), Nernstian relationships define the equilibria for the pre- and postreactions, and they can be written in the following forms:

$$e^{n'f(E_{\text{eq}}-E_{\text{pre}}^{0'})} = \frac{C_{\text{O}}^*}{(C_{\text{O}'})_{\text{eq}}} \quad e^{n''f(E_{\text{eq}}-E_{\text{post}}^{0'})} = \frac{(C_{\text{R}'})_{\text{eq}}}{C_{\text{R}}^*} \quad (3.5.13)$$

¹⁰The discussions that follow hold if either or both of n' or n'' are zero.

¹¹In the first edition and in much of the literature, one finds n_a used as the n value of the rate-determining step. As a consequence n_a appears in many kinetic expressions. Since n_a is probably always 1, it is a redundant symbol and has been dropped in this edition. The current-potential characteristic for a multistep process has often been expressed as

$$i = nFAk^0 [C_{\text{O}}(0, t)e^{-\alpha n_a f(E-E^0)} - C_{\text{R}}(0, t)e^{(1-\alpha)n_a f(E-E^0)}]$$

This is rarely, if ever, an accurate form of the i - E characteristic for multistep mechanisms.

where $E_{\text{pre}}^{0'}$ and $E_{\text{post}}^{0'}$ apply to (3.5.8) and (3.5.10), respectively. Substitution for the equilibrium concentrations of O' and R' in (3.5.12) gives

$$e^{f(E_{\text{eq}} - E_{\text{rds}}^{0'})} e^{n'f(E_{\text{eq}} - E_{\text{pre}}^{0'})} e^{n''f(E_{\text{eq}} - E_{\text{post}}^{0'})} = \frac{C_{\text{O}}^*}{C_{\text{R}}^*} \quad (3.5.14)$$

Recognizing that $n = n' + n'' + 1$ and that $E^{0'}$ for the overall process is (see Problem 2.10)

$$E^{0'} = \frac{E_{\text{rds}}^{0'} + n'E_{\text{pre}}^{0'} + n''E_{\text{post}}^{0'}}{n} \quad (3.5.15)$$

we can distill (3.5.14) into

$$e^{nf(E_{\text{eq}} - E^{0'})} = \frac{C_{\text{O}}^*}{C_{\text{R}}^*} \quad (3.5.16)$$

which is the exponential form of the Nernst equation for the overall reaction,

$$E_{\text{eq}} = E^{0'} + \frac{RT}{nF} \ln \frac{C_{\text{O}}^*}{C_{\text{R}}^*} \quad (3.5.17)$$

Of course, this is a required result if the kinetic model has any pretense to validity, and it is important that the BV model attains it for the limit of $i = 0$, not only for the simple one-step, one-electron process, but also in the context of an arbitrary multistep mechanism. The derivation here was carried out for a mechanism in which the pre-reactions and post-reactions involve net charge transfer; however the same outcome can be obtained by a similar method for any reaction sequence, as long as it is chemically reversible and a true equilibrium can be established.

3.5.3 Nernstian Multistep Processes

If all steps in the mechanism are facile, so that the exchange velocities of all steps are large compared to the net reaction rate, the concentrations of all species participating in them are always essentially at equilibrium in a local context, even though a net current flows. The result for the RDS in this nernstian (reversible) limit has already been obtained as (3.4.27), which we now rewrite in exponential form:

$$\frac{C_{\text{O}}(0, t)}{C_{\text{R}}(0, t)} = e^{f(E - E_{\text{rds}}^{0'})} \quad (3.5.18)$$

Equilibrium expressions for the pre- and post-reactions link the surface concentrations of O' and R' to the surface concentrations of O and R. If these processes involve interfacial charge transfer, as in the mechanism of (3.5.8)–(3.5.10), the expressions are of the Nernst form:

$$e^{n'f(E - E_{\text{pre}}^{0'})} = \frac{C_{\text{O}}(0, t)}{C_{\text{O}'}(0, t)} \quad e^{n''f(E - E_{\text{post}}^{0'})} = \frac{C_{\text{R}'}(0, t)}{C_{\text{R}}(0, t)} \quad (3.5.19)$$

By steps analogous to those leading from (3.5.12) to (3.5.16), one finds that for the reversible system

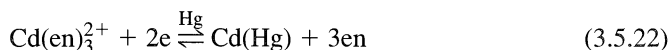
$$e^{nf(E_{\text{eq}} - E^{0'})} = \frac{C_{\text{O}}(0, t)}{C_{\text{R}}(0, t)} \quad (3.5.20)$$

which can be rearranged to

$$E = E^{0'} + \frac{RT}{nF} \ln \frac{C_{\text{O}}(0, t)}{C_{\text{R}}(0, t)} \quad (3.5.21)$$

This relationship is a very important general finding. It says that, for a kinetically facile system, the electrode potential and the surface concentrations of the initial reactant and the final product are in local nernstian balance at all times, regardless of the details of the mechanism linking these species and regardless of current flow. Like (3.5.17), (3.5.21) was derived for pre- and postreactions that involve net charge transfer, but one can easily generalize the derivation to include other patterns. The essential requirement is that all steps be chemically reversible and possess facile kinetics.¹²

A great many real systems satisfy these conditions, and electrochemical examination of them can yield a rich variety of chemical information (see Section 5.4.4). A good example is the reduction of the ethylenediamine (en) complex of Cd(II) at a mercury electrode:



3.5.4 Quasireversible and Irreversible Multistep Processes

If a multistep process is neither nernstian nor at equilibrium, the details of the kinetics influence its behavior in electrochemical experiments, and one can use the results to diagnose the mechanism and to quantify kinetic parameters. As in the study of homogenous kinetics, one proceeds by devising a hypothesis about the mechanism, predicting experimental behavior on the basis of the hypothesis, and comparing the predictions against results. In the electrochemical sphere, an important part of predicting behavior is developing the current-potential characteristic in terms of controllable parameters, such as the concentrations of participating species.

If the RDS is a heterogeneous electron-transfer step, then the current-potential characteristic has the form of (3.5.11). For most mechanisms, this equation is of limited direct utility, because O' and R' are intermediates, whose concentration cannot be controlled directly. Still, (3.5.11) can serve as the basis for a more practical current-potential relationship, because one can use the presumed mechanism to reexpress $C_{\text{O}}(0, t)$ and $C_{\text{R}}(0, t)$ in terms of the concentrations of more controllable species, such as O and R (36).

Unfortunately, the results can easily become too complex for practical application. For example, consider the simple mechanism in (3.5.8)–(3.5.10), where the pre- and postreactions are assumed to be kinetically facile enough to remain in local equilibrium. The overall nernstian relationships, (3.5.19), connect the surface concentrations of O and R to those of O' and R'. Thus, the current-potential characteristic, (3.5.11), can be expressed in terms of the surface concentrations of the initial reactant, O, and the final product, R.

$$i = nFAk_{\text{rds}}^0 C_{\text{O}}(0, t) e^{-n'f(E-E_{\text{pre}}^{0'})} e^{-\alpha f(E-E_{\text{rds}}^{0'})} - nFAk_{\text{rds}}^0 C_{\text{R}}(0, t) e^{n'f(E-E_{\text{post}}^{0'})} e^{(1-\alpha)f(E-E_{\text{rds}}^{0'})} \quad (3.5.23)$$

This relationship can be rewritten as

$$i = nFA[k_{\text{f}}C_{\text{O}}(0, t) - k_{\text{b}}C_{\text{R}}(0, t)] \quad (3.5.24)$$

¹²In the reversible limit, it is no longer appropriate to speak of an RDS, because the kinetics are not rate-controlling. We retain the nomenclature, because we are considering how a mechanism that does have an RDS begins to behave as the kinetics become more facile.

where

$$k_f = k_{\text{rds}}^0 e^{f[n'E_{\text{pre}}^0 + \alpha E_{\text{rds}}^0]} e^{-(n'+\alpha)fE} \quad (3.5.25)$$

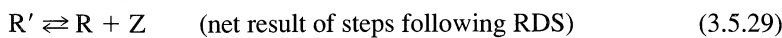
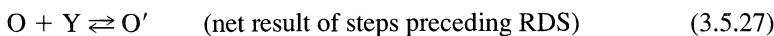
$$k_b = k_{\text{rds}}^0 e^{-f[n''E_{\text{post}}^0 + (1-\alpha)E_{\text{rds}}^0]} e^{(n'+1-\alpha)fE} \quad (3.5.26)$$

The point of these results is to illustrate some of the difficulties in dealing with a multistep mechanism involving an embedded RDS. No longer is the potential dependence of the rate constant expressible in two parameters, one of which is interpretable as a measure of intrinsic kinetic facility. Instead, k^0 becomes obscured by the first exponential factors in (3.5.25) and (3.5.26), which express thermodynamic relationships in the mechanism. One must have ways to find out the individual values of n' , n'' , E_{pre}^0 , E_{post}^0 , and E_{rds}^0 before one can evaluate the kinetics of the RDS in a fully quantitative way. This is normally a difficult requirement.

More readily usable results arise from some simpler situations:

(a) One-Electron Process Coupled Only to Chemical Equilibria

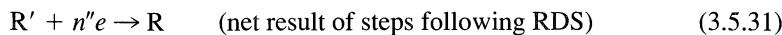
Many of the complications in the foregoing case arise from the fact that the pre- and postreactions involve heterogeneous electron transfer, so that their equilibria depend on E . Consider instead a mechanism that involves only chemical equilibria aside from the rate-determining interfacial electron transfer:



where Y and Z are other species (e.g., protons or ligands). If (3.5.27) and (3.5.29) are so facile that they are always at equilibrium, then $C_{\text{O}'}(0, t)$ and $C_{\text{R}'}(0, t)$ in (3.5.11) are calculable from the corresponding equilibrium constants, which may be available from separate experiments.

(b) Totally Irreversible Initial Step

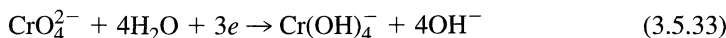
Suppose the RDS is the first step in the mechanism and is also a totally irreversible heterogeneous electron transfer:



The chemistry following (3.5.30) has no effect on the electrochemical response, except to add n'' electrons per molecule of O that reacts. Thus, the current is $n = 1 + n''$ times bigger than the current arising from step (3.5.30) alone. The overall result is given by the first term of (3.3.11) with $C_{\text{O}'}(0, t) = C_{\text{O}}(0, t)$,

$$i = nFAk^0 C_{\text{O}}(0, t) e^{-\alpha f(E - E_{\text{rds}}^0)} \quad (3.5.32)$$

Many examples of this kind of behavior exist in the literature; one is the polarographic reduction of chromate in 0.1 M NaOH:



Despite the obvious mechanistic complexity of this system, it behaves as though it has an irreversible electron transfer as the first step.

(c) Rate-Controlling Homogeneous Chemistry

A complete electrode reaction may involve homogeneous chemistry, one step of which could be the RDS. Although the rate constants of homogeneous reactions are not depen-

dent on potential, they affect the overall current-potential characteristic by their impact on the surface concentrations of species that are active at the interface. Some of the most interesting applications of electroanalytical techniques have been aimed at unraveling the homogeneous chemistry following the electrochemical production of reactive species, such as free radicals. Chapter 12 is devoted to these issues.

(d) Chemically Reversible Processes Near Equilibrium

A number of experimental methods, such as impedance spectroscopy (Chapter 10), are based on the application of small perturbations to a system otherwise at equilibrium. These methods often provide the exchange current in a relatively direct manner, as long as the system is chemically reversible. It is worthwhile for us to consider the exchange properties of a multistep process at equilibrium. The example that we will take is the overall process $O + ne \rightleftharpoons R$, effected by the general mechanism in (3.5.8)–(3.5.10) and having a standard potential $E^{0'}$.

At equilibrium, all of the steps in the mechanism are individually at equilibrium, and each has an exchange velocity. The electron-transfer reactions have exchange velocities that can be expressed as exchange currents in the manner that we have already seen. There is also an exchange velocity for the overall process that can be expressed as an exchange current. In a serial mechanism with a single RDS, such as we are now considering, the overall exchange velocity is limited by the exchange velocity through the RDS. From (3.4.4), we can write the exchange current for the RDS as

$$i_{0,\text{rds}} = F A k_{\text{rds}}^0 (C_{O'})_{\text{eq}} e^{-\alpha f (E_{\text{eq}} - E_{\text{rds}}^{0'})} \quad (3.5.34)$$

The overall exchange current is n -fold larger, because the pre- and postreactions contribute $n' + n''$ additional electrons per electron exchanged in the RDS. Thus,

$$i_0 = n F A k_{\text{rds}}^0 (C_{O'})_{\text{eq}} e^{-\alpha f (E_{\text{eq}} - E_{\text{rds}}^{0'})} \quad (3.5.35)$$

We can use the fact that the prereactions are at equilibrium to express $(C_{O'})_{\text{eq}}$ in terms of C_{O}^* . By substitution from (3.5.13),

$$i_0 = n F A k_{\text{rds}}^0 C_{\text{O}}^* e^{-n' f (E_{\text{eq}} - E_{\text{pre}}^{0'})} e^{-\alpha f (E_{\text{eq}} - E_{\text{rds}}^{0'})} \quad (3.5.36)$$

Let us multiply by unity in the form $e^{(n' + \alpha) f (E^{0'} - E^{0'})}$ and rearrange to obtain

$$i_0 = n F A k_{\text{rds}}^0 e^{n' f (E_{\text{pre}}^{0'} - E^{0'})} e^{\alpha f (E_{\text{rds}}^{0'} - E^{0'})} C_{\text{O}}^* e^{-(n' + \alpha) f (E_{\text{eq}} - E^{0'})} \quad (3.5.37)$$

Because equilibrium is established, the Nernst equation for the overall process is applicable. Taking it in the form of (3.5.16) and raising both sides to the power $-(n' + \alpha)/n$, we have

$$i_0 = n F A k_{\text{rds}}^0 e^{n' f (E_{\text{pre}}^{0'} - E^{0'})} e^{\alpha f (E_{\text{rds}}^{0'} - E^{0'})} C_{\text{O}}^* [1 - (n' + \alpha)/n] C_{\text{R}}^* [(n' + \alpha)/n] \quad (3.5.38)$$

Note that the two exponentials are constants of the system at a given temperature and pressure. It is convenient to combine them into an *apparent standard rate constant* for the overall process, k_{app}^0 , by defining

$$k_{\text{app}}^0 = k_{\text{rds}}^0 e^{n' f (E_{\text{pre}}^{0'} - E^{0'})} e^{\alpha f (E_{\text{rds}}^{0'} - E^{0'})} \quad (3.5.39)$$

so that the final result is reached:

$$i_0 = n F A k_{\text{app}}^0 C_{\text{O}}^* [1 - (n' + \alpha)/n] C_{\text{R}}^* [(n' + \alpha)/n] \quad (3.5.40)$$

This relationship applies generally to mechanisms fitting the pattern of (3.5.8)–(3.5.10), but not to others, such as those involving purely homogeneous pre- or

postreactions or those involving different rate-determining steps in the forward and reverse directions. Even so, the principles that we have used here can be employed to derive an expression like (3.5.40) for any other pattern, provided that the steps are chemically reversible and equilibrium applies. It will be generally possible to express the overall exchange current in terms of an apparent standard rate constant and the bulk concentrations of the various participants. If the exchange current can be measured validly for a given process, the derived relationship can provide insight into details of the mechanism.

For example, the variation of exchange current with the concentrations of O and R can provide $(n' + \alpha)/n$ for the sequential mechanism of (3.5.8)–(3.5.10). By an approach similar to that in Section 3.4.4, one obtains the following from (3.5.40):

$$\left(\frac{\partial \log i_0}{\partial \log C_{\text{O}}^*}\right)_{C_{\text{R}}^*} = 1 - \frac{n' + \alpha}{n} \quad (3.5.41)$$

$$\left(\frac{\partial \log i_0}{\partial \log C_{\text{R}}^*}\right)_{C_{\text{O}}^*} = \frac{n' + \alpha}{n} \quad (3.5.42)$$

Since n is often independently available from coulometry or from chemical knowledge of the reactants and products, one can frequently calculate $n' + \alpha$. From its magnitude, it may be possible to estimate separate values for n' and α , which in turn may afford chemical insight into the participants in the RDS. Practice in this direction is available in Problems 3.7 and 3.10.

As we have seen here, the apparent standard rate constant, k_{app}^0 , is usually not a simple kinetic parameter for a multistep process. Interpreting it may require detailed understanding of the mechanism, including knowledge of standard potentials or equilibrium constants for various elementary steps.

We can usefully take this discussion a little further by developing a current-overpotential relationship for a quasireversible mechanism having the pattern of (3.5.8)–(3.5.10). Beginning with (3.5.24)–(3.5.26), we multiply the first term by unity in the form of $\exp[-(n' + \alpha)f(E_{\text{eq}} - E_{\text{eq}})]$ and the second by unity in the form of $\exp[(n'' + 1 - \alpha)f(E_{\text{eq}} - E_{\text{eq}})]$. The result is

$$i = nFAk_{\text{rds}}^0 C_{\text{O}}(0, t) e^{-(n'+\alpha)fE_{\text{eq}}} e^{f[n'E_{\text{pre}}^0 + \alpha E_{\text{rds}}^0]} e^{-(n'+\alpha)f(E-E_{\text{eq}})} \quad (3.5.43)$$

$$- nFAk_{\text{rds}}^0 C_{\text{R}}(0, t) e^{(n''+1-\alpha)fE_{\text{eq}}} e^{f[n'E_{\text{post}}^0 + (1-\alpha)E_{\text{rds}}^0]} e^{(n''+1-\alpha)f(E-E_{\text{eq}})}$$

Multiplication of the first term by unity in the form of $\exp[-(n' + \alpha)f(E^{0'} - E^{0'})]$ and the second by unity in the form of $\exp[(n'' + 1 - \alpha)f(E^{0'} - E^{0'})]$ gives

$$i = nFAk_{\text{rds}}^0 C_{\text{O}}(0, t) e^{-(n'+\alpha)f(E_{\text{eq}}-E^{0'})} e^{f[n'E_{\text{pre}}^0 + \alpha E_{\text{rds}}^0 - (n'+\alpha)E^{0'}]} e^{-(n'+\alpha)f\eta}$$

$$- nFAk_{\text{rds}}^0 C_{\text{R}}(0, t) e^{(n''+1-\alpha)f(E_{\text{eq}}-E^{0'})} e^{-f[n'E_{\text{post}}^0 + (1-\alpha)E_{\text{rds}}^0 - (n''+1-\alpha)E^{0'}]} e^{(n''+1-\alpha)f\eta} \quad (3.5.44)$$

where $E - E_{\text{eq}}$ has been recognized as η . The first exponential in each of the two terms can be rewritten as a function of bulk concentrations by raising (3.5.16) to the appropriate power and substituting. The result is

$$i = nFAk_{\text{rds}}^0 C_{\text{O}}(0, t) C_{\text{O}}^{*[(n'+\alpha)/n]} C_{\text{R}}^{*[(n'+\alpha)/n]} e^{f[n'E_{\text{pre}}^0 + \alpha E_{\text{rds}}^0 - (n'+\alpha)E^{0'}]} e^{-(n'+\alpha)f\eta}$$

$$- nFAk_{\text{rds}}^0 C_{\text{R}}(0, t) C_{\text{O}}^{*[(n''+1-\alpha)/n]} C_{\text{R}}^{*[-(n''+1-\alpha)/n]} e^{-f[n'E_{\text{post}}^0 + (1-\alpha)E_{\text{rds}}^0 - (n''+1-\alpha)E^{0'}]} e^{(n''+1-\alpha)f\eta} \quad (3.5.45)$$

Division by the exchange current, as given by (3.5.40), and consolidation of the bulk concentrations provides

$$\frac{i}{i_0} = \frac{k_{\text{rds}}^0}{k_{\text{app}}^0} \frac{C_{\text{O}}(0, t)}{C_{\text{O}}^*} e^{f[n'E_{\text{pre}}^0 + \alpha E_{\text{rds}}^0 - (n' + \alpha)E^0]} e^{-(n' + \alpha)f\eta}$$

$$- \frac{k_{\text{rds}}^0}{k_{\text{app}}^0} \frac{C_{\text{R}}(0, t)}{C_{\text{R}}^*} e^{-f[n'E_{\text{post}}^0 + (1 - \alpha)E_{\text{rds}}^0 - (n'' + 1 - \alpha)E^0]} e^{(n'' + 1 - \alpha)f\eta} \quad (3.5.46)$$

where we have recognized that $n' + n'' + 1 = n$. Substitution for k_{app}^0 from (3.5.39) and consolidation of the exponentials leads to the final result,

$$\frac{i}{i_0} = \frac{C_{\text{O}}(0, t)}{C_{\text{O}}^*} e^{-(n' + \alpha)f\eta} - \frac{C_{\text{R}}(0, t)}{C_{\text{R}}^*} e^{(n'' + 1 - \alpha)f\eta} \quad (3.5.47)$$

which is directly analogous to (3.4.10).

When the current is small or mass transfer is efficient, the surface concentrations do not differ from those of the bulk, and one has

$$i = i_0 [e^{-(n' + \alpha)f\eta} - e^{(n'' + 1 - \alpha)f\eta}] \quad (3.5.48)$$

which is analogous to (3.4.11). At small overpotentials, this relationship can be linearized via the approximation $e^x \approx 1 + x$ to give

$$i = -i_0 n f \eta \quad (3.5.49)$$

which is the counterpart of (3.4.12). The charge-transfer resistance for this multistep system is then

$$R_{\text{ct}} = \frac{RT}{nFi_0} \quad (3.5.50)$$

which is a generalization of (3.4.13).

The arguments leading to (3.5.47)–(3.5.50) are particular to the assumed mechanistic pattern of (3.5.8)–(3.5.10), but similar results can be obtained by the same techniques for any quasireversible mechanism. In fact, (3.4.49) and (3.4.50) are general for quasireversible multistep processes, and they underlie the experimental determination of i_0 via methods, such as impedance spectroscopy, based on small perturbations of systems at equilibrium.

▶ 3.6 MICROSCOPIC THEORIES OF CHARGE TRANSFER

The previous sections dealt with a generalized theory of heterogeneous electron-transfer kinetics based on macroscopic concepts, in which the rate of the reaction was expressed in terms of the phenomenological parameters, k^0 and α . While useful in helping to organize the results of experimental studies and in providing information about reaction mechanisms, such an approach cannot be employed to predict how the kinetics are affected by such factors as the nature and structure of the reacting species, the solvent, the electrode material, and adsorbed layers on the electrode. To obtain such information, one needs a microscopic theory that describes how molecular structure and environment affect the electron-transfer process.

A great deal of work has gone into the development of microscopic theories over the past 45 years. The goal is to make predictions that can be tested by experiments, so that

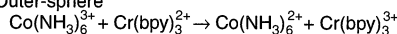
one can understand the fundamental structural and environmental factors causing reactions to be kinetically facile or sluggish. With that understanding, there would be a firmer basis for designing superior new systems for many scientific and technological applications. Major contributions in this area have been made by Marcus (37, 38), Hush (39, 40), Levich (41), Dogonadze (42), and many others. Comprehensive reviews are available (43–50), as are extensive treatments of the broader related field of electron-transfer reactions in homogeneous solution and in biological systems (51–53). The approach taken in this section is largely based on the Marcus model, which has been widely applied in electrochemical studies and has demonstrated the ability to make useful predictions about structural effects on kinetics with minimal computation. Marcus was recognized with the Nobel Prize in Chemistry for his contributions.

At the outset, it is useful to distinguish between *inner-sphere* and *outer-sphere* electron-transfer reactions at electrodes (Figure 3.6.1). This terminology was adopted from that used to describe electron-transfer reactions of coordination compounds (54). The term “outer-sphere” denotes a reaction between two species in which the original coordination spheres are maintained in the activated complex [“electron transfer from one primary bond system to another” (54)]. In contrast, “inner-sphere” reactions occur in an activated complex where the ions share a ligand [“electron transfer within a primary bond system” (54)].

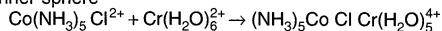
Likewise, in an *outer-sphere electrode reaction*, the reactant and product do not interact strongly with the electrode surface, and they are generally at a distance of at least a solvent layer from the electrode. A typical example is the heterogeneous reduction of $\text{Ru}(\text{NH}_3)_6^{3+}$, where the reactant at the electrode surface is essentially the same as in the bulk. In an *inner-sphere electrode reaction*, there is a strong interaction of the reactant, intermediates, or products with the electrode; that is, such reactions involve specific adsorption of species involved in the electrode reaction. The reduction of oxygen in water and the oxidation of hydrogen at Pt are inner-sphere reactions. Another type of inner-sphere reaction features a specifically adsorbed anion that serves as a *ligand bridge* to a metal ion (55). Obviously outer-sphere reactions are less dependent on electrode material than inner-sphere ones.¹³

Homogenous Electron Transfer

Outer-sphere



Inner-sphere



Homogenous Electron Transfer

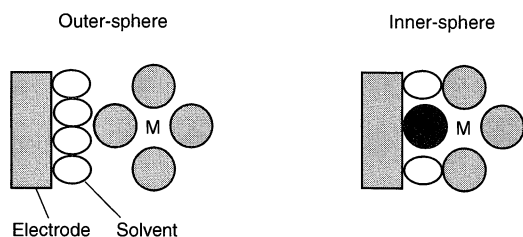


Figure 3.6.1 Outer-sphere and inner-sphere reactions. The inner sphere homogeneous reaction produces, with loss of H_2O , a ligand-bridged complex (shown above), which decomposes to $\text{CrCl}(\text{H}_2\text{O})_5^{2+}$ and $\text{Co}(\text{NH}_3)_5(\text{H}_2\text{O})^{2+}$. In the heterogeneous reactions, the diagram shows a metal ion (M) surrounded by ligands. In the inner sphere reaction, a ligand that adsorbs on the electrode and bridges to the metal is indicated in a darker color. An example of the latter is the oxidation of $\text{Cr}(\text{H}_2\text{O})_5^{2+}$ at a mercury electrode in the presence of Cl^- or Br^- .

¹³Even if there is not a strong interaction with the electrode, an outer-sphere reaction can depend on the electrode material, because of (a) double-layer effects (Section 13.7), (b) the effect of the metal on the structure of the Helmholtz layer, or (c) the effect of the energy and distribution of electronic states in the electrode.

Outer-sphere electron transfers can be treated in a more general way than inner-sphere processes, where specific chemistry and interactions are important. For this reason, the theory of outer-sphere electron transfer is much more highly developed, and the discussion that follows pertains to these kinds of reactions. However, in practical applications, such as in fuel cells and batteries, the more complicated inner-sphere reactions are important. A theory of these requires consideration of specific adsorption effects, as described in Chapter 13, as well as many of the factors important in heterogeneous catalytic reactions (56).

3.6.1 The Marcus Microscopic Model

Consider an outer-sphere, single electron transfer from an electrode to species O, to form the product R. This heterogeneous process is closely related to the homogeneous reduction of O to R by reaction with a suitable reductant, R',



We will find it convenient to consider the two situations in the same theoretical context. Electron-transfer reactions, whether homogeneous or heterogeneous, are radiationless electronic rearrangements of reacting species. Accordingly, there are many common elements between theories of electron transfer and treatments of radiationless deactivation in excited molecules (57). Since the transfer is radiationless, the electron must move from an initial state (on the electrode or in the reductant, R') to a receiving state (in species O or on the electrode) of the same energy. This demand for *isoenergetic electron transfer* is a fundamental aspect with extensive consequences.

A second important aspect of most microscopic theories of electron transfer is the assumption that the reactants and products do not change their configurations during the actual act of transfer. This idea is based essentially on the Franck–Condon principle, which says, in part, that nuclear momenta and positions do not change on the time scale of electronic transitions. Thus, the reactant and product, O and R, share a common nuclear configuration at the moment of transfer.

Let us consider again a plot of the standard free energy¹⁴ of species O and R as a function of reaction coordinate (see Figure 3.3.2), but we now give more careful consideration to the nature of the reaction coordinate and the computation of the standard free energy. Our goal is to obtain an expression for the standard free energy of activation, ΔG_f^\ddagger , as a function of structural parameters of the reactant, so that equation 3.1.17 (or a closely related form) can be used to calculate the rate constant. In earlier theoretical work, the pre-exponential factor for the rate constant was written in terms of a collision number (37, 38, 58, 59), but the formalism now used leads to expressions like:

$$k_f = K_{\text{P},\text{O}} \nu_n \kappa_{\text{el}} \exp(-\Delta G_f^\ddagger/RT) \quad (3.6.2)$$

where ΔG_f^\ddagger is the activation energy for reduction of O; $K_{\text{P},\text{O}}$ is a *precursor equilibrium constant*, representing the ratio of the reactant concentration in the reactive position at the electrode (the *precursor state*) to the concentration in bulk solution; ν_n is the *nuclear frequency factor* (s^{-1}), which represents the frequency of attempts on the energy barrier (generally associated with bond vibrations and solvent motion); and κ_{el} is the *electronic transmission coefficient* (related to the probability of electron tunneling; see Section 3.6.4). Often, κ_{el} is taken as unity for a reaction where the reactant is close to the electrode, so that there is strong coupling between the reactant and the electrode

¹⁴See the footnote relating to the use of standard thermodynamic quantities in Section 3.1.2.

(see Section 3.6.4).¹⁵ Methods for estimating the various factors are available (48), but there is considerable uncertainty in their values.

Actually, equation 3.6.2 can be used for either a heterogeneous reduction at an electrode or a homogeneous electron transfer in which O is reduced to R by another reactant in solution. For a heterogeneous electron transfer, the precursor state can be considered to be a reactant molecule situated near the electrode at a distance where electron transfer is possible. Thus $K_{P,O} = C_{O,surf}/C_O^*$, where $C_{O,surf}$ is a surface concentration having units of mol/cm². Consequently $K_{P,O}$ has units of cm, and k_f has units of cm/s, as required. For a homogeneous electron transfer between O and R', one can think of the precursor state as a reactive unit, OR', where the two species are close enough to allow transfer of an electron. Then $K_{P,O} = [OR']/[O][R']$, which has units of M⁻¹ if the concentrations are expressed conventionally. This result gives a rate constant, k_f , in units of M⁻¹s⁻¹, again as required.

In either case, we consider the reaction as occurring on a multidimensional surface defining the standard free energy of the system in terms of the nuclear coordinates (i.e., the relative positions of the atoms) of the reactant, product, and solvent. Changes in nuclear coordinates come about from vibrational and rotational motion in O and R, and from fluctuations in the position and orientation of the solvent molecules. As usual, we focus on the energetically favored path between reactants and products, and we measure progress in terms of a reaction coordinate, q . Two general assumptions are (a) that the reactant, O, is centered at some fixed position with respect to the electrode (or in a bimolecular homogeneous reaction, that the reactants are at a fixed distance from each other) and (b) that the standard free energies of O and R, G_O^0 and G_R^0 , depend quadratically on the reaction coordinate, q (49):

$$G_O^0(q) = (k/2)(q - q_O)^2 \quad (3.6.3)$$

$$G_R^0(q) = (k/2)(q - q_R)^2 + \Delta G^0 \quad (3.6.4)$$

where q_O and q_R are the values of the coordinate for the equilibrium atomic configurations in O and R, and k is a proportionality constant (e.g., a force constant for a change in bond length). Depending on the case under consideration, ΔG^0 is either the free energy of reaction for a homogeneous electron transfer or $F(E - E^0)$ for an electrode reaction.

Let us consider a particularly simple case to give a physical picture of what is implied here. Suppose the reactant is A-B, a diatomic molecule, and the product is A-B⁻. To a first approximation the nuclear coordinate could be the bond length in A-B (q_O) and A-B⁻ (q_R), and the equations for the free energy could represent the energy for lengthening or contraction of the bond within the usual harmonic oscillator approximation. This picture is oversimplified in that the solvent molecules would also make a contribution to the free energy of activation (sometimes the dominant one). In the discussion that follows, they are assumed to contribute in a quadratic relationship involving coordinates of the solvent dipole.

Figure 3.6.2 shows a typical free energy plot based on (3.6.3) and (3.6.4). The molecules shown at the top of the figure are meant to represent the stable configurations of the reactants, for example, Ru(NH₃)₆³⁺ and Ru(NH₃)₆²⁺ as O and R, as well as to provide a view of the change in nuclear configuration upon reduction. The transition state is the position where O and R have the same configuration, denoted by the reaction coordinate

¹⁵The pre-exponential term sometimes also includes a nuclear tunneling factor, Γ_n . This arises from a quantum mechanical treatment that accounts for electron transfer for nuclear configurations with energies below the transition state (48, 60).

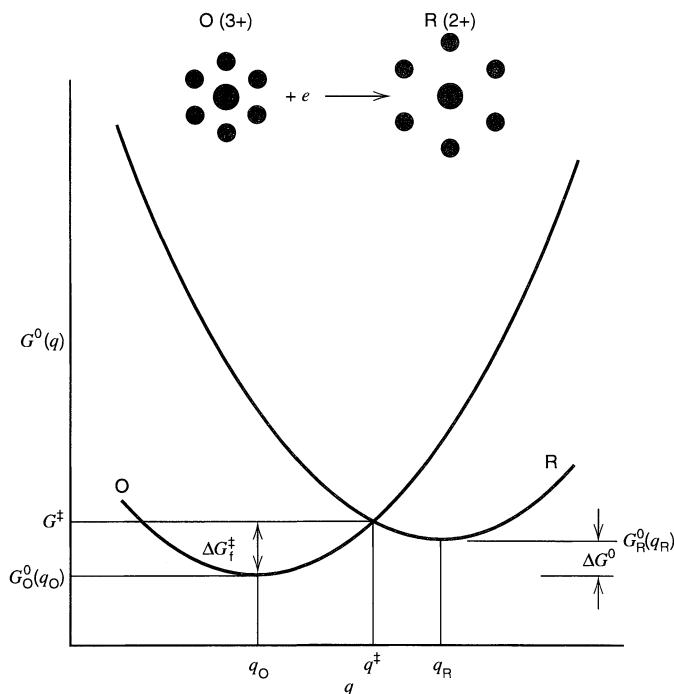


Figure 3.6.2 Standard free energy, G^0 , as a function of reaction coordinate, q , for an electron transfer reaction, such as $\text{Ru}(\text{NH}_3)_6^{3+} + e \rightarrow \text{Ru}(\text{NH}_3)_6^{2+}$. This diagram applies either to a heterogeneous reaction in which O and R react at an electrode or a homogeneous reaction in which O and R react with members of another redox couple as shown in (3.6.1). For the heterogeneous case, the curve for O is actually the sum of energies for species O and for an electron on the electrode at the Fermi level corresponding to potential E . Then, $\Delta G^0 = F(E - E^0)$. For the homogeneous case, the curve for O is the sum of energies for O and its reactant partner, R' , while the curve for R is a sum for R and O' . Then, ΔG^0 is the standard free energy change for the reaction. The picture at the top is a general representation of structural changes that might accompany electron transfer. The changes in spacing of the six surrounding dots could represent, for example, changes in bond lengths within the electroactive species or the restructuring of the surrounding solvent shell.

q^\ddagger . In keeping with the Franck–Condon principle, electron transfer only occurs at this position.

The free energies at the transition state are thus given by

$$G_O^0(q^\ddagger) = (k/2)(q^\ddagger - q_O)^2 \quad (3.6.5)$$

$$G_R^0(q^\ddagger) = (k/2)(q^\ddagger - q_R)^2 + \Delta G^0 \quad (3.6.6)$$

Since $G_O^0(q^\ddagger) = G_R^0(q^\ddagger)$, (3.6.5) and (3.6.6) can be solved for q^\ddagger with the result,

$$q^\ddagger = \frac{(q_R + q_O)}{2} + \frac{\Delta G^0}{k(q_R - q_O)} \quad (3.6.7)$$

The free energy of activation for reduction of O is given by

$$\Delta G_f^\ddagger = G_O^0(q^\ddagger) - G_O^0(q_O) = G_O^0(q^\ddagger) \quad (3.6.8)$$

where we have noted that $G_{\text{O}}^0(q_{\text{O}}) = 0$, as defined in (3.6.3). Substitution for q^{\ddagger} from (3.6.7) into (3.6.5) then yields

$$\Delta G_{\text{f}}^{\ddagger} = \frac{k(q_{\text{R}} - q_{\text{O}})^2}{8} \left[1 + \frac{2\Delta G^0}{k(q_{\text{R}} - q_{\text{O}})^2} \right]^2 \quad (3.6.9)$$

Defining $\lambda = (k/2)(q_{\text{R}} - q_{\text{O}})^2$, we have

$$\Delta G_{\text{f}}^{\ddagger} = \frac{\lambda}{4} \left(1 + \frac{\Delta G^0}{\lambda} \right)^2 \quad (3.6.10a)$$

or, for an electrode reaction

$$\Delta G_{\text{f}}^{\ddagger} = \frac{\lambda}{4} \left(1 + \frac{F(E - E^0)}{\lambda} \right)^2 \quad (3.6.10b)$$

There can be free energy contributions beyond those considered in the derivation just described. In general, they are energy changes involved in bringing the reactants and products from the average environment in the medium to the special environment where electron transfer occurs. Among them are the energy of ion pairing and the electrostatic work needed to reach the reactive position (e.g., to bring a positively charged reactant to a position near a positively charged electrode). Such effects are usually treated by the inclusion of *work terms*, w_{O} and w_{R} , which are adjustments to ΔG^0 or $F(E - E^0)$. For simplicity, they were omitted above. The complete equations, including the work terms, are¹⁶

$$\Delta G_{\text{f}}^{\ddagger} = \frac{\lambda}{4} \left(1 + \frac{\Delta G^0 - w_{\text{O}} + w_{\text{R}}}{\lambda} \right)^2 \quad (3.6.11a)$$

$$\Delta G_{\text{f}}^{\ddagger} = \frac{\lambda}{4} \left(1 + \frac{F(E - E^0) - w_{\text{O}} + w_{\text{R}}}{\lambda} \right)^2 \quad (3.6.11b)$$

The critical parameter is λ , the *reorganization energy*, which represents the energy necessary to transform the nuclear configurations in the reactant and the solvent to those of the product state. It is usually separated into inner, λ_{i} , and outer, λ_{o} , components:

$$\lambda = \lambda_{\text{i}} + \lambda_{\text{o}} \quad (3.6.12)$$

where λ_{i} represents the contribution from reorganization of species O, and λ_{o} that from reorganization of the solvent.¹⁷

¹⁶The convention is to define w_{O} and w_{R} as the work required to establish the reactive position from the average environment of reactants and products in the medium. The signs in (3.6.11a,b) follow from this. In many circumstances, the work terms are also the free energy changes for the precursor equilibria. When that is true, $w_{\text{O}} = -RT \ln K_{\text{P,O}}$ and $w_{\text{R}} = -RT \ln K_{\text{P,R}}$.

¹⁷One should not confuse the inner and outer components of λ with the concept of inner- and outer-sphere reaction. In the treatment under consideration, we are dealing with an outer-sphere reaction, and λ_{i} and λ_{o} simply apportion the energy to terms applying to changes in bond lengths (e.g., of a metal–ligand bond) and changes in solvation, respectively.

To the extent that the normal modes of the reactant remain harmonic over the range of distortion needed, one can, in principle, calculate λ_i by summing over the normal vibrational modes of the reactant, that is,

$$\lambda_i = \sum_j \frac{1}{2} k_j (q_{O,j} - q_{R,j})^2 \quad (3.6.13)$$

where the k 's are force constants, and the q 's are displacements in the normal mode coordinates.

Typically, λ_o is computed by assuming that the solvent is a dielectric continuum, and the reactant is a sphere of radius a_o . For an electrode reaction,

$$\lambda_o = \frac{e^2}{8\pi\epsilon_0} \left(\frac{1}{a_o} - \frac{1}{R} \right) \left(\frac{1}{\epsilon_{op}} - \frac{1}{\epsilon_s} \right) \quad (3.6.14a)$$

where ϵ_{op} and ϵ_s are the optical and static dielectric constants, respectively, and R is taken as twice the distance from the center of the molecule to the electrode (i.e., $2x_o$, which is the distance between the reactant and its image charge in the electrode).¹⁸ For a homogeneous electron-transfer reaction:

$$\lambda_o = \frac{e^2}{4\pi\epsilon_0} \left(\frac{1}{2a_1} + \frac{1}{2a_2} - \frac{1}{d} \right) \left(\frac{1}{\epsilon_{op}} - \frac{1}{\epsilon_s} \right) \quad (3.6.14b)$$

where a_1 and a_2 are the radii of the reactants (O and R' in equation 3.6.1) and $d = a_1 + a_2$. Typical values of λ are in the range of 0.5 to 1 eV.

3.6.2 Predictions from Marcus Theory

While it is possible, in principle, to estimate the rate constant for an electrode reaction by computation of the pre-exponential terms and the λ values, this is rarely done in practice. The theory's greater value is the chemical and physical insight that it affords, which arises from its capacity for prediction and generalization about electron-transfer reactions.

For example, one can obtain the predicted α -value from (3.6.10b):

$$\alpha = \frac{1}{F} \frac{\partial G_f^\ddagger}{\partial E} = \frac{1}{2} + \frac{F(E - E^0)}{2\lambda} \quad (3.6.15a)$$

or with the inclusion of work terms:

$$\alpha = \frac{1}{2} + \frac{F(E - E^0) - (w_O - w_R)}{2\lambda} \quad (3.6.15b)$$

Thus, the theory predicts not only that $\alpha \approx 0.5$, but also that it depends on potential in a particular way. As mentioned in Section 3.3.4, the Butler–Volmer (BV) theory can accommodate a potential dependence of α , but in its classic version, the BV theory handles α as a constant. Moreover, there is no basis in the BV theory for predicting the form of the potential dependence. On the other hand, the potential-dependent term in (3.6.15a,b),

¹⁸In some treatments of electron transfer, the assumption is made that the reactant charge is largely shielded by counter ions in solution, so that an image charge does not form in the electrode. In this case, R is the distance between the center of the reactant molecule and the electrode (24, 39).

which depends on the size of λ , is usually not very large, so a clear potential dependency of α has been difficult to observe experimentally. The effect is more obvious in reactions involving electroactive centers bound to electrodes (see Section 14.5.2.).

The Marcus theory also makes predictions about the relation between the rate constants for homogeneous and heterogeneous reactions of the same reactant. Consider the rate constant for the self-exchange reaction,



in comparison with k^0 for the related electrode reaction, $\text{O} + e \rightarrow \text{R}$. One can determine k_{ex} by labeling O isotopically and measuring the rate at which the isotope appears in R, or sometimes by other methods like ESR or NMR. A comparison of (3.6.14a) and (3.6.14b), where $a_{\text{O}} = a_1 = a_2 = a$ and $R = d = 2a$, yields

$$\lambda_{\text{el}} = \lambda_{\text{ex}}/2 \quad (3.6.17)$$

where λ_{el} and λ_{ex} are the values of λ_0 for the electrode reaction and the self-exchange reaction, respectively. For the self-exchange reaction, $\Delta G^0 = 0$, so (3.6.10a) gives $\Delta G_{\text{f}}^{\ddagger} = \lambda_{\text{ex}}/4$, as long as λ_0 dominates λ_i in the reorganization energy. For the electrode reaction, k^0 corresponds to $E = E^0$, so (3.6.10b) gives $\Delta G_{\text{f}}^{\ddagger} = \lambda_{\text{el}}/4$, again with the condition that λ_i is negligible. From (3.6.17), one can express $\Delta G_{\text{f}}^{\ddagger}$ for the homogeneous and heterogeneous reactions in common terms, and one finds that k_{ex} is related to k^0 by the expression

$$(k_{\text{ex}}/A_{\text{ex}})^{1/2} = k^0/A_{\text{el}} \quad (3.6.18)$$

where A_{ex} and A_{el} are the pre-exponential factors for self-exchange and the electrode reaction. (Roughly, A_{el} is 10^4 to 10^5 cm/s and A_{ex} is 10^{11} to 10^{12} $\text{M}^{-1} \text{s}^{-1}$.)¹⁹

The theory also leads to useful qualitative predictions about reaction kinetics. For example, equation 3.6.10b gives $\Delta G^{\ddagger} \approx \lambda/4$ at E^0 , where $k_{\text{f}} = k_{\text{b}} = k^0$. Thus, k^0 will be larger when the internal reorganization is smaller, that is, in reactions where O and R have similar structures. Electron transfers involving large structural alterations (such as sizable changes in bond lengths or bond angles) tend to be slower. Solvation also has an impact through its contribution to λ . Large molecules (large a_{O}) tend to show lower solvation energies, and smaller changes in solvation upon reaction, by comparison with smaller species. On this basis, one would expect electron transfers to small molecules, such as, the reduction of O_2 to O_2^- in 2⁻ aprotic media, to be slower than the reduction of Ar to Ar^- , where Ar is a large aromatic molecule like anthracene.

The effect of solvent in an electron transfer is larger than simply through its energetic contribution to λ_0 . There is evidence that the dynamics of solvent reorganization, often represented in terms of a solvent longitudinal relaxation time, τ_{L} , contribute to the pre-exponential factor in (3.6.2) (47, 62–65), e.g., $\nu_{\text{n}} \propto \tau_{\text{L}}^{-1}$. Since τ_{L} is roughly proportional to the viscosity, an inverse proportionality of this kind implies that the heterogeneous rate constant would decrease as the solution viscosity increases (i.e., as the diffusion coefficient of the reactant decreases). This behavior is actually seen in the decrease of k^0 for electrode reactions in water upon adding sucrose to increase the viscosity (presumably without changing λ_0 in a significant way) (66, 67). This effect was especially pronounced in other studies involving Co(III/II)tris(bipyridine) complexes modified by the addition of

¹⁹This equation also applies when the λ_i terms are included (but work terms are neglected). This is the case because the total contribution to λ_i is summed over two reactants in the homogeneous self-exchange reaction, but only over one in the electrode reaction (61).

long polyethylene or polypropylene oxide chains to the ligands, which cause large changes in diffusion coefficient in undiluted, highly viscous, ionic melts (68).

A particularly interesting prediction from this theory is the existence of an “inverted region” for homogeneous electron-transfer reactions. Figure 3.6.3 shows how equation 3.6.10a predicts $\Delta G_{\ddagger}^{\ddagger}$ to vary with the thermodynamic driving force for the electron transfer, ΔG^0 . Curves are shown for several different values of λ , but the basic pattern of behavior is the same for all, in that there is a predicted minimum in the standard free energy of activation. On the right-hand side of the minimum, there is a *normal region*, where $\Delta G_{\ddagger}^{\ddagger}$ decreases, hence the rate constant increases, as ΔG^0 gets larger in magnitude (i.e., becomes more negative). When $\Delta G^0 = -\lambda$, $\Delta G_{\ddagger}^{\ddagger}$ is zero, and the rate constant is predicted to be at a maximum. At more negative ΔG^0 values, that is for very strongly driven reactions, the activation energy becomes larger, and the rate constant smaller. This is the *inverted region*, where an increase in the thermodynamic driving force leads to a decrease in the rate of electron transfer. There are two physical reasons for this effect. First, a large negative free energy of reaction implies that the products are required to accept the liberated energy very quickly in vibrational modes, and the probability for doing so declines as $-\Delta G^0$ exceeds λ (see Chapter 18). Second, one can develop a situation in the inverted region where the energy surfaces no longer allow for adiabatic electron transfer (see Section 3.6.4). The existence of the inverted region accounts for the phenomenon of electrogenerated chemiluminescence (Chapter 18) and has also been seen by other means for several electron-transfer reactions in solution.

Even though (3.6.10b) also has a minimum, an inverted-region effect should not occur for an electrode reaction at a metal electrode. The reason is that (3.6.10b) was derived with the implicit idea that electrons always react from a narrow range of states on the electrode corresponding to the Fermi energy (see the caption to Figure 3.6.2). Even though the reaction rate at this energy is predicted to show inversion at very negative overpotentials, there are always occupied states in the metal below the Fermi energy, and they can transfer an electron to O without inversion. Any low-level vacancy created in the metal by heterogeneous reaction is filled ultimately with an electron from the Fermi energy, with dissipation of the difference in energy as heat; thus the overall energy change is as expected from thermodynamics. A similar argument holds for oxidations at metals, where unoccupied states are always available. The ideas behind this discussion are developed much more fully in the next section.

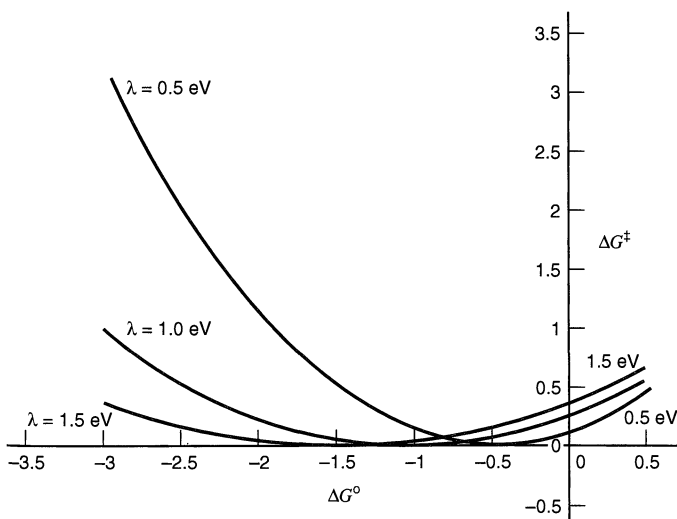


Figure 3.6.3 Effect of ΔG^0 for a homogeneous electron-transfer reaction on $\Delta G_{\ddagger}^{\ddagger}$ at several different values of λ .

An inverted region should be seen for interfacial electron transfer at the interface between immiscible electrolyte solutions, with an oxidant, O, in one phase, and a reductant, R', in the other (69). Experimental studies bearing on this issue have just been reported (70).

3.6.3 A Model Based on Distributions of Energy States

An alternative theoretical approach to heterogeneous kinetics is based on the overlap between electronic states of the electrode and those of the reactants in solution (41, 42, 46, 47, 71, 72). The concept is presented graphically in Figure 3.6.4, which will be discussed extensively in this section. This model is rooted in contributions from Gerischer (71, 72) and is particularly useful for treating electron transfer at semiconductor electrodes (Section 18.2.3), where the electronic structure of the electrode is important. The main idea is that an electron transfer can take place from any occupied energy state that is matched in energy, E , with an unoccupied receiving state. If the process is a reduction, the occupied state is on the electrode and the receiving state is on an electroreactant, O. For an oxidation, the occupied state is on species R in solution, and the receiving state is on the electrode. In general, the eligible states extend over a range of energies, and the total rate is an integral of the rates at each energy.

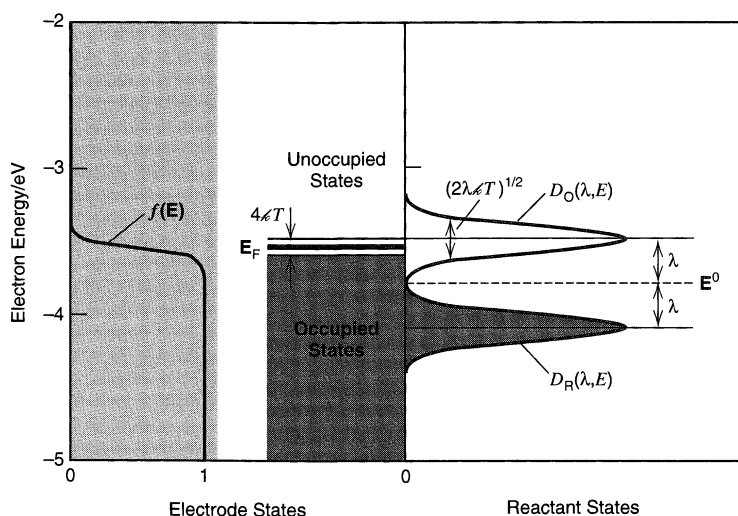


Figure 3.6.4 Relationships among electronic states at an interface between a metal electrode and a solution containing species O and R at equal concentrations. The vertical axis is electron energy, E , on the absolute scale. Indicated on the electrode side is a zone $4kT$ wide centered on the Fermi level, E_F , where $f(E)$ makes the transition from a value of nearly 1 below the zone to a value of virtually zero above. See the graph of $f(E)$ in the area of solid shading on the left. On the solution side, the state density distributions are shown for O and R. These are Gaussians having the same shapes as the probability density functions, $W_O(\lambda, E)$ and $W_R(\lambda, E)$. The electron energy corresponding to the standard potential, E^0 , is -3.8 eV, and $\lambda = 0.3$ eV. The Fermi energy corresponds here to an electrode potential of -250 mV vs. E^0 . Filled states are denoted on both sides of the interface by dark shading. Since filled electrode states overlap with (empty) O states, reduction can proceed. Since the (filled) R states overlap only with filled electrode states, oxidation is blocked.

On the electrode, the number of electronic states in the energy range between \mathbf{E} and $\mathbf{E} + d\mathbf{E}$ is given by $A\rho(\mathbf{E})d\mathbf{E}$, where A is the area exposed to the solution, and $\rho(\mathbf{E})$ is the *density of states* [having units of (area-energy) $^{-1}$, such as $\text{cm}^{-2}\text{eV}^{-1}$]. The total number of states in a broad energy range is, of course, the integral of $A\rho(\mathbf{E})$ over the range. If the electrode is a metal, the density of states is large and continuous, but if it is a semiconductor, there is a sizable energy range, called the *band gap*, where the density of states is very small. (See Section 18.2 for a fuller discussion of the electronic properties of materials.)

Electrons fill states on the electrode from lower energies to higher ones until all electrons are accommodated. Any material has more states than are required for the electrons, so there are always empty states above the filled ones. If the material were at absolute zero in temperature, the highest filled state would correspond to the *Fermi level* (or the *Fermi energy*), \mathbf{E}_F , and all states above the Fermi level would be empty. At any higher temperature, thermal energy elevates some of the electrons into states above \mathbf{E}_F and creates vacancies below. The filling of the states at thermal equilibrium is described by the *Fermi function*, $f(\mathbf{E})$,

$$f(\mathbf{E}) = \{1 + \exp[(\mathbf{E} - \mathbf{E}_F)/kT]\}^{-1} \quad (3.6.19)$$

which is the probability that a state of energy \mathbf{E} is occupied by an electron. It is easy to see that for energies much lower than the Fermi level, the occupancy is virtually unity, and for energies much higher than the Fermi level, the occupancy is practically zero (see Figure 3.6.4). States within a few kT of \mathbf{E}_F have intermediate occupancy, graded from unity to zero as the energy rises through \mathbf{E}_F , where the occupancy is 0.5. This intermediate zone is shown in Figure 3.6.4 as a band $4kT$ wide (about 100 meV at 25°C).

The number of electrons in the energy range between \mathbf{E} and $\mathbf{E} + d\mathbf{E}$ is the number of occupied states, $AN_{\text{occ}}(\mathbf{E})d\mathbf{E}$, where $N_{\text{occ}}(\mathbf{E})$ is the density function

$$N_{\text{occ}}(\mathbf{E}) = f(\mathbf{E})\rho(\mathbf{E}) \quad (3.6.20)$$

Like $\rho(\mathbf{E})$, $N_{\text{occ}}(\mathbf{E})$ has units of (area-energy) $^{-1}$, typically $\text{cm}^{-2}\text{eV}^{-1}$, while $f(\mathbf{E})$ is dimensionless. In a similar manner, we can define the density of unoccupied states as

$$N_{\text{unocc}}(\mathbf{E}) = [1 - f(\mathbf{E})]\rho(\mathbf{E}) \quad (3.6.21)$$

As the potential is changed, the Fermi level moves, with the change being toward higher energies at more negative potentials and vice versa. On a metal electrode, these changes occur not by the filling or emptying of many additional states, but mostly by charging the metal, so that all states are shifted by the effect of potential (Section 2.2). While charging does involve a change in the total electron population on the metal, the change is a tiny fraction of the total (Section 2.2.2). Consequently, the same set of states exists near the Fermi level at all potentials. For this reason, it is more appropriate to think of $\rho(\mathbf{E})$ as a consistent function of $\mathbf{E} - \mathbf{E}_F$, nearly independent of the value of \mathbf{E}_F . Since $f(\mathbf{E})$ behaves in the same way, so do $N_{\text{occ}}(\mathbf{E})$ and $N_{\text{unocc}}(\mathbf{E})$. The picture is more complicated at a semiconductor, as discussed in Section 18.2.

States in solution are described by similar concepts, except that filled and empty states correspond to different chemical species, namely the two components of a redox couple, R and O, respectively. These states differ from those of the metal in being localized. The R and O species cannot communicate with the electrode without first approaching it closely. Since R and O can exist in the solution inhomogeneously and our concern is with the mix of states near the electrode surface, it is better to express the density of states

in terms of concentration, rather than total number. At any moment, the removable electrons on R species in solution in the vicinity of the electrode²⁰ are distributed over an energy range according to a concentration density function, $D_R(\lambda, \mathbf{E})$, having units of (volume-energy)⁻¹, such as cm⁻³ eV⁻¹. Thus, the *number concentration* of R species near the electrode in the range between \mathbf{E} and $\mathbf{E} + d\mathbf{E}$ is $D_R(\lambda, \mathbf{E})d\mathbf{E}$. Because this small element of the R population should be proportional to the overall surface concentration of R, $C_R(0, t)$, we can factor $D_R(\lambda, \mathbf{E})$ in the following way:

$$D_R(\lambda, \mathbf{E}) = N_A C_R(0, t) W_R(\lambda, \mathbf{E}) \quad (3.6.22)$$

where N_A is Avogadro's number, and $W_R(\lambda, \mathbf{E})$ is a probability density function with units of (energy)⁻¹. Since the integral of $D_R(\lambda, \mathbf{E})$ over all energies must yield the total number concentration of all states, which is $N_A C_R(0, t)$, we see that $W_R(\lambda, \mathbf{E})$ is a normalized function

$$\int_{-\infty}^{\infty} W_R(\lambda, \mathbf{E}) d\mathbf{E} = 1 \quad (3.6.23)$$

Similarly, the distribution of vacant states represented by O species is given by

$$D_O(\lambda, \mathbf{E}) = N_A C_O(0, t) W_O(\lambda, \mathbf{E}) \quad (3.6.24)$$

where $W_O(\lambda, \mathbf{E})$ is normalized, as indicated for its counterpart in (3.6.23). In Figure 3.6.4, the state distributions for O and R are depicted as gaussians for reasons that we will discover below.

Now let us consider the rate at which O is reduced from occupied states on the electrode in the energy range between \mathbf{E} and $\mathbf{E} + d\mathbf{E}$. This is only a part of the total rate of reduction, so we call it a *local rate* for energy \mathbf{E} . In a time interval Δt , electrons from occupied states on the electrode can make the transition to states on species O in the same energy range, and the rate of reduction is the number that succeed divided by Δt . This rate is the instantaneous rate, if Δt is short enough (a) that the reduction does not appreciably alter the number of unoccupied states on the solution side and (b) that individual O molecules do not appreciably change the energy of their unoccupied levels by internal vibrational and rotational motion. Thus Δt is at or below the time scale of vibration. The local rate of reduction can be written as

$$\text{Local Rate}(\mathbf{E}) = \frac{P_{\text{red}}(\mathbf{E}) AN_{\text{occ}}(\mathbf{E}) d\mathbf{E}}{\Delta t} \quad (3.6.25)$$

where $AN_{\text{occ}}d\mathbf{E}$ is the number of electrons available for the transition and $P_{\text{red}}(\mathbf{E})$ is the probability of transition to an unoccupied state on O. It is intuitive that $P_{\text{red}}(\mathbf{E})$ is proportional to the density of states $D_O(\lambda, \mathbf{E})$. Defining $\varepsilon_{\text{red}}(\mathbf{E})$ as the proportionality function, we have

$$\text{Local Rate}(\mathbf{E}) = \frac{\varepsilon_{\text{red}}(\mathbf{E}) D_O(\lambda, \mathbf{E}) AN_{\text{occ}}(\mathbf{E}) d\mathbf{E}}{\Delta t} \quad (3.6.26)$$

²⁰In this discussion, the phrases "concentration in the vicinity of the electrode" and "concentration near the electrode" are used interchangeably to denote concentrations that are given by $C(0, t)$ in most mass-transfer and heterogeneous rate equations in this book. However, $C(0, t)$ is not the same as the concentration in the reactive position at an electrode (i.e., in the precursor state), but is the concentration just outside the diffuse layer. We are now considering events on a much finer distance scale than in most contexts in this book, and this distinction is needed. The same point is made in Section 13.7.

where $\varepsilon_{\text{red}}(\mathbf{E})$ has units of volume-energy (e.g., $\text{cm}^3 \text{ eV}$). The total rate of reduction is the sum of the local rates in all infinitesimal energy ranges; thus it is given by the integral

$$\text{Rate} = \nu \int_{-\infty}^{\infty} \varepsilon_{\text{red}}(\mathbf{E}) D_{\text{O}}(\lambda, \mathbf{E}) AN_{\text{occ}}(\mathbf{E}) d\mathbf{E} \quad (3.6.27)$$

where, in accord with custom, we have expressed Δt in terms of a frequency, $\nu = 1/\Delta t$. The limits on the integral cover all energies, but the integrand has a significant value only where there is overlap between occupied states on the electrode and states of O in the solution. In Figure 3.6.4, the relevant range is roughly -4.0 to -3.5 eV.

Substitution from (3.6.20) and (3.6.24) gives

$$\text{Rate} = \nu AN_{\text{A}} C_{\text{O}}(0, t) \int_{-\infty}^{\infty} \varepsilon_{\text{red}}(\mathbf{E}) W_{\text{O}}(\lambda, \mathbf{E}) f(\mathbf{E}) \rho(\mathbf{E}) d\mathbf{E} \quad (3.6.28)$$

This rate is expressed in molecules or electrons per second. Division by AN_{A} gives the rate more conventionally in $\text{mol cm}^{-2} \text{ s}^{-1}$, and further division by $C_{\text{O}}(0, t)$ provides the rate constant,

$$k_{\text{f}} = \nu \int_{-\infty}^{\infty} \varepsilon_{\text{red}}(\mathbf{E}) W_{\text{O}}(\lambda, \mathbf{E}) f(\mathbf{E}) \rho(\mathbf{E}) d\mathbf{E} \quad (3.6.29)$$

In an analogous way, one can easily derive the rate constant for the oxidation of R. On the electrode side, the empty states are candidates to receive an electron; hence $N_{\text{unocc}}(\mathbf{E})$ is the distribution of interest. The density of filled states on the solution side is $D_{\text{R}}(\lambda, \mathbf{E})$, and the probability for electron transfer in the time interval Δt is $P_{\text{ox}}(\mathbf{E}) = \varepsilon_{\text{ox}}(\mathbf{E}) D_{\text{R}}(\lambda, \mathbf{E})$. Proceeding exactly as in the derivation of (3.6.29), we arrive at

$$k_{\text{b}} = \nu \int_{-\infty}^{\infty} \varepsilon_{\text{ox}}(\mathbf{E}) W_{\text{R}}(\lambda, \mathbf{E}) [1 - f(\mathbf{E})] \rho(\mathbf{E}) d\mathbf{E} \quad (3.6.30)$$

In Figure 3.6.4, the distribution of states for species R does not overlap the zone of unoccupied states on the electrode, so the integrand in (3.6.30) is practically zero everywhere, and k_{b} is negligible compared to k_{f} . The electrode is in a reducing condition with respect to the O/R couple. By changing the electrode potential to a more positive value, we shift the position of the Fermi level downward, and we can reach a position where the R states begin to overlap unoccupied electrode states, so that the integral in (3.6.30) becomes significant, and k_{b} is enhanced.

The literature contains many versions of equations 3.6.29 and 3.6.30 manifesting different notation and involving wide variations in the interpretation applied to the integral prefactors and the proportionality functions $\varepsilon_{\text{red}}(\mathbf{E})$ and $\varepsilon_{\text{ox}}(\mathbf{E})$. For example, it is common to see a tunneling probability, κ_{el} , or a precursor equilibrium constant, $K_{\text{P,O}}$ or $K_{\text{P,R}}$, extracted from the ε -functions and placed in the integral prefactor. Often the frequency ν is identified with ν_{n} in (3.6.2). Sometimes the prefactor encompasses things other than the frequency parameter, but is still expressed as a single symbol. These variations in representation reflect the fact that basic ideas are still evolving. The treatment offered here is general and can be accommodated to any of the extant views about how the fundamental properties of the system determine ν , $\varepsilon_{\text{red}}(\mathbf{E})$, and $\varepsilon_{\text{ox}}(\mathbf{E})$.

With (3.6.29) and (3.6.30), it is apparently possible to account for kinetic effects of the electronic structure of the electrode by using an appropriate density of states, $\rho(\mathbf{E})$, for

the electrode material. Efforts in that direction have been reported. However, one must be on guard for the possibility that $\varepsilon_{\text{red}}(\mathbf{E})$ and $\varepsilon_{\text{ox}}(\mathbf{E})$ also depend on $\rho(\mathbf{E})$.²¹

The Marcus theory can be used to define the probability densities $W_{\text{O}}(\lambda, \mathbf{E})$ and $W_{\text{R}}(\lambda, \mathbf{E})$. The key is to recognize that the derivation leading to (3.6.10b) is based implicitly on the idea that electron transfer occurs entirely from the Fermi level. In the context that we are now considering, the rate constant corresponding to the activation energy in (3.6.10b) is therefore proportional to the *local rate* at the Fermi level, wherever it might be situated relative to the state distributions for O and R. We can rewrite (3.6.10b) in terms of electron energy as

$$\Delta G_{\text{f}}^{\ddagger} = \frac{\lambda}{4} \left(1 - \frac{\mathbf{E} - \mathbf{E}^0}{\lambda} \right)^2 \quad (3.6.31)$$

where \mathbf{E}^0 is the energy corresponding to the standard potential of the O/R couple. One can easily show that $\Delta G_{\text{f}}^{\ddagger}$ reaches a minimum at $\mathbf{E} = \mathbf{E}^0 + \lambda$, where $\Delta G_{\text{f}}^{\ddagger} = 0$. Thus the maximum local rate of reduction at the Fermi level is found where $\mathbf{E}_{\text{F}} = \mathbf{E}^0 + \lambda$. When the Fermi level is at any other energy, \mathbf{E} , the local rate of reduction at the Fermi level can be expressed, according to (3.6.2), (3.6.26), and (3.6.31), in terms of the following ratios

$$\begin{aligned} \frac{\text{Local Rate } (\mathbf{E}_{\text{F}} = \mathbf{E})}{\text{Local Rate } (\mathbf{E}_{\text{F}} = \mathbf{E}^0 + \lambda)} &= \frac{\nu_{\text{n}} \kappa_{\text{el}} \exp \left[-\frac{\lambda}{4\ell T} \left(1 - \frac{\mathbf{E} - \mathbf{E}^0}{\lambda} \right)^2 \right]}{\nu_{\text{n}} \kappa_{\text{el}}} \\ &= \frac{\varepsilon_{\text{red}}(\mathbf{E}) D_{\text{O}}(\lambda, \mathbf{E}) f(\mathbf{E}_{\text{F}}) \rho(\mathbf{E}_{\text{F}})}{\varepsilon_{\text{red}}(\mathbf{E}^0 + \lambda) D_{\text{O}}(\lambda, \mathbf{E}^0 + \lambda) f(\mathbf{E}_{\text{F}}) \rho(\mathbf{E}_{\text{F}})} \end{aligned} \quad (3.6.32)$$

Assuming that ε_{red} does not depend on the position of \mathbf{E}_{F} , we can simplify this to

$$\frac{D_{\text{O}}(\lambda, \mathbf{E})}{D_{\text{O}}(\lambda, \mathbf{E}^0 + \lambda)} = \exp \left[-\frac{(\mathbf{E} - \mathbf{E}^0 - \lambda)^2}{4\lambda\ell T} \right] \quad (3.6.33)$$

This is a gaussian distribution having a mean at $\mathbf{E} = \mathbf{E}^0 + \lambda$ and a standard deviation of $(2\lambda\ell T)^{1/2}$, as shown in Figure 3.6.4 (see also Section A.3). From (3.6.24), $D_{\text{O}}(\lambda, \mathbf{E})/D_{\text{O}}(\lambda, \mathbf{E}^0 + \lambda) = W_{\text{O}}(\lambda, \mathbf{E})/W_{\text{O}}(\lambda, \mathbf{E}^0 + \lambda)$. Also, since $W_{\text{O}}(\lambda, \mathbf{E})$ is normalized, the exponential prefactor, $W_{\text{O}}(\lambda, \mathbf{E}^0 + \lambda)$, is quickly identified (Section A.3) as $(2\pi)^{-1/2}$ times the reciprocal of the standard deviation; therefore

$$W_{\text{O}}(\lambda, \mathbf{E}) = (4\pi\lambda\ell T)^{-1/2} \exp \left[-\frac{(\mathbf{E} - \mathbf{E}^0 - \lambda)^2}{4\lambda\ell T} \right] \quad (3.6.34)$$

²¹Consider, for example, a simple model based on the idea that, in the time interval Δt , all of the electrons in the energy range between \mathbf{E} and $\mathbf{E} + d\mathbf{E}$ redistribute themselves among all available states with equal probability. A refinement allows for the possibility that the states on species O participate with different weight from those on the electrode. If the states on the electrode are given unit weight and those in solution are given weight $\kappa_{\text{red}}(\mathbf{E})$, then

$$P_{\text{red}}(\mathbf{E}) = \frac{\kappa_{\text{red}}(\mathbf{E}) D_{\text{O}}(\lambda, \mathbf{E}) \delta}{\rho(\mathbf{E}) + \kappa_{\text{red}}(\mathbf{E}) D_{\text{O}}(\lambda, \mathbf{E}) \delta} = \varepsilon_{\text{red}}(\mathbf{E}) D_{\text{O}}(\lambda, \mathbf{E})$$

where δ is the average distance across which electron transfer occurs, and $\kappa_{\text{red}}(\mathbf{E})$ is dimensionless and can be identified with the tunneling probability, κ_{el} , used in other representations of k_{f} . If the electrode is a metal, $\rho(\mathbf{E})$ is orders of magnitude greater than $\kappa_{\text{red}}(\mathbf{E}) D_{\text{O}}(\lambda, \mathbf{E}) \delta$; hence the rate constant becomes

$$k_{\text{f}} = \nu \int_{-\infty}^{\infty} \kappa_{\text{red}}(\mathbf{E}) \delta W_{\text{O}}(\lambda, \mathbf{E}) f(\mathbf{E}) d\mathbf{E}$$

which has no dependence on the electronic structure of the electrode.

In a similar manner, one can show that

$$W_R(\lambda, E) = (4\pi\lambda\epsilon T)^{-1/2} \exp\left[\frac{-(E - E^0 + \lambda)^2}{4\lambda\epsilon T}\right] \quad (3.6.35)$$

thus the distribution for R has the same shape as that for O, but is centered on $E^0 - \lambda$, as depicted in Figure 3.6.4.

Any model of electrode kinetics is constrained by the requirement that

$$\frac{k_b}{k_f} = e^{f(E-E^0)} = e^{-(E-E^0)/\epsilon T} \quad (3.6.36)$$

which is easily derived from the need for convergence to the Nernst equation at equilibrium (Problem 3.16). The development of the Gerischer model up through equations 3.6.29 and 3.6.30 is general, and one can imagine that the various component functions in those two equations might come together in different ways to fulfill this requirement. By later including results from the Marcus theory without work terms, we were able to define the distribution functions, $W_O(\lambda, E)$ and $W_R(\lambda, E)$. Another feature of this simple *Gerischer–Marcus model* is that $\epsilon_{\text{ox}}(E)$ and $\epsilon_{\text{red}}(E)$ turn out to be identical functions and need no longer be distinguished. However, this will not necessarily be true for related models including work terms and a precursor equilibrium.

The reorganization energy, λ , has a large effect on the predicted current-potential response, as shown in Figure 3.6.5. The top frame illustrates the situation for $\lambda = 0.3$ eV, a value near the lower limit found experimentally. For this reorganization energy, an overpotential of -300 mV (case *a*) places the Fermi level opposite the peak of the state

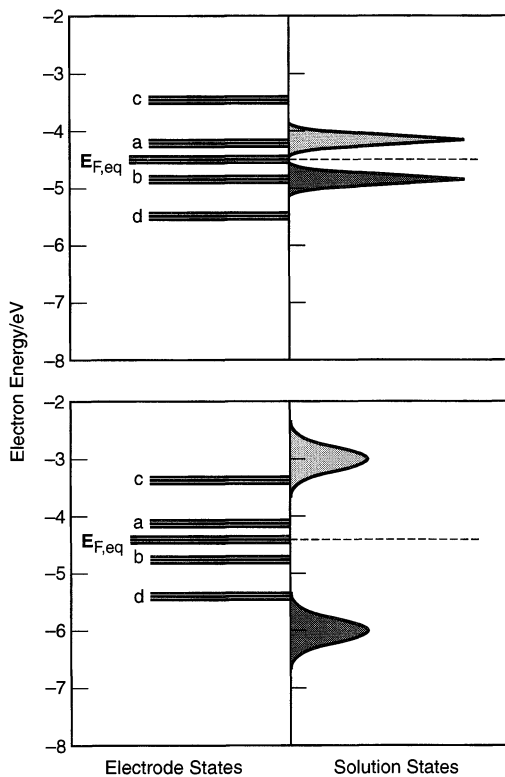


Figure 3.6.5 Effect of λ on kinetics in the Gerischer–Marcus representation. Top: $\lambda = 0.3$ eV. Bottom: $\lambda = 1.5$ eV. Both diagrams are for species O and R at equal concentrations, so that the Fermi level corresponding to the equilibrium potential, $E_{F,\text{eq}}$, is equal to the electron energy at the standard potential, E^0 (dashed line). For both frames, $E^0 = -4.5$ eV. Also shown in each frame is the way in which the Fermi level shifts with electrode potential. The different Fermi levels are for (a) $\eta = -300$ mV, (b) $\eta = +300$ mV, (c) $\eta = -1000$ mV, and (d) $\eta = +1000$ mV. On the solution side, $W_O(\lambda, E)$ and $W_R(\lambda, E)$ are shown with lighter and darker shading, respectively.

distribution for O; hence rapid reduction would be seen. Likewise, an overpotential of +300 mV (case *b*) brings the Fermi level down to match the peak in the state distribution for R and enables rapid oxidation. An overpotential of -1000 mV (case *c*) creates a situation in which $W_O(\lambda, \mathbf{E})$ overlaps entirely with filled states on the electrode, and for $\eta = +1000$ mV (case *d*), $W_R(\lambda, \mathbf{E})$ overlaps only empty states on the electrode. These latter two cases correspond to very strongly enabled reduction and oxidation, respectively.

The lower frame of Figure 3.6.5 shows the very different situation for the fairly large reorganization energy of 1.5 eV. In this case, an overpotential of -300 mV is not enough to elevate the Fermi level into a condition where filled states on the electrode overlap $W_O(\lambda, \mathbf{E})$, nor is an overpotential of +300 mV enough to lower the Fermi level into a condition where empty states on the electrode overlap $W_R(\lambda, \mathbf{E})$. It takes $\eta \approx -1000$ mV to enable reduction very effectively, and $\eta \approx +1000$ mV to do the same for oxidation. For this reorganization energy, the anodic and cathodic branches of the i - E curve would be widely separated, much as shown in Figure 3.4.2c.

Since this formulation of heterogeneous kinetics in terms of overlapping state distributions is linked directly to the basic Marcus theory, it is not surprising that many of its predictions are compatible with those of the previous two sections. The principal difference is that this formulation allows explicitly for contributions from states far from the Fermi level, which can be important in reactions at semiconductor electrodes (Section 18.2) or involving bound monolayers on metals (Section 14.5.2).

3.6.4 Tunneling and Extended Charge Transfer

In the treatments discussed above, the reactant was assumed to be held at a fixed, short distance, x_0 , from the electrode. It is also of interest to consider whether a solution species can undergo electron transfer at different distances from the electrode and how the electron-transfer rate might depend on distance and on the nature of the intervening medium. The act of electron transfer is usually considered as tunneling of the electron between states in the electrode and those on the reactant. Electron tunneling typically follows an expression of the form:

$$\text{Probability of tunneling} \propto \exp(-\beta x) \quad (3.6.37)$$

where x is the distance over which tunneling occurs, and β is a factor that depends upon the height of the energy barrier and the nature of the medium between the states. For example, for tunneling between two pieces of metal through vacuum (73)

$$\beta \approx 4\pi(2m\Phi)^{1/2}/\hbar \approx 1.02 \text{ \AA}^{-1} \text{ eV}^{-1/2} \times \Phi^{1/2} \quad (3.6.38)$$

where m is the mass of the electron, 9.1×10^{-28} g, and Φ is the work function of the metal, typically given in eV. Thus for Pt, where $\Phi = 5.7$ eV, β is about 2.4 \AA^{-1} . Within the electron-transfer theory, tunneling effects are usually incorporated by taking the transmission coefficient, κ_{el} , in (3.6.2) as

$$\kappa_{el}(x) = \kappa_{el}^0 \exp(-\beta x) \quad (3.6.39)$$

where $\kappa_{el}(x) \rightarrow 1$ when x is at the distance where the interaction of reactant with the electrode is sufficiently strong for the reaction to be *adiabatic* (48, 49).

In electron-transfer theory, the extent of interaction or electronic coupling between two reactants (or between a reactant and the electrode) is often described in terms of *adiabaticity*. If the interaction is strong, there is a splitting larger than kT in the energy curves at the point of intersection (e.g., Figure 3.6.6a). It leads to a lower curve (or surface) pro-

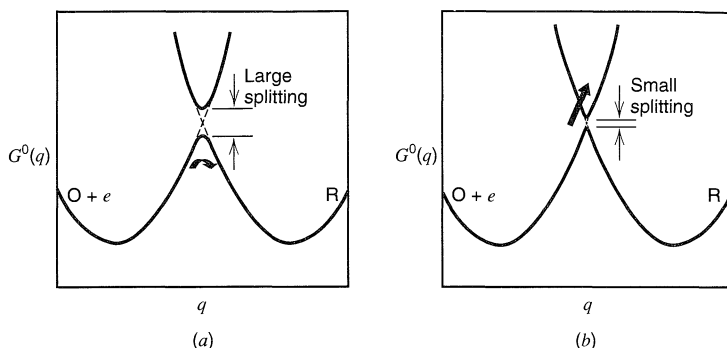


Figure 3.6.6 Splitting of energy curves (energy surfaces) in the intersection region. (a) A strong interaction between O and the electrode leads to a well-defined, continuous curve (surface) connecting O + e with R. If the reacting system reaches the transition state, the probability is high that it will proceed into the valley corresponding to R, as indicated by the curved arrow. (b) A weak interaction leads to a splitting less than kT . When the reacting system approaches the transition state from the left, it has a tendency to remain on the O + e curve, as indicated by the straight arrow. The probability of crossover to the R curve can be small. These curves are drawn for an electrode reaction, but the principle is the same for a homogeneous reaction, where the reactants and products might be O + R' and R + O', respectively.

ceeding continuously from O to R and an upper curve (or surface) representing an excited state. In this situation of strong coupling, a system will nearly always stay on the lower surface passing from O to R, and the reaction is said to be *adiabatic*. The probability of reaction per passage approaches unity for an adiabatic reaction.

If the interaction is small (e.g., when the reactants are far apart), the splitting of the potential energy curves at the point of intersection is less than kT (Figure 3.6.6b). In this case, there is a smaller likelihood that the system will proceed from O to R. The reaction is said to be *nonadiabatic*, because the system tends to stay on the original “reactant” surface (or, actually, to cross from the ground-state surface to the excited-state surface). The probability of reaction per passage through the intersection region is taken into account by $\kappa_{el} < 1$ (47, 48). For example, κ_{el} could be 10^{-5} , meaning that the reactants would, on the average, pass through the intersection region (i.e., reach the transition state) 100,000 times for every successful reaction.

In considering dissolved reactants participating in a heterogeneous reaction, one can treat the reaction as occurring over a range of distances, where the rate constant falls off exponentially with distance. The result of such a treatment (48, 74) is that electron transfer occurs over a region near the electrode, rather than only at a single position, such as the outer Helmholtz plane. However, the effect for dissolved reactants should be observable experimentally only under rather restricted circumstances (e.g., $D < 10^{-10}$ cm²/s), and is thus usually not important.

On the other hand, it is possible to study electron transfer to an electroactive species held at a fixed distance (10–30 Å) from the electrode surface by a suitable spacer, such as an adsorbed monolayer (Section 14.5.2) (75, 76). One approach is based on the use of a blocking monolayer, such as a self-assembled monolayer of an alkane thiol or an insulating oxide film, to define the distance of closest approach of a dissolved reactant to the electrode. This strategy requires knowledge of the precise thickness of the blocking layer and assurance that the layer is free of pinholes and defects, through which solution species might penetrate (Section 14.5). Alternatively, the adsorbed monolayer may itself

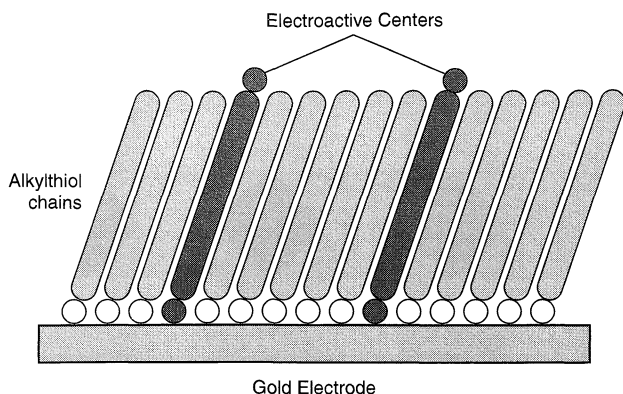


Figure 3.6.7 Schematic diagram of an adsorbed monolayer of alkane thiol containing similar molecules with attached electroactive groups held by the film at a fixed distance from the electrode surface.

contain electroactive groups. A typical layer of this kind (75) involves an alkane thiol (RSH) with a terminal ferrocene group (-Fc), that is, $\text{HS}(\text{CH}_2)_n\text{OOCFc}$ (often written as HSC_nOOCFc ; typically $n = 8$ to 18) (Figure 3.6.7). These molecules are often diluted in the monolayer film with similar nonelectroactive molecules (e.g., HSC_nCH_3). The rate constant is measured as a function of the length of the alkyl chain, and the slope of the plot of $\ln(k)$ vs. n or x allows determination of β .

For saturated chains, β is typically in the range 1 to 1.2 \AA^{-1} . The difference between this *through-bond* value and that for vacuum (*through-space*), $\sim 2 \text{ \AA}^{-1}$, reflects the contribution of the molecular bonds to tunneling. Even smaller β values (0.4 to 0.6 \AA^{-1}) have been seen with π -conjugated molecules [e.g., those with phenyleneethynyl (-Ph-C \equiv C-) units] as spacers (77, 78). Confidence in the β values found in these electrochemical studies is reinforced by the fact that they generally agree with those found for long-range intramolecular electron transfer, such as in proteins.

► 3.7 REFERENCES

- W. C. Gardiner, Jr., "Rates and Mechanisms of Chemical Reactions," Benjamin, New York, 1969.
- H. S. Johnston, "Gas Phase Reaction Rate Theory," Ronald, New York, 1966.
- S. Glasstone, K. J. Laidler, and H. Eyring, "Theory of Rate Processes," McGraw-Hill, New York, 1941.
- H. Eyring, S. H. Lin, and S. M. Lin, "Basic Chemical Kinetics," Wiley, New York, 1980, Chap. 4.
- R. S. Berry, S. A. Rice, J. Ross, "Physical Chemistry," Wiley, New York, 1980, pp. 931–932.
- J. Tafel, *Z. Physik. Chem.*, **50A**, 641 (1905).
- P. Delahay, "New Instrumental Methods in Electrochemistry," Wiley-Interscience, New York, 1954, Chap. 2.
- P. Delahay, "Double Layer and Electrode Kinetics," Wiley-Interscience, New York, 1965, Chap. 7.
- B. E. Conway, "Theory and Principles of Electrode Processes," Ronald, New York, 1965, Chap. 6.
- K. J. Vetter, "Electrochemical Kinetics," Academic, New York, 1967, Chap. 2.
- J. O'M. Bockris and A. K. N. Reddy, "Modern Electrochemistry," Vol. 2, Plenum, New York, 1970, Chap. 8.
- T. Erdey-Grúz, "Kinetics of Electrode Processes," Wiley-Interscience, New York, 1972, Chap. 1.
- H. R. Thirsk, "A Guide to the Study of Electrode Kinetics," Academic, New York, 1972, Chap. 1.
- W. J. Albery, "Electrode Kinetics," Clarendon, Oxford, 1975.
- J. E. B. Randles, *Trans. Faraday Soc.*, **48**, 828 (1952).
- C. N. Reilly in "Treatise on Analytical Chemistry," Part I, Vol. 4, I. M. Kolthoff and P. J. Elving, Eds., Wiley-Interscience, 1963, Chap. 42.

17. J. A. V. Butler, *Trans. Faraday Soc.*, **19**, 729, 734 (1924).
18. T. Erdey-Grúz and M. Volmer, *Z. Physik. Chem.*, **150A**, 203 (1930).
19. R. Parsons, *Trans. Faraday Soc.*, **47**, 1332 (1951).
20. J. O'M Bockris, *Mod. Asp. Electrochem.*, **1**, 180 (1954).
21. D. M. Mohilner and P. Delahay, *J. Phys. Chem.*, **67**, 588 (1963).
22. M. E. Peover, *Electroanal. Chem.*, **2**, 1 (1967).
23. N. Koizumi and S. Aoyagui, *J. Electroanal. Chem.*, **55**, 452 (1974).
24. H. Kojima and A. J. Bard, *J. Am. Chem. Soc.*, **97**, 6317 (1975).
25. K. J. Vetter, *op. cit.*, Chap. 4.
26. T. Erdey-Grúz, *op. cit.*, Chap. 4.
27. P. Delahay, "Double Layer and Electrode Kinetics," *op. cit.*, Chap. 10.
28. N. Tanaka and R. Tamamushi, *Electrochim. Acta*, **9**, 963 (1964).
29. B. E. Conway, "Electrochemical Data," Elsevier, Amsterdam, 1952.
30. R. Parsons, "Handbook of Electrochemical Data," Butterworths, London, 1959.
31. A. J. Bard and H. Lund, "Encyclopedia of the Electrochemistry of the Elements," Marcel Dekker, New York, 1973–1986.
32. E. Gileadi, E. Kirowa-Eisner, and J. Penciner, "Interfacial Electrochemistry," Addison-Wesley, Reading, MA, 1975, pp. 60–75.
33. K. J. Vetter and G. Manecke, *Z. Physik. Chem. (Leipzig)*, **195**, 337 (1950).
34. P. A. Allen and A. Hickling, *Trans. Faraday Soc.*, **53**, 1626 (1957).
35. P. Delahay, "Double Layer and Electrode Kinetics," *op. cit.*, Chaps. 8–10.
36. K. B. Oldham, *J. Am. Chem. Soc.*, **77**, 4697 (1955).
37. R. A. Marcus, *J. Chem. Phys.*, **24**, 4966 (1956).
38. R. A. Marcus, *Electrochim. Acta*, **13**, 955 (1968).
39. N. S. Hush, *J. Chem. Phys.*, **28**, 962 (1958).
40. N. S. Hush, *Electrochim. Acta*, **13**, 1005 (1968).
41. V. G. Levich, *Adv. Electrochem. Electrochem. Engr.*, **4**, 249 (1966) and references cited therein.
42. R. R. Dogonadze in "Reactions of Molecules at Electrodes," N. S. Hush, Ed., Wiley-Interscience, New York, 1971, Chap. 3 and references cited therein.
43. J. O'M. Bockris, *Mod. Asp. Electrochem.*, **1**, 180 (1954).
44. P. P. Schmidt in "Electrochemistry," A Specialist Periodical Report, Vols. 5 and 6, H. R. Thirsk, Senior Reporter, The Chemical Society, London, 1977 and 1978.
45. A. M. Kuznetsov, *Mod. Asp. Electrochem.*, **20**, 95 (1989).
46. W. Schmickler, "Interfacial Electrochemistry," Oxford University Press, New York, 1996.
47. C. J. Miller in "Physical Electrochemistry. Principles, Methods, and Applications," I. Rubinstein, Ed., Marcel Dekker, New York, 1995, Chap. 2.
48. M. J. Weaver in "Comprehensive Chemical Kinetics," R. G. Compton, Ed., Elsevier, Amsterdam, Vol. 27, 1987. Chap. 1.
49. R. A. Marcus and P. Siddarth, "Photoprocesses in Transition Metal Complexes, Biosystems and Other Molecules," E. Kochanski, Ed., Kluwer, Amsterdam, 1992.
50. N. S. Hush, *J. Electroanal. Chem.*, **470**, 170 (1999).
51. L. Ebersson, "Electron Transfer Reactions in Organic Chemistry," Springer-Verlag, Berlin, 1987.
52. N. Sutin, *Accts. Chem. Res.*, **15**, 275 (1982).
53. R. A. Marcus and N. Sutin, *Biochim. Biophys. Acta*, **811**, 265 (1985).
54. H. Taube, "Electron Transfer Reactions of Complex Ions in Solution," Academic, New York, 1970, p. 27.
55. J. J. Ulrich and F. C. Anson, *Inorg. Chem.*, **8**, 195 (1969).
56. G. A. Somorjai, "Introduction to Surface Chemistry and Catalysis," Wiley, New York, 1994.
57. S. F. Fischer and R. P. Van Duyne, *Chem. Phys.*, **26**, 9 (1977).
58. R. A. Marcus, *J. Chem. Phys.*, **43**, 679 (1965).
59. R. A. Marcus, *Annu. Rev. Phys. Chem.*, **15**, 155 (1964).
60. B. S. Brunshwig, J. Logan, M. D. Newton, and N. Sutin, *J. Am. Chem. Soc.*, **102**, 5798 (1980).
61. R. A. Marcus, *J. Phys. Chem.*, **67**, 853 (1963).
62. D. F. Calef and P. G. Wolynes, *J. Phys. Chem.*, **87**, 3387 (1983).
63. J. T. Hynes in "Theory of Chemical Reaction Dynamics," M. Baer, Editor, CRC, Boca Raton, FL, 1985, Chap. 4.
64. H. Sumi and R. A. Marcus, *J. Chem. Phys.*, **84**, 4894 (1986).

65. M. J. Weaver, *Chem. Rev.*, **92**, 463 (1992).
66. X. Zhang, J. Leddy, and A. J. Bard, *J. Am. Chem. Soc.*, **107**, 3719 (1985).
67. X. Zhang, H. Yang, and A. J. Bard, *J. Am. Chem. Soc.*, **109**, 1916 (1987).
68. M. E. Williams, J. C. Crooker, R. Pyati, L. J. Lyons, and R. W. Murray, *J. Am. Chem. Soc.*, **119**, 10249 (1997).
69. R. A. Marcus, *J. Phys. Chem.*, **94**, 1050 (1990); **95**, 2010 (1991).
70. M. Tsionsky, A. J. Bard, and M. V. Mirkin, *J. Am. Chem. Soc.*, **119**, 10785 (1997).
71. H. Gerischer, *Adv. Electrochem. Electrochem. Eng.*, **1**, 139 (1961).
72. H. Gerischer in "Physical Chemistry: An Advanced Treatise," Vol. 9A, H. Eyring, D. Henderson, and W. Jost, Eds., Academic, New York, 1970.
73. C. J. Chen, "Introduction to Scanning Tunneling Microscopy," Oxford University Press, New York, 1993, p. 5.
74. S. W. Feldberg, *J. Electroanal. Chem.*, **198**, 1 (1986).
75. H. O. Finklea, *Electroanal. Chem.*, **19**, 109 (1996).
76. J. F. Smalley, S. W. Feldberg, C. E. D. Chidsey, M. R. Linford, M. D. Newton, and Y.-P. Liu, *J. Phys. Chem.*, **99**, 13141 (1995).
77. S. B. Sachs, S. P. Dudek, R. P. Hsung, L. R. Sita, J. F. Smalley, M. D. Newton, S. W. Feldberg, and C. E. D. Chidsey, *J. Am. Chem. Soc.*, **119**, 10563 (1997).
78. S. Creager, S. J. Yu, D. Bamdad, S. O'Conner, T. MacLean, E. Lam, Y. Chong, G. T. Olsen, J. Luo, M. Gozin, and J. F. Kayyem, *J. Am. Chem. Soc.*, **121**, 1059 (1999).

3.8 PROBLEMS

- 3.1 Consider the electrode reaction $O + ne \rightleftharpoons R$. Under the conditions that $C_R^* = C_O^* = 1 \text{ mM}$, $k^0 = 10^{-7} \text{ cm/s}$, $\alpha = 0.3$, and $n = 1$:
- Calculate the exchange current density, $j_0 = i_0/A$, in $\mu\text{A}/\text{cm}^2$.
 - Draw a current density-overpotential curve for this reaction for currents up to $600 \mu\text{A}/\text{cm}^2$ anodic and cathodic. Neglect mass-transfer effects.
 - Draw $\log |j|$ vs. η curves (Tafel plots) for the current ranges in (b).
- 3.2 A general expression for the current as a function of overpotential, including mass-transfer effects, can be obtained from (3.4.29) and yields

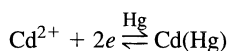
$$i = \frac{\exp[-\alpha f \eta] - \exp[(1 - \alpha) f \eta]}{\frac{1}{i_0} + \frac{\exp[-\alpha f \eta]}{i_{l,c}} - \frac{\exp[(1 - \alpha) f \eta]}{i_{l,a}}}$$

- Derive this expression.
 - Use a spreadsheet program to repeat the calculation of Problem 3.1, parts (b) and (c), including the effects of mass transfer. Assume $m_O = m_R = 10^{-3} \text{ cm/s}$.
- 3.3 Use a spreadsheet program to calculate and plot current vs. potential and $\ln(\text{current})$ vs. potential for the general i - η equation given in Problem 3.2.
- Show a table of results [potential, current, $\ln(\text{current})$, overpotential] and graphs of i vs. η and $\ln|i|$ vs. η for the following parameters: $A = 1 \text{ cm}^2$; $C_O^* = 1.0 \times 10^{-3} \text{ mol}/\text{cm}^3$; $C_R^* = 1.0 \times 10^{-5} \text{ mol}/\text{cm}^3$; $n = 1$; $\alpha = 0.5$; $k^0 = 1.0 \times 10^{-4} \text{ cm/s}$; $m_O = 0.01 \text{ cm/s}$; $m_R = 0.01 \text{ cm/s}$; $E^0 = -0.5 \text{ V vs. NHE}$.
 - Show the i vs. E curves for a range of k^0 values with the other parameters as in (a). At what values of k^0 are the curves indistinguishable from nernstian ones?
 - Show the i vs. E curves for a range of α values with the other parameters as in (a).
- 3.4 In most cases, the currents for individual processes are additive, that is, the total current, i_t , is given as the sum of the currents for different electrode reactions (i_1, i_2, i_3, \dots). Consider a solution with a Pt working electrode immersed in a solution of 1.0 M HBr and $1 \text{ mM K}_3\text{Fe}(\text{CN})_6$. Assume the following exchange current densities:

$$\begin{array}{ll} \text{H}^+/\text{H}_2 & j_0 = 10^{-3} \text{ A}/\text{cm}^2 \\ \text{Br}_2/\text{Br}^- & j_0 = 10^{-2} \text{ A}/\text{cm}^2 \\ \text{Fe}(\text{CN})_6^{3-}/\text{Fe}(\text{CN})_6^{4-} & j_0 = 4 \times 10^{-5} \text{ A}/\text{cm}^2 \end{array}$$

Use a spreadsheet program to calculate and plot the current-potential curve for this system scanning from the anodic background limit to the cathodic background limit. Take the appropriate standard potentials from Table C.1 and values for other parameters (m_O , α , ...) from Problem 3.3.

- 3.5 Consider one-electron electrode reactions for which $\alpha = 0.50$ and $\alpha = 0.10$. Calculate the relative error in current resulting from the use in each case of:
- The linear $i-\eta$ characteristic for overpotentials of 10, 20, and 50 mV.
 - The Tafel (totally irreversible) relationship for overpotentials of 50, 100, and 200 mV.
- 3.6 According to G. Scherer and F. Willig [*J. Electroanal. Chem.*, **85**, 77 (1977)] the exchange current density, j_0 , for Pt/Fe(CN) $_6^{3-}$ (2.0 mM), Fe(CN) $_6^{4-}$ (2.0 mM), NaCl (1.0 M) at 25°C is 2.0 mA/cm 2 . The transfer coefficient, α , for this system is about 0.50. Calculate (a) the value of k^0 ; (b) j_0 for a solution 1 M each in the two complexes; (c) the charge-transfer resistance of a 0.1 cm 2 electrode in a solution 10 $^{-4}$ M each in ferricyanide and ferrocyanide.
- 3.7 Berzins and Delahay [*J. Am. Chem. Soc.*, **77**, 6448 (1955)] studied the reaction



and obtained the following data with $C_{\text{Cd}(\text{Hg})} = 0.40 \text{ M}$:

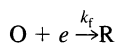
$C_{\text{Cd}^{2+}}(\text{mM})$	1.0	0.50	0.25	0.10
j_0 (mA/cm 2)	30.0	17.3	10.1	4.94

- Assume that the general mechanism in (3.5.8)–(3.5.10) applies. Calculate $n' + \alpha$, and suggest values for n' , n'' , and α individually. Write out a specific chemical mechanism for the process.
 - Calculate k_{app}^0 .
 - Compare the outcome with the analysis provided by Berzins and Delahay in their original paper.
- 3.8 (a) Show that for a first-order homogeneous reaction,



the average lifetime of A is $1/k_f$.

- (b) Derive an expression for the average lifetime of the species O when it undergoes the heterogeneous reaction,



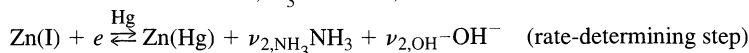
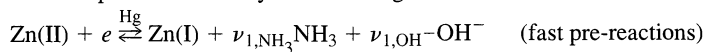
Note that only species within distance d of the surface can react. Consider a hypothetical system in which the solution phase extends only d (perhaps 10 Å) from the surface.

- (c) What value of k_f would be needed for a lifetime of 1 ms? Are lifetimes as short as 1 ns possible?
- 3.9 Discuss the mechanism by which the potential of a platinum electrode becomes poised by immersion into a solution of Fe(II) and Fe(III) in 1 M HCl. Approximately how much charge is required to shift the electrode potential by 100 mV? Why does the potential become uncertain at low concentrations of Fe(II) and Fe(III), even if the ratio of their concentrations is held near unity? Does this experimental fact reflect thermodynamic considerations? How well do your answers to these issues apply to the establishment of potential at an ion-selective electrode?
- 3.10 In ammoniacal solutions ($[\text{NH}_3] \sim 0.05 \text{ M}$), Zn(II) is primarily in the form of the complex ion Zn(NH $_3$) $_3(\text{OH})^+$ [hereafter referred to as Zn(II)]. In studying the electroreduction of this compound to zinc amalgam at a mercury cathode, Gerischer [*Z. Physik. Chem.*, **202**, 302 (1953)] found that

$$\begin{aligned} \frac{\partial \log i_0}{\partial \log [\text{Zn(II)}]} &= 0.41 \pm 0.03 & \frac{\partial \log i_0}{\partial \log [\text{NH}_3]} &= 0.65 \pm 0.03 \\ \frac{\partial \log i_0}{\partial \log [\text{OH}^-]} &= -0.28 \pm 0.02 & \frac{\partial \log i_0}{\partial \log [\text{Zn}]} &= 0.57 \pm 0.03 \end{aligned}$$

where [Zn] refers to a concentration in the amalgam.

- (a) Give the equation for the overall reaction.
 (b) Assume that the process occurs by the following mechanism:



where Zn(I) stands for a zinc species of unknown composition in the +1 oxidation state, and the ν 's are stoichiometric coefficients. Derive an expression for the exchange current analogous to (3.5.40), and find explicit relationships for the logarithmic derivatives given above.

- (b) Calculate α and all stoichiometric coefficients.
 (c) Identify Zn(I) and write chemical equations to give a mechanism consistent with the data.
 (d) Consider an alternative mechanism having the pattern above, but with the first step being rate-determining. Is such a mechanism consistent with the observations?
- 3.11 The following data were obtained for the reduction of species R to R⁻ in a stirred solution at a 0.1 cm² electrode; the solution contained 0.01 M R and 0.01 M R⁻.

η (mV):	-100	-120	-150	-500	-600
i (μA):	45.9	62.6	100	965	965

Calculate: i_0 , k^0 , α , R_{ct} , i , m_{O} , R_{mt}

- 3.12 From results in Figure 3.4.5 for 10^{-2} M Mn(III) and 10^{-2} M Mn(IV), estimate j_0 and k^0 . What is the predicted j_0 for a solution 1 M in both Mn(III) and Mn(IV)?
- 3.13 The magnitude of the solvent term ($1/\epsilon_{\text{op}} - 1/\epsilon_{\text{s}}$) is about 0.5 for most solvents. Calculate the value of λ_{O} and the free energy of activation (in eV) due only to solvation for a molecule of radius 4.0 Å spaced 7 Å from an electrode surface.
- 3.14 Derive (3.6.30).
- 3.15 Show from the equations for $D_{\text{O}}(\mathbf{E}, \lambda)$ and $D_{\text{R}}(\mathbf{E}, \lambda)$ that the equilibrium energy of a system, \mathbf{E}_{eq} , is related to the bulk concentrations, C_{O}^* and C_{R}^* and \mathbf{E}^0 by an expression resembling the Nernst equation. How does this expression differ from the Nernst equation written in terms of potentials, E_{eq} and E^0 ? How do you account for the difference?
- 3.16 Derive (3.6.36) by considering the reaction $\text{O} + e \rightleftharpoons \text{R}$ at equilibrium in a system with bulk concentrations C_{O}^* and C_{R}^* .

MASS TRANSFER BY MIGRATION AND DIFFUSION

► 4.1 DERIVATION OF A GENERAL MASS TRANSFER EQUATION

In this section, we discuss the general partial differential equations governing mass transfer; these will be used frequently in subsequent chapters for the derivation of equations appropriate to different electrochemical techniques. As discussed in Section 1.4, mass transfer in solution occurs by diffusion, migration, and convection. Diffusion and migration result from a gradient in electrochemical potential, $\bar{\mu}$. Convection results from an imbalance of forces on the solution.

Consider an infinitesimal element of solution (Figure 4.1.1) connecting two points in the solution, r and s , where, for a certain species j , $\bar{\mu}_j(r) \neq \bar{\mu}_j(s)$. This difference of $\bar{\mu}_j$ over a distance (a gradient of electrochemical potential) can arise because there is a difference of concentration (or activity) of species j (a concentration gradient), or because there is a difference of ϕ (an electric field or potential gradient). In general, a flux of species j will occur to alleviate any difference of $\bar{\mu}_j$. The flux, \mathbf{J}_j ($\text{mol s}^{-1}\text{cm}^{-2}$), is proportional to the gradient of $\bar{\mu}_j$:

$$\mathbf{J}_j \propto \mathbf{grad} \bar{\mu}_j \quad \text{or} \quad \mathbf{J}_j \propto \nabla \bar{\mu}_j \quad (4.1.1)$$

where \mathbf{grad} or ∇ is a vector operator. For linear (one-dimensional) mass transfer, $\nabla = \mathbf{i}(\partial/\partial x)$, where \mathbf{i} is the unit vector along the axis and x is distance. For mass transfer in a three-dimensional Cartesian space,

$$\nabla = \mathbf{i} \frac{\partial}{\partial x} + \mathbf{j} \frac{\partial}{\partial y} + \mathbf{k} \frac{\partial}{\partial z} \quad (4.1.2)$$

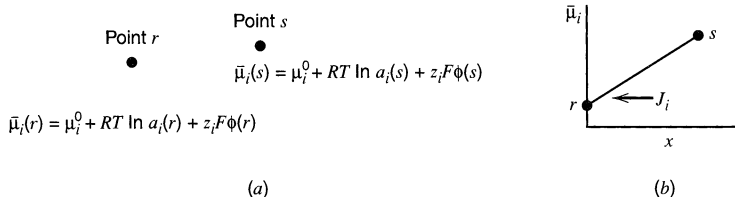


Figure 4.1.1 A gradient of electrochemical potential.

The constant of proportionality in (4.1.1) turns out to be $-C_j D_j / RT$; thus,

$$\mathbf{J}_j = -\left(\frac{C_j D_j}{RT}\right) \nabla \bar{\mu}_j \quad (4.1.3)$$

For linear mass transfer, this is

$$J_j(x) = -\left(\frac{C_j D_j}{RT}\right) \frac{\partial \bar{\mu}_j}{\partial x} \quad (4.1.4)$$

The minus sign arises in these equations because the direction of the flux opposes the direction of increasing $\bar{\mu}_j$.

If, in addition to this $\bar{\mu}$ gradient, the solution is moving, so that an element of solution [with a concentration $C_j(s)$] shifts from s with a velocity \mathbf{v} , then an additional term is added to the flux equation:

$$\mathbf{J}_j = -\left(\frac{C_j D_j}{RT}\right) \nabla \bar{\mu}_j + C_j \mathbf{v} \quad (4.1.5)$$

For linear mass transfer,

$$J_j(x) = -\left(\frac{C_j D_j}{RT}\right) \left(\frac{\partial \bar{\mu}_j}{\partial x}\right) + C_j v(x) \quad (4.1.6)$$

Taking $a_j \approx C_j$, we obtain the *Nernst-Planck equations*, which can be written as

$$J_j(x) = -\left(\frac{C_j D_j}{RT}\right) \left[\frac{\partial}{\partial x} (RT \ln C_j) + \frac{\partial}{\partial x} (z_j F \phi) \right] + C_j v(x) \quad (4.1.7)$$

$$\boxed{J_j(x) = -D_j \frac{\partial C_j(x)}{\partial x} - \frac{z_j F}{RT} D_j C_j \frac{\partial \phi(x)}{\partial x} + C_j v(x)} \quad (4.1.8)$$

or in general,

$$\boxed{\mathbf{J}_j = -D_j \nabla C_j - \frac{z_j F}{RT} D_j C_j \nabla \phi + C_j \mathbf{v}} \quad (4.1.9)$$

In this chapter, we are concerned with systems in which convection is absent. Convective mass transfer will be treated in Chapter 9. Under quiescent conditions, that is, in an unstirred or stagnant solution with no density gradients, the solution velocity, \mathbf{v} , is zero, and the general flux equation for species j , (4.1.9), becomes

$$\mathbf{J}_j = -D_j \nabla C_j - \frac{z_j F}{RT} D_j C_j \nabla \phi \quad (4.1.10)$$

For linear mass transfer, this is

$$J_j(x) = -D_j \left(\frac{\partial C_j(x)}{\partial x}\right) - \frac{z_j F}{RT} D_j C_j \left(\frac{\partial \phi(x)}{\partial x}\right) \quad (4.1.11)$$

where the terms on the right-hand side represent the contributions of diffusion and migration, respectively, to the total mass transfer.

If species j is charged, then the flux, J_j , is equivalent to a current density. Let us consider a linear system with a cross-sectional area, A , normal to the axis of mass flow. Then, J_j ($\text{mol s}^{-1} \text{cm}^{-2}$) is equal to $-i_j / z_j F A$ [$\text{C/s per } (\text{C mol}^{-1} \text{cm}^2)$], where i_j is the current

component at any value of x arising from a flow of species j . Equation 4.1.11 can then be written as

$$-J_j = \frac{i_j}{z_j F A} = \frac{i_{d,j}}{z_j F A} + \frac{i_{m,j}}{z_j F A} \quad (4.1.12)$$

with

$$\frac{i_{d,j}}{z_j F A} = D_j \frac{\partial C_j}{\partial x} \quad (4.1.13)$$

$$\frac{i_{m,j}}{z_j F A} = \frac{z_j F D_j}{RT} C_j \frac{\partial \phi}{\partial x} \quad (4.1.14)$$

where $i_{d,j}$ and $i_{m,j}$ are *diffusion* and *migration currents* of species j , respectively.

At any location in solution during electrolysis, the total current, i , is made up of contributions from all species; that is,

$$i = \sum_j i_j \quad (4.1.15)$$

or

$$i = \frac{F^2 A}{RT} \cdot \frac{\partial \phi}{\partial x} \sum_j z_j^2 D_j C_j + FA \sum_j z_j D_j \frac{\partial C_j}{\partial x} \quad (4.1.16)$$

where the current for each species at that location is made up of a migrational component (first term) and a diffusional component (second term).

We will now discuss migration and diffusion in electrochemical systems in more detail. The concepts and equations derived below date back to at least the work of Planck (1). Further details concerning the general problem of mass transfer in electrochemical systems can be found in a number of reviews (2–6).

► 4.2 MIGRATION

In the bulk solution (away from the electrode), concentration gradients are generally small, and the total current is carried mainly by migration. All charged species contribute. For species j in the bulk region of a linear mass-transfer system having a cross-sectional area A , $i_j = i_{m,j}$ or

$$i_j = \frac{z_j^2 F^2 A D_j C_j}{RT} \cdot \frac{\partial \phi}{\partial x} \quad (4.2.1)$$

The mobility of species j , defined in Section 2.3.3, is linked to the diffusion coefficient by the *Einstein–Smoluchowski equation*:

$$\boxed{u_j = \frac{|z_j| F D_j}{RT}} \quad (4.2.2)$$

hence i_j can be reexpressed as

$$i_j = |z_j| F A u_j C_j \frac{\partial \phi}{\partial x} \quad (4.2.3)$$

For a linear electric field,

$$\frac{\partial \phi}{\partial x} = \frac{\Delta E}{l} \quad (4.2.4)$$

where $\Delta E/l$ is the gradient (V/cm) arising from the change in potential ΔE over distance l . Thus,

$$i_j = \frac{|z_j| F A u_j C_j \Delta E}{l} \quad (4.2.5)$$

and the total current in bulk solution is given by

$$i = \sum_j i_j = \frac{F A \Delta E}{l} \sum_j |z_j| u_j C_j \quad (4.2.6)$$

which is (4.1.16) expressed in particular for this situation. The conductance of the solution, L (Ω^{-1}), which is the reciprocal of the resistance, R (Ω), is given by Ohm's law,

$$L = \frac{1}{R} = \frac{i}{\Delta E} = \frac{F A}{l} \sum_j |z_j| u_j C_j = \frac{A}{l} \kappa \quad (4.2.7)$$

where κ , the *conductivity* ($\Omega^{-1} \text{ cm}^{-1}$; Section 2.3.3) is given by

$$\kappa = F \sum_j |z_j| u_j C_j \quad (4.2.8)$$

Equally, one can write an equation for the solution resistance in terms of ρ , the *resistivity* ($\Omega\text{-cm}$), where $\rho = 1/\kappa$:

$$R = \frac{\rho l}{A} \quad (4.2.9)$$

The fraction of the total current that a given ion j carries is t_j , the *transference number* of j , given by

$$t_j = \frac{i_j}{i} = \frac{|z_j| u_j C_j}{\sum_k |z_k| u_k C_k} = \frac{|z_j| C_j \lambda_j}{\sum_k |z_k| C_k \lambda_k} \quad (4.2.10)$$

See also equations 2.3.11 and 2.3.18.

▶ 4.3 MIXED MIGRATION AND DIFFUSION NEAR AN ACTIVE ELECTRODE

The relative contributions of diffusion and migration to the flux of a species (and of the flux of that species to the total current) differ at a given time for different locations in solution. Near the electrode, an electroactive substance is, in general, transported by both processes. The flux of an electroactive substance at the electrode surface controls the rate of reaction and, therefore, the faradaic current flowing in the external circuit (see Section 1.3.2). That current can be separated into diffusion and migration currents reflecting the diffusive and migrational components to the flux of the electroactive species at the surface:

$$i = i_d + i_m \quad (4.3.1)$$

Note that i_m and i_d may be in the same or opposite directions, depending on the direction of the electric field and the charge on the electroactive species. Examples of three reductions—of a positively charged, a negatively charged, and an uncharged substance—are shown in Figure 4.3.1. The migrational component is always in the same direction as i_d for cationic species reacting at cathodes and for anionic species reacting at anodes. It opposes i_d when anions are reduced at cathodes and when cations are oxidized at anodes.

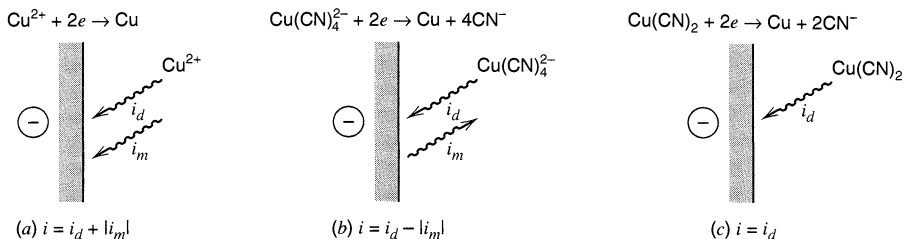


Figure 4.3.1 Examples of reduction processes with different contributions of the migration current: (a) positively charged reactant, (b) negatively charged reactant, (c) uncharged reactant.

For many electrochemical systems, the mathematical treatments are simplified if the migrational component to the flux of the electroactive substance is made negligible. We discuss in this section the conditions under which that approximation holds. The topic is discussed in greater depth in references 7–10.

4.3.1 Balance Sheets for Mass Transfer During Electrolysis

Although migration carries the current in the bulk solution during electrolysis, diffusional transport also occurs in the vicinity of the electrodes, because concentration gradients of the electroactive species arise there. Indeed, under some circumstances, the flux of electroactive species to the electrode is due almost completely to diffusion. To illustrate these effects, let us apply the “balance sheet” approach (11) to transport in several examples.

Example 4.1

Consider the electrolysis of a solution of hydrochloric acid at platinum electrodes (Figure 4.3.2a). Since the equivalent ionic conductance of H^+ , λ_+ , and of Cl^- , λ_- , relate as $\lambda_+ \approx 4\lambda_-$, then from (4.2.10), $t_+ = 0.8$ and $t_- = 0.2$. Assume that a total current equivalent to $10e$ per unit time is passed through the cell, producing five H_2 molecules

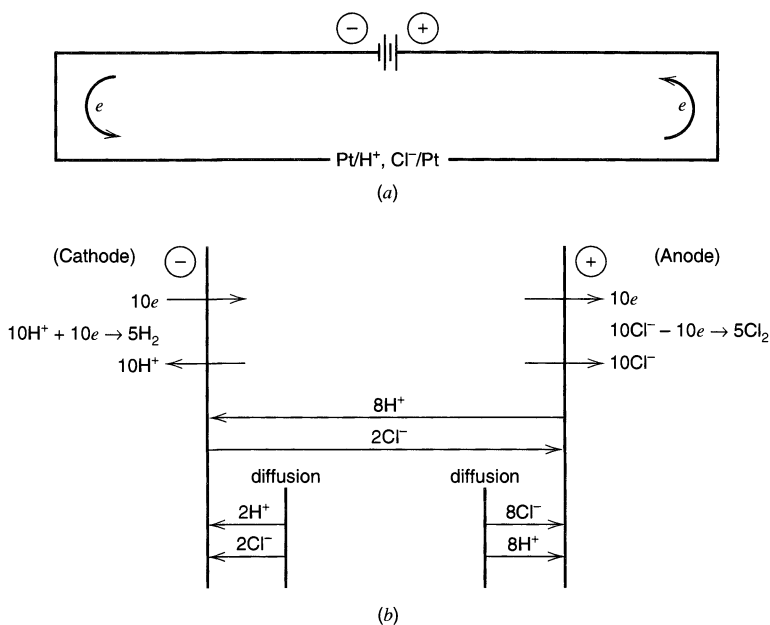


Figure 4.3.2 Balance sheet for electrolysis of hydrochloric acid solution. (a) Cell schematic. (b) Various contributions to the current when $10e$ are passed in the external circuit per unit time.

at the cathode and five Cl_2 molecules at the anode. (Actually, some O_2 could also be formed at the anode; for simplicity we neglect this reaction.) The total current is carried in the bulk solution by the movement of 8H^+ toward the cathode and 2Cl^- toward the anode (Figure 4.3.2*b*). To maintain a steady current, 10H^+ must be supplied to the cathode per unit time, so an additional 2H^+ must diffuse to the electrode, bringing along 2Cl^- to maintain electroneutrality. Similarly at the anode, to supply 10Cl^- per unit time, 8Cl^- must arrive by diffusion, along with 8H^+ . Thus, the different currents (in arbitrary e^- -units per unit time) are: for H^+ , $i_d = 2$, $i_m = 8$; for Cl^- , $i_d = 8$, $i_m = 2$. The total current, i , is 10. Equation 4.3.1 holds, with migration in this case being in the same direction as diffusion.

For mixtures of charged species, the fraction of current carried by the j th species is t_j ; and the amount of the total current, i , carried by the j th species is $t_j i$. The number of moles of the j th species migrating per second is $t_j i / z_j F$. If this species is undergoing electrolysis, the number of moles electrolyzed per second is $|t_j i| / nF$, while the number of moles arriving at the electrode per second by migration is $\pm i_m / nF$, where the positive sign applies to reduction of j , and the negative sign pertains to oxidation. Thus,

$$\pm \frac{i_m}{nF} = \frac{t_j i}{z_j F} \quad (4.3.2)$$

or

$$i_m = \pm \frac{n}{z_j} t_j i \quad (4.3.3)$$

From equation 4.3.1,

$$i_d = i - i_m \quad (4.3.4)$$

$$i_d = i \left(1 \mp \frac{nt_j}{z_j} \right) \quad (4.3.5)$$

where the minus sign is used for cathodic currents and the positive sign for anodic currents. Note that both i and z_j are signed.

In this simplified treatment, we assume that the transference numbers are essentially the same in the bulk solution and in the diffusion layer near an electrode. This will be true when the concentrations of ions in the solution are high, so that only small fractional changes in local concentration are caused by the electrolytic generation or removal of ions. This condition is met in most experiments. If the electrolysis significantly perturbs the ionic concentrations in the diffusion layer compared to those in the bulk solution, the t_j values clearly will differ, as shown by equation 4.2.10 (12).

Example 4.2

Consider the electrolysis of a solution of $10^{-3}\text{M Cu}(\text{NH}_3)_4^{2+}$, $10^{-3}\text{M Cu}(\text{NH}_3)_2^+$, and $3 \times 10^{-3}\text{M Cl}^-$ in 0.1M NH_3 at two Hg electrodes (Figure 4.3.3*a*). Assuming the limiting equivalent conductances of all ions are equal, that is,

$$\lambda_{\text{Cu(II)}} = \lambda_{\text{Cu(I)}} = \lambda_{\text{Cl}^-} = \lambda \quad (4.3.6)$$

we obtain the following transference numbers from (4.2.10): $t_{\text{Cu(II)}} = 1/3$, $t_{\text{Cu(I)}} = 1/6$ and $t_{\text{Cl}^-} = 1/2$. With an arbitrary current of $6e^-$ per unit time being passed, the migration current in bulk solution is carried by movement of one Cu(II) and one Cu(I) toward the cathode, and three Cl^- toward the anode. The total balance sheet for this system is shown in Figure 4.3.3*b*. At the cathode, one-sixth of the current for the electrolysis of Cu(II) is provided by migration and five-sixths by diffusion. The NH_3 , being uncharged, does not con-

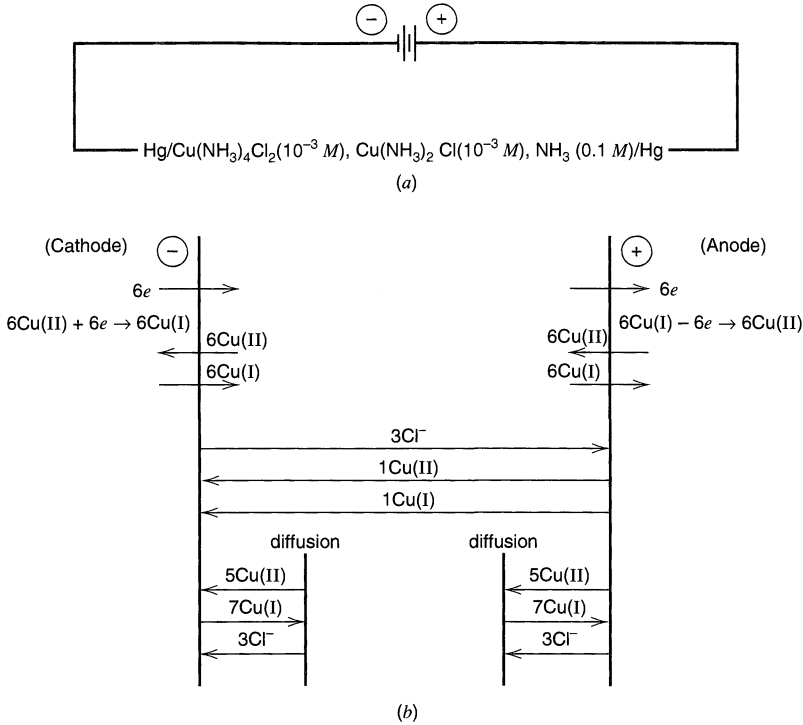


Figure 4.3.3 Balance sheet for electrolysis of the Cu(II), Cu(I), NH₃ system. (a) Cell schematic. (b) Various contributions to the current when $6e$ are passed in the external circuit per unit time; $i = 6$, $n = 1$. For Cu(II) at the cathode, $|i_m| = (1/2)(1/3)(6) = 1$ (equation 4.3.3), $i_d = 6 - 1 = 5$ (equation 4.3.4). For Cu(I) at the anode, $|i_m| = (1/1)(1/6)(6) = 1$, $i_d = 6 + 1 = 7$.

tribute to the carrying of the current, but serves only to stabilize the copper species in the +1 and +2 states. The resistance of this cell would be relatively large, since the total concentration of ions in the solution is small.

4.3.2 Effect of Adding Excess Electrolyte

Example 4.3

Let us consider the same cell as in Example 4.2, except with the solution containing 0.10 M NaClO₄ as an excess electrolyte (Figure 4.3.4a). Assuming that $\lambda_{\text{Na}^+} = \lambda_{\text{ClO}_4^-} = \lambda$, we obtain the following transference numbers: $t_{\text{Na}^+} = t_{\text{ClO}_4^-} = 0.485$, $t_{\text{Cu(II)}} = 0.0097$, $t_{\text{Cu(I)}} = 0.00485$, $t_{\text{Cl}^-} = 0.0146$. The Na⁺ and ClO₄⁻ do not participate in the electron-transfer reactions; but because their concentrations are high, they carry 97% of the current in the bulk solution. The balance sheet for this cell (Figure 4.3.4b) shows that most of the Cu(II) now reaches the cathode by diffusion, and only 0.5% of the total flux is by migration.

Thus, the addition of an excess of nonelectroactive ions (a *supporting electrolyte*) nearly eliminates the contribution of migration to the mass transfer of the electroactive species. In general, it simplifies the mathematical treatment of electrochemical systems by elimination of the $\nabla\phi$ or $\partial\phi/\partial x$ term in the mass transport equations (e.g., equations 4.1.10 and 4.1.11).

In addition to minimizing the contribution of migration, the supporting electrolyte serves other important functions. The presence of a high concentration of ions decreases

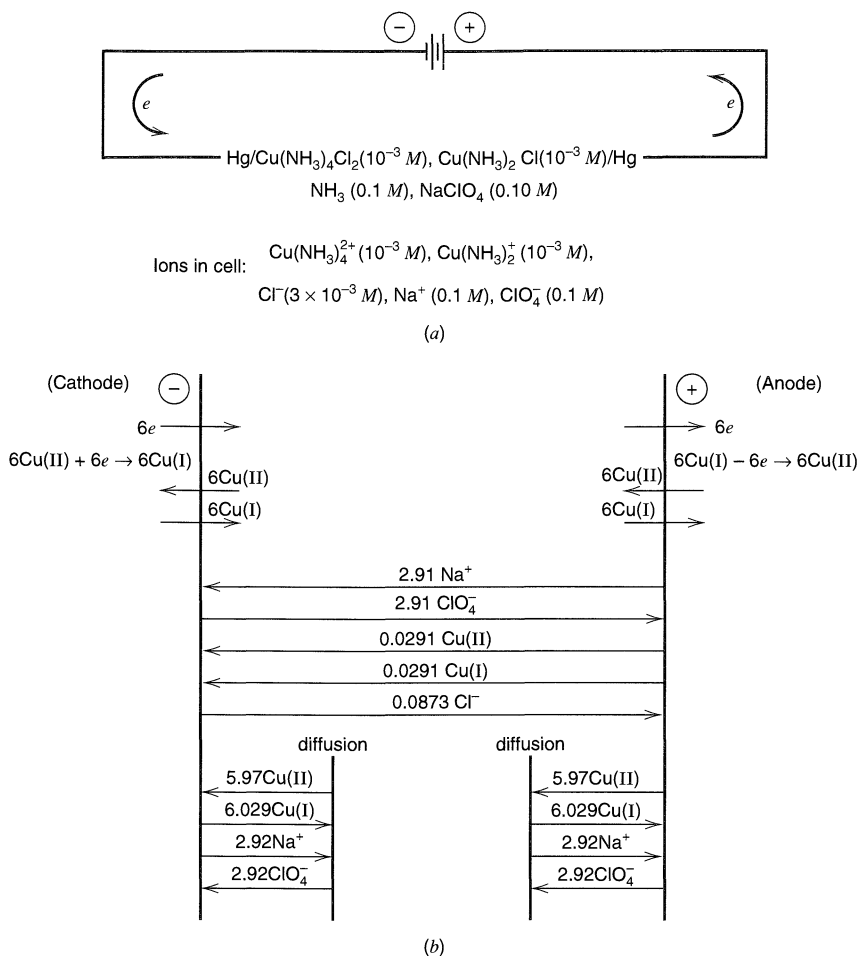


Figure 4.3.4 Balance sheet for the system in Figure 4.3.3, but with excess NaClO_4 as a supporting electrolyte. (a) Cell schematic. (b) Various contributions to the current when $6e$ are passed in the external circuit per unit time ($i = 6$, $n = 1$). $t_{\text{Cu(II)}} = [(2 \times 10^{-3})\lambda / (2 \times 10^{-3} + 10^{-3} + 3 \times 10^{-3} + 0.2)\lambda] = 0.0097$. For Cu(II) at the cathode, $|i_m| = (1/2)(0.0097)(6) = 0.03$, $i_d = 6 - 0.03 = 5.97$.

the solution resistance, and hence the uncompensated resistance drop, between the working and reference electrodes (Section 1.3.4). Consequently, the supporting electrolyte allows an improvement in the accuracy with which the working electrode's potential is controlled or measured (Chapter 15). Improved conductivity in the bulk of the solution also reduces the electrical power dissipated in the cell and can lead to important simplifications in apparatus (Chapters 11 and 15). Beyond these physical benefits are chemical contributions by the supporting electrolyte, for it frequently establishes the solution composition (pH, ionic strength, ligand concentration) that controls the reaction conditions (Chapters 5, 7, 11, and 12). In analytical applications, the presence of a high concentration of electrolyte, which is often also a buffer, serves to decrease or eliminate sample matrix effects. Finally, the supporting electrolyte ensures that the double layer remains thin with respect to the diffusion layer (Chapter 13), and it establishes a uniform ionic strength throughout the solution, even when ions are produced or consumed at the electrodes.

Supporting electrolytes also bring some disadvantages. Because they are used in such large concentrations, their impurities can present serious interferences, for example,

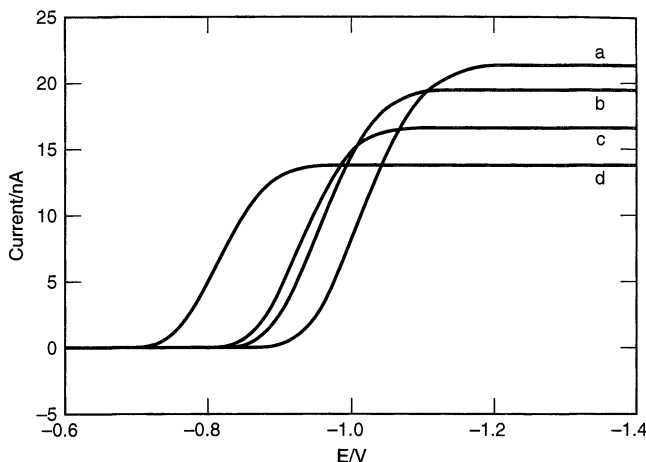


Figure 4.3.5 Voltammograms for reduction of 0.65 mM Tl_2SO_4 at a mercury film on a silver ultramicroelectrode (radius, 15 μm) in the presence of (a) 0, (b) 0.1, (c) 1, and (d) 100 mM LiClO_4 . The potential was controlled vs. a Pt wire QRE whose potential was a function of solution composition. This variability is the basis for the shifts in wave position along the potential axis. [Reprinted with permission from M. Ciszowska and J. G. Osteryoung, *Anal. Chem.*, **67**, 1125 (1995). Copyright 1995, American Chemical Society.]

by giving rise to faradaic responses of their own, by reacting with the intended product of an electrode process, or by adsorbing on the electrode surface and altering kinetics. Also, a supporting electrolyte significantly alters the medium in the cell, so that its properties differ from those of the pure solvent. The difference can complicate the comparison of results obtained in electrochemical experiments (e.g., thermodynamic data) with data from other kinds of experiments where pure solvents are typically employed.

Most electrochemical studies are carried out in the presence of a supporting electrolyte selected for the solvent and electrode process of interest. Many acids, bases, and salts are available for aqueous solutions. For organic solvents with high dielectric constants, like acetonitrile and *N,N*-dimethylformamide, normal practice is to employ tetra-*n*-alkylammonium salts, such as, Bu_4NBF_4 and Et_4NClO_4 (Bu = *n*-butyl, Et = ethyl). Studies in low-dielectric solvents like benzene inevitably involve solutions of high resistance, because most ionic salts do not dissolve in them to an appreciable extent. In solutions of salts that do dissolve in apolar media, such as Hx_4NClO_4 (where Hx = *n*-hexyl), ion pairing is extensive.

Studies in very resistive solutions require the use of UMEs, which usually pass low currents that do not give rise to appreciable resistive drops (see Section 5.9.2). The effect of supporting electrolyte concentration on the limiting steady-state current at UMEs has been treated (12–14). Typical results, shown in Figure 4.3.5, illustrate how the limiting current for reduction of Tl^+ to the amalgam at a mercury film decreases with an increase in LiClO_4 concentration (15). The current in the absence of LiClO_4 , or at very low concentrations, is appreciably larger than at high concentrations, because migration of the positively charged Tl(I) species to the cathode enhances the current. At high LiClO_4 concentrations, Li^+ migration replaces that of Tl^+ , and the observed current is essentially a pure diffusion current. A similar example involving the polarography of Pb(II) with KNO_3 supporting electrolyte was given in the first edition.¹

¹First edition, p. 127.

▶ 4.4 DIFFUSION

As we have just seen, it is possible to restrict mass transfer of an electroactive species near the electrode to the diffusive mode by using a supporting electrolyte and operating in a quiescent solution. Most electrochemical methods are built on the assumption that such conditions prevail; thus diffusion is a process of central importance. It is appropriate that we now take a closer look at the phenomenon of diffusion and the mathematical models describing it (16–19).

4.4.1 A Microscopic View—Discontinuous Source Model

Diffusion, which normally leads to the homogenization of a mixture, occurs by a “random walk” process. A simple picture can be obtained by considering a one-dimensional random walk. Consider a molecule constrained to a linear path and, buffeted by solvent molecules undergoing Brownian motion, moving in steps of length, l , with one step being made per unit time, τ . We can ask, “Where will the molecule be after a time, t ?” We can answer only by giving the probability that the molecule will be found at different locations. Equivalently, we can envision a large number of molecules concentrated in a line at $t = 0$ and ask what the distribution of molecules will be at time t . This is sometimes called the “drunken sailor problem,” where we envision a very drunk sailor emerging from a bar (Figure 4.4.1) and staggering randomly left and right (with a stagger-step size, l , one step every τ seconds). What is the probability that the sailor will get down the street a certain distance after a certain time t ?

In a random walk, all paths that can be traversed in any elapsed period are equally likely; hence the probability that the molecule has arrived at any particular point is simply the number of paths leading to that point divided by the total of possible paths to all accessible points. This idea is developed in Figure 4.4.2. At time τ , it is equally likely that the molecule is at $+l$ and $-l$; and at time 2τ , the relative probabilities of being at $+2l$, 0 , and $-2l$, are 1, 2, and 1, respectively.

The probability, $P(m, r)$, that the molecule is at a given location after m time units ($m = t/\tau$) is given by the binomial coefficient

$$P(m, r) = \frac{m!}{r!(m-r)!} \left(\frac{1}{2}\right)^m \quad (4.4.1)$$

where the set of locations is defined by $x = (-m + 2r)l$, with $r = 0, 1, \dots, m$. The mean square displacement of the molecule, $\overline{\Delta^2}$, can be calculated by summing the squares of the displacements and dividing by the total number of possibilities (2^m). The squares of the displacements are used, just as when one obtains the standard deviation in statistics, because movement is possible in both the positive and negative directions, and the sum of the displacements is always zero. This procedure is shown in Table 4.4.1. In general, $\overline{\Delta^2}$ is given by

$$\overline{\Delta^2} = ml^2 = \frac{t}{\tau} l^2 = 2Dt \quad (4.4.2)$$

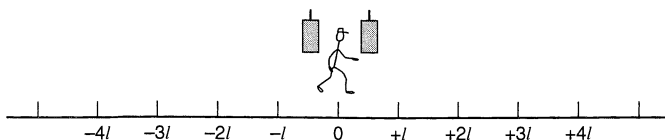


Figure 4.4.1 The one-dimensional random-walk or “drunken sailor problem.”

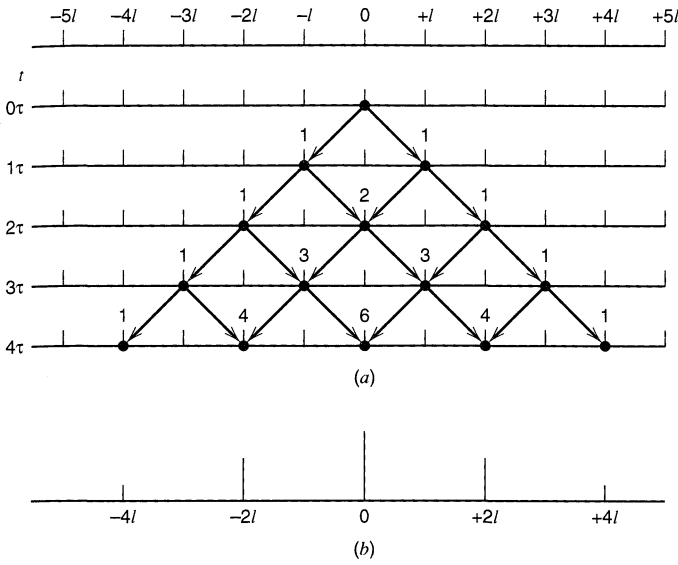


Figure 4.4.2 (a) Probability distribution for a one-dimensional random walk over zero to four time units. The number printed over each allowed arrival point is the number of paths to that point. (b) Bar graph showing distribution at $t = 4\tau$. At this time, probability of being at $x = 0$ is $6/16$, at $x = \pm 2l$ is $4/16$, and at $x = \pm 4l$ is $1/16$.

where the diffusion coefficient, D , identified as $l^2/2\tau$, is a constant related to the step size and step frequency.² It has units of length²/time, usually cm^2/s . The root-mean-square displacement at time t is thus

$$\bar{\Delta} = \sqrt{2Dt} \tag{4.4.3}$$

This equation provides a handy rule of thumb for estimating the thickness of a diffusion layer (e.g., how far product molecules have moved, on the average, from an electrode in a certain time). A typical value of D for aqueous solutions is $5 \times 10^{-6} \text{ cm}^2/\text{s}$, so that a diffusion layer thickness of 10^{-4} cm is built up in 1 ms, 10^{-3} cm in 0.1 s, and 10^{-2} cm in 10 s. (See also Section 5.2.1.)

As m becomes large, a continuous form of equation 4.4.1 arises. For N_0 molecules located at the origin at $t = 0$, a Gaussian curve will describe the distribution at some later

TABLE 4.4.1 Distributions for a Random Walk Process^a

t	n^b	Δ^c	$\Sigma \Delta^2$	$\bar{\Delta}^2 = \frac{1}{n} \Sigma \Delta^2$
0τ	$1 (= 2^0)$	0	0	0
1τ	$2 (= 2^1)$	$\pm l(1)$	$2l^2$	l^2
2τ	$4 (= 2^2)$	$0(2), \pm 2l(1)$	$8l^2$	$2l^2$
3τ	$8 (= 2^3)$	$\pm l(3), \pm 3l(1)$	$24l^2$	$3l^2$
4τ	$16 (= 2^4)$	$0(6), \pm 2l(4), \pm 4l(1)$	$64l^2$	$4l^2$
$m\tau$	2^m		$mnl^2 (= m2^m l^2)$	ml^2

^a l = step size, $1/\tau$ = step frequency, $t = m\tau$ = time interval.

^b n = total number of possibilities.

^c Δ = possible positions; relative probabilities are parenthesized.

²This concept of D was derived by Einstein in another way in 1905. Sometimes D is given as $f l^2/2$, where f is the number of displacements per unit time ($= 1/\tau$).

time, t . The number of molecules, $N(x, t)$, in a segment Δx wide centered on position x is (20)

$$\frac{N(x, t)}{N_0} = \frac{\Delta x}{2\sqrt{\pi Dt}} \exp\left(\frac{-x^2}{4Dt}\right) \quad (4.4.4)$$

A similar treatment can be applied to two- and three-dimensional random walks, where the root-mean-square displacements are $(4Dt)^{1/2}$ and $(6Dt)^{1/2}$, respectively (19, 21).

It may be instructive to develop a more molecular picture of diffusion in a liquid by considering the concepts of molecular and diffusional velocity (21). In a Maxwellian gas, a particle of mass m and average one-dimensional velocity, v_x , has an average kinetic energy of $\frac{1}{2}mv_x^2$. This energy can also be shown to be $kT/2$, (22, 23); thus the average molecular velocity is $v_x = (kT/m)^{1/2}$. For an O_2 molecule ($m = 5 \times 10^{-23}$ g) at 300 K, one finds that $v_x = 3 \times 10^4$ cm/s. In a liquid solution, a velocity distribution similar to that of a Maxwellian gas may apply; however, a dissolved O_2 molecule can make progress in a given direction at this high velocity only over a short distance before it collides with a molecule of solvent and changes direction. The net movement through the solution by the random walk produced by repeated collisions is much slower than v_x and is governed by the process described above. A “diffusional velocity,” v_d , can be extracted from equation 4.4.3 as

$$v_d = \bar{\Delta}/t = (2D/t)^{1/2} \quad (4.4.5)$$

There is a time dependence in this velocity because a random walk greatly favors small displacements from a starting point vs. large ones.

The relative importance of migration and diffusion can be gauged by comparing v_d with the steady-state migrational velocity, v , for an ion of mobility u_i in an electric field (Section 2.3.3). By definition, $v = u_i\mathcal{E}$, where \mathcal{E} is the electric field strength felt by the ion. From the Einstein-Smoluchowski equation, (4.2.2),

$$v = |z_i| FD_i\mathcal{E}/RT \quad (4.4.6)$$

When $v \ll v_d$, diffusion of a species dominates over migration at a given position and time. From (4.4.5) and (4.4.6), we find that this condition holds when

$$\frac{D_i\mathcal{E}}{RT/|z_i|F} \ll \left(\frac{2D_i}{t}\right)^{1/2}, \quad (4.4.7)$$

which can be rearranged to

$$(2D_it)^{1/2} \mathcal{E} \ll 2 \frac{RT}{|z_i|F} \quad (4.4.8)$$

where the left side is the diffusion length times the field strength, which is also the voltage drop in the solution over the length scale of diffusion. To ensure that migration is negligible compared to diffusion, this voltage drop must be smaller than about $2RT/|z_i|F$, which is 51.4/ $|z_i|$ mV at 25°C. This is the same as saying that the difference in electrical potential energy for the diffusing ion must be smaller than a few kT over the length scale of diffusion.

4.4.2 Fick's Laws of Diffusion

Fick's laws are differential equations describing the flux of a substance and its concentration as functions of time and position. Consider the case of linear (one-dimensional) diffusion. The flux of a substance O at a given location x at a time t , written as $J_O(x, t)$, is the

net mass-transfer rate of O, expressed as amount per unit time per unit area (e.g., mol s⁻¹ cm⁻²). Thus $J_O(x, t)$ represents the number of moles of O that pass a given location per second per cm² of area normal to the axis of diffusion.

Fick's first law states that the flux is proportional to the concentration gradient, $\partial C_O/\partial x$:

$$\boxed{-J_O(x, t) = D_O \frac{\partial C_O(x, t)}{\partial x}} \quad (4.4.9)$$

This equation can be derived from the microscopic model as follows. Consider location x , and assume $N_O(x)$ molecules are immediately to left of x , and $N_O(x + \Delta x)$ molecules are immediately to the right, at time t (Figure 4.4.3). All of the molecules are understood to be within one step-length, Δx , of location x . During the time increment, Δt , half of them move Δx in either direction by the random walk process, so that the net flux through an area A at x is given by the difference between the number of molecules moving from left to right and the number moving from right to left:

$$J_O(x, t) = \frac{1}{A} \frac{\frac{N_O(x)}{2} - \frac{N_O(x + \Delta x)}{2}}{\Delta t} \quad (4.4.10)$$

Multiplying by $\Delta x^2/\Delta x^2$ and noting that the concentration of O is $C_O = N_O/A\Delta x$, we derive

$$-J_O(x, t) = \frac{\Delta x^2 C_O(x + \Delta x) - C_O(x)}{2\Delta t \Delta x} \quad (4.4.11)$$

From the definition of the diffusion coefficient, (4.4.2), $D_O = \Delta x^2/2\Delta t$, and allowing Δx and Δt to approach zero, we obtain (4.4.9).

Fick's second law pertains to the change in concentration of O with time:

$$\boxed{\frac{\partial C_O(x, t)}{\partial t} = D_O \left(\frac{\partial^2 C_O(x, t)}{\partial x^2} \right)} \quad (4.4.12)$$

This equation is derived from the first law as follows. The change in concentration at a location x is given by the difference in flux into and flux out of an element of width dx (Figure 4.4.4).

$$\frac{\partial C_O(x, t)}{\partial t} = \frac{J(x, t) - J(x + dx, t)}{dx} \quad (4.4.13)$$

Note that J/dx has units of (mol s⁻¹ cm⁻²)/cm or change in concentration per unit time, as required. The flux at $x + dx$ can be given in terms of that at x by the general equation

$$J(x + dx, t) = J(x, t) + \frac{\partial J(x, t)}{\partial x} dx \quad (4.4.14)$$

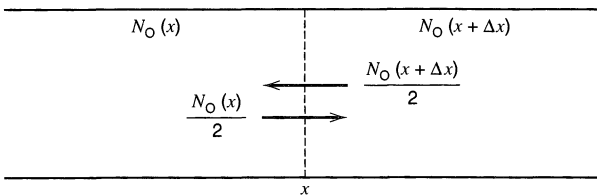


Figure 4.4.3 Fluxes at plane x in solution.

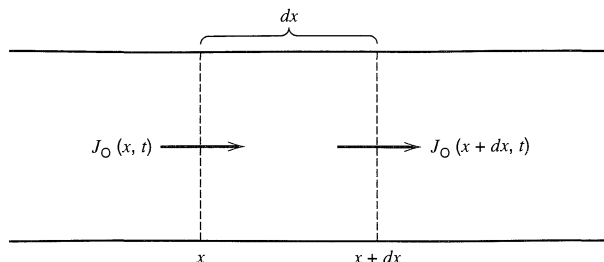


Figure 4.4.4 Fluxes into and out of an element at x .

and from equation 4.4.9 we obtain

$$-\frac{\partial J(x, t)}{\partial x} = \frac{\partial}{\partial x} D_O \frac{\partial C_O(x, t)}{\partial x} \quad (4.4.15)$$

Combination of equations 4.4.13 to 4.4.15 yields

$$\frac{\partial C_O(x, t)}{\partial t} = \left(\frac{\partial}{\partial x} \right) \left[D_O \left(\frac{\partial C_O(x, t)}{\partial x} \right) \right] \quad (4.4.16)$$

When D_O is not a function of x , (4.4.12) results.

In most electrochemical systems, the changes in solution composition caused by electrolysis are sufficiently small that variations in the diffusion coefficient with x can be neglected. However when the electroactive component is present at a high concentration, large changes in solution properties, such as the local viscosity, can occur during electrolysis. For such systems, (4.4.12) is no longer appropriate, and more complicated treatments are necessary (24, 25). Under these conditions, migrational effects can also become important.

We will have many occasions in future chapters to solve (4.4.12) under a variety of boundary conditions. Solutions of this equation yield *concentration profiles*, $C_O(x, t)$.

The general formulation of Fick's second law for any geometry is

$$\boxed{\frac{\partial C_O}{\partial t} = D_O \nabla^2 C_O} \quad (4.4.17)$$

where ∇^2 is the Laplacian operator. Forms of ∇^2 for different geometries are given in Table 4.4.2. Thus, for problems involving a planar electrode (Figure 4.4.5a), the linear diffusion equation, (4.4.12), is appropriate. For problems involving a spherical electrode

TABLE 4.4.2 Forms of the Laplacian Operator for Different Geometries^a

Type	Variables	∇^2	Example
Linear	x	$\partial^2/\partial x^2$	Shielded disk electrode
Spherical	r	$\partial^2/\partial r^2 + (2/r)(\partial/\partial r)$	Hanging drop electrode
Cylindrical (axial)	r	$\partial^2/\partial r^2 + (1/r)(\partial/\partial r)$	Wire electrode
Disk	r, z	$\partial^2/\partial r^2 + (1/r)(\partial/\partial r) + \partial^2/\partial z^2$	Inlaid disk ultramicroelectrode ^b
Band	x, z	$\partial^2/\partial x^2 + \partial^2/\partial z^2$	Inlaid band electrode ^c

^aSee also J. Crank, "The Mathematics of Diffusion," Clarendon, Oxford, 1976.

^b r = radial distance measured from the center of the disk; z = distance normal to the disk surface.

^c x = distance in the plane of the band; z = distance normal to the band surface.

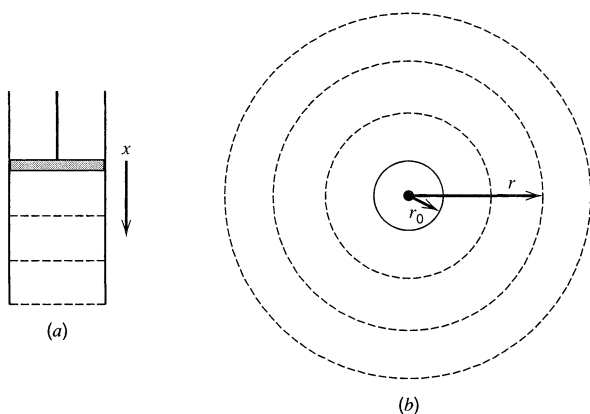


Figure 4.4.5 Types of diffusion occurring at different electrodes. (a) Linear diffusion to a planar electrode. (b) Spherical diffusion to a hanging drop electrode.

(Figure 4.4.5b), such as the hanging mercury drop electrode (HMDE), the spherical form of the diffusion equation must be employed:

$$\frac{\partial C_{\text{O}}(r, t)}{\partial t} = D_{\text{O}} \left(\frac{\partial^2 C_{\text{O}}(r, t)}{\partial r^2} + \frac{2}{r} \frac{\partial C_{\text{O}}(r, t)}{\partial r} \right) \quad (4.4.18)$$

The difference between the linear and spherical equations arises because spherical diffusion takes place through an increasing area as r increases.

Consider the situation where O is an electroactive species transported purely by diffusion to an electrode, where it undergoes the electrode reaction



If no other electrode reactions occur, then the current is related to the flux of O at the electrode surface ($x = 0$), $J_{\text{O}}(0, t)$, by the equation

$$-J_{\text{O}}(0, t) = \frac{i}{nFA} = D_{\text{O}} \left[\frac{\partial C_{\text{O}}(x, t)}{\partial x} \right]_{x=0} \quad (4.4.20)$$

because the total number of electrons transferred at the electrode in a unit time must be proportional to the quantity of O reaching the electrode in that time period. This is an extremely important relationship in electrochemistry, because it is the link between the evolving concentration profile near the electrode and the current flowing in an electrochemical experiment. We will draw upon it many times in subsequent chapters.

If several electroactive species exist in the solution, the current is related to the sum of their fluxes at the electrode surface. Thus, for q reducible species,

$$\frac{i}{FA} = - \sum_{k=1}^q n_k J_k(0, t) = \sum_{k=1}^q n_k D_k \left[\frac{\partial C_k(x, t)}{\partial x} \right]_{x=0} \quad (4.4.21)$$

4.4.3 Boundary Conditions in Electrochemical Problems

In solving the mass-transfer part of an electrochemical problem, a diffusion equation (or, in general, a mass-transfer equation) is written for each dissolved species (O, R, ...). The solution of these equations, that is, the discovery of an equation expressing C_{O} , C_{R} , ... as functions of x and t , requires that an initial condition (the concentration profile at

$t = 0$) and two boundary conditions (functions applicable at certain values of x) be given for each diffusing species. Typical initial and boundary conditions include the following.

(a) Initial Conditions

These are usually of the form

$$C_O(x, 0) = f(x) \quad (4.4.22)$$

For example, if O is uniformly distributed throughout the solution at a bulk concentration C_O^* at the start of the experiment, the initial condition is

$$C_O(x, 0) = C_O^* \quad (\text{for all } x) \quad (4.4.23)$$

If R is initially absent from the solution, then

$$C_R(x, 0) = 0 \quad (\text{for all } x) \quad (4.4.24)$$

(b) Semi-infinite Boundary Conditions

The electrolysis cell is usually large compared to the length of diffusion; hence the solution at the walls of the cell is not altered by the process at the electrode (see Section 5.2.1). One can normally assume that at large distances from the electrode ($x \rightarrow \infty$) the concentration reaches a constant value, typically the initial concentration, so that, for example,

$$\lim_{x \rightarrow \infty} C_O(x, t) = C_O^* \quad (\text{at all } t) \quad (4.4.25)$$

$$\lim_{x \rightarrow \infty} C_R(x, t) = 0 \quad (\text{at all } t) \quad (4.4.26)$$

For thin-layer electrochemical cells (Section 11.7), where the cell wall is at a distance, l , of the order of the diffusion length, one must use boundary conditions at $x = l$ instead of those for $x \rightarrow \infty$.

(c) Electrode Surface Boundary Conditions

Additional boundary conditions usually relate to concentrations or concentration gradients at the electrode surface. For example, if the potential is controlled in an experiment, one might have

$$C_O(0, t) = f(E) \quad (4.4.27)$$

$$\frac{C_O(0, t)}{C_R(0, t)} = f(E) \quad (4.4.28)$$

where $f(E)$ is some function of the electrode potential derived from the general current-potential characteristic or one of its special cases (e.g., the Nernst equation).

If the current is the controlled quantity, the boundary condition is expressed in terms of the flux at $x = 0$; for example,

$$-J_O(0, t) = \frac{i}{nFA} = D_O \left[\frac{\partial C_O(x, t)}{\partial x} \right]_{x=0} = f(t) \quad (4.4.29)$$

The conservation of matter in an electrode reaction is also important. For example, when O is converted to R at the electrode and both O and R are soluble in the solution phase, then for each O that undergoes electron transfer at the electrode, an R must be produced. Consequently, $J_O(0, t) = -J_R(0, t)$, and

$$D_O \left[\frac{\partial C_O(x, t)}{\partial x} \right]_{x=0} + D_R \left[\frac{\partial C_R(x, t)}{\partial x} \right]_{x=0} = 0 \quad (4.4.30)$$

4.4.4 Solution of Diffusion Equations

In the chapters that follow, we will examine the solution of the diffusion equations under a variety of conditions. The analytical mathematical methods for attacking these problems are discussed briefly in Appendix A. Numerical methods, including digital simulations (Appendix B), are also frequently employed.

Sometimes one is interested only in the steady-state solution (e.g., with rotating disk electrodes or ultramicroelectrodes). Since $\partial C_O/\partial t = 0$ in such a situation, the diffusion equation simply becomes

$$\nabla^2 C_O = 0 \quad (4.4.31)$$

Occasionally, solutions can be found by searching the literature concerning analogous problems. For example, the conduction of heat involves equations of the same form as the diffusion equation (26, 27);

$$\partial T/\partial t = \alpha_1 \nabla^2 T \quad (4.4.32)$$

where T is the temperature, and $\alpha_1 = \kappa/\rho s$ (κ = thermal conductivity, ρ = density, and s = specific heat). If one can find the solution of a problem of interest in terms of the temperature distribution, such as, $T(x, t)$, or heat flux, one can easily transpose the results to give concentration profiles and currents.

Electrical analogies also exist. For example, the steady-state diffusion equation, (4.4.31), is of the same form as that for the potential distribution in a region of space not occupied by electrically charged bodies (Laplace's equation),

$$\nabla^2 \phi = 0 \quad (4.4.33)$$

If one can solve an electrical problem in terms of the current density, j , where

$$-j = \kappa \nabla \phi \quad (4.4.34)$$

(where κ is the conductivity), one can write the solution to an analogous diffusion problem (as the function C_O) and find the flux from equation 4.4.20 or from the more general form,

$$-J = D_O \nabla C_O \quad (4.4.35)$$

This approach has been employed, for example, in determining the steady-state uncompensated resistance at an ultramicroelectrode (28) and the solution resistance between an ion-selective electrode tip and a surface in a scanning electrochemical microscope (29, 30). It also is sometimes possible to model the mass transport and kinetics in an electrochemical system by a network of electrical components (31, 32). Since there are a number of computer programs (e.g., SPICE) for the analysis of electric circuits, this approach can be convenient for certain electrochemical problems.

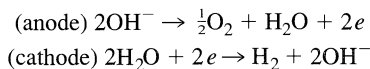
▶ 4.5 REFERENCES

1. M. Planck, *Ann. Physik*, **39**, 161; **40**, 561 (1890).
2. J. Newman, *Electroanal. Chem.*, **6**, 187 (1973).
3. J. Newman, *Adv. Electrochem. Electrochem. Engr.*, **5**, 87 (1967).
4. C. W. Tobias, M. Eisenberg, and C. R. Wilke, *J. Electrochem. Soc.*, **99**, 359C (1952).
5. W. Vielstich, *Z. Elektrochem.*, **57**, 646 (1953).
6. N. Ibl, *Chem. Ing. Tech.*, **35**, 353 (1963).
7. G. Charlot, J. Badoz-Lambling, and B. Tremillion, "Electrochemical Reactions," Elsevier, Amsterdam, 1962, pp. 18–21, 27–28.
8. I. M. Kolthoff and J. J. Lingane, "Polarography," 2nd ed., Interscience, New York, 1952, Vol. 1, Chap. 7.

9. K. Vetter, "Electrochemical Kinetics," Academic, New York, 1967.
10. J. Koryta, J. Dvořák, and V. Bohácková, "Electrochemistry," Methuen, London, 1970, pp. 88–112.
11. J. Coursier, as quoted in reference 7.
12. C. Amatore, B. Fosset, J. Bartelt, M. R. Deakin, and R. M. Wightman, *J. Electroanal. Chem.*, **256**, 255 (1988).
13. J. C. Myland and K. B. Oldham, *J. Electroanal. Chem.*, **347**, 49 (1993).
14. C. P. Smith and H. S. White, *Anal. Chem.*, **65**, 3343 (1993).
15. M. Ciszowska and J. G. Osteryoung, *Anal. Chem.*, **67**, 1125 (1995).
16. W. Jost, *Angew. Chem., Intl. Ed. Engl.*, **3**, 713 (1964).
17. J. Crank, "The Mathematics of Diffusion," Clarendon, Oxford, 1979.
18. W. Jost, "Diffusion in Solids, Liquids, and Gases," Academic, New York, 1960.
19. S. Chandrasekhar, *Rev. Mod. Phys.*, **15**, 1 (1943).
20. L. B. Anderson and C. N. Reilley, *J. Chem. Educ.*, **44**, 9 (1967).
21. H. C. Berg, "Random Walks in Biology," Princeton University, Press, Princeton, NJ, 1983.
22. N. Davidson, "Statistical Mechanics," McGraw-Hill, New York, 1962, pp. 155–158.
23. R. S. Berry, S. A. Rice, and J. Ross, "Physical Chemistry," Wiley, New York, 1980, pp. 1056–1060.
24. R. B. Morris, K. F. Fischer, and H. S. White, *J. Phys. Chem.*, **92**, 5306 (1988).
25. S. C. Paulson, N. D. Okerlund, and H. S. White, *Anal. Chem.*, **68**, 581 (1996).
26. H. S. Carslaw and J. C. Jaeger, "Conduction of Heat in Solids," Clarendon, Oxford, 1959.
27. M. N. Ozisk, "Heat Conduction," Wiley, New York, 1980.
28. K. B. Oldham in "Microelectrodes, Theory and Applications," M. I. Montenegro, M. A. Queiros, and J. L. Daschbach, Eds., Kluwer, Amsterdam, 1991, p. 87.
29. B. R. Horrocks, D. Schmidtke, A. Heller, and A. J. Bard, *Anal. Chem.*, **65**, 3605 (1993).
30. C. Wei, A. J. Bard, G. Nagy, and K. Toth, *Anal. Chem.*, **67**, 1346 (1995).
31. J. Horno, M. T. García-Hernández, and C. F. González-Fernández, *J. Electroanal. Chem.*, **352**, 83 (1993).
32. A. A. Moya, J. Castilla, and J. Horno, *J. Phys. Chem.*, **99**, 1292 (1995).

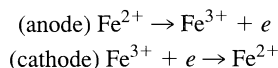
► 4.6 PROBLEMS

- 4.1 Consider the electrolysis of a 0.10 M NaOH solution at platinum electrodes, where the reactions are:



Show the balance sheet for the system operating at steady state. Assume $20e$ are passed in the external circuit per unit time, and use the λ_0 values in Table 2.3.2 to estimate transference numbers.

- 4.2 Consider the electrolysis of a solution containing 10^{-1} M $\text{Fe}(\text{ClO}_4)_3$ and 10^{-1} M $\text{Fe}(\text{ClO}_4)_2$ at platinum electrodes:



Assume that both salts are completely dissociated, that the λ values for Fe^{3+} , Fe^{2+} , and ClO_4^- are equal, and that $10e$ are passed in the external circuit per unit time. Show the balance sheet for the steady-state operation of this system.

- 4.3 For a given electrochemical system to be described by equations involving semi-infinite boundary conditions, the cell wall must be at least five "diffusion layer thicknesses" away from the electrode. For a substance with $D = 10^{-5}$ cm²/s, what distance between the working electrode and the cell wall is required for a 100-s experiment?

- 4.4 The mobility, u_j , is related to the diffusion coefficient, D_j , by equation 4.2.2. (a) From the mobility data in Table 2.3.2, estimate the diffusion coefficients of H^+ , I^- , and Li^+ at 25°C. (b) Write the equation for the estimation of D from the λ value.
- 4.5 Using the procedure of Section 4.4.2, derive Fick's second law for spherical diffusion (equation 4.4.18). [*Hint*: Because of the different areas through which diffusion occurs at r and at $r + dr$, it is more convenient to obtain the change of concentration in dr by considering the number of moles diffusing per second rather than the flux.]

BASIC POTENTIAL STEP METHODS

The next three chapters are concerned with methods in which the electrode potential is forced to adhere to a known program. The potential may be held constant or may be varied with time in a predetermined manner as the current is measured as a function of time or potential. In this chapter, we will consider systems in which the mass transport of electroactive species occurs only by diffusion. Also, we will restrict our view to methods involving only step-functional changes in the working electrode potential. This family of techniques is the largest single group, and it contains some of the most powerful experimental approaches available to electrochemistry.

In the methods covered in this chapter, as well as in Chapters 6 and 7, the electrode area, A , is small enough, and the solution volume, V , is large enough, that the passage of current does not alter the bulk concentrations of electroactive species. Such circumstances are known as *small A/V conditions*. It is easy to show on the basis of results below that electrodes with dimensions of several millimeters operating in solutions of 10 mL or more do not consume a significant fraction of a dissolved electroactive species in experiments lasting a few seconds to a few minutes (Problem 5.2). Several decades ago, Laitinen and Kolthoff (1, 2) invented the term *microelectrode* to describe the electrode's role under small A/V conditions, which is to probe a system, rather than to effect compositional change.¹ In Chapter 11, we will explore *large A/V conditions*, where the electrode is intended to transform the bulk system.

► 5.1 OVERVIEW OF STEP EXPERIMENTS

5.1.1 Types of Techniques

Figure 5.1.1 is a picture of the basic experimental system. An instrument known as a *potentiostat* has control of the voltage across the working electrode–counter electrode pair, and it adjusts this voltage to maintain the potential difference between the working and reference electrodes (which it senses through a high-impedance feedback loop) in accord with the program defined by a function generator. One can view the potentiostat

¹Recent years have seen the rapid development of extremely small working electrodes, of dimensions in the micrometer or nanometer range, which have a set of very useful properties. In much of the literature and in casual conversation, these are also called “microelectrodes,” in reference to their dimensions. They always provide small A/V conditions, so they are indeed microelectrodes within the definition given above, but much larger electrodes also belong to the class. To preserve the usefulness of the earlier term, very small electrodes have been called *ultramicroelectrodes* (see Section 5.3). That distinction is respected consistently in the remainder of this book, although it now seems likely that the new usage of the term “microelectrode” will soon displace the historic one altogether.